GLUTAMINE SYNTHETASE OF *LOTUS CORNICULATUS* ROOTS AND NODULES: CHARACTERISATION AND TISSUE-SPECIFIC INHIBITION

by JON GRAHAM BOXALL
B.Sc. (Reading), M.Sc. (York)

Thesis submitted to the University of Nottingham
for the degree of Doctor of Philosophy, May 1998

Place of research:
Biochemistry and Physiology Department,
IACR-Rothamsted,
West Common,
Harpenden,
Hertfordshire AL5 2JQ

Place of registration:
School of Biological Sciences,
Life Science Building,
University of Nottingham,
University Park,
Nottingham NG7 2RD

CONTENTS

TABLE OF CONTENTS 1

LIST OF FIGURES 6

LIST OF TABLES 9

LIST OF APPENDICES 9

ABSTRACT 10

ACKNOWLEDGEMENTS 11

ABBREVIATIONS 12

CHAPTER 1: INTRODUCTION

1.1 Higher plant glutamine synthetase (GS) and its role in nitrogen metabolism .. 13

1.1.1 GS-GOGAT cycle 13

1.1.2 Primary routes for ammonia production 14

1.1.3 Secondary sources of ammonia 16

1.1.4 GS structure and cellular compartmentalisation 18

1.1.5 Molecular basis for isoforms 21

1.1.6 Nutritional regulation 25

1.1.7 The role of GS in nitrogen remobilisation 30

1.1.8 Is there a link between GS isoforms and their role in plant nitrogen metabolism? 32

1.2 Approaches to the inhibition and down regulation of GS activity 32

1.2.1 Mutants 32

1.2.2 Antisense 33

1.2.3 Inhibitor studies 34

1.3 Phosphinothricin resistance genes and their use in plants 38

1.3.1 The *bar* and *pat* resistance genes 38

1.3.2 PPT-resistant transgenic plants expressing PAT enzymes 39

1.4 The ß-glucuronidase (GUS) reporter gene 39

1.5 Translational fusions involving PAT and GUS 40

1.6 Aims of this thesis 41

CHAPTER 2: MATERIALS AND METHODS

2.1 Materials and equipment suppliers 45

2.2 Bacterial strains and plasmids 45

2.2.1 Long-term storage 45

2.3 Bacterial transformation 46

2.3.1 Preparation of competent *E. coli* 46

2.3.2 *E. coli* transformation procedures 47

2.3.3 Transformation of *Agrobacterium* by electroporation 47

2.4 Screening bacterial transformants 48

2.4.1 Blue/white selection of bacterial transformants 48

2.4.2 Colony hybridization 49

2.4.3 GUS assays on single colonies 50

2.5 Nucleic acid extraction and purification 50

2.5.1 Small-scale plasmid preparations 50

2.5.2 Mid-scale plasmid preparations 51

2.5.3 Chloramphenicol amplification of pBIN19-based plasmids 52

2.5.4 Extraction of plant DNA 52

2.5.5 Purification of DNA fragments from gels 53

2.5.6 Electrophoresis of DNA 53

2.6 Polymerase Chain Reaction (PCR) 54

2.6.1 Template preparation 54

2.6.2 Oligonucleotide preparation 54

2.6.3 'Hot-start' PCR 54

2.6.4 Calculation of optimum primer annealing temperatures 55

2.7 DNA manipulations 55

2.7.1 Restriction digests 55

2.7.2 Ligation 55

2.7.3 Filling-in sticky ends 55

2.7.4 T/A cloning 56

2.8 DNA sequencing 56

2.8.1 Reactions 56

2.8.2 Sequencing gel 57

2.9 Plant culture, transformation and regeneration 57
2.9.1 Maintenance of plant material in culture 57
2.9.2 Stab inoculation with *Agrobacterium rhizogenes* 58
2.9.3 Regeneration of plants from hairy roots 58
2.10 Enzyme assays 59
2.10.1 Plant harvest and tissue extraction 59
2.10.2 Preparation of bacterial lysates 59
2.10.3 Protein assays 59
2.10.4 Phosphinothricin acetyltransferase 60
2.10.5 β-glucuronidase 61
2.10.6 Combined PAT and GUS assay procedure 62
2.10.7 Glutamine synthetase 62
2.10.8 Nitrogenase 63
2.10.9 Ammonium determination 63
2.11 Protein fractionation and western blotting 64
2.11.1 Size exclusion chromatography 64
2.11.2 Ion-exchange chromatography 64
2.11.3 Polyethylene glycol fractionation 65
2.11.4 Polyacrylamide gel electrophoresis (PAGE) 65
2.11.5 Electrotransfer of proteins to membranes 66
2.11.6 Membrane immunostaining 66
2.12 Conversion of glufosinate-ammonium to the sodium salt 67

CHAPTER 3: CONSTRUCTION AND TESTING OF THE *PAT::UIDA* GENE FUSION

3.1 Introduction 71
3.2 Construction of a translational fusion between the *pat* and *uidA* genes 72
3.2.1 Plasmids 72
3.2.2 PCR amplification of a modified *pat* coding sequence 72
3.2.3 Cloning the amplified *pat* fragment into pCGUS 73
3.2.4 Cloning PATGUS into a bacterial expression vector 74
3.3 Demonstration of PAT and GUS activity in *E. coli* expressing PATGUS 74
3.3.1 *E. coli* expressing PATGUS are resistant to PPT 74

3.3.2 IPTG-induced PAT and GUS activity in *E. coli* expressing PATGUS 75
3.3.3 Precipitation of PAT and GUS activities by polyethylene glycol 75
3.3.4 Elution of PAT and GUS activity in liquid chromatography studies 76
3.3.5 Immunodetection of PATGUS by GUS antibodies 77
3.4 Discussion 77

CHAPTER 4:
THE GS ISOENZYME PROFILE IN *LOTUS CORNICULATUS* ROOTS AND NODULES

4.1 Introduction 90
4.2 GS isoenzymes in roots and nodules 91
4.3 Effect of developmental stage on the isoenzyme profile 92
4.4 Effect of nitrate on the isoenzyme profile 93
4.5 A simple model of the GS isoenzyme profile in nodules 94
4.5.1 Basic principles and assumptions 94
4.5.2 Calculations involved 95
4.5.3 Model predictions 96
4.6 Discussion 96
4.6.1 General characteristics of the elution profiles of GS from roots and nodules of *L. corniculatus* 96
4.6.2 What is the molecular basis for the nodule-specific isoform? 97
4.6.3 What can the model tell us about the elution profile? 98
4.6.4 The effect of nodule developmental stage 99
4.6.5 What is the molecular basis for the effect of nitrate on GS in nodule extracts? 100
4.6.6 Why is the timing of the change in the GS elution profile variable? 102
4.6.7 Discrepancy between GS activities and GS protein levels 102
4.6.8 Summary 105

CHAPTER 5: PATGUS ACTIVITY IN TRANSGENIC *LOTUS CORNICULATUS*

5.1 Introduction 115
5.2 Gene constructs and plant transformation 116
5.3 GUS activity in constitutive PATGUS lines 117
5.4 PPT resistance in transgenic lines constitutively expressing PATGUS 117

5.5 Direction of PATGUS expression to the nodule infected zone 118
5.6 Specific protection of GS by directed PATGUS expression 119
5.7 Discussion 119
5.7.1 The GUS and PAT moieties of PATGUS are both active *in planta* 119
5.7.2 GUS activity: a quantitative marker for PAT activity *in planta*? 120
5.7.3 Expression of PATGUS in the root nodule specifically protects GS in the nodule from PPT inhibition 120

CHAPTER 6: THE EFFECT OF SPECIFIC INACTIVATION OF ROOT GLUTAMINE SYNTHETASE ON PLANT GROWTH AND NITROGEN METABOLISM IN *LOTUS CORNICULATUS*

6.1 Introduction 129
6.2 Timing of the onset of nitrogenase activity in nodulated *L. corniculatus* .. 130
6.3 Duration of the effect of a single PPT treatment on GS activity in nodules, roots, and shoots 130
6.4 Effect of long-term inhibition of root GS activity in transgenic *L. corniculatus* lines 131
6.4.1 Effect on plant growth and morphology 131
6.4.2 Effect on nodule metabolism 134
6.5 Discussion 135
6.5.1 Soil applications of PPT inhibit GS activity in all plant tissues 135
6.5.2 Effect of the hairy root phenotype on nodulation 137
6.5.3 Comparison of the effects of the two PPT treatments on line 12E, and their significance 138
6.5.4 Comparison with the effects of *Pseudomonas syringae* on *Medicago sativa* 139
6.5.5 Other observations 142
6.5.6 Conclusion 143

CHAPTER 7: GENERAL DISCUSSION

7.1 The PATGUS gene fusion and its potential use 159
7.2 The nature and regulation of GS in *L. corniculatus* 160
7.3 Comparison with the results of Knight and Langston-Unkefer (1988) 162
7.4 **Conclusion** 162

REFERENCES 177

LIST OF FIGURES

CHAPTER 1

1.1 The GS-GOGAT cycle 13

1.2 The acetylation of phosphinothricin by phosphinothricin-*N*-acetyltransferase 38

1.3a Comparison between the *bar* gene of *S. hygroscopicus* and the *pat* gene of *S. viridochromogenes* - 1: Amino acid sequence 43

1.3b Comparison between the *bar* gene of *S. hygroscopicus* and the *pat* gene of *S. viridochromogenes* - 2: Nucleic acid sequence 44

1.4 The most common histochemical assay for GUS 40

CHAPTER 3

3.1 Strategy for PCR amplification and modification of the *pat* gene 81

3.2 Construction of pCPATGUS95 82

3.3 PCR amplification of a modified form of the *pat* gene from pIB16.1 83

3.4 PPT resistance in *E. coli* expressing PATGUS 84

3.5 IPTG-induced PAT and GUS activity in *E. coli* carrying pKKPATGUS 85

3.6 PEG precipitation of PATGUS 86

3.7 Size-exclusion chromatography of PATGUS expressed in *E. coli* 87

3.8 Calibration of the Sephacryl S300-HR column with protein molecular weight standards 88

3.9 Western blots of extracts from *E. coli* expressing PATGUS probed with GUS-specific antisera 89

CHAPTER 4

4.1 Elution profiles of GS activity from ion-exchange chromatography of extracts from nodules, nodulated roots and nitrate-fed roots of *L. corniculatus*. 106

4.2 Western blots of fractions collected during ion-exchange chromatography of GS from nodules, nodulated roots and nitrate-fed roots 107

4.3 Elution profile of GS activity from ion-exchange chromatography of extracts from nodules of *L. corniculatus* using a stretched KCl gradient 108

4.4 The effect of nodule developmental stage on the elution profile of GS activity from ion exchange chromatography of extracts from nodules of *L. corniculatus* 109

4.5 The effect of nitrate on the elution profile of GS isoenzyme activity from ion exchange chromatography of nodule extracts from *L. corniculatus* 110

4.6 The effect of nitrate on the elution profile of GS isoenzyme activity from ion exchange chromatography of nodule extracts from poorly-nodulated, wild-type *L. corniculatus* 111

4.7 The effect of nitrate on the elution profile of GS isoenzyme activity from ion exchange chromatography of nodule extracts from well-nodulated, transformed *L. corniculatus* 112

4.8 A schematic representation of a simple model to explain the elution profile observed in the separation of nodule extracts by ion exchange chromatography 113

4.9 Comparison between the observed elution profile of GS from nodule extracts and the elution profile predicted for 79% A-type subunits in the computer simulation described in Section 4.5 114

CHAPTER 5

5.1 GUS activity in roots and shoots of *L. corniculatus* plants transformed with the 35S-PATGUS construct 121

5.2 PPT resistance in *L. corniculatus* lines transformed with the 35S-PATGUS construct (photographs) 122

5.3 PPT resistance in *L. corniculatus* lines transformed with the 35S-PATGUS construct (graphs) 124

5.4 Nodule-specific expression of GUS activity in *L. corniculatus* lines 12E and 11D transformed with the *gln*-γ-PATGUS construct demonstrated by histochemical staining of nodule sections 126

5.5 GUS activities in nodules of *L. corniculatus* plants transformed with the *gln*-γ-PATGUS construct, plotted against GUS activity in their roots 127

5.6 GS activity in root and nodule extracts from *L. corniculatus* plants transformed with pBINGPG 128

CHAPTER 6

6.1 Time-course of increase in nitrogenase activity as measured by acetylene reduction in wild-type *L. corniculatus* plants and in line 12E 149

6.2 The effect of soil applications of PPT on GS activity in nodules, roots and shoots of wild-type *L. corniculatus* 150

6.3 The effect of soil applications of PPT on the growth habit *L. corniculatus* 151

6.4 The effect of soil applications of PPT on the fresh weight of shoots, roots, nodules and whole plants of wild-type *L. corniculatus* and line 12E 153

6.5 The effect of soil applications of PPT on the dry weight of wild-type *L. corniculatus* and of 12E 154

6.6 The effect of soil applications of PPT on the root:shoot ratio of wild-type *L. corniculatus* and of line 12E 155

6.7 The effect of soil applications of PPT on the number and average fresh weight of nodules observed on the roots of wild-type *L. corniculatus* of line 12E 156

6.8 The effect of soil applications of PPT on nitrogenase activity, as measured by acetylene reduction, of wild-type *L. corniculatus* and in line 12E 157

6.9 The effect of soil applications of PPT on GS activity in the nodules of wild-type *L. corniculatus* and of line 12E 158

LIST OF TABLES

CHAPTER 2

2.1 Plasmids used and constructed 68

2.2 Bacterial growth media 69

2.3 Plant growth media 69

2.4 Antibiotics 70

CHAPTER 3

3.1 Calculated primer annealing temperatures 80

CHAPTER 6

6.1 Effect of PPT treatment on the growth and morphology of wild-type *L. corniculatus* and of a line expressing PATGUS in the infected zone of the nodule (12E) 145

6.2 Effect of PPT treatment on nodule GS and nitrogenase activities of wild-type *L. corniculatus* and of line 12E 147

6.3 Comparison of the main effects of PPT treatment of line 12E with the findings of Knight and Langston-Unkefer (1988) 148

LIST OF APPENDICES

I Suppliers' names and addresses 164

II A VMS-BASIC program for calculation of the optimum annealing temperature for PCR primers 167

III A VMS-BASIC program for implementing a simple model to predict the elution profile of GS from nodule extracts 172

IV Output from the program in Appendix III 174

ABSTRACT

Glutamine synthetase (GS), the enzyme responsible for the first step in the assimilation of ammonium in higher plants, generally exists in a number of isoforms associated with different tissues or cellular compartments within the plant. This study has investigated the GS isoenzyme composition of roots and N-fixing root nodules of the temperate legume, *Lotus corniculatus,* and has used a novel transgenic approach to manipulate the spatial distribution of the enzyme within these tissues.

The isoforms of GS were studied using ion-exchange chromatography and western blotting, and a nodule-specific isoform was identified. Nitrate treatment of the N_2-fixing plants had a marked effect on the nodule isoform, converting it to a form that was indistinguishable by ion-exchange chromatography from the root isoenzyme.

To allow tissue-specific manipulation of GS activity, a chimaeric gene was constructed consisting of a translational fusion between the *pat* and *uidA* genes coding for phosphinothricin acetyl transferase (PAT) and β-glucuronidase (GUS), respectively. The PAT enzyme detoxifies the GS inhibitor, phosphinothricin, while GUS is a readily assayable marker enzyme that allowed the localisation of PAT activity within the plant tissues to be inferred. The *pat::uidA* gene was shown to encode a bifunctional enzyme when expressed in *E. coli* and in transgenic *L. corniculatus* plants.

Transgenic lines carrying a nodule-specific promoter fused to *pat::uidA* were resistant to PPT only when nodulated. In some of these lines, nodule GS activity was completely resistant to soil applications of PPT under conditions where root GS was 100% inhibited. After long-term PPT treatment, one line (12E) showed a two-fold increase in nitrogenase activity, a four-fold increase in GS activity, and a 50% increase in dry matter production. Possible explanations for how specific inhibition of root GS led to these effects are discussed.

ACKNOWLEDGEMENTS

There are a number of people without whom this work would not have been possible. I would sincerely like to thank Brian Forde for his considerable help and patience whilst supervising me during my research and during the writing up period. I would also like to thank Edward Cocking who has monitored my research from up at Nottingham, offering helpful comments and advice when necessary. I extend my gratitude towards Janet Woodall and John Pearson who played a very important part in collaborating with me on the GS ion-exchange work, and who have shown constant enthusiasm for my work. Many thanks also go to Simon Driscoll who practically rebuilt an ageing GC for me without question, and all those in the B&P department at Rothamsted, past and present, who have helped with my experiments, and been involved in discussions and debates over my (sometimes peculiar) results.

Whilst at Rothamsted, I have had, and continue to benefit from, a very enjoyable time, and for that I extend sincere thanks to all my friends, both in the B&P department and in other parts of Rothamsted and beyond. Forgive me for not mentioning any names. You know who you are.

Finally, to Mum, Dad, Clare, Maurice, Joan and Shahnaz, who have supported me greatly, and appear to have more faith in my abilities than I have myself; my heartfelt thanks for putting up with me.

Jon Boxall, February 1998

ABBREVIATIONS

ADP	adenosine diphosphate
ATP	adenosine triphosphate
APS	ammonium persulfate
ATP	adenosine triphosphate
bp	base pairs
BSA	bovine serum albumin, fraction V
CaMV	cauliflower mosaic virus
CAT	chloramphenicol acetyltransferase
DTNB	5,5'-dithiobis-2-nitrobenzoic acid
DTT	dithiothreitol
EDTA	ethylenediaminetetraacetic acid
FAD	flavin adenine dinucleotide
fwt	fresh weight
GDH	glutamate dehydrogenase
GOGAT	glutamate synthase
GS	glutamine synthetase
GUS	β-glucuronidase
IAA	indole-acetic acid
kb	kilobases
MES	2-[N-Morpholino]ethanesulfonic acid
MSO	3-amino-3-carboxypropylmethyl-sulphoximine
MUG	4-methylumbelliferyl glucuronide
NiR	nitrite reductase
NPTII	neomycin phosphotransferase II
NR	nitrate reductase
PAGE	polyacrylamide gel electrophoresis
PAT	phosphinothricin acetyltransferase
PEG	polyethylene glycol
3-PGA	3-phosphoglycerate
PMSF	phenylmethylsulphonylfluoride
PPT	phosphinothricin
PVPP	polyvinylpolypyrrolidone
Rubisco	ribulose-bisphosphate carboxylase/oxygenase
RuBP	ribulose-bisphosphate
SDS	sodium dodecyl sulphate
T-β-L	tabtoxinine-β-lactam
TBS	tris-buffered saline
TCA	trichloroacetic acid
TEMED	N,N,N',N'-tetramethyl ethylenediamine
TLC	thin-layer chromatography
Tween 20	polyoxyethylsorbitan monolaurate
X-Gal	5-bromo-4-chloro-3-indolyl-β-D-galactopyranoside
X-Gluc	5-bromo-4-chloro-3-indolyl-β-D-glucuronic acid

CHAPTER 1:

INTRODUCTION

1.1 Higher plant glutamine synthetase and its role in nitrogen metabolism

1.1.1 GS-GOGAT cycle

Glutamine synthetase (GS; EC 6.3.1.2) is a key enzyme in nitrogen metabolism. It is the route by which all nitrogen from primary assimilation must pass, and is also responsible for the reassimilation of ammonia liberated by secondary metabolic processes. It catalyses the addition of ammonia to glutamate to synthesise glutamine, and works in conjunction with glutamate synthase (GOGAT; EC 1.4.7.1 and EC 1.4.1.14) in the GS-GOGAT cycle (Fig. 1.1). The net outcome of this cycle is the assimilation of ammonia and the synthesis of glutamate, at the expense of ATP and reducing power (Miflin and Lea, 1976). The glutamine and glutamate thus produced serve as organic nitrogen sources for the rest of the plant and are used as the basis for other nitrogenous compounds.

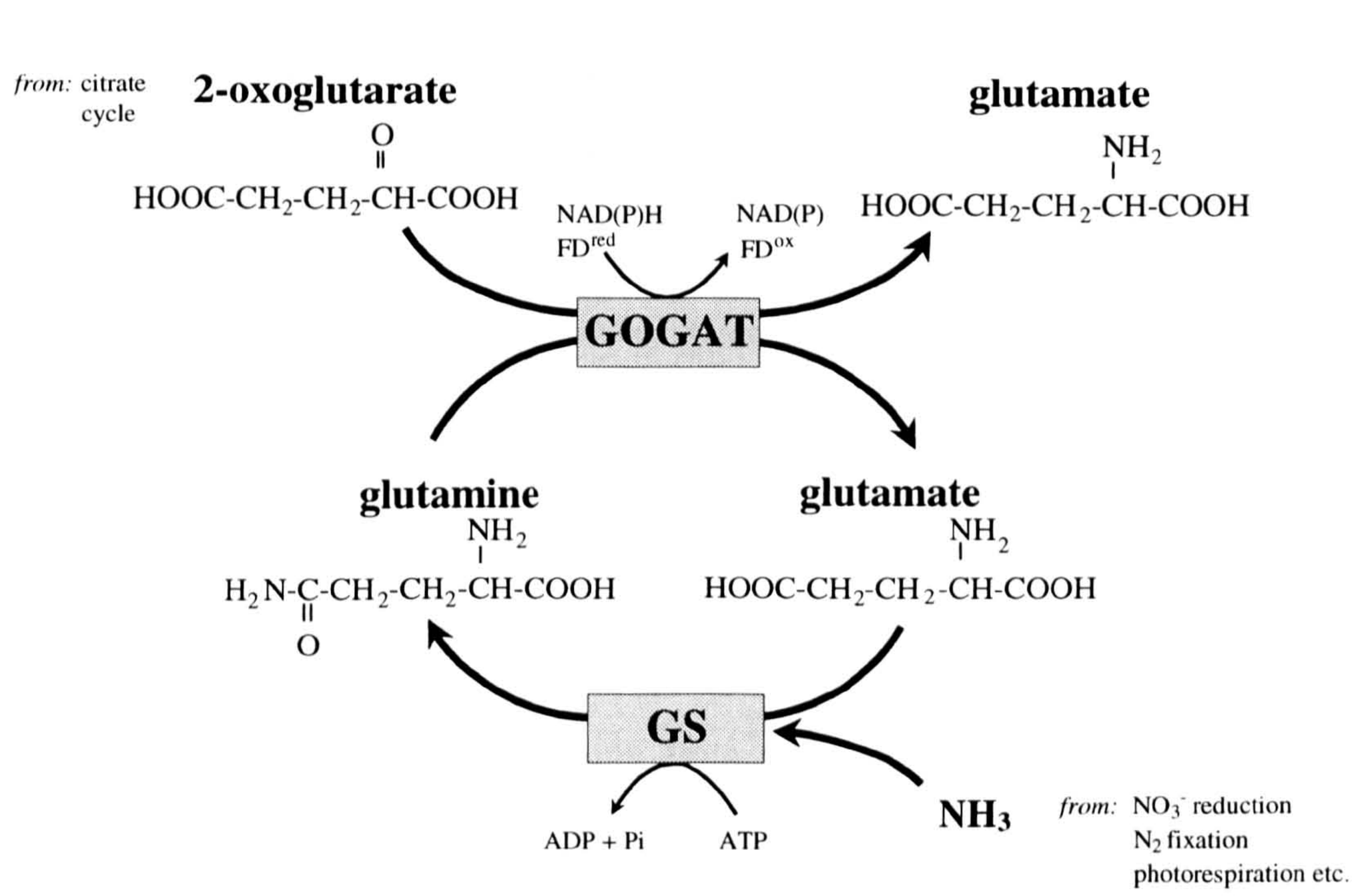

Figure 1.1: The GS-GOGAT cycle

1.1.2 Primary routes for ammonia production

Reduction of nitrate

The primary source of ammonia in the majority of plants growing in well-aerated soils is from the reduction of nitrate. In many agricultural soils, nitrate can be considered to be the predominant form of nitrogen in the soil, since ammonium in the soil is rapidly converted into nitrate through the nitrifying action of *Nitrosomonas* and *Nitrobacter* spp., bacteria which are found in most soils (Haynes, 1986; Marschner, 1995). Nitrate in the soil is taken up by the plant against an electrochemical gradient, requiring active transport systems (Trueman *et al.*, 1996). Once inside the plant, the nitrate is reduced to nitrite by cytosolic nitrate reductase (NR) in the root, or is transported in the xylem to the shoot, and then reduced there. It may also be stored in the vacuoles of both shoot and root cells if supply exceeds demand (Andrews, 1986). Whether nitrate reduction occurs primarily in the root or the shoot depends on such factors as the concentration of nitrate in the soil, the developmental stage of the plant, and plant species (Andrews, 1986; Woodall and Forde, 1996). Nitrite is reduced further to ammonium by nitrite reductase (NiR) in the root plastid or leaf chloroplast, and the ammonium thus produced is then available to the GS-GOGAT cycle.

Direct uptake of ammonium from the soil

Despite the tendency for soil ammonium to be converted into nitrate, there are still many situations in which it is a significant, if not the predominant form of available nitrogen (Popp, 1993). For example, ammonium is a significant form of soil nitrogen in grazed pastures where it is present at high concentrations in the urine of grazing animals (Ryden *et al.*, 1984; Jarvis *et al.*, 1989). Soil ammonium concentrations may also be significant in the Arctic tundras, forest ecosystems and in rice cultivation where soil nitrification is significantly inhibited (Frommer *et al.*, 1994). The steps of the nitrate assimilatory pathway are among the most energy-intensive processes in plants (Bloom *et al.*, 1992), and so it is not surprising that plants have also evolved the ability to take up ammonium directly from the soil in addition to, and perhaps preferentially to nitrate (Hatch and Macduff, 1991). Like nitrate uptake, this process involves at least two uptake systems, and ammonium transporters have been cloned and shown in *Lycopersicon esculentum* to be preferentially expressed in root hairs (Frommer *et al.*, 1994; Ninnemann *et al.*, 1994; Lauter *et al.*, 1996). Once in the root,

the ammonium is available for assimilation by the GS-GOGAT cycle, but unlike nitrate is not usually transported in the xylem, so its assimilation is restricted to the root.

Nitrogen fixation

Leguminous plants are able to fix nitrogen directly from dinitrogen in the air by forming a symbiotic relationship with certain members of the bacterial genera *Rhizobium, Bradyrhizobium*, and *Azorhizobium* (Hirsch, 1992). Free-living soil bacteria of these genera have the ability to infect root cells of leguminous species, causing cortical cell divisions in the host, which result in the formation of a specialised organ, the nodule. Nodules are separated into two categories based on their macrostructure: determinate and indeterminate. The type of nodule formed is dictated by plant species, for example, *Glycine max*, *Phaseolus vulgaris* and *Lotus* spp. produce determinate nodules whereas those of *Medicago sativa* and *Vicia faba* are indeterminate. Determinate nodules result from expansion of plant-derived cells of the outer cortex, and have a discrete growth phase whereas indeterminate nodules are produced by cell divisions of the inner cortex and have a persistent meristem (Hirsch, 1992).

The central region of the nodule is composed mainly of cells which have been infected by the bacteria, the latter having undergone major morphological and physiological changes to become bacteroids. The bacteroids express the enzyme nitrogenase, which reduces dinitrogen to ammonium, and this is exported into the cytosol of the infected cell where it can be assimilated by cytosolic GS of the host plant. To cope with the considerable flux of ammonium from the bacteroids, the plant-derived fraction of the root nodule generally expresses a large amount of GS protein, well above that of normal root tissue. In fact, GS represents 1-2% of soluble protein in nodules (Miflin and Cullimore, 1984). This nodule isoform of GS has been the subject of much research, and has been found to be the product of specific expression of a novel gene ('nodule-specific') in some cases, and due to up-regulation of a root form ('nodule-enhanced') in others (Forde and Cullimore, 1989). By dissecting the central region of *P. vulgaris* nodules from the cortical region and comparing western blots from these regions, Chen and Cullimore (1989) demonstrated that the predominant isoenzyme in the central region differs from that in the cortex. This was confirmed by Forde *et al.* (1989) who fused the promoter of

a nodule-specific GS gene (*gln-γ*) to the β-glucuronidase (GUS) reporter gene and demonstrated that it directed expression to the infected cells of the central region of the nodule, corresponding to the cells in which N_2 fixation takes place. Studies such as these have prompted speculation that the infected cells are primarily involved in assimilation of ammonium whereas the uninfected cells convert the glutamate from the GS-GOGAT cycle into transport compounds for export from the nodule (Forde and Cullimore, 1989). The type of further metabolism of glutamine to transport compounds is dependent on the type of nodule, with determinate nodules producing and exporting ureides in the majority of cases whereas most species with indeterminate nodules produce and export amides (Hirsch, 1992).

1.1.3 Secondary sources of ammonia

Photorespiration

In photosynthetic tissues of C3 plant species, photorespiration can be a major source of ammonia. Photorespiration is a complex series of reactions that compensates for the tendency of ribulose-bisphosphate carboxylase/oxygenase (Rubisco) to oxygenate ribulose-bisphosphate (RuBP) to phosphoglycollate, in an alternative reaction to its photosynthetic role of carboxylation of RuBP to 3-phosphoglycerate (3-PGA). Under conditions of moderate to high light intensity, high O_2:CO_2 ratios in the chloroplast can lead to high rates of the oxygenation reaction, resulting in the production of glycollate: a net loss of two carbon atoms from photosynthesis. This glycollate is transported to the peroxisome where it is oxidised to glyoxylate, which is in turn transaminated to glycine. The glycine then passes to the mitochondrion where two molecules are converted to one molecule of serine, with a net loss of one molecule of carbon dioxide and one molecule of ammonia. This process results in the reassimilation of up to three quarters of the carbon lost from photosynthesis, but also leads to the production of considerable amounts of ammonia which must be reassimilated by the GS-GOGAT cycle (Keys *et al.*, 1978; Givan *et al.*, 1988; Lea *et al.*, 1990). It has been estimated that in C3 plants the rate of flux of nitrogen through the photorespiratory nitrogen cycle is 10-fold greater than through primary assimilation (Miflin *et al.*, 1980).

Senescence and nitrogen remobilisation during germination

Far from being the passive decay of plant tissues, senescence is a highly controlled process involving the co-ordinated breakdown of cell components and their remobilisation to other parts of the plant (Feller and Fischer, 1994). Thus, a senescing organ becomes a source of nitrogen compounds for transport to other sinks such as developing grains or tap roots and tubers. A high percentage of cellular nitrogen is bound as phloem-immobile protein, which cannot be exported without first being broken down. The deamination reactions that effect this result in the release of ammonium, which must be reassimilated by GS. Glutamine itself is a common amino acid used for nitrogen transport, or it may be further metabolised to other phloem-mobile amino acids such as asparagine, glutamate or aspartate for transport (Pate *et al.*, 1979; Joy, 1988).

At the sink organ, some of these nitrogen transport compounds are in turn catabolised to release their nitrogen for use in the sink tissue. For example, asparagine is deaminated by asparaginase in developing *Nicotiana* and *Lupinus* seeds (Grant and Bevan, 1994), and ureides such as allantoin and allantoic acid which are the major transport compounds in tropical legumes must be catabolised to release their nitrogen (Joy, 1988). Each of these reactions releases ammonia, which can then be reassimilated by the GS-GOGAT cycle.

During germination, a similar process of nitrogen remobilisation occurs, as seed storage proteins are broken down again to phloem-mobile amino acids, which can then be sent to the developing seedling. Cotyledons of developing seedlings often show high levels of GS activity, primarily to cope with this high turnover of protein (Vézina and Langlois, 1989; Elmlinger and Mohr, 1992; Watanabe *et al.*, 1994).

Lignin biosynthesis

Lignin, a major structural component of the cell wall, is a high molecular weight polymer of phenylpropane. The pathway of lignin biosynthesis involves the conversion of L-phenylalanine to *trans*-cinnamic acid by phenylalanine ammonia lyase, a process that results in the evolution of ammonia (Goodwin and Mercer, 1986).

Thus, within the plant, GS is required to assimilate the ammonia arising from a number of different, sometimes spatially and sometimes temporally separated sources.

1.1.4 GS Structure and cellular compartmentalisation

Glutamine synthetase of higher plants is an oligomeric enzyme assembled from eight similar or identical subunits of M_r 38,000-45,000 into a native enzyme of M_r 350-400 kDa (Stewart *et al.*, 1980). The enzyme was categorised into two main isoforms, GS1 and GS2, based on the order of their elution from ion exchange columns (Mann *et al.*, 1979; McNally and Hirel, 1983) and it was demonstrated by subcellular fractionation that GS1 was the cytosolic isoform and GS2 was the chloroplast or plastidic isoform (Guiz *et al.*, 1979; Hirel and Gadal, 1980; Wallsgrove *et al.*, 1980; Barratt, 1981; Ochs *et al.*, 1995). The subunit of the plastidic isoenzyme was generally reported to be larger than the cytosolic one (43-45 kDa for the plastidic; 37-43 kDa for the cytosolic), allowing their separation by SDS-PAGE (McNally and Hirel, 1983). Charge differences also allowed separation of the two isoenzymes by ion exchange chromatography (Mann *et al.*, 1979), GS1 traditionally being seen to elute at a lower KCl concentration than GS2. These data were, however, based on the analysis of very few species, mainly *P. vulgaris*, *Pisum sativum* and *Nicotiana tabacum* (Forde and Cullimore, 1989), and more recent work has suggested that extrapolation from these species to a broader range of species is invalid. In studies of GS isoforms from a number of different species, Woodall and co-workers (1996a, b) have found that in some species, such as *Pinus sylvestris*, the chloroplast form can elute first in ion exchange, with the second peak being cytosolic. Furthermore, the distinction based on the electrophoretic mobility of the subunits may also be invalid. They identified two species which did not fit into the traditional GS1/GS2 classification: the chloroplast subunit of *Trientalis europaea* appears to be composed of a subunit of M_r 39,000 (the smallest of the subunits seen in this species) with the cytosolic form being composed of a mixture of subunits of M_r 40,000 and 44,000 (Woodall *et al.*, 1996b). Similarly they have found only one GS peak in *Pyrola media*, which is chloroplast-derived and composed only of subunits of the smaller type (Woodall *et al.*, 1996a).

In the light of these recent findings, it is evident that care must be taken in analysing the results of ion exchange separations of GS, and these data need to be backed up with western blotting experiments and more detailed subcellular fractionations.

Chloroplast and plastidic GS

A survey by McNally and co-workers (1983) of GS isoforms from the leaves of a number of different plant species from contrasting habitats indicated four distinct patterns of isoenzyme distribution; (a) a group of achlorophyllous plant parasites from which only GS1 could be isolated, (b) plants which possessed only GS2, (c) plants in which GS2 was the predominant form but which also had small amounts of the cytosolic enzyme, and (d) plants which had high levels of both GS1 and GS2. Other early work on the separation of GS into different isoforms suggested that GS2 was present only in green tissues as it could not be detected in roots (Suzuki *et al.*, 1981; McNally and Hirel, 1983). However, it is now known also to be present in the root plastids of many species, including *Lotus corniculatus*, *P. sativum*, *Vicia faba*, *Medicago media*, *H. vulgare* and *Zea mays* (Emes and Fowler, 1974; Miflin, 1974; Barratt, 1981; Emes and Fowler, 1983; Vézina *et al.*, 1987; Vézina and Langlois, 1989; Woodall and Forde, 1996), although not in most tropical legumes (Woodall and Forde, 1996).

In the majority of species studied so far, only one form of GS2 is evident from SDS-PAGE analysis, but 2D electrophoresis has in many cases revealed a number of charge variants. Four charge variants have been reported in *N. tabacum*, *P. sativum*, *P. vulgaris*, *H. vulgare*, *Lotus* species and *Beta vulgaris* (Lara *et al.*, 1984; Nato *et al.*, 1984; Tingey *et al.*, 1987; Mäck and Tischner, 1994; Woodall, 1994; Mäck, 1995), whilst two appear to be present in *Sinapis alba* (Höpfner *et al.*, 1991), and only one in *Nicotiana plumbaginifolia* and *Spinacia oleracea* (Ericson, 1985; Tingey and Coruzzi, 1987). Nato and co-workers (1984) reported that these charge variants in tobacco were due to glycosylation, but later studies have found no evidence for this in *P. sativum*, *N. plumbaginifolia*, *S. oleracea* or *Lotus japonicus* (Ericson, 1985; Tingey and Coruzzi, 1987; Tingey *et al.*, 1987; Woodall, 1994).

The enzyme from *P. vulgaris* appears as a doublet on SDS-PAGE, arising from the use of two distinct cleavage sites by the processing peptidase that removes the N-terminal transit peptide from the subunit precursor (Lightfoot *et al.*, 1988). A doublet has also been reported for GS2 in chloroplasts of *Brassica napus* (Ochs *et al.*, 1995). Mäck and Tischner (1990) present intriguing evidence that GS2 in

chloroplasts of *H. vulgare* exists as a tetramer as well as an octamer. The octamer is homomeric, whereas the tetramer consists of four charge variants. This is the first such report for plant GS, although there are other examples from mammals and fungi (Mäck and Tischner, 1994).

In an extensive study of 55 legume species, Woodall and Forde (1996) found a strong correlation between species climatic origin and the presence in the root of a form of GS consistent in size with the expected plastid isoform, with all temperate species tested exhibiting this phenomenon, but the great majority of tropical species lacking it. They suggest that this may point to a more general adaptation towards root assimilation of nitrate in temperate species, and shoot assimilation in tropical species. However, in the light of the more recent work by Woodall *et al.* (1996a) already discussed, it is no longer clear whether the larger subunit seen in the roots of the temperate legumes was in all cases GS2, further complicating the interpretation of their findings.

Cytosolic GS

Lara and co-workers (1983) found that GS1 from root nodules of *P. vulgaris* could be resolved by ion exchange into two distinct isoforms, one which was chromatographically indistinguishable from the root cytosolic form, and one which was unique to the nodule. Work on the genetic basis of this and studies in many other species has shown the existence of multiple isoforms of GS1 in different tissues to be common (Lam *et al.*, 1996). However, the classification of GS1 into distinct isoforms based on the distribution of variants of the holoenzyme is somewhat misleading, since it is known to be assembled from a number of distinct polypeptide subunits which in many species are differentially expressed spatially and developmentally in the plant (Forde and Cullimore, 1989). Thus, the holoenzyme can be composed of varying proportions of the different subunits in different parts of the plant and at different stages of development, and a specific 'isoform' often really consists of a range of heterooctamers, rather than being homogeneous. The precise complement of these subunits varies considerably between species, and a review of these follows in the next Section.

1.1.5 Molecular basis for isoforms

Plastidic GS

All studies to date indicate that a single gene encodes the plastidic form of the enzyme, with charge and size variants of the subunits arising from post-translational modifications and/or variations in transcriptional start site or transcript splicing as described above (see Section 1.1.4).

Cytosolic GS

In *Phaseolus* species

In *P. vulgaris*, one of the plant species most extensively studied to date, there are three isoforms of GS1 subunit; α, β and γ, these being located mainly in leaf and root, root and nodule, and nodule respectively (Forde and Cullimore, 1989). Equal amounts of the β and γ subunits have been shown to be present in the nodule (Cullimore *et al.*, 1984), and isoforms corresponding to the nine different possible combinations of the β and γ subunits ($\beta_8\gamma_0$- $\beta_0\gamma_8$) appear to be present in *P. vulgaris* and *P. lunatus* nodules, indicating that the subunits can assemble in any ratio (Robert and Wong, 1986; Cai and Wong, 1990). One-dimensional native and two-dimensional SDS-PAGE studies on GS from nodules of the Tepary bean, *Phaseolus acutifolius*, indicate that its GS subunits can indeed assemble in any ratio into a heterologous native holoenzyme (Green and Wong, 1992).

Studies in *P. vulgaris* have revealed that the subunits in this species are encoded by a small gene family. Cullimore and co-workers (1984) identified a cDNA clone from a library prepared from root nodules and showed by hybrid-select translation studies that it encoded a GS-like protein. The clone (later assigned to the *gln*-γ gene) was also shown to hybridise at different stringencies to mRNA species of different electrophoretic mobilities from leaves and roots, suggesting a multigene family that was differentially expressed in different tissues of the plant. Subsequently two more cDNAs (corresponding to the *gln*-α and *gln*-β genes) were identified from a root cDNA library which were similar to, but distinct from, *gln*-γ cDNA (Gebhardt *et al.*, 1986), and a cDNA encoding a chloroplast form (*gln*-δ) was also isolated (Lightfoot *et al.*, 1988). The *gln*-α and *gln*-γ cDNAs have been expressed in *E. coli* mutants lacking GS and shown to complement this mutation, providing clear evidence that

they encode functional GS subunits (Bennett and Cullimore, 1990). Later work by Bennett *et al.* (1989) showed that the *gln-γ* mRNA is present in stems, petioles and green cotyledons in addition to nodules, but at much lower levels. Studies in which the promoter regions of the *gln-γ* and *gln-β* genes were fused to the GUS reporter gene confirmed these expression patterns in transgenic *L. corniculatus* (Forde *et al.*, 1989). They also demonstrated for the first time that the two genes are expressed in very different spatial patterns within the nodule. While the *gln-γ* gene was expressed primarily in infected cells, the *gln-β* gene was expressed most strongly in the vascular region of the cortex which surrounds the infected zone. This was later confirmed by dissection of *P. vulgaris* nodules (Chen and Cullimore, 1989).

It is now generally accepted that the cytosolic subunits arise from differential expression of these three distinct genes: *gln-α* is expressed in leaves and roots, *gln-β* in leaves, roots and nodule cortex, and *gln-γ* primarily in the infected cells of the nodule, although with a low level of expression in stems, petioles and green cotyledons (Bennett and Cullimore, 1989). A single gene, *gln-δ*, has been shown to encode the chloroplast subunits (Lightfoot *et al.*, 1988), and thus the existence of four distinct subunit variants is likely to arise from post-translational modifications. A final gene, *gln-ε* has been found (Forde *et al.*, 1989), although no gene product has yet been demonstrated (B. G. Forde, personal communication).

In Other Legumes

There are considerable differences between legume species with respect to the expression of GS1 within the root nodule. Nodule-specific or enhanced genes analogous to *gln-γ* have also been reported in *Glycine max*, *Lupinus angustifolius*, *Lupinus luteus* and *Vigna aconitifolia* (Sengupta-Gopalan and Pitas, 1986; Boron *et al.*, 1989; Grant *et al.*, 1989; Lin *et al.*, 1995). These have been correlated with isoenzyme studies for *L. angustifolius* and *G. max*, but the data for *L. luteus* and *V. aconitifolia* are based solely on DNA sequence homologies and further work has yet to be done to validate this at the protein level. Recent work by Temple and co-workers (Kunjibettu *et al.*, 1996; Temple *et al.*, 1996) on GS from nodules of *G. max* has established it to be very similar to *P. vulgaris*, in that there is expression of both nodule- and root-type subunits in the same cells, resulting in heterooctamers

composed of both types of subunit. In addition to expression of the nodule-specific subunit in *G. max*, there is also strong enhancement of expression of the root subunit during nodule development (Hirel *et al.*, 1987).

In contrast to the species mentioned above, *P. sativum* expresses three cytosolic subunit types which are encoded by separate genes, each of which is expressed in all tissues, and none of which is nodule-specific. The increase in GS activity in *P. sativum* nodules is achieved by increased expression of all three cytosolic subunits (Tingey *et al.*, 1987; Walker and Coruzzi, 1989). Similarly, in *Medicago sativa* and *M. truncatula*, the increase in GS activity in nodules may be achieved by increased expression of one or more subunits also present in the rest of the root (Stanford *et al.*, 1993; Temple *et al.*, 1995b).

In addition to this interspecific variation in GS expression, in some cases there is also evidence for considerable quantitative differences in nodule GS between cultivars of the same species. The specific activity of GS in nodules of *V. faba* has been shown to differ by up to 65% between cultivars (Caba *et al.*, 1994). It should, however, be noted that this study did not address the question of whether there were any qualitative differences in nodule GS between cultivars, and no subunit separation data are available to ascertain the molecular basis for this. Conversely, *M. sativa* appears to be much less variable, with smaller differences between different genetic lines (Groat *et al.*, 1984).

<u>In Non-legumes</u>

The existence of multiple isoforms is by no means restricted to legumes. For example, *Z. mays* has been shown to express five distinct genes for putative GS1, each of which exhibits a different pattern of expression (Li *et al.*, 1993). Although these genes have yet to be correlated with their polypeptide products, studies by other groups have identified distinct cytosolic isoenzymes in *Z. mays*. The pedicel region, for example, appears to express a novel isoform which is different in DEAE-Sephacel elution characteristics from either leaf GS2 or root GS1 (Muhitch, 1989). Li and co-workers did not examine expression of the transcripts they found in this region, so it is unclear whether or not one of the mRNA species they identified encodes this isoform. A novel root isoform which is chromatographically distinct has also been

identified (Sakakibara *et al.*, 1992a). Again, this study failed to identify from four different mRNA species one which showed the same pattern of expression, and clearly more work is needed to correlate genetic and protein data.

Z. mays is a C4 plant, and exhibits two distinct patterns of ammonia production due to the spatial separation of photorespiration and nitrate assimilation in the mesophyll and bundle sheath cells respectively. This may partly explain why a number of different GS isoforms exist in this species, but a number of non-legume species which have C3 metabolism have also been shown to express a number of different GS isoforms in the cytosol. In *B. vulgaris* seedlings, two isoforms have been identified depending on plant age (Mäck and Tischner, 1994) and more may be present (Mäck and Tischner, 1990). There is genetic evidence for three cytosolic subunits in *Arabidopsis thaliana* which are differentially expressed at the mRNA level in leaves, roots and germinating seeds (Peterman and Goodman, 1991). Only one GS1 isoform has so far been isolated from *Helianthus annuus*, (Cabello *et al.*, 1991; Cabello *et al.*, 1994) and similarly, only one isoform has been detected in *L. esculentum* at the protein and RNA levels (Cánovas *et al.*, 1984; Cánovas *et al.*, 1986; Pérez-García *et al.*, 1995). One species, *S. alba*, appears to have no GS1 at all. Here, GS2 is present in all tissues, and only a single gene encoding this has been detected (Höpfner *et al.*, 1991).

In general under normal physiological conditions, these studies have found that the amount of GS1 in green tissues is much lower than that of GS2, with the opposite often being true for roots. Furthermore, in *N. plumbaginifolia* there is no detectable GS1 in leaves, although very low levels of mRNA may be present (Tingey and Coruzzi, 1987). The situation is often different during senescence, either natural or pathogen-induced, where the plastids are broken down, and GS1 may well be induced, perhaps to compensate for the loss of the GS2 and cope with the remobilised nitrogen (Bernhard and Matile, 1994; Feller and Fischer, 1994; Watanabe *et al.*, 1994; Pérez-García *et al.*, 1995). Immunolocalisation of GS1 has added to the evidence that at least some of it is specifically associated with the vascular system, implicating it in phloem loading and transport (Carvalho *et al.*, 1992; Pereira *et al.*, 1992; Becker *et al.*, 1993).

1.1.6 Nutritional regulation

Superimposed on the developmental pattern of GS regulation, there are likely to be mechanisms within the plant whereby its activity is regulated by substrate availability and product repression. As pointed out by Stewart et al. (1980), almost any endogenous nitrogen-containing compound can be considered to be an end-product of nitrogen assimilation and may inhibit GS activity *in vivo*, but the significance of such compounds has not been established. There are a number of potential candidates for GS induction. In the pathway of nitrate assimilation, nitrate itself might be expected to regulate GS activity, as might nitrite, although levels of nitrite are usually kept very low. Parameters affecting nitrogenase activity such as the oxygen status of the nodule are indicators of its nutritional status, and in green tissues, photosynthetic status acts as an indicator for the amount of photorespiration that might be expected to occur. As previously stated, each of these processes ultimately results in the release of ammonium which is the common substrate and thus a strong candidate for the regulation of GS.

Both NR and NiR are induced by nitrate (Redinbaugh and Campbell, 1991; Pelsey and Caboche, 1992), as are a number of other physiologically related processes such as nitrate uptake (Redinbaugh and Campbell, 1991). In the case of NR, mRNA has been detected in the leaves of tobacco seedlings within minutes of nitrate treatment, with protein being detected after a few hours (Galangau *et al.*, 1988). Thus, the response of GS to nitrate is of significant interest. As NiR is located in the plastid, work has focused on GS2, although there is also evidence that GS1 may be sufficient for the assimilation of ammonium from primary assimilation (Woodall and Forde, 1996).

The distinction should if possible be made between those enzymes for which the gene is modulated as a primary response to nitrate and those that are a secondary response. As defined by Redinbaugh and Campbell (1991), primary response genes are those which are activated rapidly (in minutes), specifically (a limited number of genes are affected), and directly (not requiring protein synthesis), whereas secondary response genes require new protein synthesis for their expression.

In green tissues

It is well established that light is the major factor regulating the expression of the GS2 in chloroplasts, whilst having little effect on GS1 (Schmidt and Mohr, 1989; Elmlinger and Mohr, 1992). This is thought to be a phytochrome-mediated response rather than a nutritional one (Becker *et al.*, 1992), although there is evidence that it may also be a response to changes in chloroplast metabolism (Edwards and Corruzzi, 1989; Peterman and Goodman, 1991). Elevated CO_2, which suppresses photorespiration, causes a decrease in mRNA for GS2 in *P. sativum* and *P. vulgaris* whilst having no effect on GS1 mRNA levels (Edwards and Corruzzi, 1989; Cock *et al.*, 1991). In these two examples, the effect was not seen until 7-14 d after the treatment began, suggesting a secondary response rather than a direct effect of photorespiratory ammonia. In contrast, Woodall and co-workers (1996a) observed a much more rapid decrease in GS2 activity of *H. vulgare* and *P. sativum* when photorespiration was reduced by a controlled decrease in ambient temperature. Other indirect evidence linking GS and photorespiration comes from *Z. mays* where GS2 has been shown to exhibit a light-mediated increase in activity in bundle sheath cells but not in mesophyll cells, corresponding with the location of the photorespiratory apparatus (Sakakibara *et al.*, 1992b).

In roots

A certain amount of care must be taken in the interpretation of studies published to date on the effects of nutritional parameters on GS in roots. Peat and Tobin (1996) have recently shown that GS isoform composition, total activity levels and response to nitrogen nutrition can vary with root age and developmental stage, and this may make it difficult to compare earlier studies which did not take this into account. Their study also points toward the possibility that GS may be present in both active and inactive forms: immunocytochemical localisation of GS in *H. vulgare* roots revealed a discrepancy between GS activity levels and amounts of GS protein detected. Plants grown without a nitrogen source appeared to have higher densities of immunogold labelling but less GS activity, suggesting that GS is actively synthesised in plants grown without a nitrogen source, but in an inactive form which can subsequently be rapidly activated when needed. In this respect it is particularly interesting that GS1

has very recently been identified as a target for binding to 14-3-3 proteins (C. MacKintosh, personal communication). 14-3-3 proteins are known to be involved in the post-translational regulation of both nitrate reductase and the plasma membrane protein pump (Huber *et al.*, 1996; Moorhead *et al.*, 1996; MacKintosh, 1997).

By ammonium

There is conflicting evidence on the possible induction of GS in the root by ammonium. Cock and co-workers (1990) found no evidence of induction in *P. vulgaris*, whereas in *G. max* the abundance of GS mRNA noticeably increased within 2 h and had reached levels comparable with that of the nodule within 8 h when nitrogen-starved plants were treated with 5 mM ammonium; an effect which was not seen by Hirel and co-workers when they treated plants with 10 mM nitrate (Hirel *et al.*, 1987). The gene in *G. max* was cloned by direct complementation of an *E. coli* mutant and promoter::GUS fusions used to determine its pattern of expression and regulation (Miao *et al.*, 1991; Marsolier and Hirel, 1993). This work showed the promoter to be up-regulated threefold in transgenic *L. corniculatus* by 10 mM ammonium, but there was no effect in transgenic *N. tabacum*, possibly indicating that the promoter needs a leguminous background for proper function (Marsolier *et al.*, 1993). Temple and co-workers (1996) have recently shown that this root GS gene is expressed at higher levels in nodules, but the increase in expression is dependent on N_2 fixation (see below), providing further evidence that it is ammonium-induced.

By nitrate

To a certain extent, whether a species would be expected to show nitrate induction of GS in the root will be determined by its site of nitrate reduction. Some plant species assimilate the majority of the nitrate they receive in the root, and thus would be expected to show some form of induction; others tend to transport nitrate to the shoot before it is assimilated, and consequently would not be expected to show this pattern of induction (Woodall, 1994).

In root tissues of plants growing on nitrate, ammonia is primarily derived from the assimilation of nitrate by NR, which is located in the cytoplasm, and NiR, which is plastidic. In *V. faba* roots treated with nitrate, there was reported to be an isoform with the same characteristics as leaf GS2, and which is absent in ammonia-grown

plants (Barratt, 1981). Similarly, *P. sativum* plants show a specific increase in root GS2 protein and activity in nitrate-grown plants as compared to ammonium-grown controls (Emes and Fowler, 1983; Vézina and Langlois, 1989). A study in *Z. mays* showed the accumulation of root GS2 transcripts was unaffected by cycloheximide treatment. The cycloheximide concentrations used were sufficient to inhibit 85% of protein synthesis, preventing the accumulation of NR protein and thus indicating that the increase in abundance of GS mRNAs is a primary response (Redinbaugh and Campbell, 1993).

In the nodule infected zone

By ammonium

Direct measurement of the effect of ammonium on GS isoforms in nodules is difficult, as ammonium applied exogenously promotes nodule senescence (Chen *et al.*, 1990). However, a correlation between a nodule-specific increase in GS activity, protein and mRNA levels with the onset of N_2 fixation, and hence ammonium export from the bacteroids, is well documented in a number of species (Lara *et al.*, 1983; Sengupta-Gopalan and Pitas, 1986; Konieczny *et al.*, 1988; Egli *et al.*, 1989). This led to speculation that ammonium is the signal for the induction of GS in the nodule, but there is now good evidence that this is not the case. In *P. vulgaris* and *L. angustifolius* there is evidence that the nodule-specific subunit is primarily under developmental control as its presence has been reported prior to the onset of nitrogenase activity (Robertson *et al.*, 1975; Padilla *et al.*, 1987). Further evidence comes from studies of *nifA*$^-$ mutants of *Bradyrhizobium* strains infecting *G. max.* Infection with these mutants results in the formation of highly abnormal nodules which are incapable of fixing nitrogen, but which have been shown to express the nodule-enhanced form of GS despite this (Studer *et al.*, 1987; Temple *et al.*, 1996). Similarly, there is a specific increase in GS activity in nodules of *M. sativa* and *P. sativum* even when infected with *fix*$^-$ mutants of *Rhizobium meliloti* and *R. leguminosarum* respectively, despite the fact that these nodules do not fix nitrogen (Dunn *et al.*, 1988; Walker and Coruzzi, 1989). Cock and co-workers (1990) failed to demonstrate induction of GS mRNA by exogenous ammonium, nor did they find an effect on synthesis of the subunits themselves. In these studies, *gln-γ* was induced 2- to 4-fold more in *fix*$^+$ over *fix*$^-$ nodules, and in N_2/O_2 over Ar/O_2 air mixtures, suggesting that N_2 supply has a

quantitative effect on expression. Switching to Ar/O_2 atmospheres in one case led to an 85% reduction in the γ subunit. In contrast to this, high concentrations of CO_2 have been shown to significantly decrease expression of the γ subunit, whilst increasing the rate of N_2 fixation and nitrogenase activity (Ortega *et al.*, 1992). Thus both high and low nitrogenase activity (and hence rates of ammonium production) have been correlated to decreases in nodule-specific GS activity. This may suggest that it is the C/N ratio that is affecting nodule-specific GS levels, with an increasing C/N ratio correlating with a quantitative decrease in the amount of the nodule-specific subunit, and a qualitative shift to the root-specific form (Ortega *et al.*, 1992).

By nitrate

The effect of nitrate on a number of parameters of nodule metabolism has received much attention (Streeter, 1988; Vessey and Waterer, 1992; Parsons *et al.*, 1993). In general, nitrogenase activity is inhibited by nitrate, but the degree of inhibition is species-dependent. For example, 10 mM nitrate inhibited nitrogenase activity in *G. max* by 48% after 2 d, with complete inhibition by 7 d (Schuller *et al.*, 1986) whereas 20 mM nitrate had an inhibitory effect on nitrogenase activity in *Lupinus albus* within 24 h (Lang *et al.*, 1993) and 15 mM inhibited nitrogenase activity by 80% within 24 h in some *Vigna unguiculata* and *L. angustifolius* symbioses (Manhart and Wong, 1980). This is likely not to be a primary response: there is considerable evidence that in many species nitrate does not even enter the nodule to a very large extent (Sprent *et al.*, 1987; Mizukoshi *et al.*, 1995), but exerts its inhibitory effect by other means, such as affecting the oxygen tension within the nodule, a parameter which must be kept within strict upper and lower limits (Layzell and Hunt, 1990; Denison *et al.*, 1992; Denison and Kinraide, 1995). The effect also appears to be biphasic; the first few days of inhibition appear to be reversible when nitrate is removed or the oxygen tension is artificially rebalanced, whereas prolonged exposure to nitrate causes irreversible inhibition (Faurie and Soussana, 1993). There is also evidence from split root experiments that, whilst nitrate has a local inhibitory effect on nodule initiation and development, its effect on nitrogenase is systemic, implying a more complex feedback mechanism involving signals from the shoot (Carroll and Gresshoff, 1983; Arnone *et al.*, 1994).

Since nitrate has been shown to have an inhibitory effect on N_2 fixation, one might expect an analogous effect on GS. However the effect of nitrate on GS in the nodule is poorly documented. In *M. sativa*, 20 mM nitrate has been shown to lead to a 50% decrease in GS activity in the nodule region after 7 d, but both higher and lower concentrations had much less effect (Becana *et al.*, 1984). Schuller and co-workers (1986) failed to find any effect of 10 mM nitrate on GS activity in *G. max*, although 1 mM nitrate has been shown to cause a decrease in glutamine concentrations and a corresponding increase in glutamate in both the infected and the cortical regions of the nodule.

Nitrate probably has a secondary effect on GS activity, either through the decrease in nitrogenase activity, which is in turn regulated by as yet undetermined mechanisms, or as a result of the promotion of nodule senescence. Nitrate-induced nodule senescence is a very different response to natural nodule senescence, being more a stress response than a controlled breakdown and remobilisation process (Walsh, 1995). It is characterised by the loss of membrane integrity of bacteroids, conversion of leghemoglobin to a green, non-functional form, legcholeglobin, diversion of photosynthate away from the nodule and a general shut-down of the N_2 fixation apparatus (Sutton, 1983; Naisbitt and Sprent, 1993; Schubert, 1995).

1.1.7 The role of GS in nitrogen remobilisation

During leaf senescence, ammonium is released in the process of protein breakdown and amino acid remobilisation. The ammonium is reassimilated via GS and used in the synthesis of amino acids suitable for transport in the phloem, such as glutamine and asparagine (in temperate species) or the ureides allantion and allantoic acid (in tropical species; Feller and Fischer, 1994). GS1 is the most likely candidate for this role, since the chloroplast is rapidly broken down in senescent tissues, and hence GS2 activity rapidly lost. Evidence to support this has been documented both at the protein and mRNA levels. In deciduous trees, GS2 activity rapidly declines in the autumn, to be replaced by GS1 activity which increases from undetectable levels in midsummer to become the major isoform just prior to abscission in late autumn (Pearson and Ji, 1994). In *B. vulgaris*, a species that shows top senescence with the above-ground parts of the plant senescing as the tuber fills, GS1 activity increases in senescing

leaves whilst GS2 activity is lost (Mäck and Tischner, 1994). During senescence of the flag leaf of wheat, which expresses both GS1 and GS2 isoforms during most stages of development, GS2 activity decreases whilst GS1 activity persists during senescence and the remobilisation of nitrogen to the grain (Peeters and Van Laere, 1994). Interestingly, Downs and co-workers (1994a) found that these changes in GS profile could be seen in asparagus spears even after harvest, where GS2 dropped to below 20% initial activity within a few days whilst GS1 activity recovered to 80% of initial activity after a brief decrease.

At the molecular level, Berhard and Matile (1994) have found that the mRNA for one GS subunit is induced during senescence in *Arabidopsis thaliana* rosette leaves, and Watanabe and co-workers (1994) showed the abundance of mRNA for one form of cytosolic GS to be maximal during germination and senescence, both of which are periods of nitrogen remobilisation. GUS fusion studies in *N. tabacum* with the promoter from one of the GS1 clones isolated from *P. sativum* have shown it to direct expression to the phloem cells of the vasculature in leaves, stems and roots, and to the vasculature of the cotyledons and root tips of germinating seedlings, all tissues in which nitrogen remobilisation is an active process (Edwards *et al.*, 1990; Brears *et al.*, 1991). Similarly, immunocytolocalisation of the enzyme in rice leaves using antibodies specific to GS1 have shown it to be located mainly in the vascular bundles of the leaf blade, in keeping with a proposed role in nitrogen remobilisation and in contrast to the plastidic form, which was present mainly in the mesophyll cells (Kamachi *et al.*, 1992). The study also found that GS1 was present in both mature and senescent leaves, in contrast to GS2, which decreased in abundance during leaf senescence.

Vascular-located GS1 may well be of vital importance to the plant. A study which attempted to use antisense to down-regulate GS specifically in the vasculature of *M. sativa* plants, using the promoter for *A. thaliana* acidic chitinase which has enhanced expression in vascular tissues and also enhanced expression in root tissues, failed to generate any transformants (Temple *et al.*, 1995a). This probably indicates that down regulation in such a manner is lethal (or at least detrimental to regeneration), underlining the importance of GS in these tissues.

1.1.8 Is there a link between GS isoforms and their role in plant nitrogen metabolism?

It is clear from the above overview that the constantly changing ammonium pools that arise during different stages of development and in different physiological conditions are handled by modulation of the activity of a dynamic complement of GS isoenzymes. This complement of isoenzymes responds differentially to developmental signals and physiological parameters, with evidence that in some cases, individual isoforms play a specialised role in the assimilation of a specific, defined pool of ammonia, while other isoforms perhaps have a more generalised role. Investigations designed to determine these relative roles have focused in three main areas; (a) the study of GS mutants, (b) the use of antisense to artificially modulate GS activity, and (c) inhibitor studies with a number of potent GS inhibitors including methionine sulphoximine, tabtoxinine-β-lactam, and phosphinothricin. The following Section reviews this body of work.

1.2 Approaches to the inhibition and down regulation of GS activity

A popular approach to establishing the role and relative importance of a specific enzyme or isoform in a metabolic system is to attempt to down-regulate or inhibit its activity *in vivo*, and then to measure the effect of this loss of activity on metabolic and growth parameters. This Section reviews this approach as applied to the study of GS in plants.

1.2.1 Mutants

Mutants deficient in chloroplast GS activity have been identified in *H. vulgare* (Blackwell *et al.*, 1987; Wallsgrove *et al.*, 1987) based on the premise that such plants would show stress symptoms such as chlorosis in air, but would grow normally in high CO_2 (1%) atmospheres. This is because in air these mutants cannot reassimilate the C3 intermediates of the Calvin cycle which are lost as a result of photorespiration, leading to a considerable drain of photosynthetic products. Conditions of high CO_2 alleviate this problem because the CO_2 competitively inhibits RuBP oxygenase, the first step of photorespiration (Somerville and Ogren, 1979). Whilst this approach has proven successful for isolation of mutants deficient in GS2 and such mutants are now well characterised (Blackwell *et al.*, 1988; Freeman *et al.*, 1990), it is clearly not suitable for the identification of GS isoenzymes not involved in photorespiration.

As an alternative to the production and screening of mutants, Gao and Wong (1994) screened 104 cultivars of *P. vulgaris* and identified two that lacked the nodule-specific isoform. They did not report any other obvious effects on the phenotype of the plants due to this absence of the nodule-specific isoform. They found no examples of cultivars in which the root isoform was absent.

1.2.2 Antisense

For enzymes for which the gene has been cloned, a popular alternative to mutations has been antisense technology. In this approach, a cDNA transcript of the gene encoding the enzyme to be manipulated is introduced back into the plant in the reverse orientation, under the control of a strong (usually constitutive) promoter (Bourque, 1995; Stitt and Sonnewald, 1995). This results in transcription of the opposite, non-coding DNA strand of the introduced gene. The mechanism by which this effects down-regulation of the endogenous gene is at present unclear, although degradation of double-stranded RNAs by specific RNases is thought to be the main mechanism in stabley transformed plants (Moffat, 1991).

The antisense technique has been successful in a number of diverse systems (Bourque, 1995), but has had only limited success when applied to GS. In *N. tabacum* leaves, antisense *M. sativa* GS driven by the constitutive Cauliflower Mosaic Virus (CaMV) 35S promoter has been shown to lead to a 25-40% decrease in GS activity on a fresh weight basis, which was attributed to a reduction in the chloroplast form as the cytosolic form is not present at a significant level in these tissues (Temple *et al.*, 1993). However, in this case the decrease in activity could simply have reflected an effect on protein content in the two antisense lines, since total protein content per g fresh weight was reduced by 30%. In another study, the group failed to generate *M. sativa* and *L. japonicus* transformants in which antisense expression of this full-length *M. sativa* gene had any effect on cytosolic GS (Temple *et al.*, 1994). It seems likely that in this situation, where the transformants are genetically more closely related, antisense expression is lethal, the transformants succumbing to nitrogen starvation or ammonia toxicity during the regeneration procedure. The two cytosolic genes in *M. sativa* show significant sequence divergence at their 3' ends (Temple *et al.*, 1995b), and antisense expression of this

region of one of the genes was successful in specifically down-regulating its mRNA. Surprisingly, this was not reflected in the amount of cytosolic GS protein, which was unaffected. Similarly, root-enhanced expression of a full-length antisense construct in *M. sativa* (using the *A. thaliana* acidic chitinase promoter, see Section 1.1.7) caused dramatic decreases in transcript levels in all organs, and also a significant decrease in cytosolic GS protein in the nodule, but had no significant effect on GS protein in roots (Temple *et al.*, 1994).

The results of these studies indicate that, whilst antisense expression of GS can be successful in down-regulation of genes at the transcript level, the plant is often able to compensate for the effects of the transgene by as yet to be determined mechanisms. Possible candidates for this are regulation at the level of translation, modulation of holoenzyme assembly and/or turnover, compensatory effects of other isoenzymes, and responses to the altered nitrogen status of the plant (Temple *et al.*, 1994).

Studies such as those presented above also bring out an important drawback of the antisense approach to down-regulation of critical genes such as GS: transformants that express the antisense construct well may be non-viable, and thus selected against during the regeneration procedure.

1.2.3 Inhibitor studies

Methionine sulphoximine (3-amino-3-carboxypropylmethyl-sulphoximine; MSO)

Originally isolated as the toxic agent in zein preparations treated with nitrogen trichloride which caused convulsive fits in rabbits, and later as an antibiotic, MSO was found to be a potent inhibitor of GS (Bentley *et al.*, 1949). At low concentrations, MSO acts competitively with glutamate (Wedler *et al.*, 1980; Logusch *et al.*, 1989), but it is an irreversible inhibitor in the presence of metal ions and ATP due to phosphorylation *in vivo* (Meister, 1980).

Studies using MSO to inhibit GS were of crucial importance during the introduction and subsequent widespread acceptance of the GS-GOGAT cycle proposed by Miflin and Lea (1976) as the principle mechanism by which ammonia is assimilated in plants. The effect of MSO was studied in a wide and diverse variety of plant tissues

and, with very few exceptions, it was found that even low concentrations resulted in increases in free ammonia and decreases in soluble amino acids in the treated tissues (Lea and Ridley, 1989). The few exceptions to this rule were generally in lower plants where glutamate dehydrogenase (GDH) is thought to be important (Lea, 1991). MSO was also used to help establish rates of ammonia evolution as a result of photorespiration (Keys *et al.*, 1978), and thus its use has been instrumental in the elucidation of some of the key biochemical pathways involving GS.

Whilst MSO has been widely used and its effects on metabolism characterised, a certain amount of care must be taken in its use: it has been shown to inhibit γ-glutamylcysteine synthetase, the first step in glutathione metabolism (Griffith and Meister, 1978; Griffith and Meister, 1979). Furthermore, MSO is of little use in determining the relative importance of different GS isoenzymes, as it is non-selective for the different isoforms.

Tabtoxinine-β-lactam

The irreversible GS inhibitor, tabtoxinine-β-lactam (T-β-L), is the active component of tabtoxin, a dipeptide produced by *Pseudomonas syringae*, which is hydrolysed *in vivo* to yield T-β-L and threonine (Sinden and Durbin, 1968; Langston-Unkefer *et al.*, 1987; Lea, 1991). In the field, infection by toxin-producing strains of the pathogen causes circular lesions on a wide range of crops including *Z. mays*, *P. vulgaris*, *G. max* and *Avena sativa* (Lea, 1991). These symptoms are correlated with an increase in ammonia concentrations in the infected tissues. Using plants infected by *P. syringae*, it has been possible to study differential inhibition of specific isoforms of GS since it appears that not all isoforms are equally susceptible to inhibition by the toxin.

Knight and co-workers (1988) identified an *A. sativa* population that was tolerant to *P. syringae* infection. Cytoplasmic and chloroplast GS from leaves of these plants was found to be partially tolerant to T-β-L, whereas GS from roots was not. Surprisingly, infected plants grew better than controls, indicating perhaps that shoot assimilation of ammonium was more efficient in this species than root assimilation.

In another study, the same group found that infection of nodulated *M. sativa* by *P. syringae* completely inhibited root GS activity, but only reduced nodule GS activity by 50% (Knight and Langston-Unkefer, 1988). The striking effect of this abnormal change in the distribution of GS activity was that infected plants exhibited a near two-fold increase in plant growth, nitrogenase activity, and nodule weight and number. Furthermore, the effect was only observable in Tox^+ strains. This was a very significant result, which may have wide implications for the control of nodule carbon and nitrogen metabolism (Lea, 1991). Analysis of the nodules of these infested plants showed concentrations of ammonia in the tissues to be more than 30 times greater than controls. They also contained 50% more glutamate and only a fraction of the glutamine present in the controls: a situation consistent with a loss of GS activity.

The physiological basis of these observations is unclear, although it is likely to be due either to a disruption of the control and feedback mechanisms that operate in the legume-*Rhizobium* symbiosis, or to a change in nitrogen cycling within the plant (Knight and Langston-Unkefer, 1988). It has been suggested that nitrogenase activity may be regulated by the glutamine pool, as is the case with free-living bacteria, which respond to a decrease in glutamine concentration with an increase in the expression of nitrogenase (Oaks, 1992). This may be a direct response of the bacteroid fraction to glutamine concentrations or to a specific metabolite derived from glutamine (Gussin *et al.*, 1986). Alternatively, Parsons and co-workers (1993) have suggested that the nutrient status of the plant is sensed by the nodule as fluctuations in the concentrations of reduced nitrogen compounds (such as amino acids) in the phloem. The nodule then responds to a drop in the concentration of certain amino acids with a compensatory increase in nitrogenase activity. It would therefore be of considerable interest to know what was the effect of *P. syringae* infestation on the phloem sap composition. Unfortunately, an experiment such as that reported by Knight and Langston-Unkefer has limitations since infestation by the pathogen is difficult to achieve in a controlled way, and has proven difficult to repeat in other laboratories (J. V. Cullimore, personal communication).

Phosphinothricin (2-amino-methylphosphinyl-butanoic acid)

Phosphinothricin (PPT) is an irreversible inhibitor of GS produced by the fungus *Streptomyces hygroscopicus* (Ogawa *et al.*, 1973). It is also the active component of the tripeptide antibiotics bialaphos (L-phosphinothricyl-L-alanyl alanine), produced by *S. viridochromogenes* (Bayer *et al.*, 1972), and phosalacine (L-phosphinothricyl-L-alanyl leucine), produced by *Kitatosporia phosalacinea* (Õmura *et al.*, 1984a; Õmura *et al.*, 1984b). Bialaphos and phosalacine are not GS inhibitors in themselves, and must be broken down *in planta* to release PPT: Tachibana and co-workers (1986) demonstrated that bialaphos did not inhibit GS purified from shoots of *Echinochloa utilis* unless first incubated with cell free extracts. Similarly, Õmura (1984b) failed to inhibit purified GS from leaves of *Spinacia oleracea* with phosalacine without prior treatment of the antibiotic in a similar manner. PPT can be chemically synthesised and the ammonium salt (glufosinate ammonium) is marketed as a non-selective, post-emergence herbicide by AgrEvo under the trade names *Basta* and *Challenge*. The potent herbicidal effect of the compound has been demonstrated in many species (Ridley and McNally, 1985; Lea and Ridley, 1989) and it has the added advantage of being quickly broken down by soil microorganisms (Bartsch and Tebbe, 1989; Abell and Villafranca, 1991; Tebbe and Reber, 1991).

In addition to its agricultural and horticultural use as a herbicide, PPT has been used extensively in laboratory studies of GS inhibition. It has largely replaced MSO in this respect, as it is both more potent and does not have the same effect on glutathione metabolism (Lea and Ridley, 1989). PPT has for example been used in studies of the inhibition of GS on photosynthesis and respiration of both C3 and C4 plants (Wild *et al.*, 1987; Wendler *et al.*, 1990; Lacuesta *et al.*, 1992; Wendler *et al.*, 1992; Diaz *et al.*, 1995), to provide evidence against the assumption that the toxic effect of GS inhibition is simply the accumulation of ammonia (Downs *et al.*, 1994b; Downs *et al.*, 1994c), and to examine the effect of GS inhibition on nitrate reduction (Lacuesta *et al.*, 1993).

The discovery in some bacterial strains of resistance genes capable of detoxifying PPT has increased the scope of such experiments, and is described below.

1.3 Phosphinothricin resistance genes and their use in plants

1.3.1 The *bar* and *pat* resistance genes

The *Streptomyces* strains that produce bialaphos have also evolved genes that encode enzymes capable of detoxifying PPT. These genes encode PPT-*N*-acetyltransferases (PATs) which acetylate PPT to the inactive derivative, *N*-acetyl-phosphinothricin (Ac-PPT):

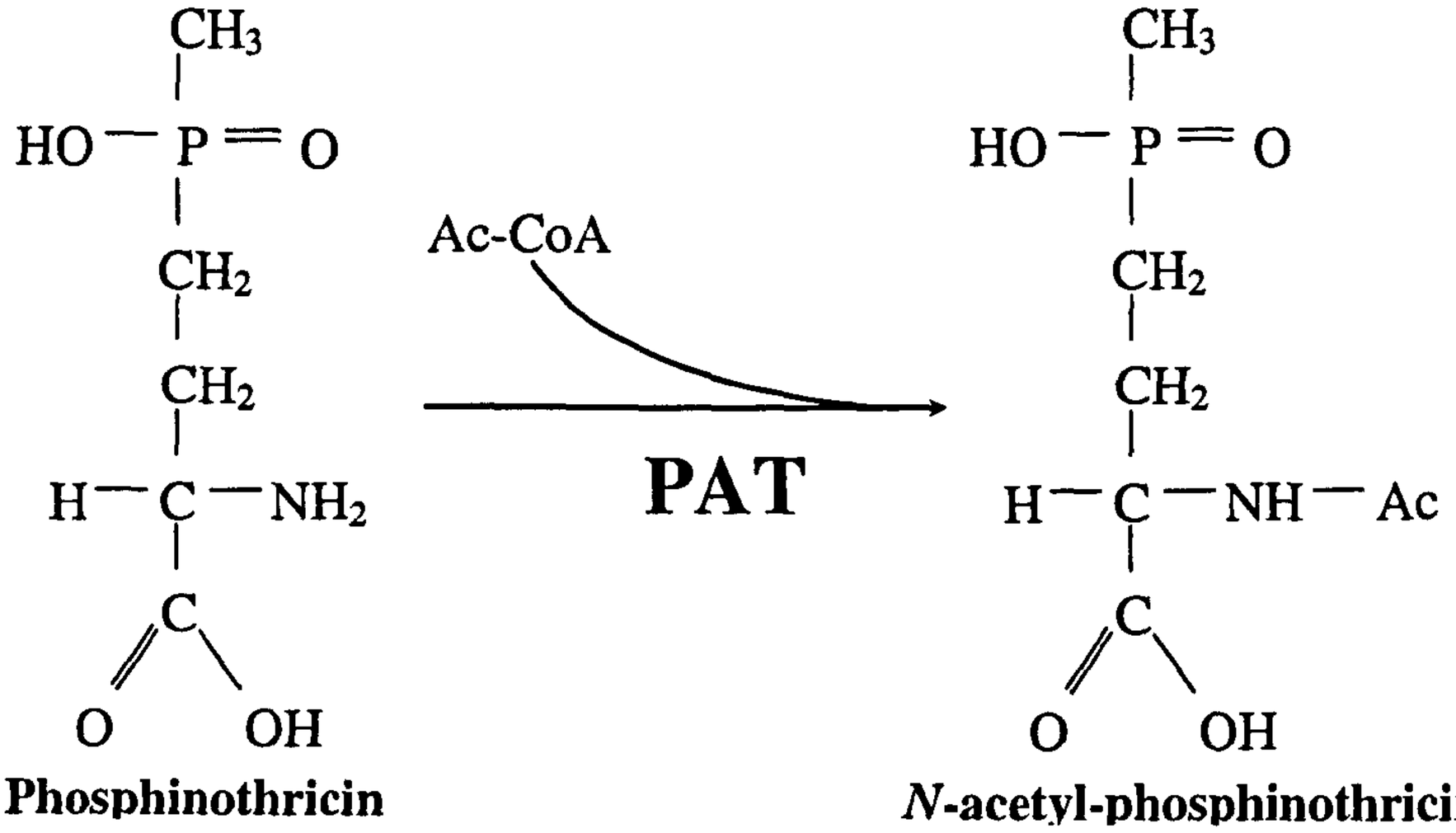

Figure 1.2: The acetylation of phosphinothricin by phosphinothricin-*N*-acetyltransferase

N-acetylation is a common way in which *Streptomyces* strains avoid self-toxicity from the antibiotic compounds they produce (Cundliffe, 1989). The bialaphos resistance gene (*bar*) from *S. hygroscopicus* and the phosphinothricin acetyl-transferase gene (*pat*) from *S. viridochromogenes* have been independently isolated and cloned (De Block *et al.*, 1987; Thompson *et al.*, 1987; Strauch *et al.*, 1988; Wohlleben *et al.*, 1988), and their products characterised (Botterman *et al.*, 1991; Vinnemeier *et al.*, 1995; Wehrmann *et al.*, 1996). They have 87% nucleotide identity and both encode polypeptides of 183 residues in length with 85% identity in their amino acid sequences (Fig 1.3a,b). Subsequently, a similar gene from another strain, *S. coelicolor*, was isolated and shown to encode a PAT, the amino acid sequence of which has about 30% identity to the *bar* and *pat* gene products (Bedford *et al.*, 1991).

1.3.2 PPT-resistant transgenic plants expressing PAT enzymes

Both *bar* and *pat* have been used successfully to engineer plant resistance to PPT. The *bar* gene has been used much more extensively than *pat*, although both genes are equally suitable for use in plants (Wehrmann *et al.*, 1996) and there is some evidence to suggest that the enzyme encoded by *pat* may be slightly more efficient *in planta* (Vinnemeier *et al.*, 1995). Transgenic *N. tabacum* plants expressing *bar* were the first example of the successful transfer of PAT to plants (De Block *et al.*, 1987), and subsequently, PPT resistance from *pat* expression was demonstrated (Wohlleben *et al.*, 1988). Since then, PAT-determined resistance to PPT has been demonstrated in a wide range of transgenic plant species of agronomic importance, and field trials have been successful with *Solanum tuberosum*, *M. sativa*, *B. vulgaris* and *Linum usitatissimum* (De Greef *et al.*, 1989; D'Halluin *et al.*, 1992a, b; McHughen and Holm, 1995). The majority of studies to date have concentrated on constitutive expression of PAT, although van der Hoeven and co-workers (1994) have demonstrated that root-specific expression is sufficient for herbicide tolerance in *N. tabacum*.

One area of research in which the *bar* and *pat* genes have shown particular promise has been in cereal transformation systems, where they have been used as a selectable marker. Traditional selectable markers such as kanamycin are not suitable for cereal transformation systems, since the plant material exhibits a high degree of natural resistance to the antibiotic (McElroy and Brettell, 1994). Successful gene transfer of *bar* to *Z. mays*, *Oryza sativa*, *H. vulgare* and *Secale cereale* has been demonstrated, and fertile transgenic plants regenerated (Cao *et al.*, 1992; Spencer *et al.*, 1992; Castillo *et al.*, 1994; Wan and Lemaux, 1994).

1.4 The ß-glucuronidase (GUS) reporter gene

Since its isolation in 1985 by Jefferson, the *uidA* gene, which encodes an *E. coli* β-glucuronidase (GUS), has become the most widely used reporter gene for transgenic research in plants (Jefferson, 1985; Guivarch *et al.*, 1996). The enzyme hydrolyses β-D-glucuronides (see Fig. 1.4), and much of its popularity has been due to the availability of a wide range of substrates, both quantitative such as the fluorogenic methyl-umbelliferyl glucuronide (MUG), and histochemical such as 5-bromo-4-chloro-3-indolyl-β-D-glucuronide (X-Gluc), the product of which is a blue precipitate

(Jefferson, 1987). The enzyme is very stable, with a broad pH range (pH optimum between 5.2 and 8.0 and 50% activity at pH 4.3), a half-life of 2 hours at 55°C, and retains activity for several days in the standard staining buffer (Jefferson, 1987; Wilson *et al.*, 1995). The fluorimetric assay can easily be carried out in a microtitre plate (Rao and Flynn, 1992). In addition there is a negligible amount of endogenous GUS activity in most tissues of the majority of plant species and GUS activity is also absent from many bacteria, including *Rhizobium*, *Bradyrhizobium* and *Agrobacterium* species (Wilson *et al.*, 1992). Thus it has been demonstrated to be suitable for use as a marker gene in studies of the expression of both plant and bacterial genes in root nodules (Forde *et al.*, 1989; Streit *et al.*, 1992; Marsolier *et al.*, 1995; Wilson, 1995; Wilson *et al.*, 1995; Andersson *et al.*, 1997).

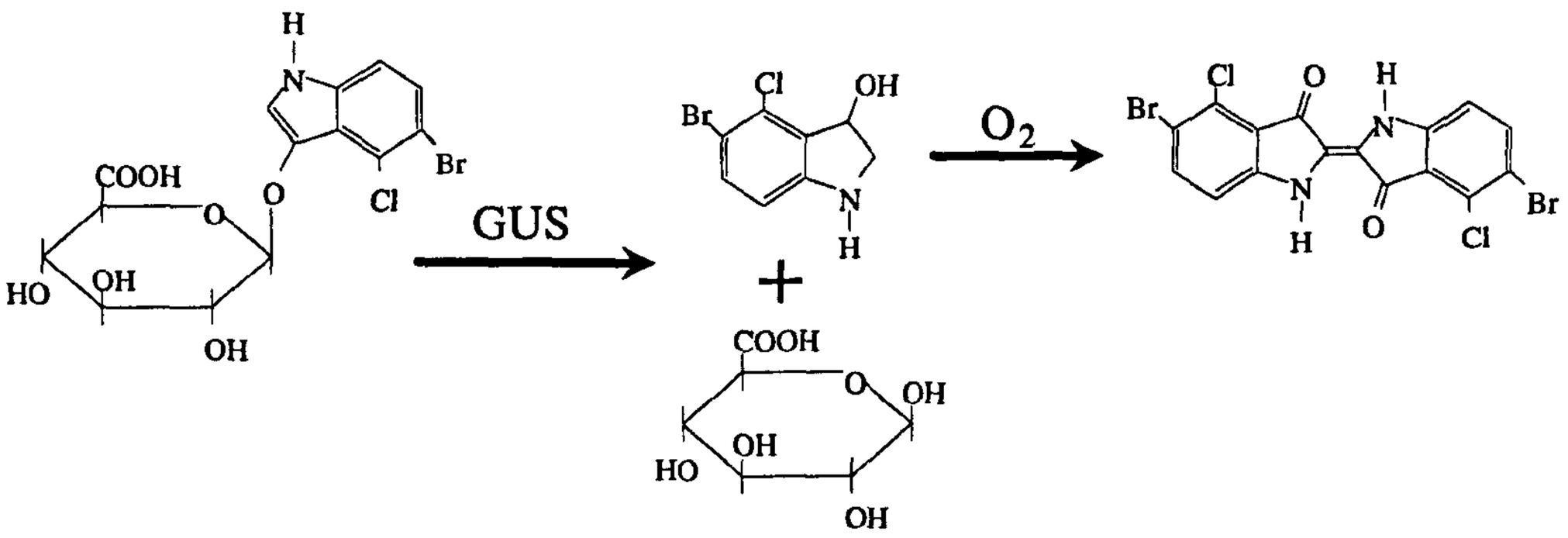

Figure 1.4: The most common histochemical assay for β-glucuronidase (GUS). 5-bromo-4-chloro-3-indolyl-β-D-glucuronide (X-Gluc) is hydrolysed by the enzyme to glucuronic acid and a soluble indoxyl intermediate that oxidises to form an insoluble indigo compound which is seen as a blue precipitate.

1.5 Translational fusions involving PAT and GUS

Prior to this work, both PAT and GUS enzymes had been shown to be capable of retaining activity when fused to foreign polypeptides. PAT from *S. hygroscopicus* has been shown to tolerate C-terminal extensions with no discernible effect on catalytic activity (Botterman *et al.*, 1991). Although no reports of such studies with the homologue from *S. viridochromogenes* exist to date, the high degree of homology between the two enzymes indicated that the *pat* gene product should also be amenable to such extensions. GUS has been shown to tolerate an N-terminal

fusion of 2 kDa (Jefferson, 1987), and has also been successfully fused via its C-terminus to the neomycin phosphotransferase II (NPTII) selectable marker enzyme, and shown to retain enzymatic activity (Datla *et al.*, 1991).

1.6 Aims of this thesis

As we have seen, none of the available approaches for manipulating GS activity *in planta* is ideal for use in physiological studies, particularly if we wish to inhibit the enzyme in both a tissue-specific and short-term manner. The aims of this thesis were therefore:

1. To develop a tool to facilitate the short-term or long-term manipulation of GS activity in specific tissues or organs of a plant.

2. To use this tool to investigate the role of the root GS isoform in the nitrogen metabolism of a N_2-fixing legume.

The first of these aims was pursued by constructing a novel gene fusion (*pat::uidA*) which would encode a bifunctional enzyme with both PAT and GUS activities (Chapter 3). It was hypothesised that this gene, when combined with a tissue-specific promoter, would be able to target PAT activity to selected plant tissues and to protect these tissues from inhibition of GS activity when the plant was treated with PPT. By combining PAT and GUS activity in one polypeptide it would be possible to use histochemical analysis to identify transgenic lines in which the PAT activity was correctly targeted. Many studies have shown that the expression pattern of a transgene can be influenced by its site of integration in the genome (Jones *et al.*, 1985; Hobbs *et al.*, 1990; Peach and Velten, 1991), so it was particularly important that the spatial localisation of the PAT activity could be confirmed in any transgenic lines that were to be used for physiological studies.

The second major aim was pursued by fusion of the *pat::uidA* gene to the nodule-specific *gln-γ* promoter (Forde *et al.*, 1989) in an attempt to generate transgenic *L. corniculatus* plants in which PAT activity was targeted to the infected zone of the nodule. It was hoped that this would make it possible to inhibit root GS activity without affecting nodule GS, so mimicking the tabtoxin experiments of Knight and

Langston-Unkefer (discussed in Section 1.2.3). Prior to using this approach to manipulate the distribution of GS activity between roots and nodules and to study its consequences (Chapters 5 and 6), it was considered important to undertake a detailed analysis of the GS isoenzymes and polypeptides and their spatial distribution in *L. corniculatus* (Chapter 4).

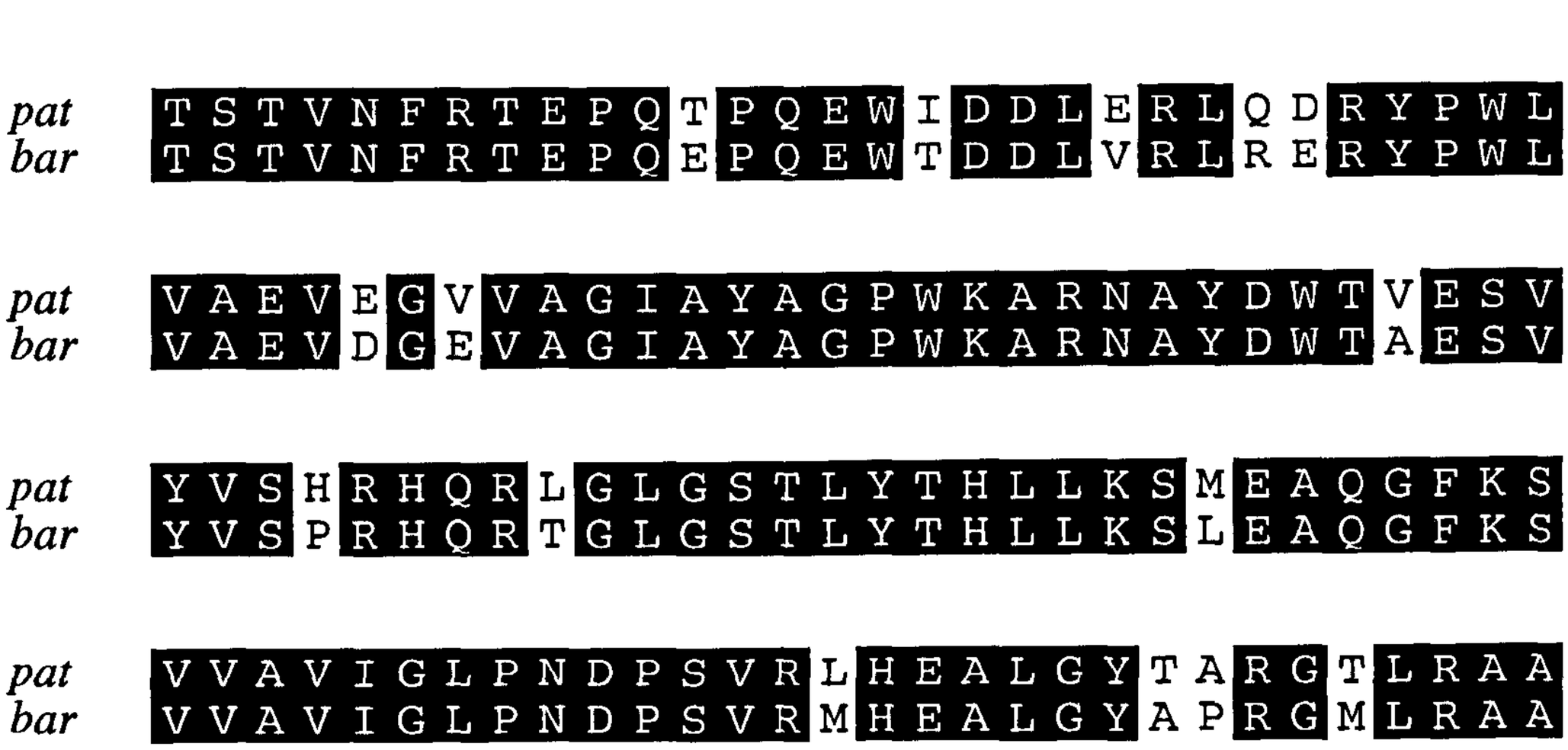

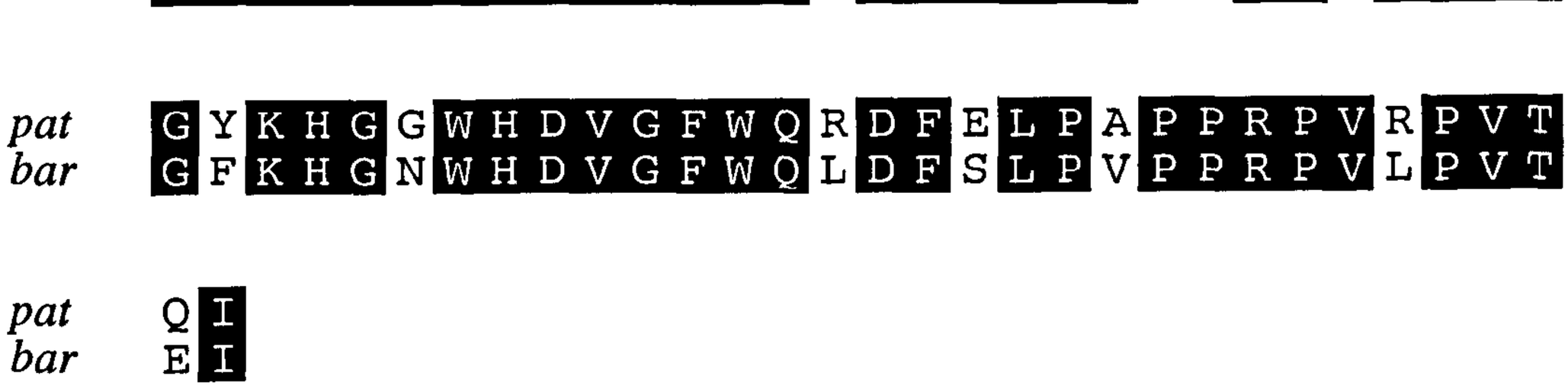

Figure 1.3a: Comparison between the *bar* gene of *Streptomyces hygroscopicus* and the *pat* gene of *S. viridochromogenes* - 1: Amino acid sequence. Homologous residues are shown in inverse type.

Figure 1.3b: Comparison between the *bar* gene of *Streptomyces hygroscopicus* and the *pat* gene of *S. viridochromogenes* - 2: Nucleic acid sequence. Homologous bases are shown in inverse type.

CHAPTER 2:

MATERIALS AND METHODS

2.1 Materials and equipment suppliers

All chemicals used in this thesis were purchased from Sigma (Poole, UK) or BDH (Merck Ltd., Poole, UK) unless otherwise stated. Radioactive nucleotides were supplied by Amersham International (Amersham, UK). Appendix I contains a list of suppliers used and their addresses.

2.2 Bacterial strains and plasmids

Unless otherwise stated, the *Escherichia coli* strain used for the propagation of plasmids in all experiments was XL1-Blue (Bullock *et al.*, 1987, supplied by Stratagene, Cambridge, UK). The *Agrobacterium rhizogenes* strain used for plant transformations was LBA9402 (Hooykaas, 1979) and the *Rhizobium loti* strain was NZP2037 (Chua *et al.*, 1985). Details of the plasmids used or generated in the course of this work can be found in Table 2.1.

2.2.1 Long-term storage

Glycerol stocks

E. coli cells were grown overnight at 37°C on LB agar, and *A. rhizogenes* for 2 d at 29°C on YMB (Table 2.2) containing the appropriate antibiotics (Table 2.4). A single colony was resuspended either in liquid LB (Table 2.2) in the case of *E. coli*, or 523 medium (Table 2.2) in the case of *A. rhizogenes*, and grown overnight at 37°C or 29°C respectively. Aliquots of 0.5 ml were dispensed into Nalgene 2 ml screw-topped vials (Techmate, Milton Keynes, UK) containing 0.5 ml of 40% (v/v) glycerol and quick-frozen in liquid nitrogen. Samples prepared in this way could be stored at -70°C for at least 12 months. On recovery from freezing, samples could be either re-streaked on agar plates, used to inoculate liquid cultures, or plasmids recovered directly using the miniprep procedure described in Section 2.5.1

Lyophilization

For very long-term storage of bacterial strains, cells were freeze-dried. Cultures were grown on agar plates as described above and then several colonies were removed and a suspension made in 300 mM sucrose, 50 $mg.ml^{-1}$ peptone, pH 6.8. Aliquots of 0.5 ml were transferred to small sterile glass vials (4 ml; Fisher, Loughborough, UK) containing a plug of non-absorbent cotton wool. Lyophilization was carried out overnight in an Edwards Modulyo freeze-drier according to the manufacturer's instructions and then the lid closed under vacuum and sealed with an air-tight rubber insert and an aluminium cap. Samples could be stored indefinitely at 4°C and recovered by resuspension in the appropriate liquid medium and streaking on agar plates.

2.3 Bacterial transformation

2.3.1 Preparation of competent *E. coli*

Competent *E. coli* cells were prepared using a method described by Alexander *et al.* (1984). An overnight culture was set up by inoculating 25 ml of 2XL broth (Table 2.2) with a single colony of XL1-Blue and grown overnight at 30°C with shaking at 300 rpm. A pre-warmed 100 ml culture was inoculated with 1 ml of overnight culture and incubated at 30°C with shaking at 300 rpm for about 60 min, until the OD_{600} of the culture had reached 0.2. At this point, 1 ml of 2 M $MgCl_2$ was added and the culture incubated for a further 40 to 50 min, until the OD_{600} had reached 0.45 to 0.55. The culture was then quick-cooled in ice-cold water and left on ice for 2 h. After chilling, the cells were pelleted by centrifugation at 7,000 *g* for 5 min at 4°C and the supernatant discarded. The cells were resuspended gently in 50 ml of sterile ice-cold Ca^{2+}/Mn^{2+} solution (40 mM Na^+ acetate, 100 mM $CaCl_2$, 70 mM $MnCl_2$, pH 5.5) and incubated on ice for 2 h. Cells were then pelleted at 5,000 *g* for 5 min at 4°C and resuspended very gently in Ca^{2+}/Mn^{2+} solution containing 15% (v/v) glycerol. Aliquots of 0.3 ml were dispensed into microtubes, quick-frozen in liquid nitrogen and could be stored at -80°C for up to 12 months.

2.3.2 *E. coli* transformation procedures

Standard method

High efficiency transformation of *E. coli* was achieved using the following protocol modified from the procedure described by Alexander *et al.* (1984). Frozen aliquots of competent cells prepared as described in Section 2.3.1 were thawed on ice, split into 50 µl aliquots and mixed with 2 to 5 ng of plasmid DNA in up to 25 µl of TE. The mixture was incubated on ice for 30 min and then heat-shocked by incubation at 30°C for 5 min. Immediately after the heat shock, 1 ml of 2XL broth pre-warmed to 37°C was added and incubated at 37°C for 45 min with shaking at 300 rpm. The cells were then concentrated by spinning at 4,000 *g* for 3 min in a microcentrifuge to pellet the cells, removing all but 100 to 200 µl of the supernatant, and resuspending gently in the remaining supernatant. The resulting cell suspension was then spread on an LB-agar plate (Table 2.2) containing appropriate antibiotics for selection of the introduced plasmid (Table 2.4).

Quick method

If the plasmid to be introduced had already been purified and characterised, and was available as a homogeneous mixture, then a less efficient but rapid heat-shock procedure could be used. A 3 µl aliquot of competent cells prepared as described in Section 2.3.1 was mixed with 1 µl of plasmid DNA (1 to 100 ng in TE) on ice. The mixture was heat-shocked for 1 min at 44°C and then 100 µl of 2XL broth immediately added and the cell suspension spread on a suitable selective agar plate.

2.3.3 Transformation of *Agrobacterium* by electroporation

Cultures of *Agrobacterium rhizogenes* were transformed with pBIN19 derivatives using the method described by Shen and Forde (1989).

Preparation of electrocompetent cells

A single colony of *A. rhizogenes* was used to inoculate a 100 ml culture of 523 medium (Table 2.2) and incubated at 29°C overnight with shaking at 300 rpm until the OD_{600} was between 0.5 and 0.7. The cells were subsequently quick-cooled on ice, and pelleted by centrifugation at 3,000 *g* for 10 min at 4°C. The supernatant was replaced with an equal vol of sterile ice-cold 10% (v/v) glycerol and the cells

resuspended in this. The cells were then pelleted and washed successively in 1, 0.5, 0.1, and 0.02 culture vol of sterile 10% (v/v) glycerol before finally being resuspended in 0.5 ml sterile 10% (v/v) glycerol. Aliquots of this were quick-frozen in liquid nitrogen and could be stored at -80°C for up to 6 months.

Electroporation

A 40 µl aliquot of cells prepared as described above was transferred to a pre-cooled 0.2 cm electroporation cuvette (Bio-Rad, Hemel Hempstead, UK) and mixed with 2 to 10 ng of plasmid DNA (in 0.5 to 2 µl TE). This was electroporated at 12.5 $kV.cm^{-1}$ with a capacitance of 25 µF and with a resistor of 400 Ω in parallel with the sample, in a Gene Pulser system (Bio-Rad). The sample was then immediately mixed with 0.96 ml YMB (Table 2.2), transferred to a sterile test tube with an aluminium cap and incubated at 29°C for 3 h with shaking at 250 rpm. The cells were then spread onto YMB plates containing the appropriate antibiotic for selection (Table 2.4), and incubated at 29 °C for 2 to 3 d.

2.4 Screening bacterial transformants

2.4.1 Blue/white selection of bacterial transformants

E. coli colonies transformed with derivatives of pUC19, pBIN19 and pBluescript were screened for inserts using the blue/white selection procedure described by Messing *et al.* (1977). The multiple cloning site in these vectors is located in the coding region of a gene, *lacZ*, which encodes for the α-polypeptide of β-galactosidase. Disruption of the *lacZ* gene by insertion of foreign DNA at the multiple cloning site disables production of β-galactosidase in *lacZ*⁻ strains of *E. coli*. Inactivation of the *lacZ* gene can be detected by a histochemical reaction in which clones with β-galactosidase activity (and without inserts) are coloured blue in the presence of the artificial chromogenic substrate 5-bromo-4-chloro-3-indolyl-β-D-galactopyranoside (X-Gal) and those lacking enzyme activity (with inserts) are white. Prior to plating the transformants (see Section 2.3.2), 50 µl of 2% X-gal (in N,N'-dimethylformamide) was spread onto the plate. After incubation as described in Section 2.3.2, blue colonies were clearly distinguishable.

2.4.2 Colony hybridization

Colony transfer and liberation of bound DNA

Filters carrying bacterial colonies ready for hybridization to radiolabelled DNA probes were prepared by the method of Grunstein and Hogness (1975). A nylon Hybond-N filter (Amersham) was placed on an LB-agar plate containing the appropriate antibiotic and up to 100 colonies were picked onto it using sterile cocktail sticks. The colonies were picked simultaneously onto a master plate, and both plates were incubated at 37°C (*E. coli*) or 29°C (*A. rhizogenes*) overnight. If the vector supported blue/white selection, then a single blue colony was also picked onto the plate as a negative control. The DNA was liberated from the colonies by wetting the filter twice with 0.5 M NaOH. This was done by pipetting 0.75 ml of 0.5 M NaOH onto a small sheet of cling film, placing the filter onto this and leaving at room temperature for 2 to 3 min. The procedure was then repeated twice with 1 M Tris-HCl, pH 7.4 for 5 min, and then once with 1.5 M NaCl, 0.5 M Tris-HCl, pH 7.4 for 2 to 3 min. The DNA was bound permanently to the filter by placing the filter on a paper towel moistened with transfer buffer (1.5 M NaCl, 0.15 M Na^+ citrate, pH 7.0), and crosslinking by irradiation with 120 mjoules.cm^{-1} of UV light at 254 nm in a Stratalinker Model 1800 (Stratagene), and stored at 4°C in 0.3 M NaCl, 30 mM trisodium citrate pH 7.0.

Probe radiolabelling by nick-translation

Radiolabelled probes were used to check for the presence of insert DNA in recombinant colonies. A nick translation kit supplied by Amersham International was used to label DNA with [α-^{32}P]-dATP. The reaction mixture contained 100 ng DNA, 20 µCi [α-^{32}P]-dATP, 3 mg.ml^{-1} BSA, 3 U of Klenow fragment, and 7 µl nick-translation buffer (as supplied in the kit), 20 µM dCTP, 20 µM dGTP and 20 µM dTTP, in a final vol of 50 µl. The reaction was incubated at room temperature for 2 h, after which the probe was purified from unincorporated nucleotides by passing through a Sephadex G-50 column (Pharmacia, St. Albans, UK) and collecting and pooling the fractions corresponding to the first radioactivity peak.

Hybridization

Since in all instances in this work, the probe was identical in sequence to the target DNA, all DNA hybridizations were carried out under high stringency conditions.

Filters were incubated in glass hybridization tubes (Techne, Duxford, UK) in prehybridization buffer (0.3 M NaCl, 30 mM trisodium citrate, 0.1% (v/v) Ficoll, 0.1% (w/v) PVP, 0.1% (w/v) BSA, 0.1% (w/v) SDS, 100 $\mu g.ml^{-1}$ herring sperm DNA) for 2 h at 65°C in a rotating hybridization oven (Techne). The probe was boiled for 5 min and added to the prehybridization mix and filters. Hybridization was carried out overnight at 65°C. Filters were washed 4 times in 50 ml of 0.3 M NaCl, 30 mM trisodium citrate, 0.1% (w/v) SDS; twice briefly and twice at 65°C for 30 min. Filters were wrapped in cling film and exposed to blue-light-sensitive X-ray film (X-Ograph, Wiltshire, UK) at -80°C in autoradiography cassettes containing intensifier screens for 4 h to 24 h depending on the strength of the signal. Autoradiographs were developed in an X-Ograph model X-2 automatic developer.

2.4.3 GUS assays on single colonies

Colonies of *E. coli* and *A. rhizogenes* could be screened for the presence of many plasmids containing the *uidA* gene by assaying for the presence of high levels of GUS activity. A toothpick was used to transfer a small portion of each colony into a microtitre well containing 200 µl of GUS grinding buffer (see Section 2.10.5). The microplate was incubated at 37°C for up to 24 h (although in some cases no incubation was necessary) and viewed on a UV transilluminator (see Section 2.5.6) for fluorescence. This technique worked well for plasmids in which the inserted gene was in the same orientation as the *lacZ* promoter.

2.5 Nucleic acid extraction and purification

2.5.1 Small-scale plasmid preparations

From E. coli

For routine preparation of plasmids from *E. coli*, Promega 'Magic Minipreps' were used as described in the manufacturer's protocol (Promega, 1991). In this system, alkaline cell lysates are applied to a silica-based column under high salt conditions in which the DNA binds to the column. After several high-salt washes, the DNA can be eluted from the column in an appropriate buffer.

From A. rhizogenes

A modification of the miniprep procedure of Birnboim and Doly (1979) was used for preparing plasmid DNA from *A. rhizogenes*. A single colony was used to inoculate a 50 ml culture of 523 medium (Table 2.2) with the appropriate antibiotic (Table 2.4) and grown overnight at 29°C. Cultures were cooled on ice and cells pelleted at 5,000 *g* for 5 min at 4°C. The pellet was resuspended in 200 µl of cell lysis solution (50 mM glucose, 10 mM EDTA, 100 µg/ml lysosyme, 25 mM Tris-HCl, pH 8.0) and incubated on ice for 60 min, prior to the addition of 400 µl of 0.2 N NaOH, 1% (w/v) sodium dodecyl sulphate (SDS). The tube was inverted 5 to 10 times to mix and then 300 µl of ice cold 3 M potassium acetate, pH 5.2 was added. The tube was vortexed for 10 s and then incubated on ice for a further 5 min. The debris was pelleted at 12,000 *g* for 10 min at 4°C and the supernatant recovered and extracted twice with phenol:chloroform:isoamyl alcohol (25:24:1). The DNA was precipitated with 2 vol of absolute ethanol and resuspended in 50 µl TE (10 mM Tris-HCl, pH 7.4, 1 mM EDTA). Plasmid DNA prepared in this way was suitable for restriction analysis to confirm that no rearrangements had occurred. If larger amounts of plasmid were required, a small amount of the plasmid DNA was used to re-transform *E. coli* (using the quick transformation method described in Section 2.3.2) and the plasmid DNA extracted from liquid cultures of the *E. coli* transformant, as described above.

2.5.2 Mid-scale plasmid preparations

Preparation of larger amounts of plasmid DNA was done using a method modified from that described by Holmes and Quigley (1981). A 400 ml overnight culture was pelleted at 10,000 *g* for 10 min at 4°C and resuspended in 10 ml of STET buffer (100 mM NaCl, 1 mM EDTA, 0.5% (v/v) Triton X-100, 10 mM Tris-HCl, pH 8.0). The resuspended cells were transferred to a conical flask and 2 ml of lysozyme solution (10 $mg.ml^{-1}$) added. The flask was heated until boiling and transferred to a boiling water bath for 40 s before quick-cooling on ice. A further 5 ml of STET was added and the lysate was spun at 10,000 *g* for 40 min at 4°C in a Beckman ultracentrifuge with a 60 Ti rotor to pellet cell debris. The supernatant was transferred to a new tube and the DNA precipitated by adding 0.5 vol isopropanol

and 0.05 vol 2.5 M sodium acetate pH 5.5, and spinning at 1,000 *g* for 15 min at 4°C. The supernatant was discarded, the pellet drained well and washed in ice-cold 70% (v/v) ethanol and resuspended in 4 ml of TE buffer. RNA was removed by adding 200 µl RNAse solution (10 mg.ml^{-1} RNAse A) and incubating at 37°C for 2 h. Finally, the sample was extracted twice with an equal vol of phenol:chloroform (1:1), then once with an equal vol of chloroform, ethanol precipitated and redissolved in TE buffer.

2.5.3 Chloramphenicol amplification of pBIN19-based plasmids

The copy number of pBIN19-based plasmids could be increased substantially by the addition of chloramphenicol (final concentration, 500 µM) to the bacterial culture when the OD_{600} was approximately 0.4, with further overnight incubation. This treatment arrests protein synthesis but not DNA replication resulting in higher plasmid yields per g of culture (Sambrook *et al.*, 1989).

2.5.4 Extraction of plant DNA

Total plant DNA was extracted using the method of Dellaporta *et al.* (1983). Up to 0.75 g of leaf tissue was ground to a powder in liquid nitrogen before adding 10 ml of ice-cold extraction buffer (50 mM EDTA, 500 mM NaCl, 10 mM β-mercaptoethanol, 100 mM Tris-HCl, pH 8.0) and ground further to homogeneity. The extract was transferred to a 30 ml Corex tube and the mortar washed into this with a further 5 ml extraction buffer. One ml of 20% (w/v) SDS was added and the tube shaken vigorously before incubating at 65°C for 10 min. After incubation, 5 ml of 5 M potassium acetate was added and the tube shaken vigorously and incubated on ice for 20 min. The debris was pelleted by spinning at 10,000 *g* for 30 min at 4°C and the supernatant filtered through miracloth into a clean 30 ml Corex tube containing 10 ml isopropanol. After mixing and incubating at -20°C for 30 min, the DNA was pelleted by spinning at 10,000 *g* for 30 min and the supernatant discarded. The pellet was washed with 80% (v/v) ethanol, resuspended in 700 µl of 50 mM Tris-HCl, pH 8.0, 10 mM EDTA, and transferred to a 1.5 ml microtube. The sample was spun at 17,000 *g* for 10 min to remove insoluble debris, and the supernatant transferred to a fresh microtube and extracted with an equal volume of phenol:chloroform:isoamyl-

alcohol (25:24:1). The aqueous phase was transferred to a fresh microtube and the DNA precipitated using 0.1 vol 3 M sodium acetate and 0.6 vol isopropanol. The DNA was pelleted at 17,000 *g* for 30 s, washed with ice-cold 80% (v/v) ethanol, air-dried and redissolved in 100 µl TE with 200 $\mu g.ml^{-1}$ RNase A.

2.5.5 Purification of DNA fragments from gels

The silica-based Prep-A-Gene system from Bio-Rad was used for the recovery of DNA from bands in agarose or acrylamide gels. The band was cut out of the gel and incubated in 3 vol 'Prep-a-Gene' binding buffer at 50°C for 10 min to dissolve the gel. Once the gel had dissolved, the mixture was vortexed briefly and 5 µl of binding matrix was added for every µg of DNA in the slice. After incubation at room temperature for 10 min, the matrix was pelleted by spinning at 17,000 *g* for 30 s and washed twice in 500 ml binding buffer and 3 times in 500 ml wash buffer. The DNA was eluted from the matrix by incubation in 10 µl of elution buffer at 30°C for 5 min. The elution step was repeated and the samples pooled and spun briefly to remove traces of the matrix.

2.5.6 Electrophoresis of DNA

For DNA fragments of less than ca. 1,000 bp such as PCR products, polyacrylamide gels were used because of their higher resolution in this size range. For larger fragments, such as those produced by restriction digests, agarose gels were sufficient. Samples were prepared by adding 0.2 to 0.5 vol loading buffer (0.25% (w/v) bromophenol blue, 0.25% (w/v) xylene cyanol FF, 30% (v/v) glycerol), and then loaded onto the gel along with suitable markers for size estimation. After electrophoresis, the gel was viewed on a long wavelength (300 to 360 nm) UV transilluminator, and photographed using a Polaroid Land camera with a yellow filter or digitally captured and printed using an 'Eagle Eye II' gel documentation system (Stratagene).

Polyacrylamide gels

Gels of 8% (w/v) acrylamide (10:1 acrylamide:bis-acrylamide) were prepared as described by Sambrook *et al.* (1989) and run for 5 h at 40 mA. To visualise the DNA, the gel was transferred to a solution of ethidium bromide (0.5 $\mu g.ml^{-1}$ in distilled water), stained for 30 min, and destained in distilled water for a further 30 min.

Agarose gels

Gels of 0.8% to 1.2% (w/v) were prepared in 1 x E buffer (20 mM Na^+ acetate, 2 mM EDTA, 40 mM Tris-HCl, pH 7.8) depending on the size of the fragments to be separated. Electrophoresis was carried out at 10 $V.cm^{-1}$ for 1 h or 1 $V.cm^{-1}$ overnight in 1 x E buffer.

2.6 Polymerase Chain Reaction (PCR)

2.6.1 Template preparation

Template plasmid DNA to be used in PCR was prepared by the mid-scale method as described in Section 2.5.2. The target DNA was linearised by adding 10 U of *Hin*dIII to the reaction mix and incubating at 37°C for 30 min prior to commencing PCR cycling.

2.6.2 Oligonucleotide preparation

Oligonucleotides were synthesised by the phosphoramidite method (Caruthers *et al.*, 1987), using a Biosearch 3810 DNA synthesizer (New Brunswick Scientific, Hatfield, UK). They were released from the synthesis column by incubating at room temperature in 1 ml concentrated ammonia solution (880) for 1 hour and then the solution was transferred to a microtube, sealed with parafilm and incubated at 55°C overnight for deprotection. The DNA was purified and concentrated by transferring the solution to a siliconised 30 ml Corex tube, adding 10 vol butan-1-ol and vortexing vigorously. The tube was spun at 17,000 *g* for 4 min at room temperature to pellet the DNA, and the pellet was resuspended in 200 µl sterile distilled water.

2.6.3 'Hot-start' PCR

A 50 µl PCR reaction mix containing 50 ng of each primer, 250 pg of template DNA, 250 µM dATP, 250 µM dCTP, 250 µM dGTP, 250 µM dTTP, 50 mM KCl, 1.5 mM $MgCl_2$ and 10 mM Tris-HCl, pH 8.3 was prepared in a 0.5 ml microtube. The reaction mix was overlaid with 50 µl of mineral oil and the tube was heated to 94°C for 3 min before adding 1 U of Taq polymerase (AmpliTaq; Perkin-Elmer, Warrington, UK) and subsequent thermocycling. The conditions used for the amplification cycles are described in Chapter 3. At the end of the run, 100 µl of chloroform was added to remove the mineral oil, and the PCR products were recovered by ethanol precipitation and redissolved in 10 µl TE.

2.6.4 Calculation of optimum primer annealing temperatures

A computer program was written to calculate the optimum annealing temperature based on the length and base composition of the oligonucleotides and the target DNA. It was based on the thermodynamic calculations of Breslauer *et al.* (1986) and Rychlik *et al.* (1990) and is included in Appendix II.

2.7 DNA manipulations

2.7.1 Restriction digests

Many of the DNA manipulations carried out involved digesting DNA to provide suitable fragments for cloning and to provide compatible cut ends in plasmids into which the fragments could be ligated. Digests with restriction enzymes were carried out according to the supplier's instructions. Digests usually contained 0.5 to 5 µg DNA, 5 µl 10 x restriction enzyme buffer as supplied, 1 µl (10 U) restriction enzyme and 100 $\mu g.ml^{-1}$ BSA (nuclease-free; Life Technologies) in a total vol of 50 µl. Reactions were incubated at the appropriate temperature for the enzyme for 0.5 to 3 h.

DNA fragments were used directly in ligation procedures (see Section 2.7.2) but vector DNA was further purified by extraction with phenol:chloroform:isoamyl alcohol (25:24:1) and precipitated with ethanol (Sambrook *et al.*, 1989).

2.7.2 Ligation

DNA ligations were done using T4 DNA ligase (Life Technologies). Typically, 10 to 100 ng of vector was ligated to 50 to 300 ng of insert DNA. The ratio of insert to vector was varied to obtain optimal ligation rates, but was usually between 1:1 and 3:1. To this was added 1 µl of 5 x ligation cocktail containing ATP as supplied by the manufacturer, 1 Weiss-unit of T4 DNA ligase, and the volume was made up to 5 µl with sterile distilled water. The reaction was incubated overnight at 14°C. For blunt-ended ligations, the concentration of the ligation cocktail and the amount of enzyme was doubled, and the incubation temperature reduced to 12°C.

2.7.3 Filling-in sticky ends

Sticky-ended fragments of DNA could be converted to blunt-ended fragments by filling in the 5' overhang using the large fragment of *E. coli* DNA polymerase I

(Klenow fragment; Jacobsen *et al.*, 1974; Joyce and Grindley, 1983). The reaction mixture used contained 250 μM dATP, 250 μM dCTP, 250 μM dGTP, 250 μM dTTP, 10 mM $MgCl_2$, 50 mM NaCl, 4 U Klenow fragment and 50 mM Tris-HCl, pH 8.0 in a total vol of 25 μl. The reaction was incubated at 30°C for 30 min and then could be heated to 65°C for 10 min to inactivate the enzyme if further digests were to be performed, or extracted with phenol:chloroform:isoamyl alcohol (25:24:1), ethanol precipitated and redissolved in TE ready for further manipulations.

2.7.4 T/A cloning

Taq DNA polymerase has a tendency to add an extra deoxyadenosine residue onto the 3' end of DNA fragments at the end of the amplification cycle (Clark, 1988). Thus, the efficiency of cloning of PCR fragments could be increased if blunt-ended vectors were modified to include a 3' overhanging thymine residue (Mead *et al.*, 1991). The efficiency of blunt-ended ligations could also be increased significantly by modifying vectors in this way and modifying inserts to include the 3' overhanging adenosine residue.

Up to 500 ng of *Sma*I-cut vector DNA to be T-tailed was incubated at 70°C for 2 h with 1 U AmpliTaq in 50 mM KCl, 0.4 mM $MgCl_2$, 2 mM dTTP and 10 mM Tris-HCl, pH 8.3 in a total vol of 25 μl. Blunt-ended fragments were A-tailed using the same procedure but substituting dATP for dTTP.

2.8 DNA sequencing

Constructs were verified by sequencing the plasmid DNA around the regions modified in the cloning procedure using the dideoxy method as described by Sanger *et al.* (1977) and a kit supplied by United States Biochemical (USB).

2.8.1 Reactions

Five μg of double-stranded plasmid DNA was denatured by adding 0.1 vol 2 M NaOH to the plasmid sample in TE and incubating at room temperature for 5 min. The DNA was then precipitated with 4 vol ice-cold ethanol and 0.5 vol 1 M Na^+ acetate, pH 5.0, pelleted at 17,000 *g* for 10 min at 4°C and washed in 75% (v/v) ethanol and dried under vacuum. The DNA was resuspended in 1 μl of a suitable primer in sterile

distilled water, and then made up to 10 µl in 40 mM Tris-HCl, pH 7.5, 20 mM $MgCl_2$ and 50 mM NaCl. Primers were annealed to the template by heating to 65°C for 2 min, cooled to room temperature on the bench (about 30 min) and kept on ice until needed. To label the DNA with ^{35}S, the volume of the mix was increased to 15 µl with the addition of 10 mM DTT, 0.55 µCi [α-^{35}S]-dATP, 1.5 µM dCTP, 1.5 µM dGTP, 1.5 µM dTTP and 5 U Sequenase T7 DNA polymerase (USB), and incubated for 5 min at room temperature. Four aliquots of 2.5 µl were taken from each sequencing reaction and each transferred to a termination reaction, pre-warmed to 37°C, containing 33.3 µM of each deoxynucleotide and 3.3 µM of either ddATP, ddCTP, ddGTP or ddTTP. The termination reactions were incubated at 37°C for 5 min and then stopped by the addition of 4 µl of stop solution (95% (v/v) formamide, 20 mM EDTA, 0.05% (w/v) bromophenol blue, 0.05% (w/v) xylene cyanol FF). The completed reactions could be stored at -20°C, and were boiled for 5 min immediately prior to loading on the sequencing gel.

2.8.2 Sequencing gel

Samples were run on a 6% (w/v) bis/acrylamide gel containing 8 M urea and 1 x TBE buffer, in a Bio-Rad Sequi-Gen II gel system with 21 cm x 40 cm plates. The gel was pre-run at 2,000 V in 1.5 x TBE until it had warmed up to 50°C, and then the samples loaded and run at 50 W for 90 min. The gel was fixed in 10% (v/v) methanol, 10% (v/v) acetic acid, vacuum-dried for 30 min at 60°C and autoradiographed overnight.

2.9 Plant culture, transformation and regeneration

2.9.1 Maintenance of plant material in culture

Plant culture conditions

Lotus corniculatus cv. Leo plants were used in all experiments and were maintained in culture in sterile sausage and bean jars (7 cm high, 7.5 cm diameter; Fisons, Loughborough, UK) containing MS20 medium (Table 2.3). Because of the genetic variability of the cultivar, a line that had been vegetatively propagated from a single plant was used in all experiments. Plants were grown in a culture room at 25°C, 16 h light : 8 h dark and subcultured every 1 to 2 months as necessary, by cutting stem segments just above the node and planting these in fresh media. Light intensity in the

room was 50 to 100 μeinsteins.m^{-2}.s^{-1}. For nodulation experiments, plants were subcultured onto MS20 medium for 10 to 12 d, until they had produced roots of 0.3 to 1.5 cm length. They were then transplanted into Terra-Green (Turfpro, Staines, UK) and inoculated with *R. loti* strain NZP2037. Plants were acclimatised for 3 to 4 d in propagators, and then transferred to a controlled environment cabinet and grown in 16 h light : 8 h dark, 22°C day : 18°C night, 70% humidity for 6 to 8 weeks with regular watering with Fåhraeus medium (Table 2.3), before treatments and analyses.

Long-term storage of transgenic lines

Plants were also maintained in sterile plastic, screw-topped culture tubes (10 ml; Bibby-Sterilin, Staffordshire, UK) on Fåhraeus medium (Table 2.3). This minimal medium limited growth and allowed plants to be stored for 3 to 4 months before subculturing was necessary.

2.9.2 Stab inoculation with *Agrobacterium rhizogenes*

Untransformed *L. corniculatus* plantlets were propagated under sterile conditions by subdividing them onto fresh MS20 medium as described in Section 2.9.1, and maintained in a growth room under the conditions described in Section 2.9.1 for 4 to 6 weeks. The *A. rhizogenes* strain carrying the chimaeric gene in pBin19 was cultured on YMB medium (Table 2.2) containing 50 μg.ml^{-1} kanamycin for 2 to 3 d, until a thick lawn of bacteria were present on the plate. The tip of a sterile 50 mm long 19 gauge needle (Terumo; Fisher) was dipped into the *A. rhizogenes* culture and the plants infected by stabbing their internodes with this. Each stem could be stabbed in a number of different locations using this method. Plants were returned to the growth room, and hairy roots usually developed at the infection sites within 3 to 4 weeks.

2.9.3 Regeneration of plants from hairy roots

When the hairy roots were clearly visible, the infection sites were excised from the stem and placed on MS20 plates containing 250 μg.ml^{-1} cefotaxime (Table 2.4; Roussel Laboratories, Uxbridge, UK) to kill the *Agrobacterium.* These plates were wrapped in aluminium foil to exclude light and grown for 2 to 3 weeks at 25°C to allow the hairy roots to grow. Hairy roots were then cut into sections 6 to 8 mm long

and transferred to fresh MS20 plates containing 1 $\mu g.ml^{-1}$ zeatin to induce callus. These plates were kept at standard growth conditions (see Section 2.9.1) in the light, with the developing calli transferred to fresh plates at weekly intervals. After 4 to 6 weeks, the root cultures had produced callus, which subsequently produced shoots within another 3 to 4 weeks. The shoots were excised from the callus cultures and transferred to MS20 jars where they rapidly produced roots. Transformants could subsequently be maintained in tissue culture and transferred to Terra-Green as described Section 2.9.1.

2.10 Enzyme assays

2.10.1 Plant harvest and tissue extraction

Plant material was separated into nodules, roots and shoots, and then quick-frozen in liquid nitrogen and kept in liquid nitrogen until needed. Up to 0.5 g of frozen material was ground to a powder on ice before addition of up to 2 ml of appropriate grinding buffer, with continued grinding on ice to homogeneity. A small amount of acid-washed sand (40-100 mesh; Fisons) was added if necessary. The crude extract was clarified by spinning at 17,000 *g* for 15 min at 4°C.

2.10.2 Preparation of bacterial lysates

Cells were harvested from 40 ml of late log-phase cultures by spinning at 7,000 *g* for 30 min at 4°C. Cells were resuspended in 100 ml of sonication buffer (10 mM NaH phosphate, pH 7.0, 10 mM NaCl) and sonicated on ice at a frequency of 23 kHz and an amplitude of 20 microns in an MSE Soniprep 150 (Fisons) for six 5-s bursts separated by 25-s intervals. The extract was clarified by spinning at 10,000 *g* for 5 min at 4°C.

2.10.3 Protein assays

Protein concentrations in plant and bacterial extracts were measured by a modification of the method described by Bradford (1976), using a kit supplied by Bio-Rad. The method was scaled down and performed in a 96-well microtitre plate. Up to 20 µl of extract was added to 200 µl of Bio-Rad reagent diluted 1 in 4 with distilled water and mixed thoroughly. Bovine serum albumin Fraction V (BSA) was used to generate a

standard curve. Plates were left to stand for 5 min and then the absorbance at 595 nm was read using a Dynatech 5000 plate reader (Dynatech, Billingshurst, UK).

2.10.4 Phosphinothricin acetyltransferase

Colorimetric assay

The colorimetric phosphinothricin acetyltransferase (PAT) assay as described by Thompson *et al.* (1987) was used for determination of PAT activity in *E. coli* extracts. This is a modification of the CAT assay of Shaw (1975) in which the free CoA sulphhydryl group generated by the transfer of the acetyl group from acetyl-CoA to PPT reacts with 5,5'-dithiobis-2-nitrobenzoic acid (DTNB) to yield the mixed disulphide of CoA and thionitrobenzoic acid, and free 5-thio-2-nitrobenzoate. The molar equivalent of the 5-thio-2-nitrobenzoate produced has a molar extinction coefficient of 13,600 at 412 nm.

One hundred µl of bacterial extract prepared by sonication (see Section 2.10.2) was added to 1 ml of PAT assay mix (50 mM Tris pH 7.5, 1 mM DTNB, 100 µM acetyl-CoA) in a cuvette at 37°C and the absorption rate at 412 nm determined. After establishing a baseline rate for 1 min, PPT (glufosinate ammonium; Greyhound chromatography, Birkenhead, UK) was added to 200 µM and the rate of acetylation determined. One unit of PAT activity is defined as 1 µmol of PPT acetylated per minute at 37°C.

Chromatographic assay

The baseline rate of acetylation measured using the colorimetric method for determination of PAT activity in plant extracts was too high so a thin layer chromatographic (TLC) method was used as described by De Block *et al.* (1987).

Thirteen µl of a 1 in 10 dilution of extract prepared as described (see Section 2.4.1) in PATGUS extraction buffer (50 mM Tris pH 7.5, 2 mM ethylenediaminetetraacetic acid (EDTA), 1 mM phenylmethylsulfonylfluoride (PMSF), 0.3 mM leupeptin, 2 mM dithiothrietol (DTT)) was added to 1 µl of 10 mM PPT and 1 µl of ^{14}C-acetyl-CoA (ICN) in a 0.5 ml microtube and incubated for 5 min at 37°C. The reaction was stopped by the addition of 15 µl of 12% (w/v) trichloroacetic acid (TCA) and 10 µl

spotted onto a Whatman LK6D silicagel TLC plate (Whatman International, Maidstone, UK). Chromatography was carried out in a 3:2 mixture of propan-1-ol and ammonia (880) for 4 h. Plates were measured using a Berthold Tracemaster 20 and analysed using Chroma 2D analysis software (Berthold Instuments, St. Albans, UK). The software was used to determine the percentage of radioactivity on the TLC plate that was transferred from the position corresponding to acetyl-CoA to that corresponding to acetylated PPT, and this figure used to calculate PAT activity. One unit of PAT activity is defined as for the colorimetric assay above.

2.10.5 β-glucuronidase

Fluorimetric assay

Crude extracts were prepared as described (see Sections 2.10.1 and 2.10.2) in GUS grinding buffer (50 mM Na^+ phosphate, pH 7.0, 100 mM NaCl, 1 mM EDTA, 0.1% (v/v) Triton X-100, 10 mM β-mercaptoethanol) and their protein concentrations determined (see Section 2.10.3). Enough crude extract for 10 μg protein was made up to 200 μl with grinding buffer in a black microtitre plate. The plate was warmed to 37°C and the reaction started by addition of 4-methylumbelliferyl glucuronide (MUG) to a final concentration of 1 mM. At various times from 5 to 120 min, a 50 μl aliquot was removed and dispensed into a fresh well containing 200 μl of 0.2 M Na_2CO_3 to stop the reaction and enhance fluorescence. Fluorescence at 460 nm was read immediately in a Titretek Fluoroskan II microplate reader (ICN Flow, High Wycombe, UK) with excitation at 355 nm and concentrations deduced from a standard curve generated using known concentrations of 4-methylumbelliferone (4-MU) in 0.2 M Na_2CO_3 (Jefferson, 1987; Rao and Flynn, 1992). One unit of GUS activity is defined as 1 μmol of 4-MU liberated from MUG per minute at 37 °C.

Histochemical staining

Individual nodules were sectioned longitudinally by hand with a double-edged razor blade and immersed in GUS staining buffer (1 mM 5-bromo-4-chloro-3-indolyl-β-D-glucuronic acid (X-gluc), 50 mM Na^+ phosphate, pH 7.0, 0.5 mM potassium ferricyanide, 0.5 mM potassium ferrocyanide) and vacuum-infiltrated for 1 min. Samples were incubated at 37°C for up to 24 h depending on the amount of activity present in the tissue (Pearse, 1972; Jefferson, 1987).

2.10.6 Combined PAT and GUS assay procedure

When extracts were to be assayed for both PAT and GUS activity, then PATGUS extraction buffer (see Section 2.10.4) was used for both protocols. It was established in preliminary experiments that PATGUS grinding buffer could be used with no significant reduction in the activity of either enzyme moiety. The enzyme assays were as described in Sections 2.10.4 and 2.10.5.

2.10.7 Glutamine synthetase

Transferase assay

For routine estimates of glutamine synthetase (GS) activity, the transferase assay based on that of Cullimore and Sims (1980) was used, in which GS catalyses the reaction of glutamine with hydroxylamine to yield γ-glutamylhydroxamate and ammonia. This reaction is more sensitive but less accurate than the semi-biosynthetic assay described below. One hundred µl of tissue extract prepared in GS extraction buffer (10 mM EDTA, 10 mM $MgSO_4$, 6 mM DTT, 15 mM β-mercaptoethanol, 6 mM reduced glutathione, 25 mM Tris-HCl, pH 8.0) was added to 800 µl of assay mix (80 mM glutamine, 20 mM hydroxylamine, 3 mM $MnCl_2$, 0.3 mM adenosine diphosphate (ADP), 100 mM 2-[N-Morpholino]ethanesulfonic acid (MES), pH 6.4). The mixture was warmed to 30°C and the reaction was started by the addition of 100 µl of arsenate mix (250 mM sodium arsenate, 25 mM MES, pH 6.4) and incubated at 30°C for 10 min. The reaction was stopped by adding 1 ml of ferric chloride solution (4% (w/v) TCA, 100 mM $FeCl_3$, 8% (v/v) HCl). Control reactions were set up with 100 µl Tris-HCl buffer in place of the arsenate solution. Reaction mixtures were spun at 17,000 *g* for 10 min and the absorbance of the supernatant read at 505 nm. An absorbance of 1 is equivalent to 3 µmol glutamylhydroxylammonium in a 1 cm light path. One unit of GS activity is defined as 1 µmol of γ-glutamyl-hydroxamate formed per minute at 30°C.

Semi-biosynthetic assay

The semi-biosynthetic assay based on that of Stewart *et al.* (1988) was often used to confirm the validity of the transferase assay as described above. One hundred µl of extract prepared in synthetase assay buffer (10 mM EDTA, 10 µM flavin adenine dinucleotide (FAD), 10 µM leupeptin, 1 µM Na_2MoO_4, 1% (v/v) Nonidet, 3% (w/v) polyvinylpolypyrrolidone (PVPP), 6 mM DTT, 50 mM Tris-HCl, pH 8.5) was added

to 800 µl of 50 mM Tris-HCl, pH 7.6, and 100 µl of GS assay buffer (0.4 M adenosine triphosphate (ATP), 150 mM $MgSO_4$, 300 mM glutamic acid, 40 mM hydroxylamine) prewarmed to 30°C. The reaction was incubated for 60 min at 30°C and then stopped with 1 ml ferric chloride solution (see above). Tubes were spun at 17,000 *g* and the OD_{505} read as above.

2.10.8 Nitrogenase

A modification of the acetylene reduction assay for nitrogenase activity, as described by Hirota *et al.* (1978), was used. Single plants were grown in 9 cm square pots in vermiculite. When the plants were 4 to 6 weeks old, the whole pot was transferred to a 4 L glass vacuum desiccator (Jencons, Leighton Buzzard, UK) modified to include a suba-seal (Fisons) at the inlet, and sealed so that it was air tight with vacuum grease and PVC insulating tape. A 50 ml aliquot of air was removed from the chamber and replaced with acetylene, and the desiccator incubated in the controlled environment chamber used for the growth of the plants. Air samples of 1 ml were removed with a syringe at regular intervals for up to 24 h and analysed for ethylene content using an Ai model 93 gas chromatograph (Ai, Cambridge, UK) fitted with a 150 cm glass column of OD 0.6 cm and iD 0.4 cm, packed with Porapak R (Jones Chromatography, Mid-Glamorgan, UK), and a flame-ionization detector.

2.10.9 Ammonium determination

For the detection of ammonium ions in solutions (for example before and after their replacement with sodium in glufosinate-ammonium solutions) a method after McCullough (1967) was used. To 100 µl of the sample in a microtube, 0.5 ml of phenol solution (1% (w/v) phenol, 0.005% (w/v) Na^+ nitroprusside) and 0.5 ml of alkaline solution (125 mM NaOH, 344 mM Na_2HPO_4, 1% (v/v) Na^+ hypochlorite solution containing 10-14% available chlorine) was added. The tube was capped, mixed by inversion and incubated at 37°C for 30 min. At high pH, ammonium ions in the solution react with the phenol and hypochlorite, resulting in the formation of stoichiometric quantities of indophenol. The indophenol has a deep blue colour that can be quantified by measuring optical absorbance at 625 nm. The reaction was calibrated using known concentrations of ammonium ions.

2.11 Protein fractionation and western blotting

2.11.1 Size exclusion chromatography

Size exclusion chromatography was used for the analysis of *E. coli* strains expressing the *pat::uidA* gene fusion. A 1.3 cm x 73 cm glass chromatography column was packed with Sephacryl S300-HR size exclusion matrix and connected to a peristaltic pump, UV detector and fraction collector. The whole set-up was kept in a cold room at 4°C. The column was calibrated using known size markers (Bio-Rad; Fig. 3.8) and then equilibrated by passing 200 ml of the appropriate sample buffer through it at a flow rate of 0.5 ml.min^{-1}. Up to 5 ml of *E. coli* extract prepared by sonication (see Section 2.10.2) was applied to the top of the column, and eluted through the column at a flow rate of 0.5 ml.min^{-1}. Fractions of 1 ml were collected and stored at 4°C prior to assaying for PAT and GUS activity.

2.11.2 Ion exchange chromatography

Different isoforms of plant GS can be separated on the basis of differences in the overall charge of the holoenzymes (Mann *et al.*, 1979; McNally and Hirel, 1983). The ion exchange system used was a Memsep 1010 cartridge (PerSeptive Biosystems, Hertford, UK) fitted to a Consep LC100 4-way gradient mixer (Millipore, Watford, UK). The Memsep cartridge is a tightly compacted stack of charged membranes, which act like a conventional column, but with improved performance speed at lower pressures. The plant extract, prepared in GS grinding buffer (see Sections 2.10.1 and 2.10.7), was filtered through a 0.45 μm filter (Millipore) and then up to 2 ml was applied to a PD10 column for desalting and removal of detergent. This was washed into the column with 1.5 ml of loading buffer (grinding buffer without detergent) and eluted in a further 3 ml of loading buffer. The eluent was further filtered with a 0.22 μm filter (Millipore) prior to injection into the Memsep cartridge. The Memsep cartridge was pre-equilibrated by passing at least 10 ml of 20 mM Tris-HCl, pH 7.6 through it. The sample was then injected onto the column and eluted with an increasing KCl gradient into fractions that were subsequently assayed for GS activity (see Section 2.10.7). Details of the gradients used and fraction volumes collected can be found in Chapter 4.

2.11.3 Polyethylene glycol fractionation

Polyethylene glycol (PEG) was added to 1 ml of sample extract prepared as described (see Sections 2.10.1 and 2.10.2) in a microtube to a final concentration of between 30% and 70% saturation at 0°C. The tube was shaken vigorously until all the PEG had dissolved and then the tube was incubated on ice for 15 min. The supernatant was removed to a fresh microtube, and the precipitated protein was resuspended in an equal vol of sample buffer.

2.11.4 Polyacrylamide gel electrophoresis (PAGE)

Denaturing gels

Denaturing SDS-PAGE gels were run as described by Laemmli (1970), using a Bio-Rad Mini Protean II system. Gels were 0.75 mm thick, with a 10% (w/v) bis/acrylamide separating gel (0.1% (w/v) SDS, 0.05% (w/v) ammonium persulfate (APS), 0.005% (v/v) N,N,N',N'-tetramethyl ethylenediamine (TEMED), 375 mM Tris-HCl, pH 8.8), and a 4% (w/v) bis/acrylamide stacking gel (0.1% (w/v) SDS, 0.05% (w/v) APS, 0.005% (v/v) TEMED, 125 mM Tris-HCl, pH 6.8). Samples were extracted in protein extraction buffer (10 mM $MgSO_4$, 5 mM DTT, 10% (v/v) ethanediol, 0.05% (v/v) Triton X-100, 50 $\mu g.ml^{-1}$ leupeptin, 0.01% (v/v) β-mercapto-ethanol, 50 mM Tris-HCl, pH 7.8), assayed for protein (see Section 2.10.3) and up to 10 µg protein diluted 1 in 4 with sample loading buffer (62.5 mM Tris-HCl, pH 6.8, 10% (v/v) glycerol, 2% (w/v) SDS, 0.001% (w/v) bromophenol blue, 5% (v/v) β-mercaptoethanol). Samples were heated to 95°C for 5 min prior to loading on the gel. The running buffer was 25 mM Tris-HCl, pH 8.3, 192 mM glycine, 0.1% (w/v) SDS and electrophoresis was at a constant 200 V for 45 min to 60 min.

Non-denaturing gels

To preserve the quaternary structure of GS, and thus separate it on the basis of the size of the holoenzyme, some non-denaturing gels were run in which SDS was omitted from all solutions and the samples were not heated prior to loading. All conditions other than these were the same as for denaturing gels.

2.11.5 Electrotransfer of proteins to membranes

A sheet of Hybond-C Extra nitrocellulose membrane (Amersham) was cut to the size of the separating gel and equilibrated by incubating in transfer buffer (25 mM Tris-HCl, pH 8.3, 192 mM glycine, 15% (v/v) methanol) for 5 min. The gel to be blotted was also incubated in transfer buffer for 20 min, and then blotted onto the membrane at a constant 90 V for 1 h using a Bio-Rad Minitransfer cell. After blotting, the membrane was blocked overnight in Tris-buffered saline (TBS; 50 mM Tris-HCl, pH 7.4, 150 mM NaCl) plus 5% (w/v) BSA and stored in TBS at 4°C prior to immunostaining.

2.11.6 Membrane immunostaining

Membranes were washed once in TBS for 5 min and then incubated for 30 min in TBS+BSA (TBS containing 0.5% (w/v) BSA) and the appropriate dilution of primary antiserum. Unless otherwise stated, antibody dilutions were 1:100,000 for GS, 1:10,000 for GUS and 1:10,000 for PAT. After incubation with the primary antibody, the membrane was washed 3 times for 10 min in wash buffer (TBS, 0.5% (w/v) BSA, 0.05% (v/v) polyoxyethylsorbitan monolaurate (Tween 20)) and then incubated for 30 min in a 1 in 50,000 dilution of biotinylated secondary antibody (anti-rabbit IgG for GS and GUS; anti-goat IgG for PAT; both supplied by Sigma) in TBS+BSA. The membrane was again washed for 3 x 10 min in wash buffer and then for 3 x 5 min in TBS, prior to incubation for 1 h in a 1:5,000 dilution of ExtrAvidin horseradish peroxidase (Sigma). After a final 3 washes in wash buffer followed by 3 washes in TBS as before, the membrane was ready for antibody detection. The detection system was enhanced chemiluminescence using an Amersham ECL kit and the protocol was as described in the manufacturer's instructions. Exposure times ranged from 30 s to overnight and the X-ray film was developed in an automatic developer (X-Ograph model X-2).

The GS antibody used was a polyclonal raised in rabbit against the *Phaseolus vulgaris* γ subunit (Cullimore and Miflin, 1984), which has been shown to recognise all plant GS isoforms tested to date. The PAT antibody was a monoclonal raised in goat against native *S. hygroscopicus* PAT enzyme (supplied by AgrEvo, Saffron Walden, UK). The GUS antibody was a monoclonal raised in rabbit against native *E. coli* GUS enzyme (supplied by Clontech, Basingstoke, UK).

2.12 Conversion of glufosinate-ammonium to the sodium salt

The only commercially available form of phosphinothricin is the ammonium salt, glufosinate-ammonium (Greyhound Chromatography, Birkenhead, UK). Since the experiments described here were designed to investigate nitrogen metabolism, it was important that no external nitrogen source of any kind was introduced with the treatment. Thus, prior to use, solutions of glufosinate ammonium were passed through a Bio-Rad AG50W cation exchange column (Bio-Rad, Hemel Hempstead, UK). The column was first converted to the Na^+ form by flushing through with two bed volumes of 1 M NaOH and washed with four bed volumes of deionised water before passing the stock solution (10 $mg.ml^{-1}$ PPT) through it. The PPT stock was analysed for ammonium content as described in Section 2.10.9 before and after cation replacement and the procedure was found to replace at least 95% of the ammonium ions (data not shown).

Table 2.1: Plasmids used and constructed

Plasmid	Description	Reference
pIB16.1	A derivative of pROK1 (Baulcombe *et al.*, 1986) carrying the *pat* gene.	Wohlleben *et al.*, 1988
pCGUS	The $35S_{pro}$::*uidA*::nos_{ter} gene in pUC19.	Shen, 1991
pBA68	The *gln*-β promoter sequence in pUC8.	Forde *et al.*, 1989
pUC19	A high copy-number *E. coli* vector with *lacZ*-derived blue/white selection.	Vieira and Messing, 1982
pBIN19	A wide host-range binary vector for *Agrobacterium*-mediated plant transformation.	Bevan, 1984
pKK223-3	A pBR322-derived (Bolivar *et al.*, 1977) *E. coli* expression vector containing the strong IPTG-inducible *tac* promoter.	Brosius and Holy, 1984
pBluescript II SK+	A high copy-number *E. coli* vector with *lacZ*-derived blue/white selection.	Short *et al.*, 1988; Alting-Mees and Short, 1989
pCPATGUS95	The $35S_{pro}$::*pat*::*uidA*::nos_{ter} gene in pUC19. Derived from cloning the PCR-amplified *pat* fragment into pCGUS.	*This work, Section 3.2.1*
pKKPATGUS	The *pat*::*uidA* fusion in *E. coli* expression vector pKK223-3.	*This work, Section 3.2.3*
pPATGUS1.1	The *pat*::*uidA* fusion in pUC19 (*Xba*I/*Eco*RI sites).	*This work, Section 5.2*
pPATGUS2.1	The *pat*::*uidA* fusion in pUC19 (T/A cloned into *Sma*I site).	*This work, Section 5.2*
pBII76	The *gln*-γ promoter fragment from pBA68 (*Hin*dIII/*Eco*RI) in pBluescript II SK+.	*This work, Section 5.2*
pGPATGUS4.1	The *gln*-γ_{pro}::*pat*::*uidA*::nos_{ter} gene in pBluescript II SK+.	*This work, Section 5.2*
pBINCPG	The $35S_{pro}$::*pat*::*uidA*::nos_{ter} gene in pBIN19.	*This work, Section 5.2*
pBINGPG	The *gln*-γ_{pro}::*pat*::*uidA*::nos_{ter} gene in pBIN19.	*This work, Section 5.2*

Table 2.2: Bacterial growth media

Medium	Recipe (per litre)[§]		Reference
LB	10 g bacto-tryptone, 5 g yeast extract[†], 5 g NaCl[††], pH 7.4		Sambrook *et al.*, 1989
YMB	10 g mannitol, 0.4 g yeast extract[†], 0.2 g $MgSO_4.7H_2O$, 0.1 g NaCl, 0.5 g K_2HPO_4, pH 7.0		Dye, 1979
2XL	20 g bacto-tryptone[†], 10 g yeast extract[†], 2 g glucose, pH 7.0		Alexander *et al.*, 1984
523	8 g casein, 4 g yeast extract[†], 0.3 g $MgSO_4.7H_2O$, 10 g sucrose, 3 g K_2HPO_4, pH 7.0		Kado and Heskett, 1970
M9 minimal	6 g Na_2HPO_4, 1 g NH_4Cl, 2 mM $MgSO_4$, 0.1 mM $CaCl_2$, 2 g glucose, 0.5 g NaCl, 3 g KH_2PO_4, pH 7.4		Sambrook *et al.*, 1989

[§] Unless otherwise stated, solid media was made by adding 15 $g.l^{-1}$ bacto-agar to the medium prior to autoclaving.

[†] Supplied by Difco (Michigan, USA)

[††] For solid media, 10 g NaCl was used

Table 2.3: Plant growth media

Medium	Recipe (per litre)[§]		Reference
MS20(10)	4.41g MS salts (ICN biomedicals), 20 g (10 g) sucrose		Murashige and Skoog, 1962
Fåhraeus (no NO_3^-)	0.15 g $Na_2HPO_4.12H_2O$, 0.1 g KH_2PO_4, 0.1 g $CaCl_2.2H_2O$, 0.12 g $MgSO_4.7H_2O$, 5 mg ferric citrate, 1.6 mg $MnSO_4.4H_2O$, 2.9 mg H_3BO_3, 0.22 µg $ZnSO_4.7H_2O$, 80 µg $H_2MoO_4.H_2O$, 80 µg $CuSO_4.5H_2O$,		Fåhraeus, 1957
Fåhraeus (+ NO_3^-)	As above with 0.5g KNO_3 added.		Fåhraeus, 1957

[§] For solid media 8 $g.l^{-1}$ agar-agar was added to the medium prior to autoclaving.

Table 2.4 Antibiotics

Antibiotic[§]	Use	Working Concentration ($\mu g.ml^{-1}$)
Ampicillin	Maintenance of pUC19, pKK223-3, pBluescript and their derivatives in *E. coli*.	100
Kanamycin	Maintenance of pBIN19 and derivatives in *E. coli* and *A. rhizogenes*.	50
Rifampicin	Maintenance of Ti plasmid transfer functions in *A. rhizogenes* LBA 9402.	100
Chloramphenicol	Amplification of pBIN19 derivatives in *E. coli*.	34
Cefotaxime	Removal of *A. rhizogenes* from plant material after transformation.	250

[§] All antibiotics apart from cefotaxime were prepared as 1,000 x stocks in water (ampicillin; kanamycin) or ethanol (rifampicin; chloramphenicol) which were filter-sterilized and stored at 4°C. Cefotaxime was supplied as a sterile powder and dissolved in SDW to a final concentration of 100 $mg.ml^{-1}$. Antibiotics were added to solid media just prior to pouring, and to liquid media just before use. Solid media to which kanamycin or rifampicin had been added could be stored at 4°C for up to 3 months, but media containing ampicillin could be stored no longer than 2 weeks.

CHAPTER 3:

CONSTRUCTION AND TESTING OF THE *PAT::UIDA* GENE FUSION

3.1 Introduction

One of the aims of this project was to obtain differential protection of GS in different tissues from inhibition by phosphinothricin (PPT), so that the role of individual GS isoenzymes could be investigated. This was to be achieved by fusing a bacterial phosphinothricin acetyltransferase gene (*pat*) to suitable plant promoters and introducing these into *Lotus corniculatus*. However, it is well known that even with a well-characterised promoter, individual transformed lines can vary widely in their expression patterns, due to the effects of integration at different locations within the host genome, i.e. positional effects (e.g. Jones *et al.*, 1985; Hobbs *et al.*, 1990; Peach and Velten, 1991; Wilkinson *et al.*, 1997). Thus, it was necessary to determine that the desired patterns of expression were being achieved in the transformed plant lines. Unfortunately, there is no known histochemical assay for PAT activity, and the quantitative assays available are insensitive and tedious. To visualise the spatial distribution and accurately quantify PAT activity, I therefore fused it to the β-glucuronidase (GUS) reporter gene (*uidA*) from *E. coli* (Jefferson, 1987). GUS has gained wide popularity as a reporter enzyme for plant transformation, due to its high stability, wide range of substrates, and the low level of endogenous plant β-glucuronidase activity (Jefferson, 1987; Gallagher, 1992; Wilson *et al.*, 1995). There is a convenient histochemical assay for GUS, and this can be used as a sensitive indicator of expression levels in different tissues. Furthermore, there is a more sensitive quantitative assay for GUS than for PAT, and so accurate measurements of expression levels in specific tissues are possible (Jefferson, 1987; Rao and Flynn, 1992). If PAT and GUS could be fused together in one bifunctional protein, then the distribution and relative levels of PAT activity present in the tissues of transformed plants should be identical to that of GUS.

In this Chapter I describe the design and construction of a chimaeric *pat::uidA* gene and the demonstration that it encodes a bifunctional PATGUS enzyme when expressed in *E. coli*.

3.2 Construction of a translational fusion between the *pat* and *uidA* genes

At the time this work was initiated, PAT had been shown to tolerate C-terminal extensions of up to 24 kDa without loss of catalytic activity (Botterman *et al.*, 1991), and GUS to tolerate an N-terminal extension of 2 kDa (Jefferson, 1987). To link the PAT and GUS activities together in a single fusion protein, a flexible peptide sequence was designed which would link the C-terminus of PAT to the N-terminus of GUS and a PCR approach was adopted to generate the construct.

3.2.1 Plasmids

The *pat::uidA* gene fusion (PATGUS) was derived from two parent plasmids, pIB16.1 (Wohlleben *et al.*, 1988) and pCGUS (see below). pIB16.1, kindly supplied by AgrEvo (Saffron Walden, UK), is a pROK derivative which contains the *pat* coding sequence (Fig. 3.1), and was used as a template for amplification of *pat* by PCR. pCGUS is a pUC derivative which contains a CaMV35S$_{pro}$*::uidA::nos*$_{ter}$ cassette from pBI121 (Jefferson *et al.*, 1987; see Forde *et al.*, 1989 and Fig. 3.1). The modified *pat* gene was designed to be cloned between the 35S promoter (Franck *et al.*, 1980; Odell *et al.*, 1985) and *uidA* regions of pCGUS, creating the translational fusion, *pat::uidA* in pCPATGUS95 (Fig. 3.2). The *pat::uidA::nos* cassette was then cloned from pCPATGUS95 into a variety of subsequent vectors, including a prokaryotic expression vector, pKK223-3 (see Section 3.2.4) for analysis of its expression in *E. coli*.

3.2.2 PCR amplification of a modified *pat* coding sequence

The forward primer (Primer A; Fig. 3.1) was designed with a 5' mismatched region which contained an *Xba*I site upstream of the ATG start codon of the *pat* sequence, to facilitate cloning into pCGUS (Fig. 3.2). The reverse primer (Primer B) included a 3' mismatched extension that was designed to replace the *pat* stop codon with a linker

sequence suitable for a translational fusion with the 5' end of *uidA* (Fig. 3.2). The PCR reactions were carried out as described in Section 2.6 and conditions were as stated in Fig. 3.3. These were optimised for the production of a single product of about 580 bp, the expected size of the modified *pat* fragment (Fig. 3.3).

To increase the efficiency of the PCR reaction, and obtain enough of the product for subsequent cloning, a pre-PCR step was introduced in which the template pIB16.1 DNA was linearised with *Hin*dIII. A 'hot-start' PCR approach was adopted in which the reaction mix was heated to 94°C for 3 min prior to addition of the AmpliTaq T4 DNA polymerase and commencing thermocycling. This eliminates the possibility of any non-specific primer-template extensions occurring at room temperature prior to thermal cycling (Arnheim and Erlich, 1992). The temperature used for the annealing step was based on that calculated using a computer program (see Appendix II), which applies the thermodynamic data of Breslauer *et al.* (1986) and the equations of Rychlik *et al.* (1990) to a given primer sequence and expected target DNA length and GC content. These equations combine predictions of the optimum annealing temperature of the primer-template pairs and of the product-product pairs to give an overall optimum value for the suggested temperature to be used for each primer. The values predicted by the program are presented in Table 3.1. Taking an average of the values for primers A and B, the optimal annealing temperature is predicted to be 55.5°C at the start of the reaction (when the primers are mainly annealing to the initial, mismatched template), rising to 68.9°C (when the primers are annealing to perfectly matched products of the earlier cycles). The final reaction scheme included a ramp time of 90 s between the denaturing and annealing steps, which was designed to allow the primers a greater chance to anneal to the template. The annealing temperatures used were 40°C for 5 cycles followed by 50°C for 30 cycles. The products of three PCR reactions were pooled and electrophoresed, and a single, intensely staining band of the expected mobility (580 bp) was obtained (Fig. 3.3).

3.2.3 Cloning the amplified pat fragment into pCGUS

The 580 bp *pat* fragment from Section 3.2.2 was digested with *Xba*I and cloned between the CaMV35S promoter and the *uidA* coding sequence in *XbaI/Sma*I-digested

pCGUS to create pCPATGUS95 (Fig. 3.2). *E. coli* transformants were readily identifiable from their increased levels of GUS activity (see Section 2.4.3), but their PAT activities were less easily measured. The colorimetric method of Thompson *et al.* (1987; see Section 2.10.4) proved inappropriate for use with crude cell extracts from the *E. coli* strain used in the cloning experiments, since there was a high basal rate of increase in absorbance at 412 nm before addition of PPT. This phenomenon was noted by Shaw (1975) who attributed this competing hydrolysis of acetyl-CoA to high levels of endogenous thioesterase activity present in some strains of *E. coli*. Consequently, transformants harbouring pCPATGUS were distinguished from those harbouring pCGUS by Southern blotting, using a *pat* fragment as probe. Positives were then tested for functional expression of the PAT moiety using the chromatographic method (see Section 2.10.4).

3.2.4 Cloning PATGUS into a bacterial expression vector

The PATGUS gene fusion was excised from pCPATGUS95 by digestion at the flanking *Sma*I and *Eco*RI sites, the *Eco*RI sticky end was filled in with Klenow and then the fragment was A-tailed. The *E. coli* expression vector pKK223-3 (Brosius and Holy, 1984; supplied by Stratagene, UK) was cut downstream of its promoter with *Sma*I and T-tailed, and the PATGUS fragment inserted to create pKKPATGUS. pKK223-3 contains the *tac* promoter which is strongly induced by addition of IPTG to the growth medium (de Boer *et al.*, 1983). This construct was used for characterisation of PATGUS activity in *E. coli*.

3.3 Demonstration of PAT and GUS activity in *E. coli* expressing PATGUS

3.3.1 *E. coli* cells expressing PATGUS are resistant to PPT

E. coli clones harbouring pKKPATGUS were tested for PPT resistance by plating suspensions of single colonies onto M9 minimal agar plates (Table 2.2) containing thiamine and a range of concentrations of PPT. Colonies grew within 3 d on concentrations of up to 300 $\mu g.ml^{-1}$ PPT (Fig. 3.4). Untransformed *E. coli* did not grow on these plates, but could grow on the medium if the concentration of PPT was lowered to 200 $\mu g.ml^{-1}$, a concentration considerably higher than that needed for most

antibiotics to suppress bacterial growth. Resistance to 300 $\mu g.ml^{-1}$ PPT was also seen in the transformants when IPTG was omitted from the growth media, suggesting that the *tac* promoter is not completely silenced in the absence of IPTG (data not shown).

3.3.2 IPTG-induced PAT and GUS activity in *E. coli* expressing PATGUS

In an attempt to correlate the activities of PAT and GUS in *E. coli* harbouring pKKPATGUS, the IPTG-inducibility of the two enzyme activities was compared (Fig. 3.5). At the time of inoculation, IPTG was added to liquid cultures at concentrations ranging from 0.1 to 10 μM and the cultures grown to late-log phase before preparing crude cell extracts and assaying for enzyme activities. Addition of 0.1 μM IPTG was sufficient to induce low-level expression of PAT and GUS activity, although PAT activity appeared to be induced to a much greater extent than GUS. Addition of 1 μM IPTG resulted in a 100% increase in PAT activity over that seen in the 0.1 μM IPTG treatments, but GUS activity was still barely above the background level of endogenous GUS activity present in *E. coli* strain XL-1 Blue. Addition of 10 μM IPTG produced a further 50% increase in PAT activity, and was also sufficient to induce high levels of GUS activity in the cultures. Thus, both PAT and GUS activity could be induced by IPTG, but there did not appear to be a strong correlation between the two enzyme activities. Untransformed *E. coli* had GUS activity comparable with the uninduced transformed cultures and had no detectable PAT activity at any of the IPTG concentrations used in these experiments (data not shown).

3.3.3 Precipitation of PAT and GUS activities by polyethylene glycol

To examine further the disparity between PAT and GUS activities in the IPTG-induction experiments described above, and to investigate the possibility that the PATGUS fusion protein was being cleaved in *E. coli*, extracts were prepared from cultures induced with 10 μM IPTG and the soluble protein fraction precipitated with polyethylene glycol (PEG) at concentrations in the range 5% to 35% (w/v). The precipitates and the supernatants were then assayed for PAT and GUS activity (Fig. 3.6). All of the GUS activity precipitated at PEG concentrations of 10% and above. A small, but significant amount (5%) of PAT activity could still be detected in the supernatant of this fraction. The PEG concentration had to be increased to 15% to

precipitate all detectable PAT activity. Thus some of the PAT activity in the sample was not associated with GUS activity and so it seems likely that some cleavage of PATGUS had occurred, either *in vivo* or during the extraction procedure. Up to 90% of the GUS activity present in the original sample could be recovered in the resuspended pellet, but PAT assays on this fraction achieved no more than 70% recovery. This may be evidence that PAT is less stable than GUS once cleaved, although this is in contradiction with the results of the IPTG induction experiment (Section 3.3.2) and the size-exclusion chromatography presented later (Section 3.3.4). Another explanation for this is that some aspect of the precipitation procedure interfered with the PAT assay: either traces of PEG adversely affected it, or some of the enzyme was degraded during the time taken to resuspend the pellet.

3.3.4 Elution of PAT and GUS activity in liquid chromatography studies

To confirm that most of the product of the *pat::uidA* gene was stable as a fusion protein in the *E. coli* cells, extracts were fractionated by size-exclusion chromatography on a Sephacryl S-300HR column (Pharmacia, UK) and fractions were collected and analysed for PAT and GUS activities (Fig. 3.7). As expected, most of the PAT and GUS activity eluted together in a single peak (Fig. 3.7A). The column was calibrated by applying protein standards of known molecular weight, and it was estimated from the elution time that this peak coincided with a M_r of about 130 kDa (Fig. 3.8). This is considerably larger than the M_rs of the native PAT and GUS enzymes which are 42 and 68 kDa respectively (the PAT holoenzyme is a dimer of two 21 kDa subunits while GUS is a monomer; see Vinnemeier, 1995; Jefferson, 1985). It is also much larger than expected for a monomeric PATGUS enzyme (90 kDa), suggesting that it represents a dimeric PATGUS holoenzyme formed by intermolecular interactions between the two PAT domains. Although such a protein complex would have a M_r of about 160 kDa, it is clear from the calibration curve that the observed peak correlated closely with the elution of the aldolase standard (158 kDa), and this may give a better indication of its size than the fitted, straight-line regression.

It was further found that if PMSF was omitted from the extraction buffer (Fig. 3.7B), PAT activity eluted in two peaks, one of which co-eluted with the GUS standard

while the other eluted much later, corresponding to a M_r of approximately 35 kDa. These two peaks are probably due to cleavage of the fusion protein into its constituent PAT and GUS moieties during extraction, as PMSF is a serine protease inhibitor and is likely to be preventing proteolytic attack of the areas around the synthetic linker. This second peak of PAT activity also corresponded to a shoulder on the PATGUS peak obtained with PMSF present, suggesting that a small amount of degradation was also occurring here. There was no corresponding second GUS peak in any of the samples. However, the profiles of PAT and GUS activity seen in Fig. 3.7B are very similar to those reported by Datla and co-workers (1991), who characterised a *uidA::nptII* fusion product. They believed the lack of a second GUS activity peak in their extracts to be due to protein degradation. This suggests that the cleaved GUS domain is more labile in the crude extract than the cleaved PAT domain.

The PATGUS elution volume that was observed in Fig. 3.7B suggests that the protein was much larger than expected (ca. 245 kDa). However, the elution volume was close to the column void volume, and may indicate that this was simply due to overloading of the column in this instance.

3.3.5 Immunodetection of PATGUS by GUS antibodies

Extracts prepared as above were separated by SDS-PAGE and electroblotted onto Hybond-C Extra membranes. These were probed with antibodies raised against native GUS protein (Fig. 3.9). An IPTG-inducible band of above 90 kDa could be detected in *E. coli* harbouring pKKPATGUS, but not in untransformed *E. coli*. This indicates that the fusion protein is present and IPTG-inducible as expected.

3.4 Discussion

This Chapter has described the construction of a chimaeric *pat::uidA* gene and the demonstration that when expressed in *E. coli* it is able to direct the synthesis of a stable fusion protein with both PAT and GUS activities. The construction of a bifunctional selectable-scorable marker by fusion of two independent coding sequences is not in itself a novel concept. Datla and co-workers (1991) reported the construction and use of a *uidA::nptII* translational fusion, the product of which

possessed both GUS activity and resistance to aminoglycoside antibiotics. They also demonstrated by size exclusion chromatography that the fusion product was active. Similarly, while the work reported in this thesis was in progress, Sunito and co-workers (1994) described using a *lacZ::nptII* gene fusion as a bifunctional reporter for gene-tagging studies. However, this is the first study of this type to use the *pat* gene, and is the first in which the reporter moiety has been fused downstream of the selectable marker. This may well be unimportant for studies where the selectable marker is used simply as a screen for transformants, but is an important advantage in a study of this type, since it ensures that expression of the reporter moiety indicates integration of the whole transgene, rather than a truncated version. If the *uidA* coding sequence were placed in front of the *pat* coding sequence, then it would be possible to obtain transgenic plants carrying a truncated version of the gene in which *pat* had been deleted, probably with no adverse effect on GUS activity.

The lack of a direct 1:1 correlation between increases in PAT and GUS activity in response to IPTG (Fig. 3.5) may have a number of explanations: (1) it may indicate that PATGUS was being cleaved *in vivo* or *in vitro* when its expression exceeded a certain level, the resultant products having different stabilities or catalytic activities relative to the fusion product. In this case PAT may have been less stable than GUS, or GUS was more active once cleaved from its N-terminus extension. However, this explanation contradicts the results of the PEG-precipitation and size-exclusion chromatography experiments (Sections 3.3.3 and 3.3.4). (2) A small amount of PATGUS cleavage may have occurred during the extraction procedure, but only to a noticeable degree when PATGUS was present at the higher levels of expression induced by 10 μM IPTG. (3) The high levels of PAT activity in the extract from cultures supplemented with 10 μM IPTG may have been above the linear range of the PAT assay used (the linear range of the GUS assay was found to be 2 orders of magnitude greater - data not shown), and such non-linearity prevented a direct correlation of induction of the two enzyme activities. The data are also complicated by the existence of high levels of background GUS activity in the XL1-Blue cells, which had no measurable background PAT activity.

The results of the IPTG-induction experiment also conflict with the result from the PPT-resistance experiment presented in Section 3.3.1, in which PPT resistance was clearly demonstrated in uninduced *E. coli* cultures carrying pKKPATGUS. This is likely to be highlighting the insensitivity of the *in vitro* PAT assay at these low levels of expression.

The molecular weight of the fusion protein, as estimated from the results of the size-exclusion chromatography experiments presented in Section 3.3.4, clearly suggests that it is a dimer, and the fact that both PAT and GUS activities elute together clearly indicate that the fusion is active. There was also evidence that the fusion was cleaved, making a direct correlation between PAT and GUS activity levels unreliable, although it seems likely that this was mainly happening during the extraction procedure: the cleavage appeared to be strongly correlated to the omission of the serine protease inhibitor PMSF from the extraction buffer, and much less free PAT enzyme could be identified when the inhibitor was included in the extraction buffer.

In conclusion, this Chapter has demonstrated the construction of a bifunctional gene, PATGUS, which, when expressed in *E. coli*, has both PAT and GUS activity. The amount of activity retained by both enzyme moieties was easily demonstrated when the fusion was expressed in *E. coli*. Although there was some evidence for cleavage of the fusion product, this was thought mainly to be an artifact of the extraction procedure, and maintenance of the fusion is not necessary in this study, as GUS activity can still be used as a marker for PAT activity, based on its production in the same cell. In Chapter 5, the PATGUS gene is introduced into *L. corniculatus* plants, and its properties *in planta* are investigated.

Table 3.1 Calculated primer annealing temperatures

Primer	Sequence	Tm_{OPT} (°C)
Primer A	CGG TCT AGA CCC GGG AGG AAG AAC AAT GAG CCC AG	68.9
Primer A (disregarding 5' degenerate sequence)	AAG AAC AAT GAG CCC AG	57.2
Primer B	GGC AGT GTG TCT AGC CTC CAC CTT CGC C	67.1
Primer B (disregarding 3' degenerate sequence)	CCT CCA CCT TCG CC	53.7

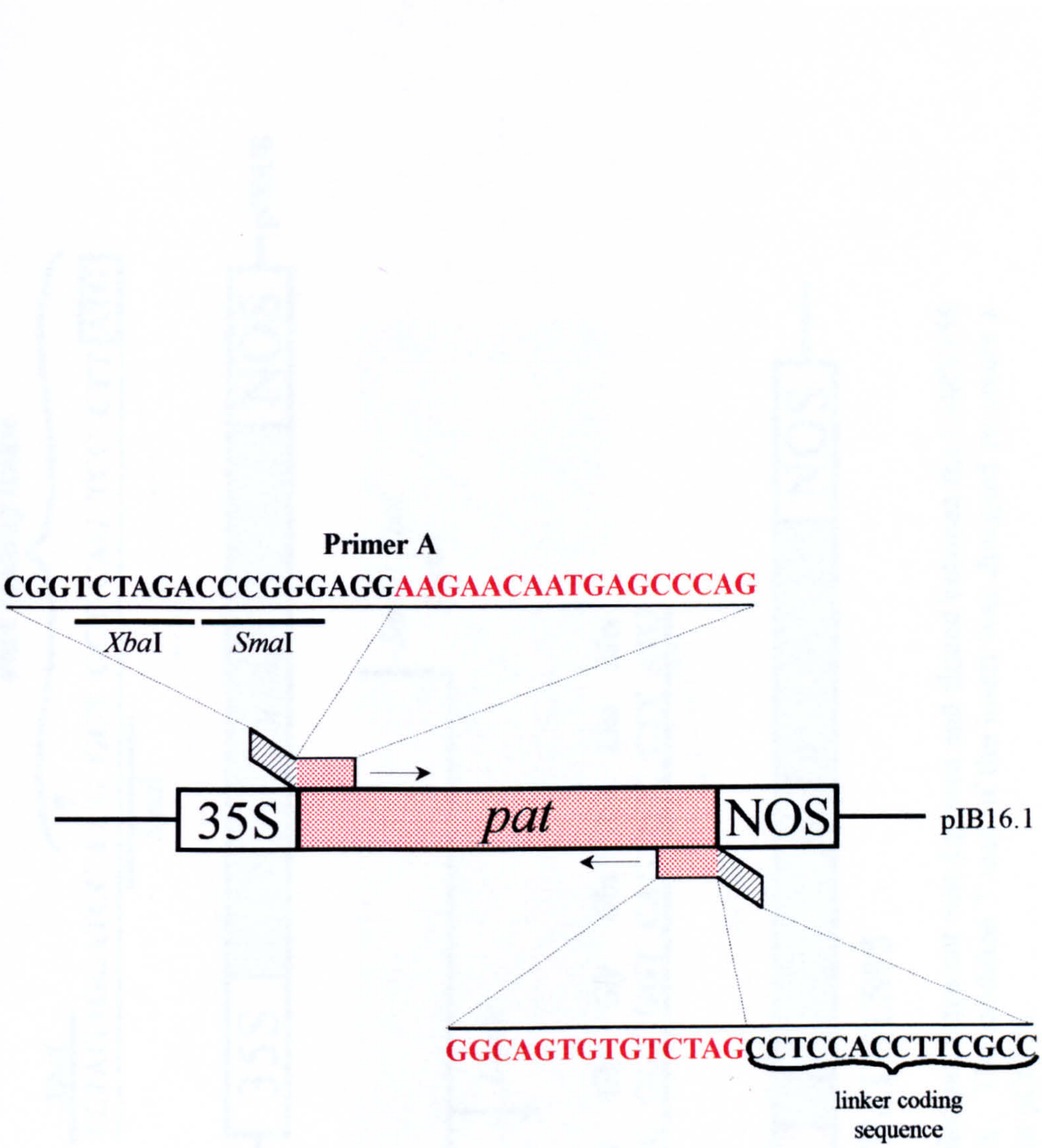

Figure 3.1: Strategy for PCR amplification and modification of the *pat* gene. Primer A was designed to anneal to the sequence surrounding the ATG codon of the *pat* coding sequence, and to include a mismatched 5' extension that included the two restriction sites, *Xba*I and *Sma*I to be used for subsequent cloning. Primer B included a mismatched 3' extension designed to replace the stop codon of the *pat* gene with a sequence encoding a flexible linker peptide (*Gly-Gly-Gly-Ser-Gly*).

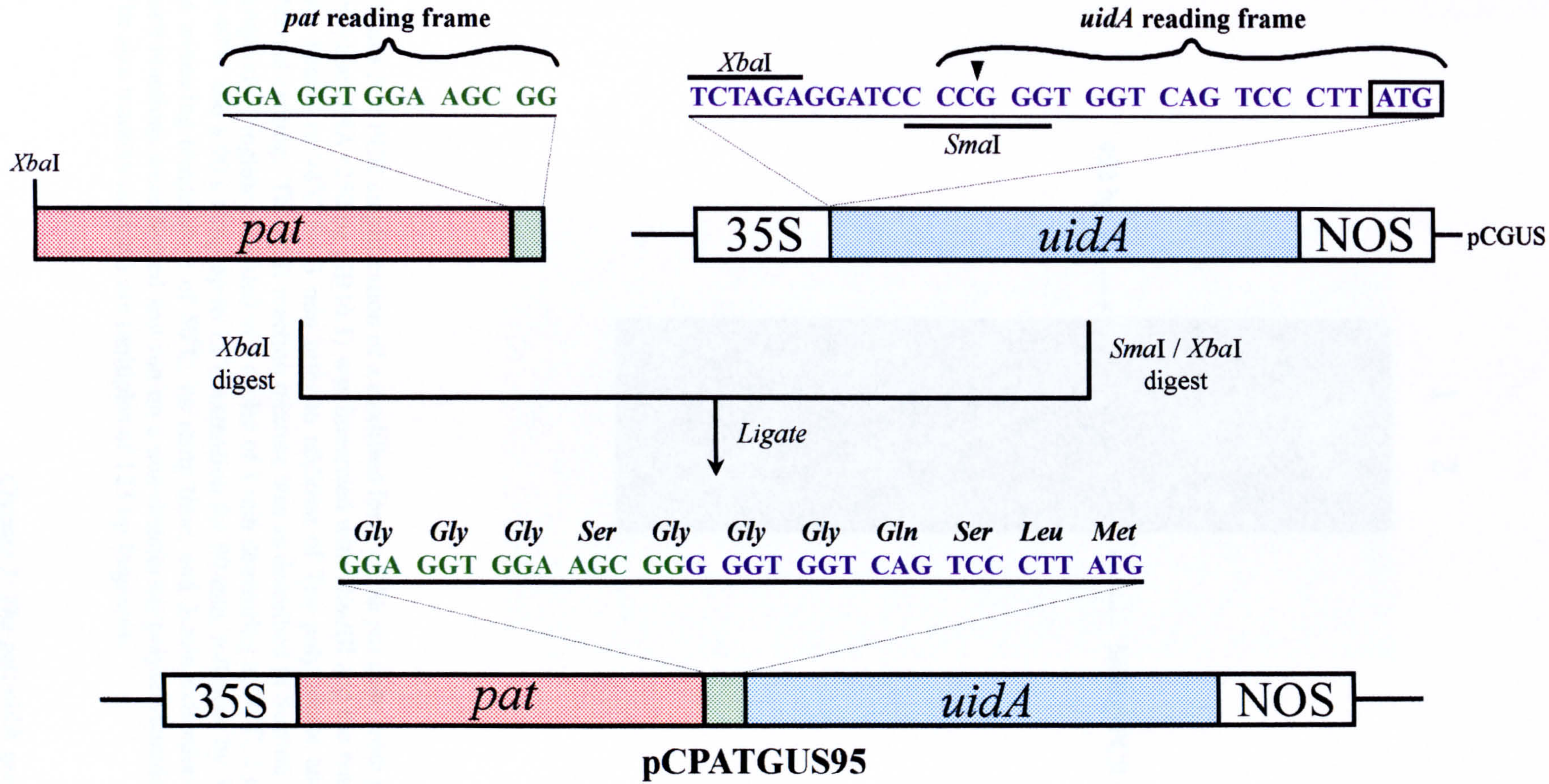

Fig 3.2: Construction of pCPATGUS95. The modified *pat* fragment was digested and cloned between the CaMV35S promoter and the *uidA* coding sequence of pCGUS. The modified 3' end of the insert was designed to create a translational fusion when blunt-end ligated to *Sma*I-cut pCGUS.

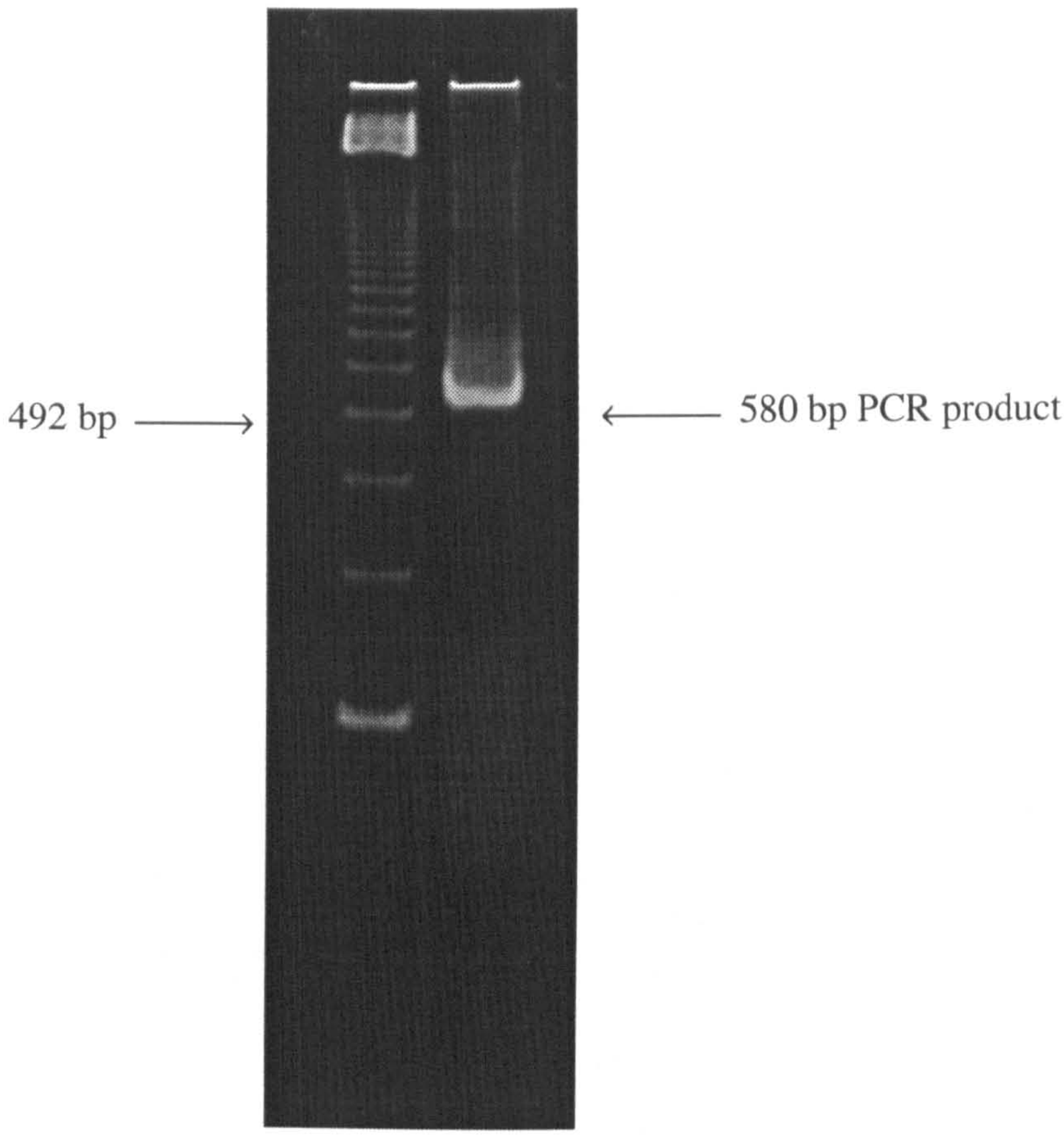

Figure 3.3: PCR amplification of a modified form of the *pat* gene from pIB16.1. The template DNA (250 pg pIB16.1) was linearised with *Hin*dIII and the reaction mixture was heated to 94°C for 3 min prior to addition of Taq polymerase and the start of thermal cycling. The PCR reaction mixture was as described in Section 2.6.3, and the temperature regime consisted of 5 cycles of 1 min denaturing at 94°C, 2 min annealing at 40°C and a 90 s ramp up to 72°C extension for 90 min, followed by 30 cycles with an annealing temperature of 50°C, no ramp time, and 2 min extension time. Three such reactions were pooled and run on a non-denaturing polyacrylamide gel (lane 2). The size markers in lane 1 are multiples of 123 bp fragments.

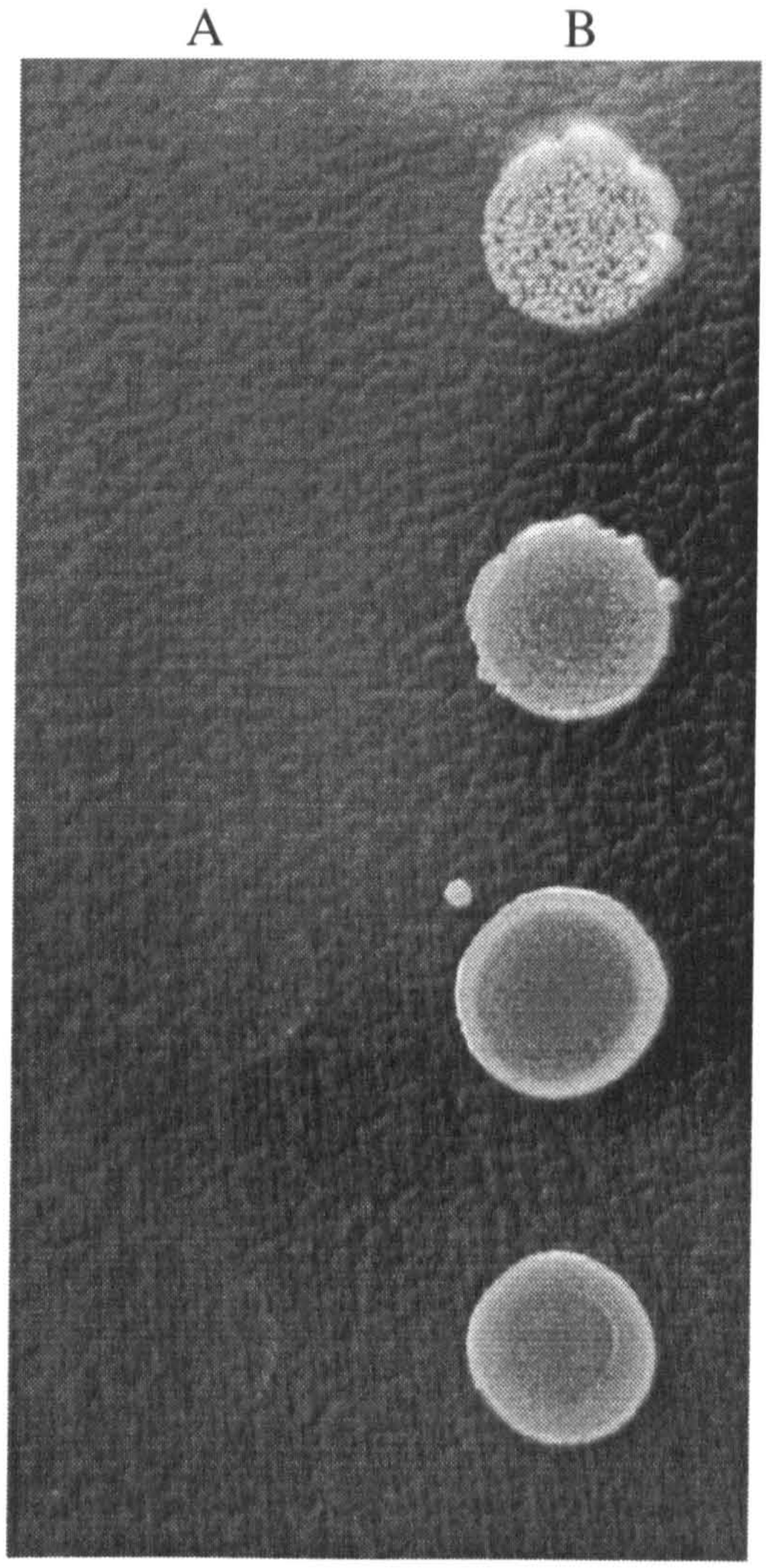

Figure 3.4: PPT resistance in *E. coli* expressing PATGUS. Single colonies of untransformed *E. coli* (A) and *E. coli* harbouring pKKPATGUS (B) were suspended in M9 minimal media (see Table 2.2). Cell density was estimated from the OD_{600} of the suspension, and then dilutions equivalent to 100, 1000, 10^4 and 10^5 cells in 10 μl made and spotted onto M9 agar plates containing 300 $\mu g.ml^{-1}$ PPT and 1 μM IPTG. Plates were incubated at 37°C for 3 days and then photographed.

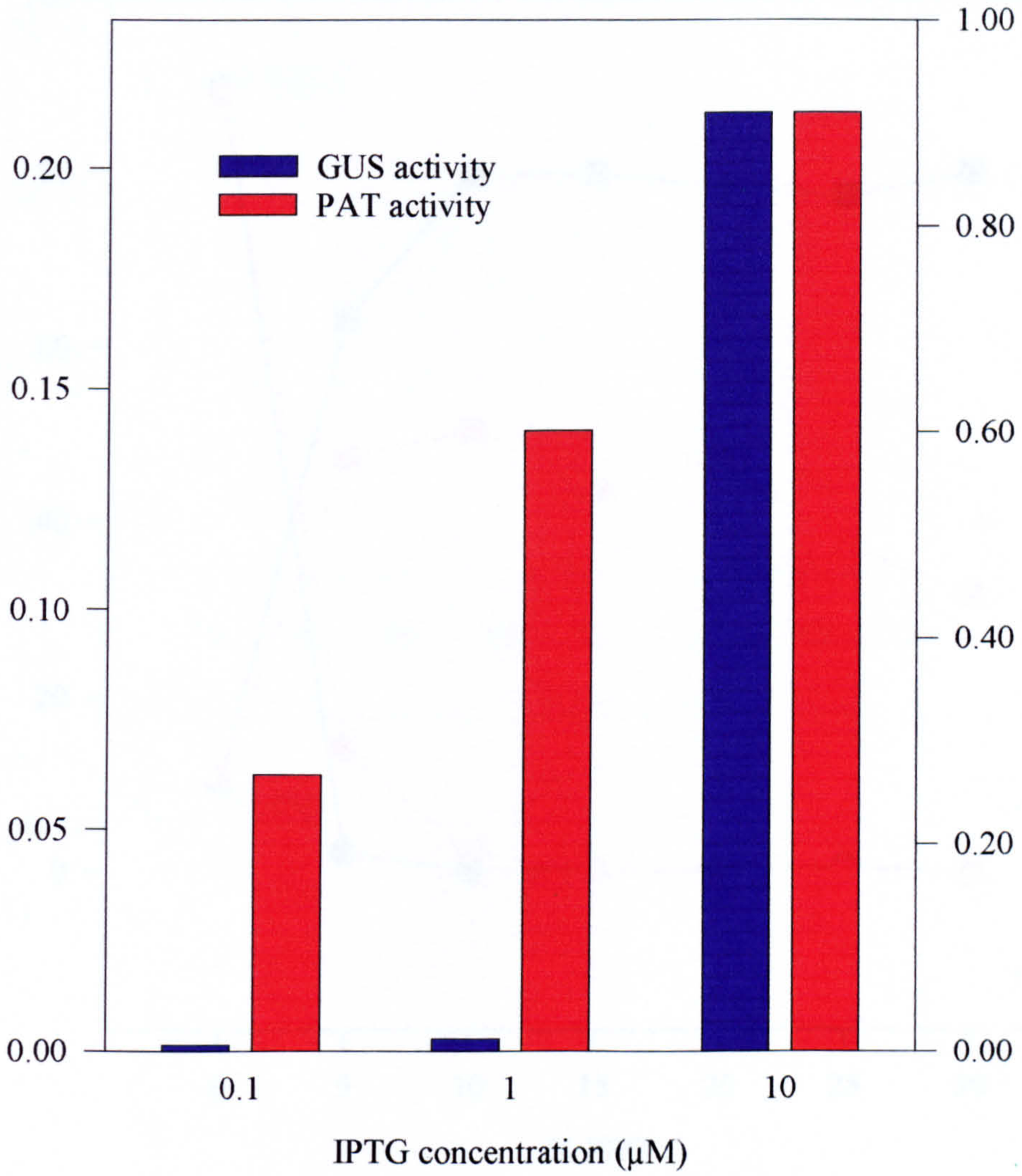

Figure 3.5: IPTG-induced PAT and GUS activity in *E. coli* carrying pKKPATGUS. Liquid cultures containing different concentrations of IPTG were inoculated with *E. coli* strain XL1-Blue harbouring pKKPATGUS (see Section 3.2.4) and grown to late-log phase. Crude cell extracts were prepared by sonication and clarified by centrifugation as described in Section 2.10.2. These were then assayed for PAT and GUS activity (see Sections 2.10.4 - 2.10.6.). GUS activity represented here is that obtained after subtracting the background level of endogenous activity measured in untransformed cultures of XL1-Blue. No background PAT activity was measured.

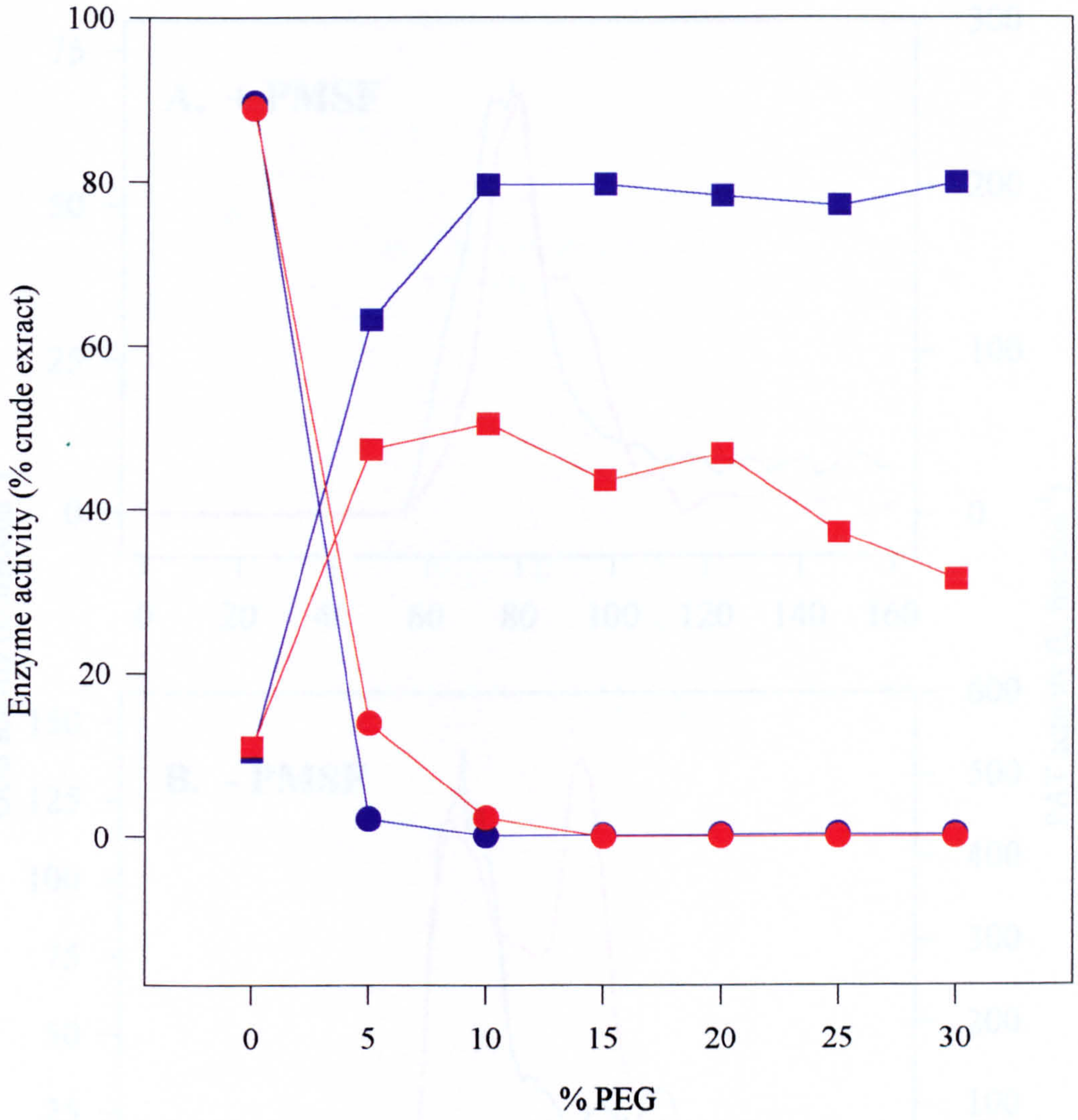

Figure 3.6: PEG precipitation of PATGUS. Crude extracts from *E. coli* expressing PATGUS were precipitated with PEG at different concentrations and centrifuged as described in Section 2.11.3, and the amount of GUS (●;■) and PAT (●;■) activity in the supernatant (●;●) and pellet (■;■) determined (see Sections 2.10.4 - 2.10.6) and is expressed as a percentage of the activity of the crude extract.

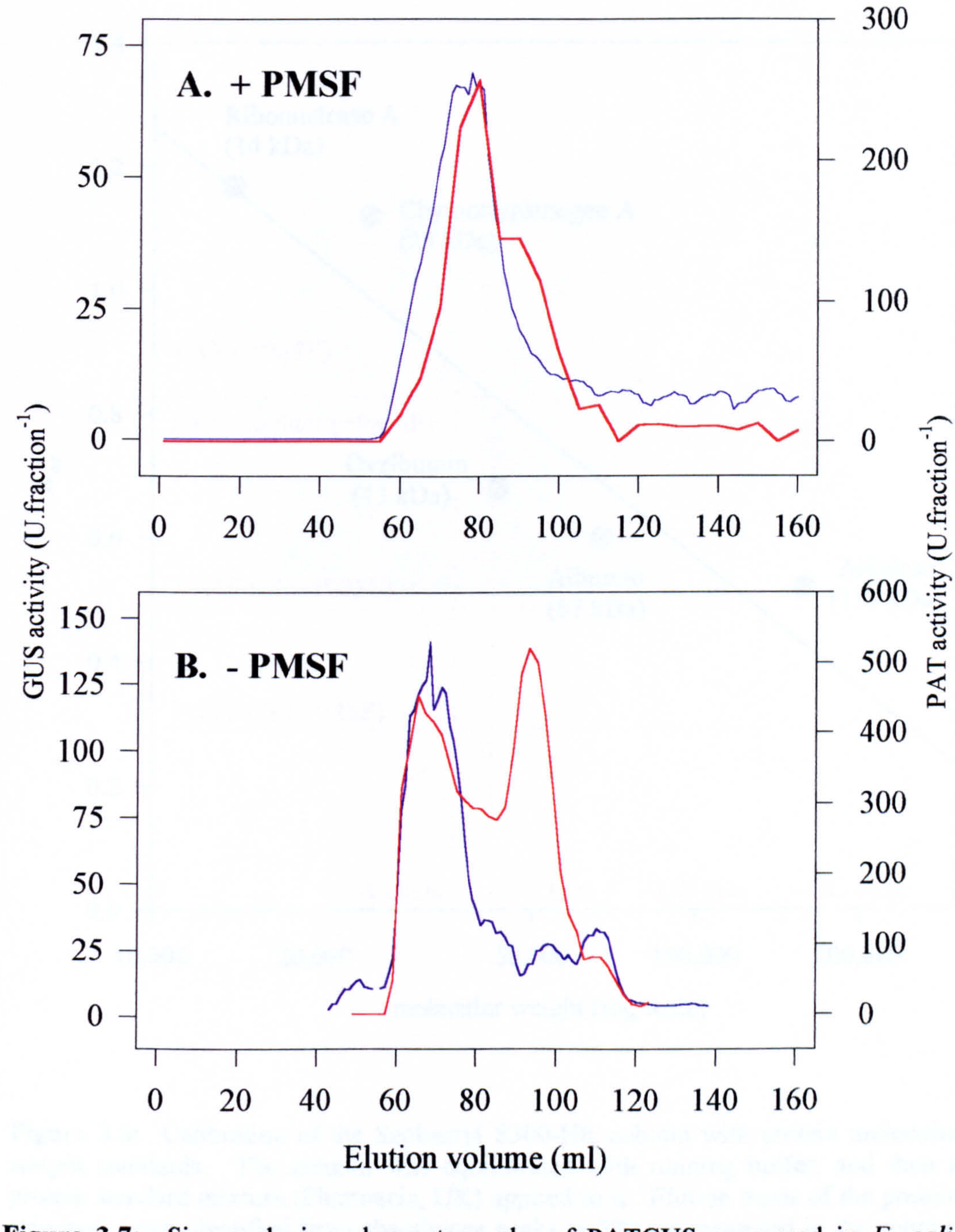

Figure 3.7: Size-exclusion chromatography of PATGUS expressed in *E. coli*. A: PMSF included in the extraction buffer. B: PMSF omitted. Crude extracts from *E. coli* expressing PATGUS were applied to an S300-HR size-exclusion column and 1 ml fractions collected and analysed for PAT (---) and GUS (---) activities (see Sections 2.10.4 - 2.10.6).

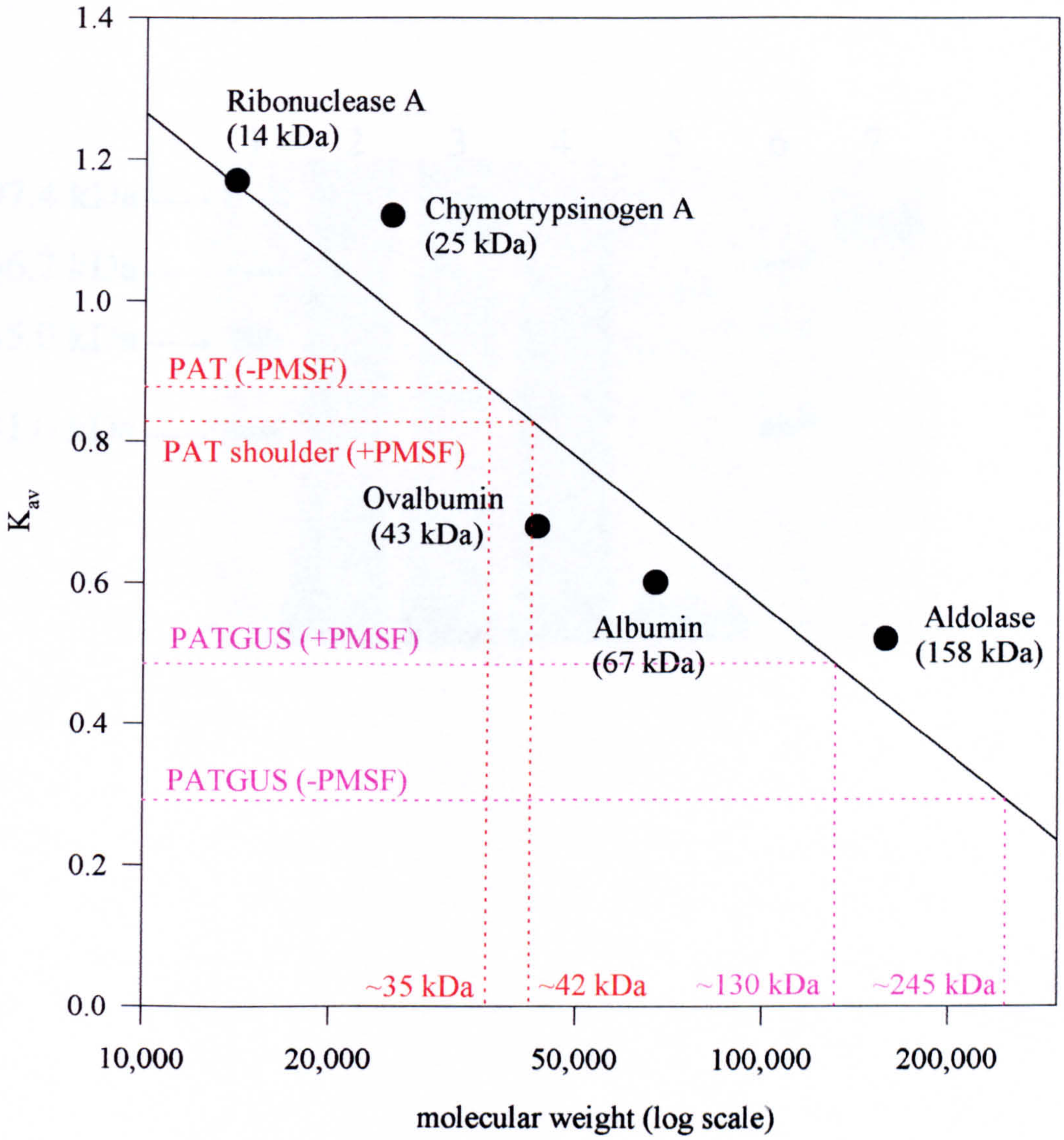

Figure 3.8: Calibration of the Sephacryl S300-HR column with protein molecular weight standards. The column was equilibrated with running buffer, and then a protein standard mixture (Pharmacia, UK) applied to it. Elution times of the protein standards were identified from absorbance peaks at 280 nm measured in the column eluent. Sample elution times were estimated from the enzyme activity profiles presented in Fig. 3.7. The K_{av}, a function of the column characteristics and the size of the protein, is calculated from the elution time thus (Pharmacia, 1995):

$$K_{av} = \frac{V_e - V_0}{V_t - V_0}$$

Where:

V_t = Total bed vol = $\pi r^2 . h$ = 97 ml.
V_0 = Column void vol = elution vol for blue dextran 2000 = 56 ml.
V_e = Elution vol of protein.

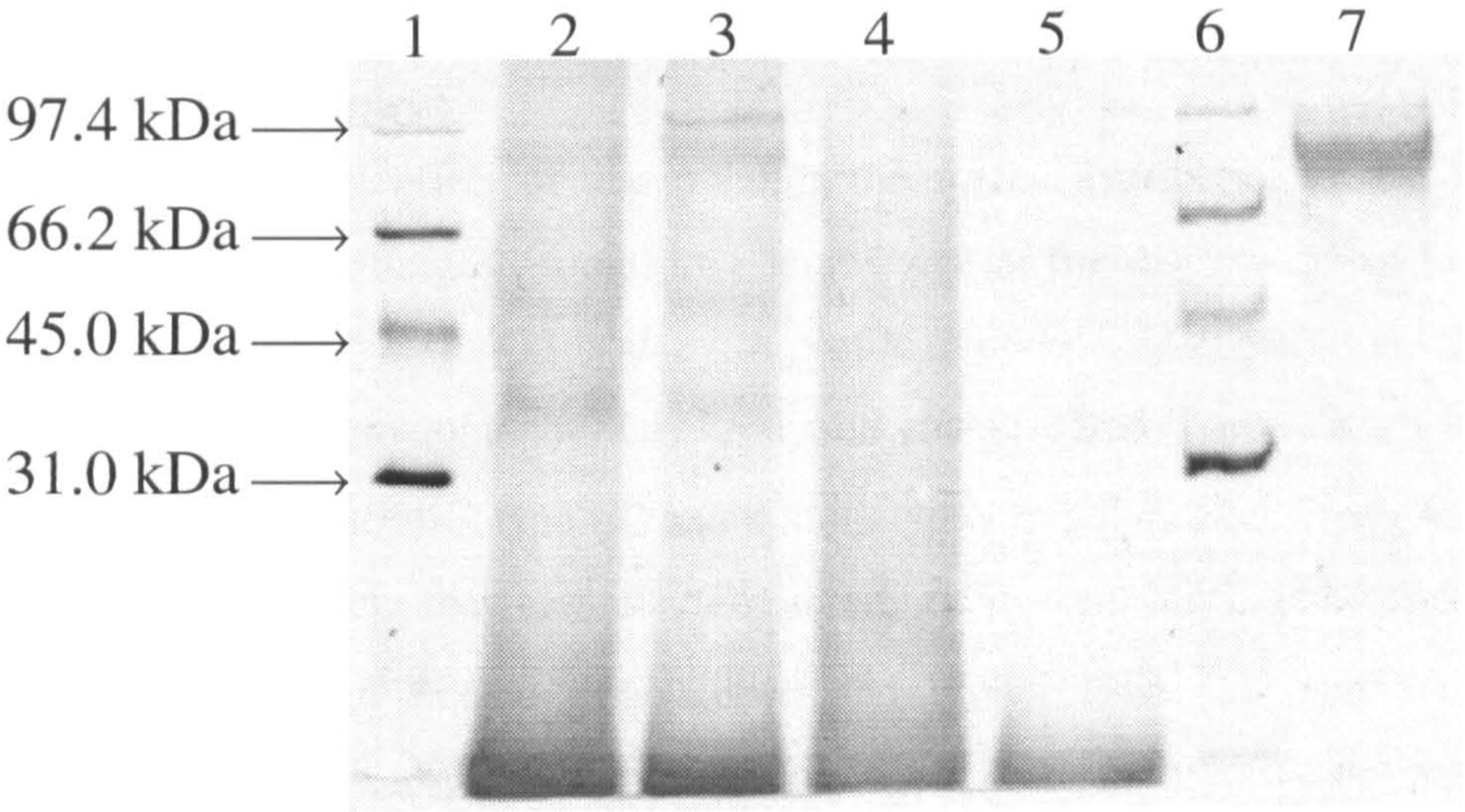

Figure 3.9: Western blots of extracts from *E. coli* expressing PATGUS probed with GUS-specific antisera. Ten μl of crude extract from *E. coli* expressing PATGUS were electrophoresed on a 10% polyacrylamide SDS-PAGE gel. The gel was blotted and probed with antibodies raised against GUS protein as described in Section 2.11.6. Lanes 1, 6: Protein molecular weight markers. Lane 2: *E. coli* harbouring pKKPATGUS, no IPTG induction. Lane 3: *E. coli* harbouring pKKPATGUS, induced with 1 mM IPTG. Lanes 4, 5: Untransformed *E. coli* (10 μl and 2 μl respectively). Lane 7: 2 μg GUS protein.

CHAPTER 4:

THE GS ISOENZYME PROFILE IN *LOTUS CORNICULATUS* ROOTS AND NODULES

4.1 Introduction

For a study of the effect of manipulating the spatial distribution of GS activity in nodules to be meaningful, some prior knowledge of the distribution of GS in these tissues is necessary. The GS isoenzyme profile in nodules of *P. vulgaris* (obtained by ion-exchange chromatography) has been well characterised (Lara *et al.*, 1983), and it is thought that both root-type (β) and nodule-type (γ) polypeptides are present in the infected cells, where they can assemble in any ratio, resulting in the formation of all combinations from $\beta_8\gamma_0$ to $\beta_0\gamma_8$ (Robert and Wong, 1986; Cai and Wong, 1990). Information is also available on GS isoforms and their distribution and regulation in *P. sativum*, *G. max*, and *M. sativa* (Sengupta-Gopalan and Pitas, 1986; Vézina *et al.*, 1987; Walker and Coruzzi, 1989). Species to date have been shown to achieve high levels of GS activity in the nodule either by up-regulating one of the isoforms found in roots, as is seen in *P. sativum* (Walker and Coruzzi, 1989), or, more commonly, by the expression of a nodule-specific isoform, as has been shown to be the case in *P. vulgaris, G. max* and *M. sativa* (Lara *et al.*, 1983; Sengupta-Gopalan and Pitas, 1986; Vézina *et al.*, 1987). However, at the time of writing there are no published data on the GS isoenzymes in *L. corniculatus* nodules.

Knight and Langston-Unkefer (1988) were able to demonstrate clearly that tabtoxin inhibited the root-type GS of *M. sativa* (whilst leaving the nodule-type largely unaffected) by comparing isoenzyme profiles of plants infected with Tox^+ and Tox^- strains of *P. syringae*, and showing that the peak that eluted with the root isoform was absent when the plants were infected with the Tox^+ strain. Like *P. vulgaris*, *M. sativa* expresses a nodule-specific form of GS, which can be resolved from the root isoenzyme by this technique (Knight and Langston-Unkefer, 1988), making such an approach possible. It was hoped that the corresponding isoenzymes of *L. corniculatus* would also be resolvable in this way, allowing a similar comparison to be made.

This chapter describes the elucidation of the GS isoenzyme profile in nodules of *L. corniculatus*, and the effect of nitrate on this profile. A simulation model is described which was used to examine the proposition that the profiles obtained resulted from the interactions of two distinct isoforms in the infected cells of the nodule.

4.2 GS isoenzymes in roots and nodules

The GS isoenzymes were separated by ion-exchange chromatography of extracts as described in Section 2.11.2. The method chosen was based on that used by Lara *et al.* (1983) to separate GS isoforms from *P. vulgaris* and *P. sativum* nodules, and employed a KCl gradient rising from 0 mM to 400 mM KCl over 60 fractions.

Fig. 4.1 shows the results obtained with extracts from roots and nodules of N_2-fixing plants harvested 28 d after rhizobial inoculation, and from roots of unnodulated, nitrate-fed plants of the same age. There are very marked differences between the three isoenzyme profiles. Roots of unnodulated plants showed two peaks of GS activity (peaks I and III in Fig. 4.1): only one of these peaks (peak III) was detectable in the roots of nodulated plants and contained much less GS activity than in the nitrate-fed roots (expressed per g fresh weight of tissue).

Western blots of selected fractions showed that peak I from nitrate-fed roots contained a GS polypeptide of M_r 45 kDa, which corresponded in size to the major leaf form (Fig. 4.2C, lane 3). Peak I, therefore, appears to correspond to GS2. Peak III in nitrate-fed and nodulated roots contained a 39 kDa polypeptide, which is most probably a GS1 subunit.

Nodules showed one peak of GS activity (peak II), which eluted between, but overlapped with, the two peaks seen in unnodulated roots. This peak was specific to nodules, being absent from all preparations from other tissues examined, and thus appears to correspond to a nodule-specific form of GS1. Western blots showed that peak II was composed of more than one size of polypeptide (Fig. 4.2A). The leading edge of this peak contained mainly a GS polypeptide identical in size to that of the putative GS2 subunit in peak I from unnodulated roots, suggesting that there was some GS2 in the nodule, and that peak I was not resolved from peak II in this fractionation. All fractions from peak II that were analysed contained a GS

polypeptide corresponding in size to that found in peak III (Fig. 4.2A, lanes 3-6), and fractions up to and including fraction 41 also contained a slightly larger polypeptide, forming a doublet of M_r 39 kDa with the other GS1-type polypeptide (lanes 3-5). Thus, peak II contains at least two GS1-type polypeptides, the leading edge being enriched for a slightly larger form, whilst the most abundant polypeptide present is indistinguishable, in both size and charge, from that found in the root in peak III.

The major peaks in root and nodule extracts run on this initial gradient eluted at 270 and 220 mM KCl respectively, which was too close to allow a clear demonstration of the existence of a root-type GS isoform in nodule extracts. In an attempt to obtain better resolution in this region, the gradient was modified so that the KCl concentration rose rapidly to 150 mM over 20 fractions, then climbed slowly to 300 mM over 30 fractions, and then rose rapidly over the final 20 fractions (Fig 4.3). This revealed a number of shoulders to peak II (IIa-IId in Fig. 4.3). It would appear from this that the nodule-specific form can be resolved into at least 4 different isoforms. There was also a minor peak at the trailing edge of peak II, which corresponded to peak III from root extracts, suggesting that a small amount of the isoform found in roots was also present in the nodule extracts.

4.3 Effect of developmental stage on the isoenzyme profile

In *P. vulgaris*, the GS isoenzyme profile changes with nodule age. In young nodules, the root-type isoform predominates, whereas as the nodule matures, this activity decreases and is replaced by the nodule-specific isoform (Lara *et al.*, 1983). To examine the changes that occur in the GS isoenzyme composition during nodule development in *L. corniculatus*, nodules were separated into three broad categories at harvest: small, almost white nodules with very little leghemoglobin (stage I), medium-sized, bright pink nodules (stage II), and large, deep-red nodules (stage III). Fig. 4.4 shows the isoenzyme profiles obtained in this experiment. Although GS activity clearly increased between stages I and III, there were no major qualitative differences in the isoenzyme profiles. Unlike *P. vulgaris*, there was no evidence of a transition from a root-type profile to a nodule-type: the profile characteristic of the nodule was seen even in the youngest nodules.

4.4 Effect of nitrate on the isoenzyme profile

Nitrate has been shown to induce GS in the roots of a number of species, including *V. faba, P. sativum, L. corniculatus* and *L. japonicus* (Barratt, 1981; Vézina and Langlois, 1989; Woodall, 1994), and the increase in GS activity has in all cases been shown to be due partly to induction of GS2 (the marked effect of nitrate nutrition on the GS composition of *L. corniculatus* roots can be seen in Fig. 4.1). In contrast, the effect of nitrate on GS in nodules has received little attention. To investigate whether nitrate treatment of already nodulated roots would alter the GS composition of the nodule, N_2-fixing plants 28 d after rhizobial inoculation were treated with 10 mM nitrate for 5 d prior to harvesting. Extracts were run on a KCl gradient which rose from 0 mM KCl to 300 mM KCl over 20 fractions, then eluted at 300 mM KCl for a further 50 fractions. Fig. 4.5 shows how the nitrate treatment affected the profile. Nitrate appeared to shift the elution profile so that the main peak moved from fraction 33 to fraction 39. However, the overall shape of the peak appeared to be largely unaltered, and was intermediate in its elution characteristics between the peak seen with untreated nodules and the major root peak which eluted at fraction 50 in this experiment.

More detailed examination of this phenomenon confirmed this result but showed that the timing of the changes was variable between experiments (Figs 4.6 and 4.7). In the experiment shown in Fig. 4.6, the nitrate-induced changes in the elution profile were seen after only 12 h of treatment, and by 24 h the profile was indistinguishable from that of the root. When the experiment was repeated (Fig. 4.7), no changes in the profile were evident at 2 d and it was only after 6 d that the transition to the root-type profile had been completed. A possible explanation for the difference between the timing of events in these two experiments is that the plants used in Fig. 4.6 were poorly nodulated while those used in Fig. 4.7 were well-nodulated. Although the results shown in Fig. 4.7 were from an *A. rhizogenes*-transformed line, this is not thought to be significant since similar results were obtained with well-nodulated plants of an untransformed line (not shown).

4.5 A simple model of the GS isoenzyme profile in nodules

The rapid change in the GS isoenzyme profile seen in response to nitrate treatment was unexpected and intriguing. It could be caused by modifications to the holoenzyme, such as glycosylation or phosphorylation, or could be the result of a shift in the relative abundance of the individual polypeptide types present in the cytosol of the infected and/or uninfected cells.

As an aid to examining this phenomenon, and as an attempt to explain the complex elution profile seen in nodule extracts, a simple model was constructed to predict the pattern of elution peaks that would be expected for a range of ratios of two different types of polypeptides present in the cytosol. Based on this model, a computer simulation was constructed which predicted elution profiles based on hypothetical ratios of subunits with different elution properties. It was hoped that this simulation would help to discriminate between the alternative hypotheses.

4.5.1 Basic principles and assumptions

To produce a working model, it was necessary to adopt a number of assumptions and general principles with which to work. These are shown graphically in Fig. 4.8, and explained below.

1. *GS isoenzymes in nodules of* L. corniculatus *are octameric and assembled from two distinct polypeptides that confer different elution characteristics on the holoenzyme.* The polypeptide composition of the holoenzyme from *L. corniculatus* nodules has not yet been elucidated. One major assumption of the model is that this holoenzyme is assembled from two distinct polypeptide populations in a situation analogous to that seen in *P. vulgaris*, where both β and γ polypeptides are expressed in the infected cells of the nodule (Cullimore *et al.*, 1984). This assumption would appear to be reasonable since the peak of GS activity seen in the ion exchange separations is more complex than that which would be expected for a homogeneous population (Fig. 4.3). Furthermore, two GS1 polypeptides with slightly different electrophoretic mobilities were detected in Peak II of the isoenzyme profile from nodules (Fig. 4.2A). The two populations of polypeptide in the model will be referred to as A-type and B-type, with A-type polypeptides

eluting at a lower salt concentration than B-type. The possibility that the upper band of the doublet corresponds to A-type and the lower band to B-type is discussed in Section 4.6.3.

2. *The elution characteristics of the holoenzyme are altered in a predictable way by changes in the relative amounts of the two subunit types.* It is assumed that the octameric holoenzyme will elute at a position that reflects the relative proportions of the two polypeptide types. Thus, for example, a holoenzyme composed of five A-type polypeptides and three B-type polypeptides will elute at a lower salt concentration than one composed of three A-type polypeptides and five B-type polypeptides, but at a higher salt concentration than the A-type homooctamer. The observed profile will be the composite result of a heterogeneous population of such octamers with slightly different elution characteristics reflecting their differing subunit compositions. It is also assumed that this would affect elution from the column in a linear way, so that each successive substitution of A-type by B-type would result in the same increase in the salt concentration at which the holoenzyme eluted.

3. *Polypeptides assemble randomly within the cell.* It is assumed that within a cell that is expressing both types of polypeptides, the octameric holoenzyme is randomly assembled, and the different polypeptide types show no preferences to assembly with polypeptides of the same type. Thus, the ratio of A-type to B-type subunits in the holoenzyme will tend to reflect their relative proportions in the overall subunit population, which in turn will be determined by the relative levels of expression and turnover of the subunit types.

4.5.2 Calculations involved

The computer program that was written to calculate the relative heights of the individual sub-peaks making up the overall complex peak is presented in Appendix III, and details of the calculations involved are included in the accompanying text.

4.5.3 Model predictions

Fig. 4.9 shows the result of superimposing a normal distribution onto each of these values to simulate the effect of the column, and summing to give the final profile. As Fig. 4.9 illustrates, small changes in the relative proportions of the two subunit types have a considerable effect on the predicted elution profile. A range of profiles were compared visually with the observed profile, and the results predicted for 79% A-type found to correlate most closely with the experimental data. The similarity between the observed and predicted profiles is quite striking, suggesting that in mature nodule tissues there is a roughly 4:1 ratio of A-type to B-type polypeptides.

4.6 Discussion

4.6.1 General characteristics of the elution profiles of GS from roots and nodules of *L. corniculatus*

The elution profile in Fig. 4.1 clearly shows that the main peak of nodule GS activity eluted earlier than the main peak of GS activity observed in roots (either from nodulated or nitrate-grown plants). A smaller peak, which eluted before any of the other GS samples, was also present in extracts from nitrate-grown roots. All of the peaks eluted within the ionic range usually reported for GS2: the majority of reports so far indicate that GS1 elutes up to about 150 mM KCl, with GS2 eluting from 150 mM to 330 mM KCl (Cullimore *et al.*, 1983; Lara *et al.*, 1983; McNally and Hirel, 1983). However, isoforms of GS1 which elute in the range seen here have been reported for *Hordeum vulgare* (200-230 mM; Wallsgrove *et al.*, 1987; Mäck, 1995) and Bennett and Cullimore (1989; 1990) reported values of 190 mM and 280 mM for isolated β_8 and α_8 GS octamers respectively from *P. vulgaris* when subjected to re-chromatography or heterologous expression in *E. coli*. Western blotting of the fractions as presented in Fig. 4.2 clearly identified the peak at 190 mM as being the band of lower electrophoretic mobility. Since this was also the predominant band present in shoot extracts, it seems reasonable to assume that this represents the plastidic form, GS2, and contrasts with the other peaks, which corresponded to the presumed GS1 doublet of higher electrophoretic mobility. This situation is also very unusual, as it indicates that GS2 is eluting *before* GS1 in *L. corniculatus* extracts. However, a similar situation has also been observed in some species of *Pinus*, in

which GS2 elutes at a concentration of about 90 mM KCl whilst GS1 elutes at 200 mM KCl (Vézina *et al.*, 1988; Vézina and Margolis, 1990; Elmlinger and Mohr, 1992).

4.6.2 What is the molecular basis for the nodule-specific isoform?

The fractionations presented here clearly show the presence of a distinct peak of GS activity that is associated with the nodule (Fig. 4.1, peak II). Furthermore, 1D western analysis revealed that this peak was composed of two polypeptides of similar size; one which was indistinguishable from that found in the root peak, and one which was slightly larger (Fig. 4.2). The two polypeptides in this putative GS1 doublet showed different elution patterns. Both polypeptides were detectable in roots and nodules and the lower band always predominated, although the upper band appeared to be associated primarily with the leading edge of the nodule peak. Further analysis of fractions from peak II by 2D SDS-PAGE revealed that it contained 4 distinct isoelectric-focussing variants (J. Woodall, personal communication), but the pattern in roots and leaves has been shown to be identical to this (Woodall, 1994), and no distinct nodule-specific polypeptide has yet been identified by 2D analysis (J. Woodall, personal communication). Using a *P. vulgaris gln-β* probe, Thykjær and co-workers have since isolated a GS1 clone from a *L. japonicus* nodule cDNA library (Thykjær *et al.*, 1997) and found it to be the same as that independently isolated from a root library by Waterhouse and co-workers (Waterhouse *et al.*, 1996). Neither group has yet identified any other GS1 sequences in *L. japonicus*, which may suggest it is the same gene being expressed in both tissues. If this is the case in *L. corniculatus*, then either the novel GS isoenzyme identified in nodules, or the root isoenzyme, must be the result of some post-translational modification of the holoenzyme (or subunits) which does not show up on 2D gels. However, it should be noted that the Southern blots presented by Thykjær *et al.* had more bands at low stringency, which suggests the existence of more than one GS gene. It is also worth mentioning that, unlike *L. japonicus*, *L. corniculatus* is a tetraploid and therefore will have 2 similar copies of any GS gene. Using a PCR approach with primers designed from highly conserved regions in known plant GS sequences, Woodall (1994) demonstrated up to 5 reaction

products of different sizes, although this is far from proof for multiple GS genes. At the time of writing, there are no accessions in either the GENBANK or EMBL databases for GS genes from *L. corniculatus*, and further work on the molecular basis for the isoforms observed in this study is clearly needed.

The lower band of the GS1 doublet eluted over a very broad range of salt concentration, which started prior to fraction 34 (200 mM KCl) and was still detectable in fraction 52 (340 mM KCl). This is much broader than would be expected for a single protein, and has two possible explanations: it may indicate that the lower band detected in the western blots is itself not homogeneous, or it may be evidence that the polypeptide is associating with another polypeptide (e.g. the upper of the 39 kDa doublet) to form an array of heterologous holoenzymes with slightly different elution characteristics. The computer simulation model was constructed as a way of testing the latter hypothesis, and is discussed in Section 4.6.3 below.

4.6.3 What can the model tell us about the elution profile?

The presence of greatly increased amounts of GS activity in the nodule compared to the root can be explained in a number of ways. It could be due to up-regulation of the root isoform, enhancement of one or more of a number of isoforms which are also found in the root, expression of a nodule-specific isoform, or a combination of these. The elution profiles presented in this Chapter clearly show that the nodule isoform eluted at a lower KCl concentration from ion exchange chromatography, indicating the presence of a distinct isoform which appears not to be present in roots, pointing to a similar situation to that found in *P. vulgaris*. The model presented in Section 4.5 was constructed as a way of testing the hypothesis that the GS holoenzyme in *L. corniculatus* is constructed from heterologous subunits, as is thought to be the case in *P. vulgaris*. The assumption was that cytosolic GS in the nodule is made up of two different species of polypeptides, one (B-type), which is expressed in the root and the cortical and infected zone of the nodule, and another (A-type), which is expressed solely in the infected cells of the nodule (see Forde *et al.*, 1989). In all the profiles of nodule extracts that were obtained, the peak of GS activity appeared to be characterised by a sharp leading edge with no more than one shoulder, followed by a long tail in which a number of shoulders could be identified. The model predicts

that for high A-type:B-type subunit ratios in the nodule, the profile should have this characteristic shape (see Appendix IV). Close comparison between a typical profile and the prediction which matches it most closely (Fig. 4.9; 79% A-type) shows a very significant correlation between the predicted and experimental data.

This clearly suggests that peak II is, in fact, a range of heterooctamers produced by the association of two polypeptides with different elution positions. However, since the model also predicts a 4:1 ratio of A-type to B-type subunits, it very unlikely that the slower-moving polypeptide of the 39 kDa doublet is the A-type subunit in question: it is less abundant than the lower band in the fractions blotted from peak II (Fig. 4.2A). Thus, the nodule-specific polypeptide may be indistinguishable in size from the root polypeptide.

Comparison with the model also highlights the small peak at the trailing end of the profile, which is not present in the prediction (Fig. 4.9). This may be attributable to the presence of the root isoform, and thus may represent expression of solely B-type polypeptides in a small fraction of cells in the nodule, where they are unable to interact with A-type polypeptides (presumably in uninfected cells within the nodule and/or in the cortical region surrounding the infected zone; see Forde *et al.*, 1989).

4.6.4 The effect of nodule developmental stage

Nodules harvested at very early stages of development (Fig. 4.4; stage I) contained very little leghemoglobin, indicating that they were at or just prior to the onset of N_2 fixation, as has been shown to be the case for *P. vulgaris* (Robertson *et al.*, 1975; Padilla *et al.*, 1987). Previous reports on a number of species (Lara *et al.*, 1983; Sengupta-Gopalan and Pitas, 1986; Konieczny *et al.*, 1988; Egli *et al.*, 1989) indicate this to be approximately coincident with the onset of nodule-specific GS activity. Even at this very early stage in development, the profile is clearly that of the nodule isoform. This may suggest that the onset of this nodule-specific peak of GS activity in *L. corniculatus* is earlier than the onset of N_2 fixation, thus implying primarily developmental regulation of its expression in this species. Whilst work needs to be done to confirm this preliminary observation, it is of interest as there has been considerable debate as to whether GS in the nodule is under primarily developmental or nutritional control (see Section 1.1.6).

Under nitrate-free conditions, none of the GS isoenzyme profiles obtained from nodules showed more than a very minor peak with the elution characteristics of that found in roots, regardless of nodule developmental stage. Thus, the nodule-specific form is by far the major form present in nodules of *L. corniculatus*. This contrasts with the situation in *P. vulgaris*, where the root form represents a significant fraction of the total nodule GS (Lara *et al.*, 1984; Bennett and Cullimore, 1989; Cai and Wong, 1990).

4.6.5 What is the molecular basis for the effect of nitrate on GS in nodule extracts?

As seen in Figs 4.5 - 4.7, nitrate has a dramatic effect on the elution profile of nodule extracts, apparently causing it to revert to the profile seen in roots. This seems to be the first report of a qualitative effect of nitrate on GS isoenzymes in the nodule. Assuming the holoenzyme is heterologous as was discussed earlier (see Sections 4.6.2 and 4.6.3), there are two plausible explanations for this: (a) changes in the ratio of subunit types within the cell, or (b) post-translational modifications to the existing nodule-specific holoenzyme.

(a) Changes in subunit composition

This hypothesis has two requirements. Firstly, there must be rapid breakdown or inactivation of the GS holoenzyme present in the cytosol at the initial timepoint, to account for the rapid disappearance of the nodule-specific activity peak. Evidence presented later in this thesis suggests that the turnover of GS within the nodule is rapid, as it is quickly replaced after irreversible inhibition with PPT (see Section 6.3 and Fig. 6.2A). There are also reports suggesting that nitrate causes rapid shutdown of N_2 fixation concomitant with changes in oxygen tension within the central infected region of the nodule (Faurie and Soussana, 1993; Denison and Harter, 1995). This is at first reversible, but becomes irreversible after a few days and marks the start of nitrate-induced nodule senescence in which first leghemoglobin and subsequently the majority of soluble proteins are broken down and remobilised (Walsh, 1995). GS present in the nodule may also be rapidly broken down under these conditions. Temple and co-workers, for example, have recently presented evidence that the maintenance of the nodule-specific GS isoenzyme from *G. max* in a stable, correctly assembled, active form is dependent on active N_2 fixation, with

the nodule-specific form from *fix*$^-$ nodules being considerably more labile *in vitro* than the same enzyme from *fix*$^+$ nodules (Kunjibettu *et al.*, 1996; Temple *et al.*, 1996; Temple and Sengupta-Gopalan, 1997).

Secondly, there must be a gradual decrease in the production of nodule-type subunits, coupled with their replacement in the cytosol by a gradual increase in the production of root-type subunits. If the different isoforms of GS in roots and nodules of *L. corniculatus* are the product of differential expression of two genes as is the case in *P. vulgaris*, then this would be achieved by gradual inhibition of expression of the nodule-type subunit, coupled with gradual induction of the root-type subunit in the same cells. Alternatively, if the difference between the two subunit types is derived from post-translational modifications prior to holoenzyme assembly, then the shift would be seen either if there was a gradual decrease in the efficiency of the modification mechanism (if the polypeptide in nodules represents a modified form of the polypeptide expressed in roots), or vice-versa. Likely candidates for modification mechanisms are glycosylation and/or phosphorylation (discussed below with reference to holoenzyme modifications).

(b) Post-translational modifications and/or changes in activation of the holoenzyme

Alternatively, changes in the elution characteristics of the holoenzyme could be the result of post-assembly modification of the holoenzyme. Glycosylated GS has been reported in leaves of *Nicotiana tabacum* (Nato *et al.*, 1984) but, whilst Woodall (1994) found that some charge variants of GS from *L. japonicus* were glycosylated, removal of these residues had no effect on migration of the protein, indicating little effect on overall charge. The possibility of glycosylation of GS in *L. corniculatus* under the unusual conditions described here has not been investigated and warrants further attention.

Phosphorylation is another mechanism that could be implicated. Nitrate reductase (NR) is known to be subject to regulatory control by phosphorylation (Douglas *et al.*, 1995; Chandok and Sopory, 1996; MacKintosh, 1997). Whilst phosphorylation as a method of GS regulation has not yet been reported, recent work by MacKintosh (personal communication) suggests that it may be subject to a similar mechanism. This possibility is discussed further in Section 4.6.7.

4.6.6 Why is the timing of the change in the GS elution profile variable?

Figs 4.5 and 4.7 clearly indicate that the shift in the elution profile of GS in response to nitrate can take about 5-6 days to complete. This was seen in both untransformed plants, and in plants transformed with *Agrobacterium rhizogenes*, thus expressing the hairy root phenotype. However, as Fig. 4.6 shows, the shift can take place over a much shorter time period, but the plants used in this experiment were poorly nodulated, and this may be the reason for the difference. When a nodulated plant is exposed to nitrate, there may be some regulatory mechanism that senses that the nodules are no longer needed, and diverts nitrogen assimilation from N_2 fixation to nitrate reduction. In a well-nodulated plant, there is a large flux of nitrogenous compounds from the N_2-fixing nodule, and it could take some time for nitrate reduction in the roots to reach a level that challenges this. However, in poorly-nodulated plants, the flux of nitrogen from the nodules is much smaller. Thus, the proportion of plant nitrogen intake by nitrate uptake and reduction rapidly surpasses that contributed by N_2 fixation, switching the plant from fixation to assimilation much more rapidly. This shift is accompanied by changes in the elution characteristics back to that of a root-type profile.

4.6.7 Discrepancy between GS activities and GS protein levels

There is some discrepancy between the total amounts of immunoreactive polypeptides as detected on the western blots and the activities of the corresponding fractions from the ion exchange column. One source of this anomaly could be the GS assay employed. The measurements of GS activity shown were all based on the GS transferase assay (GS_t; see Section 2.4.7) which is more sensitive than the semi-biosynthetic 'synthetase' assay (GS_s), but measures the GS-catalysed reaction of glutamine with hydroxylamine rather than the physiological addition of ammonia to glutamate measured by the biosynthetic assay. It has been reported that different GS isoenzymes isolated from the same species can have very different GS_t:GS_s activity ratios, making direct comparisons of GS activity peaks based on the transferase method unreliable (Cullimore *et al.*, 1983). In crude extracts from *P. vulgaris* nodules, for example, the ratio decreases as the nodule matures, and this is thought to reflect the induction of the nodule-induced γ subunit which has a much lower ratio

than the β subunit of the root (Bennett and Cullimore, 1989). Further analysis of the GS1 peaks from different tissues of *L. corniculatus* by Woodall (personal communication) has revealed that the GS_t:GS_s ratio varies between tissues, and depends on the nitrogen source. Her results show that the ratio is about 40 in nodules, nodulated roots and roots supplied with ammonium, but only about 20 in nitrate-fed roots and leaves.

There are a number of examples of observed changes in the GS_t:GS_s ratio of prokaryotic GS in response to changes in nitrogen status: Manco and co-workers (1992) reported that inhibition of GS_t activity of derepressed GSII from *Rhizobium leguminosarum* bv. *viceae* by ammonium occurred more rapidly than did inhibition of the corresponding GS_s activity. Similar investigations by Bravo and Mora into the effect of nitrate and ammonium on GS of *R. phaseoli* indicated that GS_t of GSI was the same in both treatments but GS_s was halved by nitrate (Bravo and Mora, 1988). Mérida and co-workers purified the enzyme from two cyanobacteria strains, *Synechocystis* sp. and *Calothrix* sp., and found that GS_t was inhibited up to 90% by alanine, glycine and serine, but GS_s was unaffected by glycine and serine (Mérida *et al.*, 1990). They subsequently found that ammonium had a 90% inhibitory effect on both GS_t and GS_s (Mérida *et al.*, 1991). Glutamine and ammonia have been shown to inhibit *in vivo* GS_s but not GS_t of *Saccharomyces cerevisiae* (Mitchell and Magasanik, 1984). Kim and Rhee (1987), commenting on their investigations into the partial inhibition of the *S. cerevisiae* enzyme by L-methionine sulfoximine (MSO) suggested that the irreversible inactivation of any given subunit of the octamer has a complex effect on neighbouring subunits: their GS_t is also decreased, but they are subsequently less likely to be completely inactivated, and the GS_s of these subunits is actually enhanced. Thus, at least under certain conditions in bacteria and yeast, changes in GS_t and GS_s can be dissociated.

Data on the effect of nitrogen nutrition on plant GS_t:GS_s is limited to one report by Sakakibara and co-workers (1996) on the short-term effect of supplying 3-4-d old seedlings of *Zea mays* with 10 mM ammonium. They found that the ammonium treatment induced a novel form of GS in the roots within 6 h, with a corresponding decrease in the GS_t:GS_s ratio. The change in the GS_t:GS_s ratio in this case can clearly be correlated to the induction of the GS_r isoform, and they demonstrated corresponding changes in the mRNA levels of four of the five GS genes present in *Zea mays*. More

work needs to be done to determine the precise origin of the differences in the GS_t:GS_s ratio in *L. corniculatus* under different nitrogen sources, which could be due to either changing subunit composition or modifications of the holoenzyme.

Another explanation for the discrepancy between measured GS activity and amounts of immunoreactive protein detected could be the existence of inactive forms of the enzyme in some of the tissues. The existence of largely inactive, immunoreactive forms of GS has been demonstrated in the roots of N-deficient *P. vulgaris*, *G. max* and *P. sativum* (Hoelzle *et al.*, 1992) and *H. vulgare* (Peat and Tobin, 1996), where it has been postulated that the existence of an inactive form allows rapid activation should ammonium become available. As already mentioned, NR is known to be subject to regulation by phosphorylation. This is a two-step process in which phosphorylation of a single serine residue on the enzyme is thought to cause a conformational change, exposing a binding site for an inhibitor protein, NIP (MacKintosh, 1997). NIP has been purified and found to be a mixture of several isoforms of a 14-3-3 protein. 14-3-3 proteins are common signalling proteins, and it was suggested that the NR-NIP-14-3-3 complex may itself be a signal that interacts with other cellular processes (Moorhead *et al.*, 1996). MacKintosh has since demonstrated that GS1 from *Spinacea oleracea* also binds to a 14-3-3-like protein (personal communication), and more work is clearly necessary to determine whether a similar process is involved in GS regulation.

A further discrepancy can be seen from close examination of the upper band of the 39 kDa GS doublet. It eluted at fraction 34, and was present in the crude extracts of both nodulated roots and nodules, although there was virtually no measurable activity in fraction 34 of the profile from nodulated roots. It may therefore represent a subunit that is inactive in roots, but activated in nodules. It is possible, for example, that, in roots, this polypeptide is incapable of assembling into an active holoenzyme. There is evidence that GS2 in the leaves of some plants may require the help of a chaperonin to assemble (Lubben *et al.*, 1992; Tsuprun *et al.*, 1992), and Gao and Wong (1994) postulated a similar mechanism may be necessary for assembly of nodule-specific subunits in *P. vulgaris*. Temple *et al.* (1996) suggested that stable assembly of the nodule-specific polypeptide of *G. max* requires active N_2 fixation, the deciding factor being ammonium concentration in the cytosol.

4.6.8 Summary

The isoenzyme profile of GS in roots and nodules of *L. corniculatus* and the effect of nitrate on this profile has been presented. Nodules of *L. corniculatus* express a GS isoform that was distinct in its ion-exchange elution characteristics from the isoform found in roots, but that was indistinguishable from the root form by 1D-gel electrophoresis and western blot analysis. This isoform elutes earlier than the root isoform, and there was little evidence of a root-type isoform in profiles from nodule extracts.

Nitrate was found to have a dramatic effect on the elution profile of GS in the nodule, shifting the main elution peak to a position that corresponded to the root peak. The origin of the nodule-specific peak is unclear, as is the mechanism behind the nitrate-induced shift in the profile and the reported changes in the GS_t:GS_s ratio. Possibilities include changes in subunit composition, and post-translational alterations to the subunits or the holoenzyme, resulting in changes in elution characteristics and activation states or holoenzyme assembly. These possibilities clearly warrant further investigation.

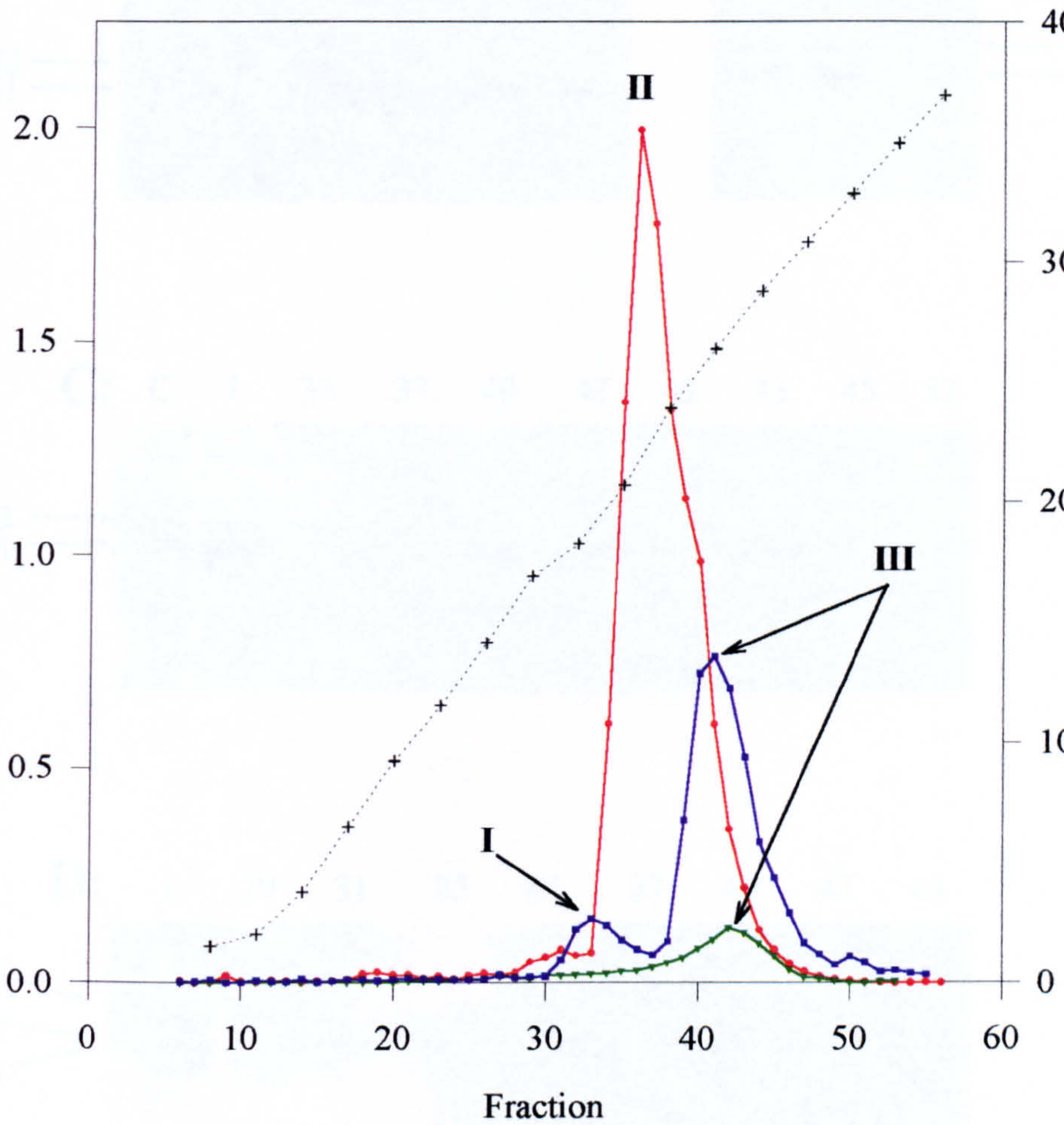

Figure 4.1: Elution profiles of GS activity from ion-exchange chromatography of extracts from nodules (•), nodulated roots (▼) and nitrate-fed roots (■) of *L. corniculatus*. Chromatography was carried out as described in Section 2.11.2 and KCl concentrations (+) were determined using a conductivity meter. GS transferase activity (GS_t) was determined as described in Section 2.10.7, and is expressed per g fresh weight of tissue. One unit (U) of GS activity catalyses the formation of one µmol of γ-glutamyl-hydroxamate from glutamine and hydroxylammonium per minute at 30°C.

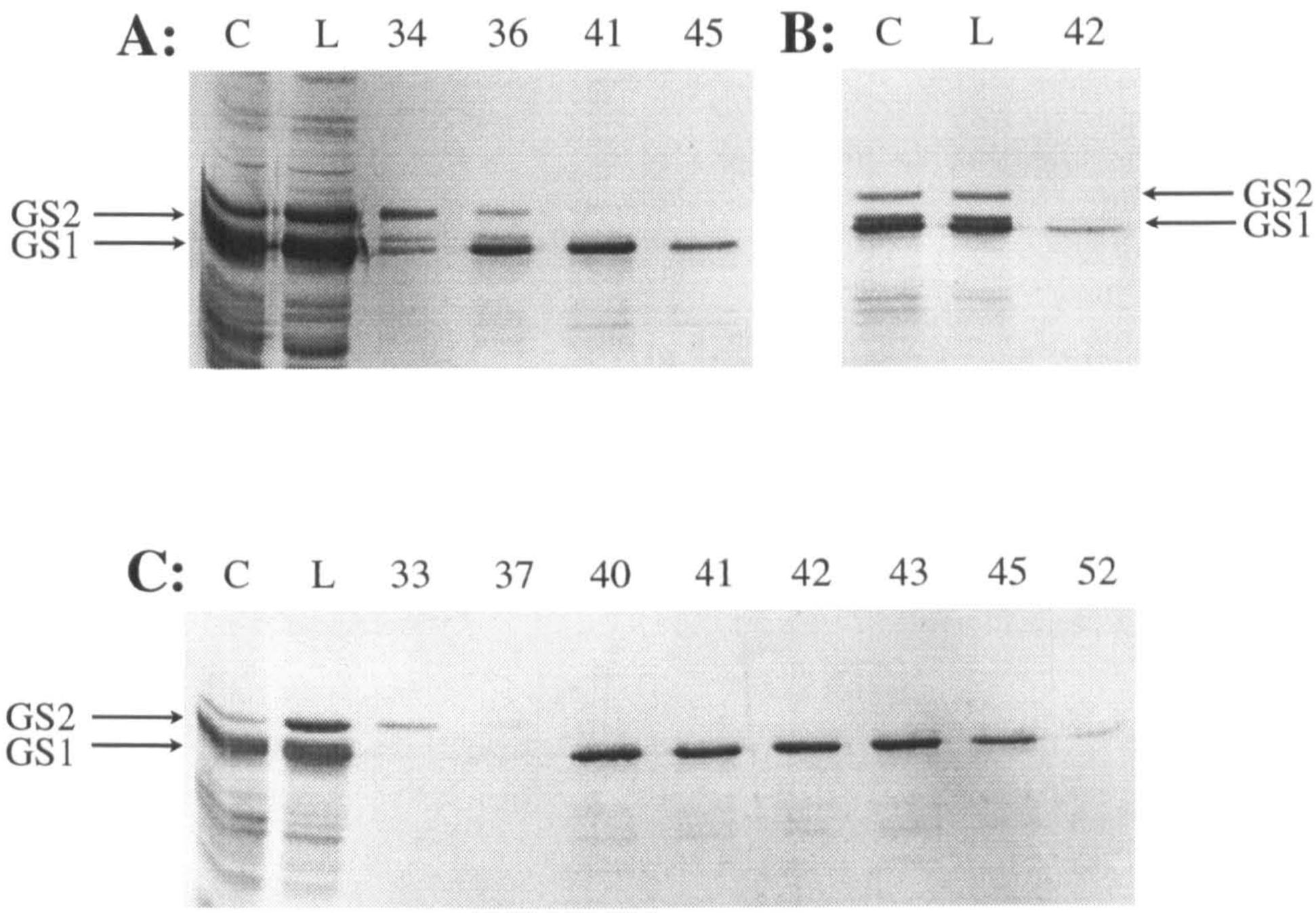

Figure 4.2: Western blots of fractions collected during ion-exchange chromatography of GS from nodules, nodulated roots and nitrate-fed roots (Fig. 4.1). Blots shown are from **A:** nodules, **B:** nodulated roots, **C:** nitrate-fed roots and **D:** shoots from nitrate-fed plants (included for comparison). Samples of equal volume (10 µl) from eluted fractions were separated by SDS-PAGE and electroblotted onto membranes which were then immunostained for GS polypeptides (see Sections 2.11.4 - 2.11.6). LSU = Rubisco large subunit which cross-reacts with the GS antibody (data not shown); C = crude extract; L = PD10-purified extract as loaded onto MemSep cartridge. Fraction numbers are shown above the relevant lane. The blots shown were produced by J. Woodall and are reproduced with permission.

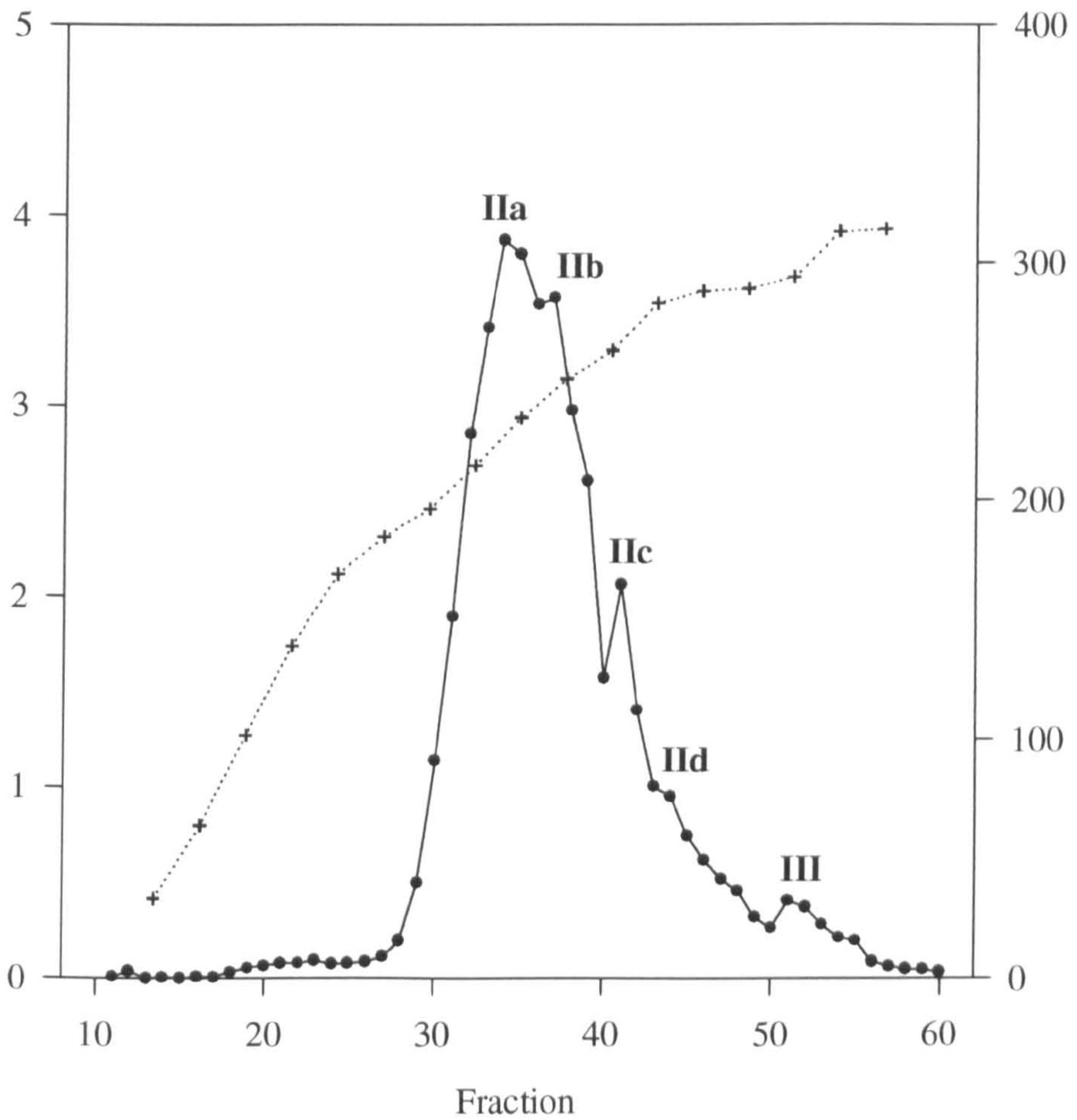

Figure 4.3: Elution profile of GS activity (•) from ion-exchange chromatography of extracts from nodules of *L. corniculatus* using a stretched KCl gradient. Chromatography was carried out as described in Section 2.11.2 and KCl concentrations (+) were determined using a conductivity meter. GS transferase activity (GS_t) was determined as described in Section 2.10.7.

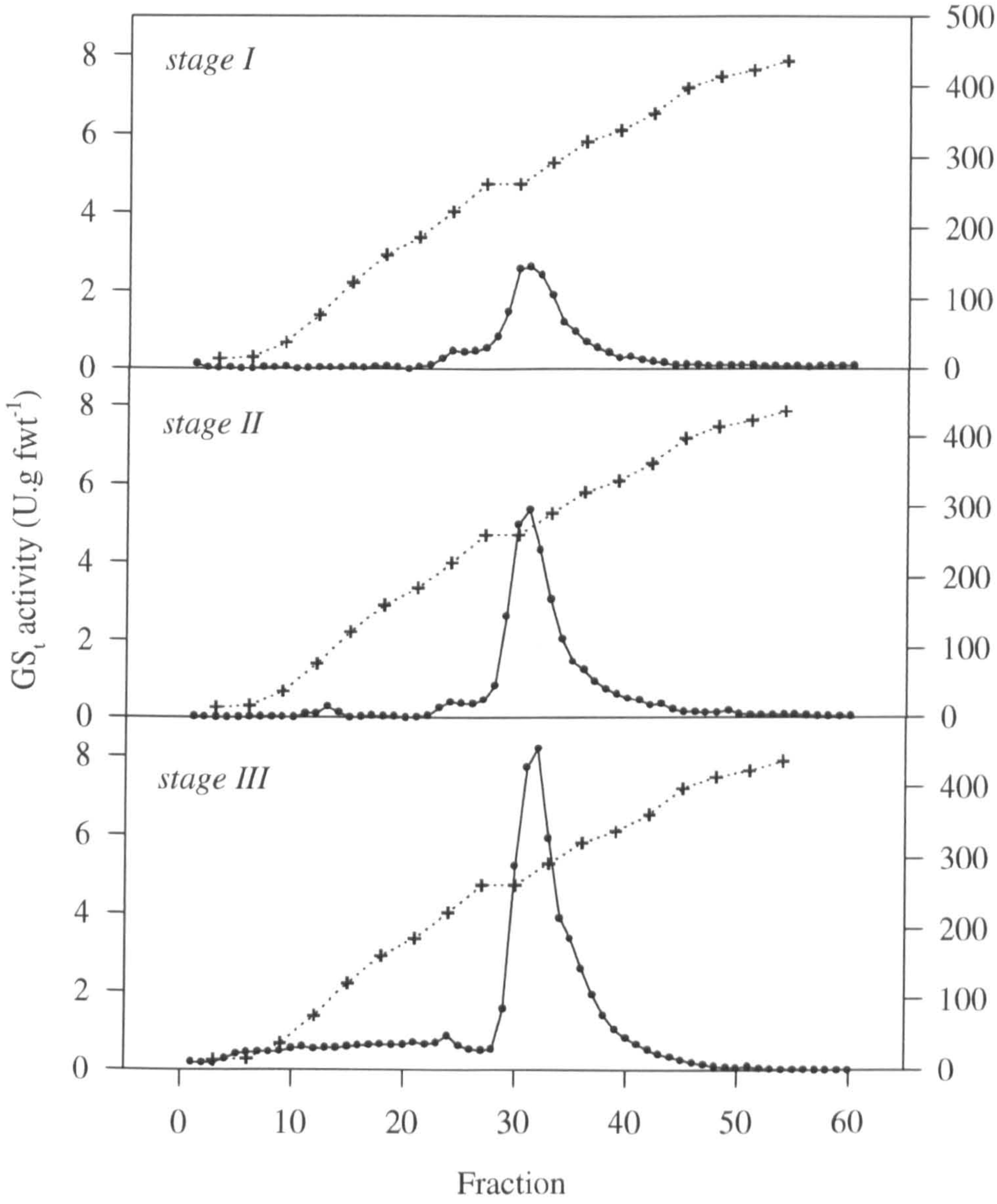

Figure 4.4: The effect of nodule developmental stage on the elution profile of GS activity (•) from ion exchange chromatography of extracts from nodules of *L. corniculatus*. Chromatography was carried out as described in Section 2.11.2 and KCl concentrations (+) were determined using a conductivity meter. GS transferase activity (GS_t) was determined as described in Section 2.10.7.

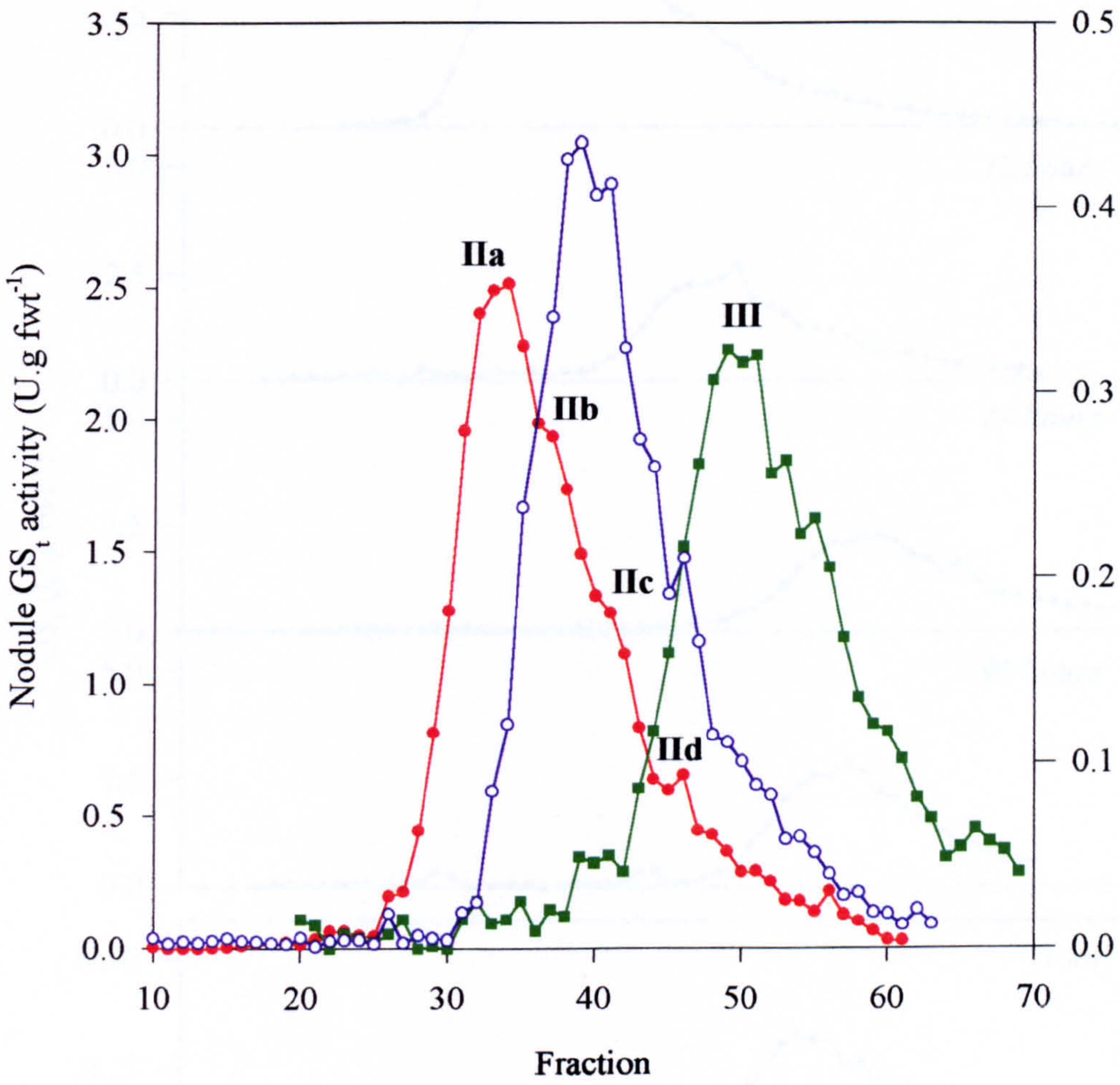

Figure 4.5: The effect of nitrate on the elution profile of GS isoenzyme activity from ion exchange chromatography of nodule extracts from *L. corniculatus*. Treated plants (○) were watered with Fåhraeus medium (see Table 2.3) supplemented with 10 mM nitrate for 5 d prior to harvest while control plants (•) continued to receive Fåhraeus medium with no added nitrate. Chromatography was carried out as described in Section 2.11.2 and GS transferase activity (GS_t) was determined as described in Section 2.10.7. A typical root elution profile is shown for comparison (■).

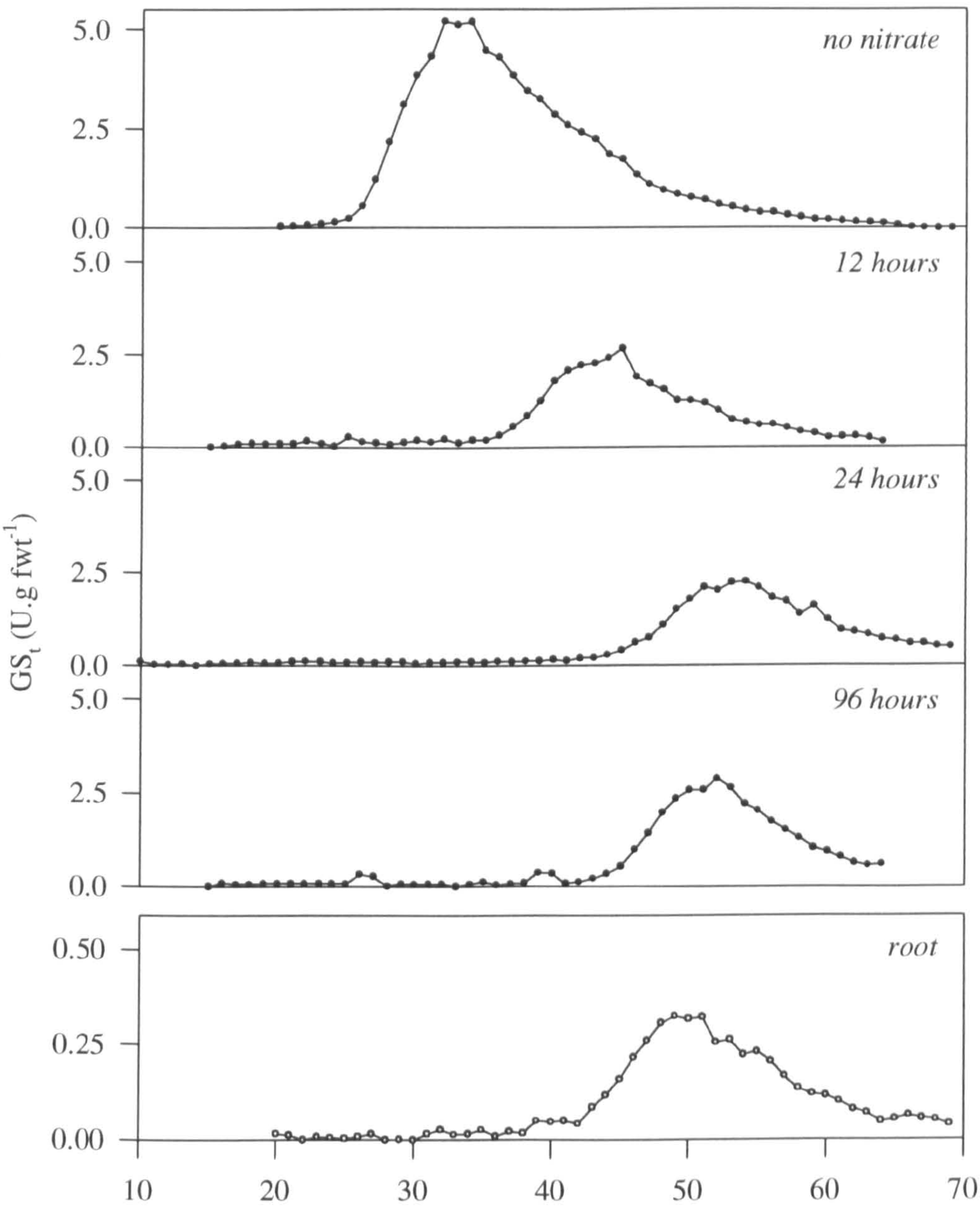

Figure 4.6: The effect of nitrate on the elution profile of GS isoenzyme activity from ion exchange chromatography of nodule extracts from poorly-nodulated, wild-type *L. corniculatus*. Chromatography was carried out as described in Section 2.11.2 and GS transferase activity (GS_t) was determined as described in Section 2.10.7. A typical root elution profile is shown for comparison.

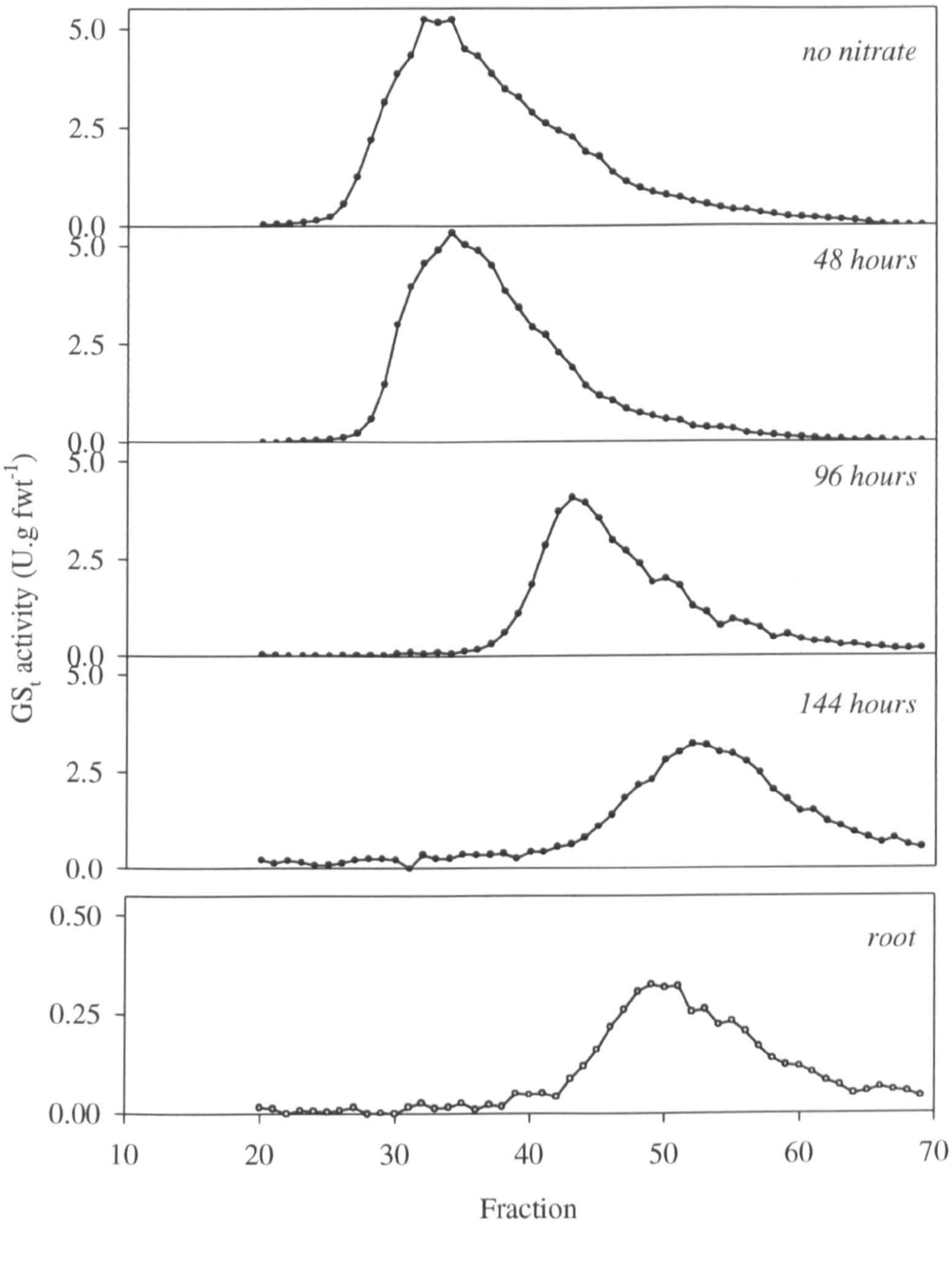

Figure 4.7: The effect of nitrate on the elution profile of GS isoenzyme activity from ion exchange chromatography of nodule extracts from well-nodulated, transformed *L. corniculatus*. Chromatography was carried out as described in Section 2.11.2 and GS transferase activity (GS_t) was determined as described in Section 2.10.7. A typical root elution profile is shown for comparison.

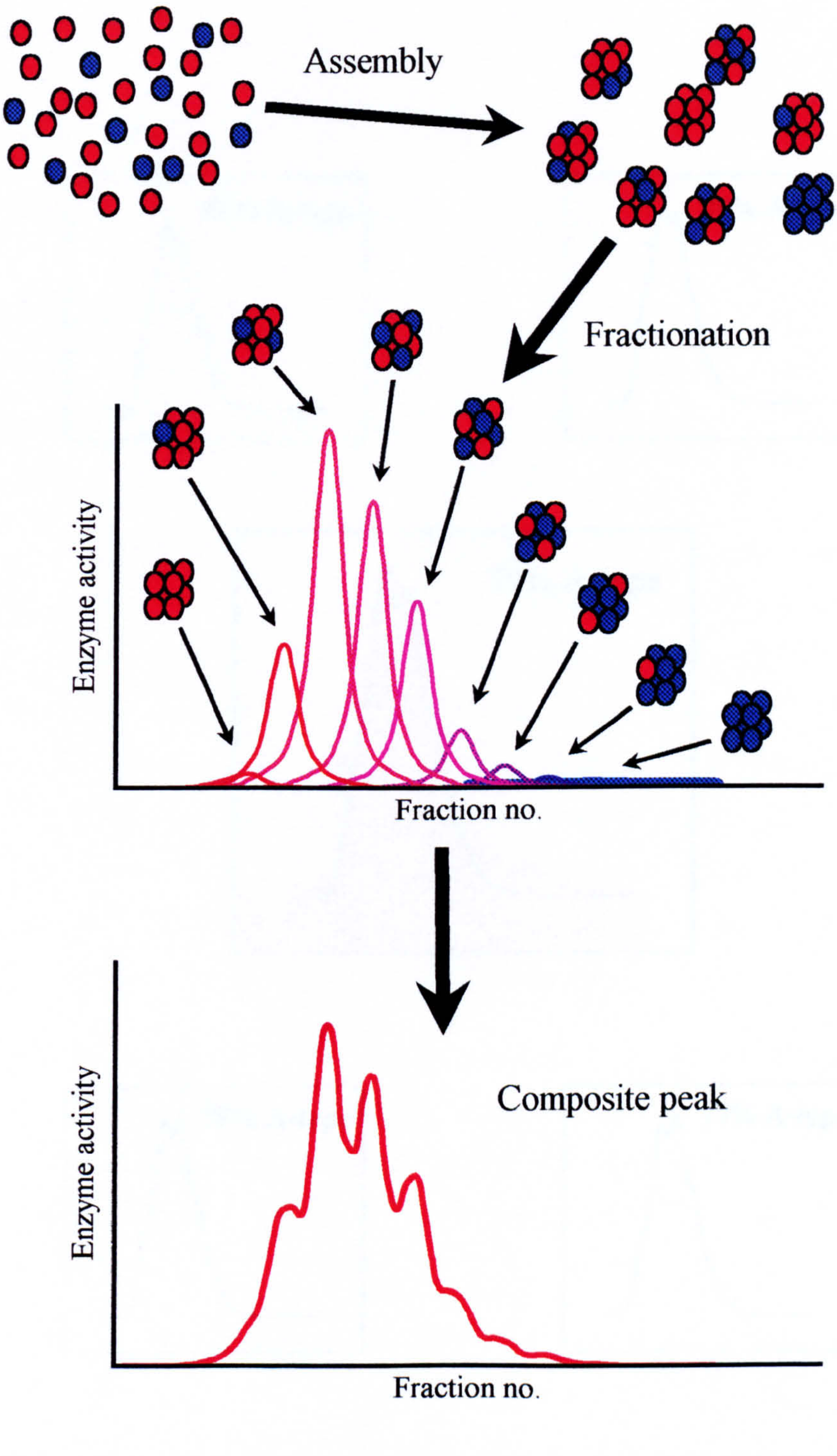

Figure 4.8: A schematic representation of a simple model to explain the elution profile observed in the separation of nodule extracts by ion exchange chromatography. A-type subunits are represented in red, B-type subunits in blue. See Section 4.6 for a full discussion.

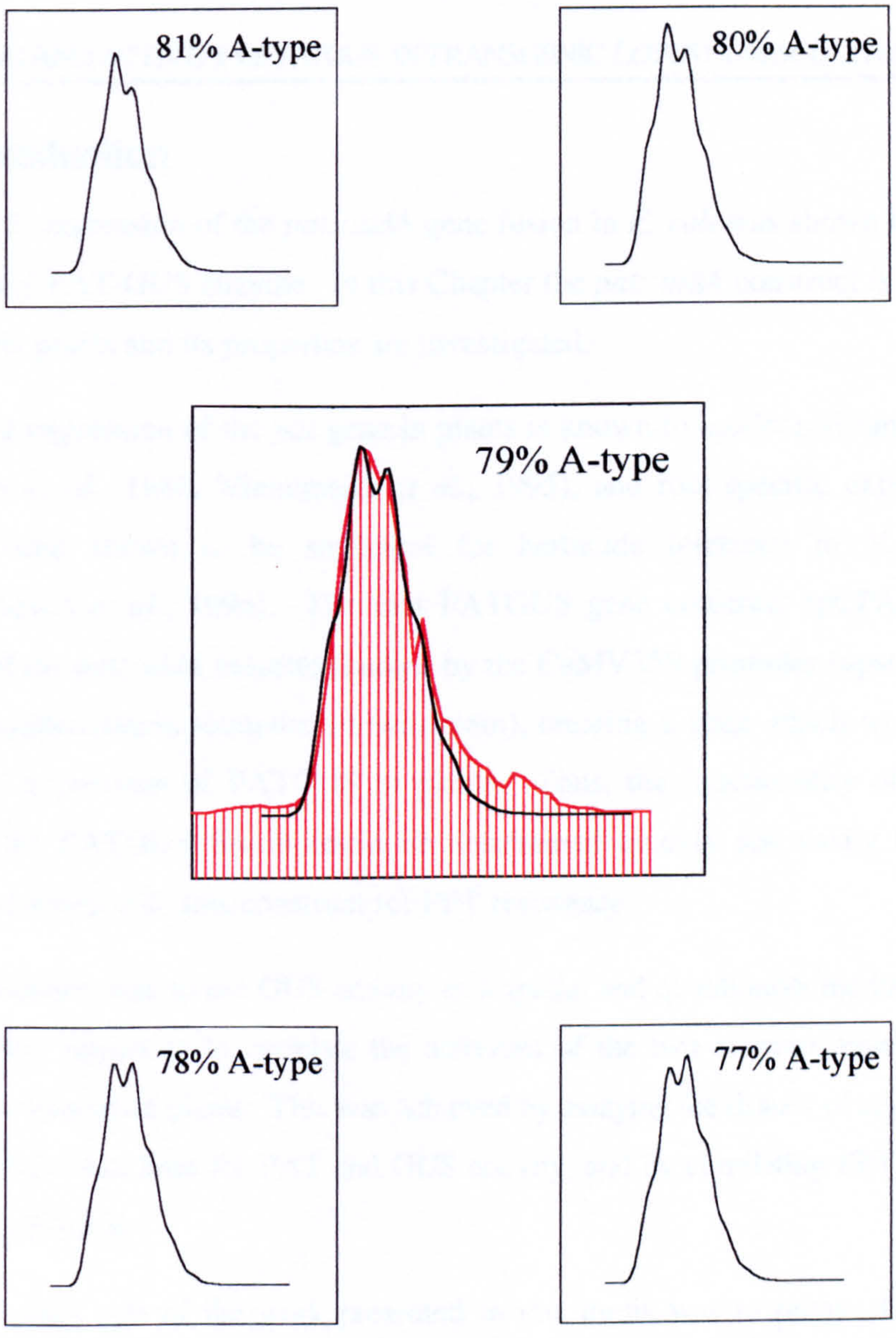

Figure 4.9: Comparison between the observed elution profile of GS from nodule extracts (red shaded region, reproduced from Fig. 4.3) and the elution profile predicted for 79% A-type subunits in the computer simulation described in Section 4.5. The horizontal axis represents increasing elution volume, and the vertical axis represents GS activity, both in arbitrary units.

CHAPTER 5:

EXPRESSION AND ACTIVITY OF PATGUS IN TRANSGENIC *LOTUS CORNICULATUS*

5.1 Introduction

In Chapter 3, expression of the *pat::uidA* gene fusion in *E. coli* was shown to produce a bifunctional PAT-GUS enzyme. In this Chapter the *pat::uidA* construct is expressed in transgenic plants and its properties are investigated.

Constitutive expression of the *pat* gene in plants is known to confer resistance to PPT (Wohlleben *et al.*, 1988; Vinnemeier *et al.*, 1995), and root-specific expression of PAT has been shown to be sufficient for herbicide tolerance in *N. tabacum* (van der Hoeven *et al.*, 1994). The first PATGUS gene construct (pCPATGUS95) consisted of the *pat::uidA* cassette flanked by the CaMV35S promoter (upstream) and the *nos* polyadenylation sequence (downstream), creating a gene which would direct constitutive expression of PATGUS in plants. Thus, the functionality of the PAT moiety of the PATGUS fusion could be determined quickly and easily by testing plants transformed with this construct for PPT resistance.

Since the intention was to use GUS activity as a spatial and quantitative marker for PAT activity, it was important to correlate the activities of the two enzyme moieties in the tissues of the transgenic plants. This was achieved by assaying the tissues of constitutively expressing PATGUS lines for PAT and GUS activity, and by correlating PPT resistance with GUS expression.

The second main aim of the work presented in this thesis was to protect GS activity specifically in the infected zone of the nodule by nodule-specific expression of PATGUS. These demonstrations of PATGUS activity in plants could be taken as good evidence that (1): expression of the chimaeric gene in nodule tissues would confer PAT activity to those tissues, and (2): GUS activity could be used to screen transformants for those which expressed the gene in the desired, nodule-specific fashion. The *pat::uidA* gene would be introduced into plants under the control of the *P. vulgaris gln-γ* promoter for nodule-

directed expression and transformants regenerated and screened for GUS activity specifically in the nodule. Only those lines in which the stain was confined to the central infected zone (indicating the correct targeting of PAT activity) would be suitable for further examination of the effect of PATGUS expression on GS inhibition by PPT, and for the subsequent physiological studies described in Chapter 6.

5.2 Gene constructs and plant transformation

Experimental details of the cloning techniques used are given in Section 2.7. For constitutive expression of PATGUS, the *35S*$_{pro}$*::pat::uidA::nos*$_{ter}$ cassette was excised from pCPATGUS95 by digestion with *Eco*RI and *Hin*dIII, and ligated into the binary plant transformation vector pBIN19 (Bevan, 1984) to create pBINCPG. For nodule-directed expression of PATGUS, the *P. vulgaris gln-γ* promoter, previously cloned by Forde *et al.* (1989), was used. The promoter fragment was excised from pBA68 (Forde *et al.*, 1989) using *Hin*dIII and *Eco*RI, blunt-ended and T/A cloned into *Eco*RV-cut pBluescript SK+ (Alting-Mees and Short, 1989) to create pBII76. This plasmid contained a number of restriction sites downstream of the *gln-γ* promoter for easy insertion of genes to be expressed under its control. In a similar way, a *pat::uidA::nos*$_{ter}$ cassette was excised from pCPATGUS95 using *Eco*RI and *Sma*I, blunt-ended and T/A cloned into *Sma*I-cut pUC19 (Vieira and Messing, 1982), creating pPATGUS2.1 from which the cassette could be excised using a variety of restriction sites. The *pat::uidA::nos*$_{ter}$ gene construct was then excised from pPATGUS2.1 by digestion with *Pst*I and *Hin*dIII, and cloned into *Pst*I/*Hin*dIII-cut pBII76 to create pGPATGUS4.1 which contains PATGUS under the control of the *gln-γ* promoter. For plant transformation, pBINGPG was constructed by excising the *gln-*γ_{pro}*::pat::uidA::nos*$_{ter}$ cassette from pGPATGUS4.1 with *Hin*dIII and *Eco*RI and ligating it into *Hin*dIII/*Eco*RI-cut pBIN19. The pBIN19-derived constructs thus created were used subsequently to transform *L. corniculatus* plants via *A. rhizogenes* mediated transformation (see Section 2.9).

5.3 GUS activity in constitutive PATGUS lines

Transgenic lines carrying the pBINCPG construct were identified at the hairy root stage using the GUS histochemical assay (see Section 2.10.5) and regenerated as described in

Section 2.9. These lines were assayed again after 3 months in culture (after subculturing twice) and five of them were found to have retained GUS activity. Roots and shoots of these lines were assayed fluorimetrically and these were found to exhibit a range of GUS activities (Fig. 5.1). The GUS activities in these lines varied from very low (cA4) to very high (cC7 and cD2), with two transformants showing intermediate levels (cD4 and cD6). In all lines, the level of GUS activity detected in the roots was greater on a protein basis than that detected in shoots. On a fresh weight basis, however, the GUS activity in roots was very much lower than in shoots (data not shown).

5.4 PPT resistance in transgenic lines constitutively expressing PATGUS

The transgenic *L. corniculatus* lines were tested for PPT resistance by examining the ability of cuttings to grow on MS20 media containing up to 25 $mg.l^{-1}$ PPT. The cuttings were grown for 28 d under standard culture conditions as described in Section 2.3.1. Fig. 5.2 shows the appearance of the cuttings after this time. When no PPT was present in the culture media (Fig. 5.2A), there was little discernible difference between the lines, other than that which could be attributable to expression of the hairy root phenotype, as a consequence of the transformation procedure. PPT at concentrations of up to 0.8 $mg.l^{-1}$ had no adverse effect on any of the lines (Fig. 5.2B), but at concentrations of 1 $mg.l^{-1}$ and above, differences between lines became apparent. Untransformed control plants failed to root on media containing 1 $mg.l^{-1}$ PPT (Fig. 5.2C), and the stem segments were severely stunted in growth but not killed. Transformed line cA4 managed to produce very stunted roots, but shoot growth was affected in the same manner as the untransformed controls. Line cD4 showed stunted root and shoot growth, but this was not as severe as the control or cA4 lines. Lines cD6, cC7 and cD2 showed no adverse effects at this concentration of PPT. When the PPT concentration of the medium was doubled to 2 $mg.l^{-1}$ (Fig. 5.2D), the control, cA4 and cD4 lines produced no root or shoot growth, and were showing signs of chlorosis by the end of the study. Line cD6 exhibited stunted root and shoot growth and some chlorosis at this concentration, but cC7 and cD2 were still unaffected. Doubling the concentration of PPT in the media again to 4 $mg.l^{-1}$ (Fig. 5.2E) killed control, cA4, cD4 and cD6 lines, whereas cC7 and cD2 were still largely unaffected, and even at 25 $mg.l^{-1}$ (Fig. 5.2F), the highest concentration of PPT used, these lines were tolerant.

Cuttings that would subsequently die without any establishment could be identified after 7 d due to the onset of necrosis at the base of the stem, chlorosis of stems and leaves and wilting leaves. However, the more subtle effects on root growth were not apparent until later in the experiment when the highly resistant lines established themselves whereas those with less tolerance grew less vigorously and produced stunted root systems.

At the end of the experiment, the plants were harvested and the fresh weights of the root and shoot determined (Fig. 5.3). These data confirmed the visual observations, and revealed a small but significant increasing inhibitory effect of increasing PPT concentration on root establishment of lines cC7 and cD2.

5.5 Direction of PATGUS expression to the nodule infected zone

Plants transformed with pBINGPG, which carries the *gln-*γ_{pro}*::pat::uidA::nos*$_{ter}$ construct (see Section 5.2), were regenerated and nodulated, and the nodules sectioned and stained histochemically for GUS activity (Fig. 5.4). Strong staining was seen in the infected region of the nodule, indicating a high level of PATGUS expression in these tissues. The staining was also confined to the central, infected area of the nodule in these examples, indicating that the *gln-*γ promoter is directing expression specifically to the infected zone as previously reported (Forde *et al.*, 1989). To quantify the level of PATGUS expression in the regenerated lines, GUS activity in roots and nodules was also measured fluorimetrically (Fig. 5.5). The majority of the lines examined showed high levels of GUS activity in the nodule but little or no activity above background levels in the root, again confirming the results obtained previously with the *gln-*γ promoter (Forde *et al.*, 1989). Line 12E had the highest ratio of nodule GUS activity to root GUS activity (ca. 10^4:1).

5.6 Specific protection of GS by directed PATGUS expression

Lines 8C and 12E, in which PATGUS was being expressed specifically in the infected zone of the nodule (shown for 12E in Fig. 5.4), were tested for nodule-specific protection of GS from PPT inhibition by flushing different concentrations of PPT through the soil every 24 h for 7 d. Roots and nodules were then harvested, and GS activity determined on a protein basis. Fig. 5.6 shows the effect of these PPT

treatments on the GS activity in roots and nodules of transgenic plants and untransformed controls. When the treatments were applied to untransformed control plants (Fig. 5.6A), there was no detectable GS activity in the root at concentrations of 10 mM and above. The activity in the nodules of these control plants was 70% inhibited by 10 mM PPT, and at 25 mM this inhibition was greater than 95%. At PPT concentrations of 50 mM and above there was no detectable activity in the nodule. GS in roots of transformed plants (Figs 5.6B and C) was equally sensitive to inhibition by PPT as the control, untransformed lines, but GS activity in the nodules of these lines was not inhibited even by 75 mM PPT. Thus expression of PATGUS under the control of the *gln-γ* promoter specifically and effectively protected GS activity in the nodule from inhibition by PPT.

5.7 Discussion

5.7.1 The GUS and PAT moieties of PATGUS are both active *in planta*

GUS activity due to constitutive expression of PATGUS in *L. corniculatus* was clearly demonstrated (Fig. 5.1). Expression levels varied considerably between lines, and this may be due to the effects of integration at different positions in the genome (Dean *et al.*, 1988; Peach and Velten, 1991), or to the number of copies of the integrated gene (Hobbs *et al.*, 1990; Mlynárová *et al.*, 1995). PPT resistance due to the transgene can be attributed to activity of the PAT moiety (Botterman *et al.*, 1991), and the transformed plants clearly had varying degrees of tolerance to PPT above that observable in the wild type control (Figs 5.2 and 5.3). The level of tolerance demonstrated in lines cC7 and cD2 is comparable with that shown in other studies of transgenic plants expressing the *pat* and *bar* genes (De Block *et al.*, 1987; Wohlleben *et al.*, 1988; Datta *et al.*, 1992; McHughen and Holm, 1995). Thus PATGUS can confer PPT resistance on *L. corniculatus* plants constitutively expressing it in the same way as has been shown for PAT expression in other species.

5.7.2 GUS activity: a quantitative marker for PAT activity *in planta*?

It is clear, from comparing Fig. 5.1 with Figs 5.2 and 5.3, that there was a positive correlation between the amount of GUS activity observed in the tissues of the constitutive PATGUS lines and their ability to survive when subcultured onto media

containing PPT. Line cA4 which showed only a very small amount of GUS activity above background was barely more PPT-resistant than wild-type *L. corniculatus*, whereas lines cC7 and cD2 were tolerant of the highest concentration of PPT used, consistent with their high GUS expression levels. Lines cD4 and cD6 showed intermediate levels of PPT resistance corresponding to the moderate amounts of GUS activity measurable in their tissues. Thus it was demonstrated that GUS activity could be used as at least a semi-quantitative marker of PPT resistance, and hence PAT activity in the tissues of these plants.

5.7.3 Expression of PATGUS in the root nodule specifically protects GS in the nodule from PPT inhibition

The *gln-γ* promoter was used to direct expression of PATGUS to the infected zone of the root nodule and its tissue-specificity was confirmed by histochemical and fluorimetric assays. The aim of using this promoter was to obtain plants in which root GS could be inhibited, without affecting nodule GS. The data in Fig. 5.6 clearly showed that this objective had been achieved. With both lines tested (12E and 8C) it was possible to reduce root GS activity to almost undetectable levels by treating the roots with concentrations of PPT above 10 mM, while nodule GS was unaffected. Similar treatments to the control line markedly inhibited both root and nodule GS activities. Line 12E was a line that showed a very high level of nodule-specific GUS activity and no significant GUS activity above background in the roots; line 8C, on the other hand, showed much weaker expression of GUS in the nodule, and thus might have been expected to show evidence of GS inhibition. This was not the case, indicating that protection of GS activity from PPT inhibition can be achieved even with moderate levels of PATGUS expression. It is possible that longer term exposure to PPT would have revealed less tolerance in line 8C.

In the next Chapter, the effects on the transgenic lines of differential manipulation of GS activity are investigated.

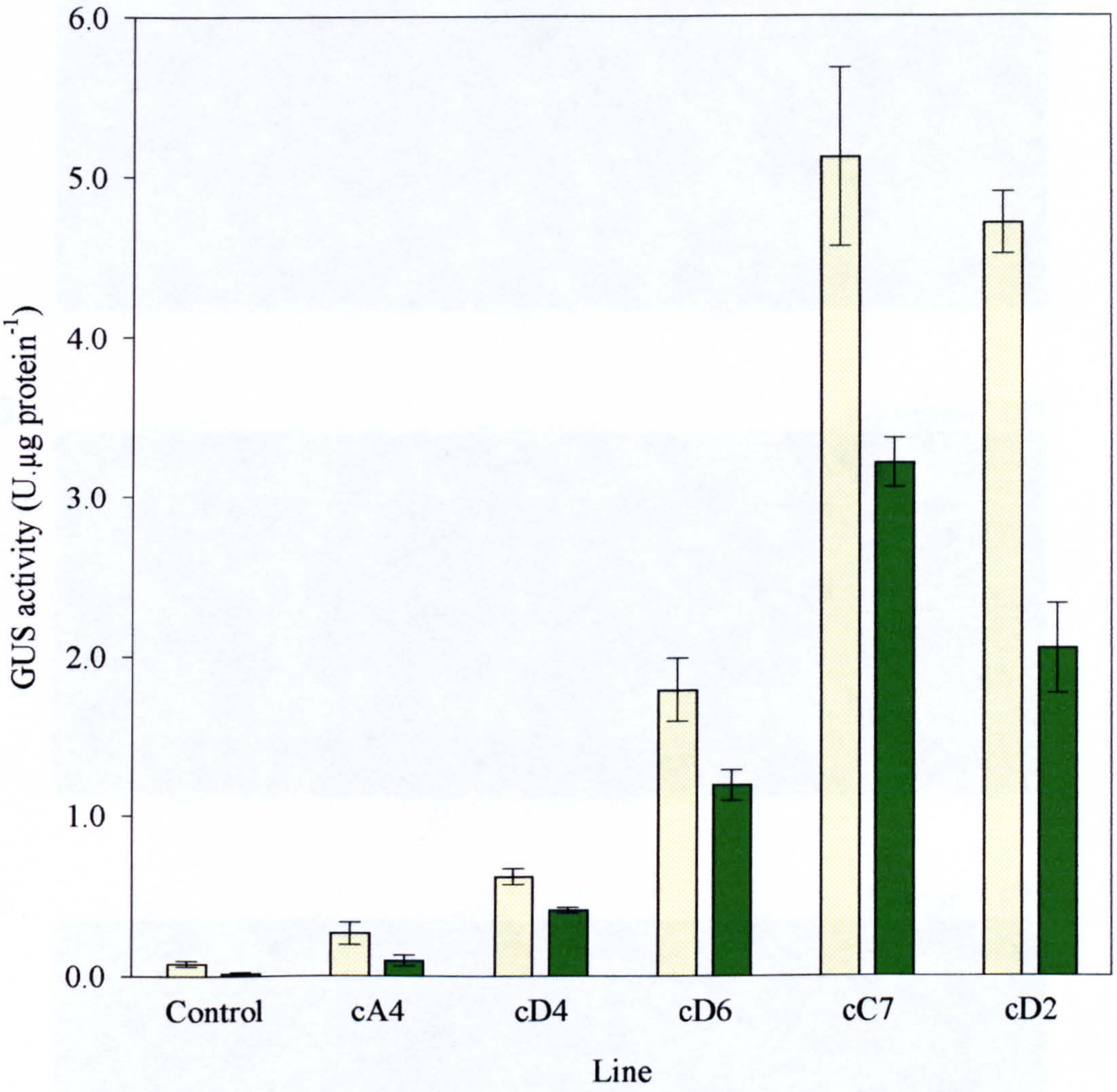

Figure 5.1: GUS activity in roots (■) and shoots (■) of *L. corniculatus* plants transformed with the 35S-PATGUS construct. Plants were grown in tissue culture as described in Section 2.9.1. Tissues were harvested and GUS activity determined fluorimetrically as described in Sections 2.10.1 and 2.10.5 respectively. One unit of GUS activity catalyses the conversion of 1 µmol MUG to 4-MU. Values are shown are the mean of 4 replicates ± standard error.

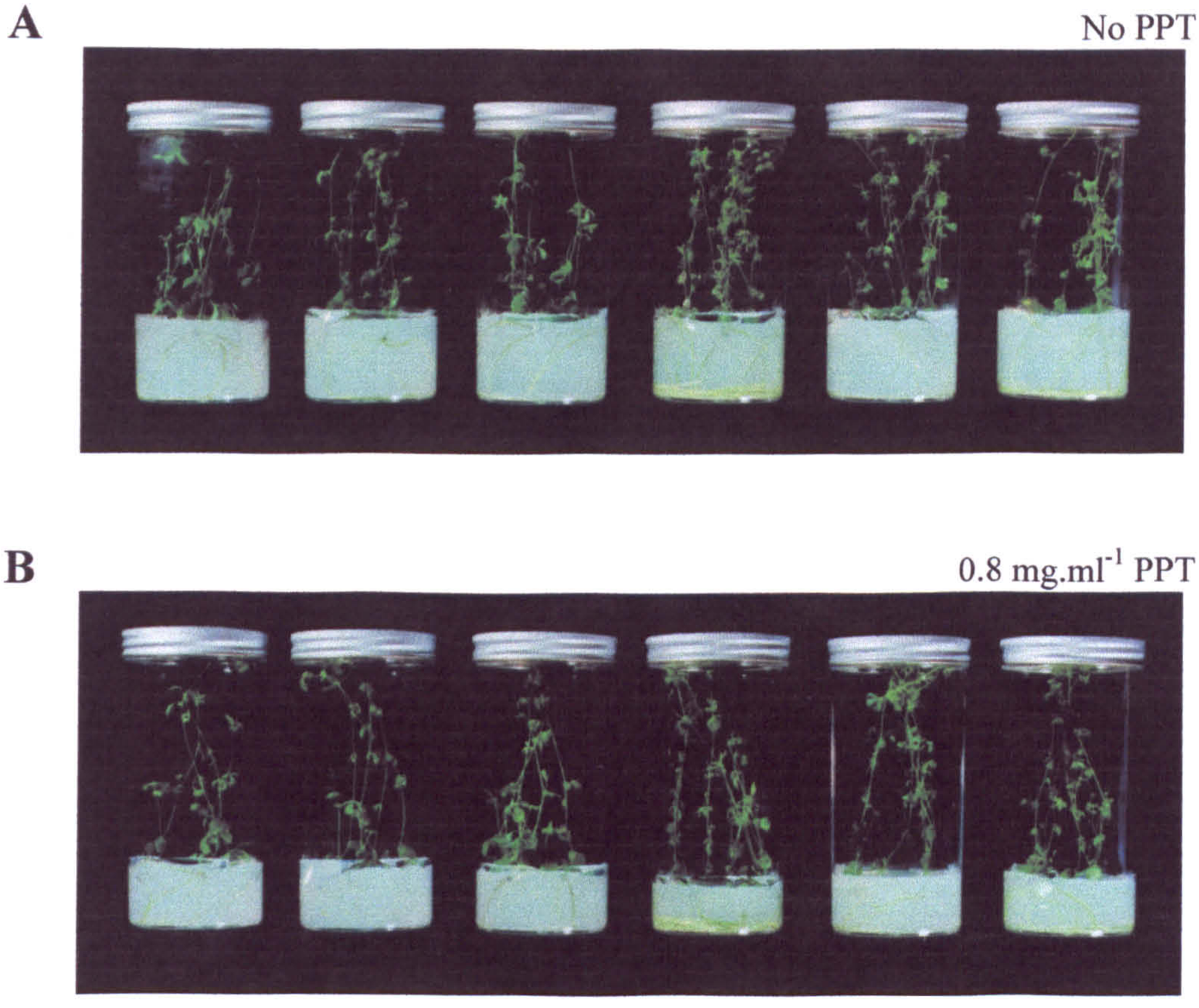

Figure 5.2: PPT resistance in *L. corniculatus* lines transformed with the 35S-PATGUS construct. Healthy stem segments were subcultured onto MS20 media supplemented with a range of concentrations of PPT and grown for 28 d under standard culture conditions as described in Section 2.9.1 before being photographed. Subculturing was as described in Section 2.9.1, but to ensure healthy tissue only the top 2-3 stem segments were used. (*continued overleaf*)

D

2 mg.ml^{-1} PPT

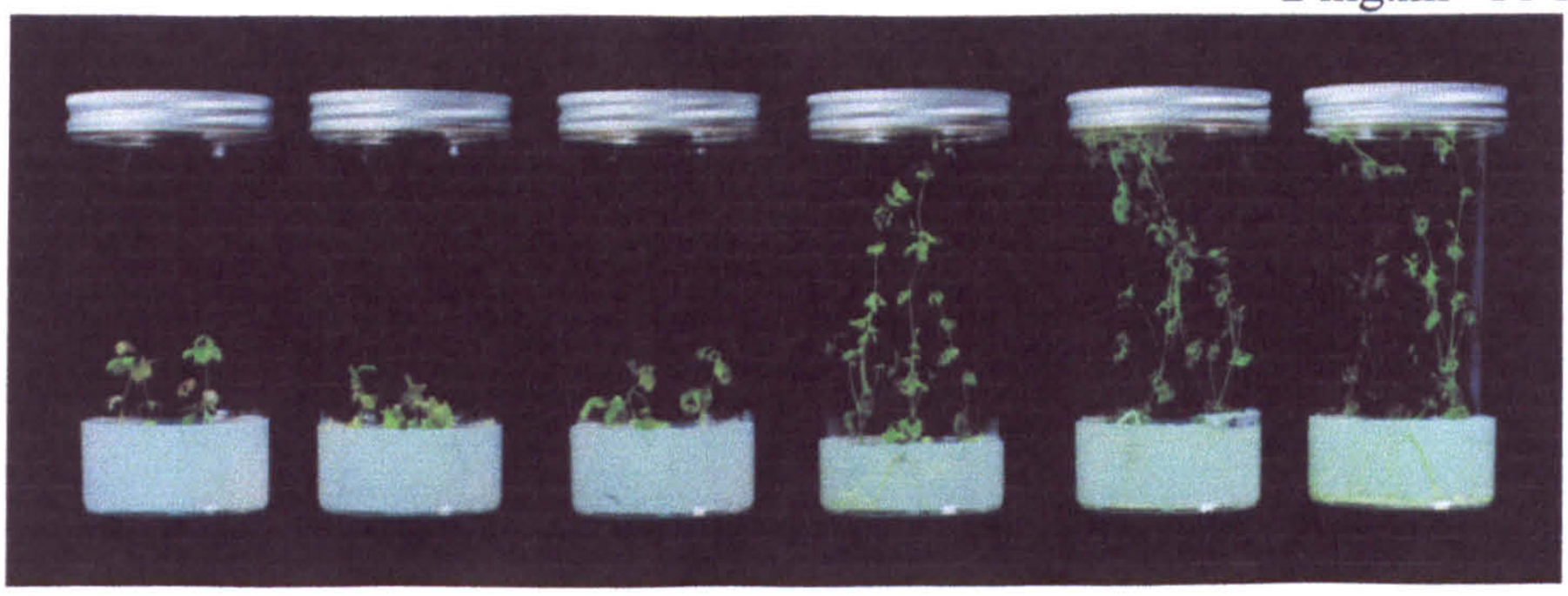

E

4 mg.ml^{-1} PPT

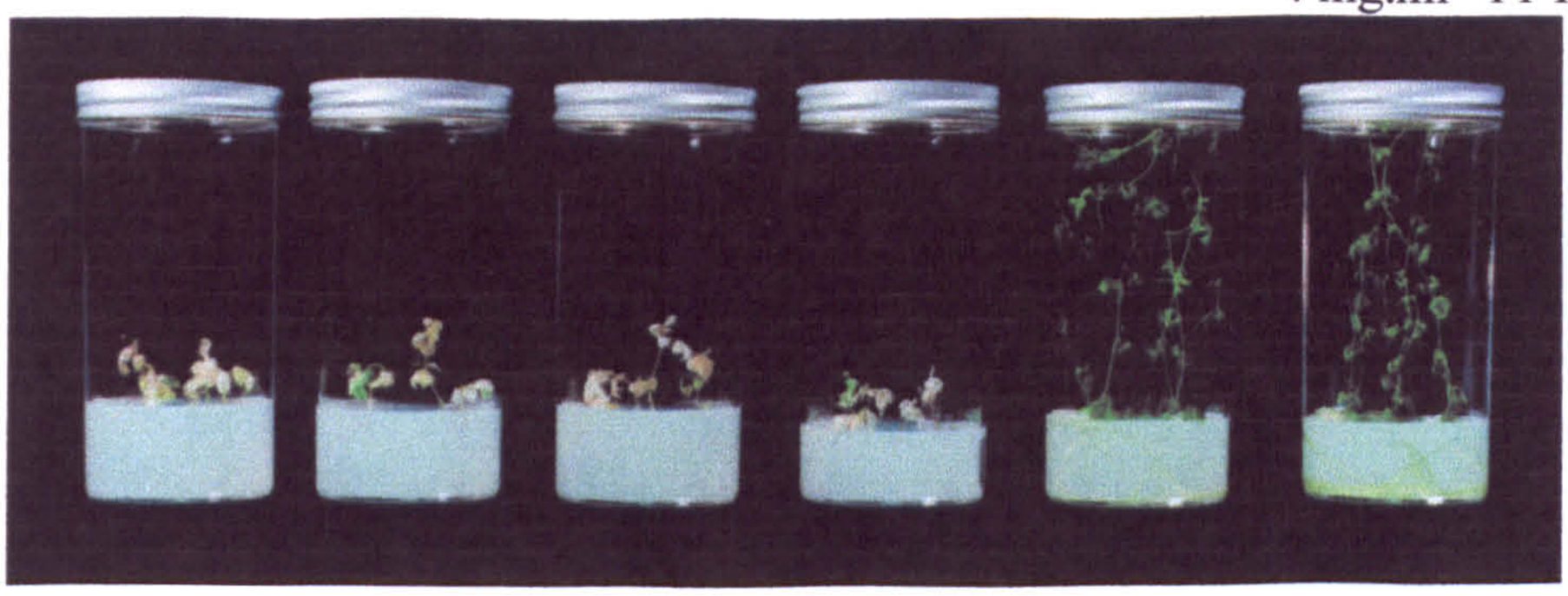

F

25 mg.ml^{-1} PPT

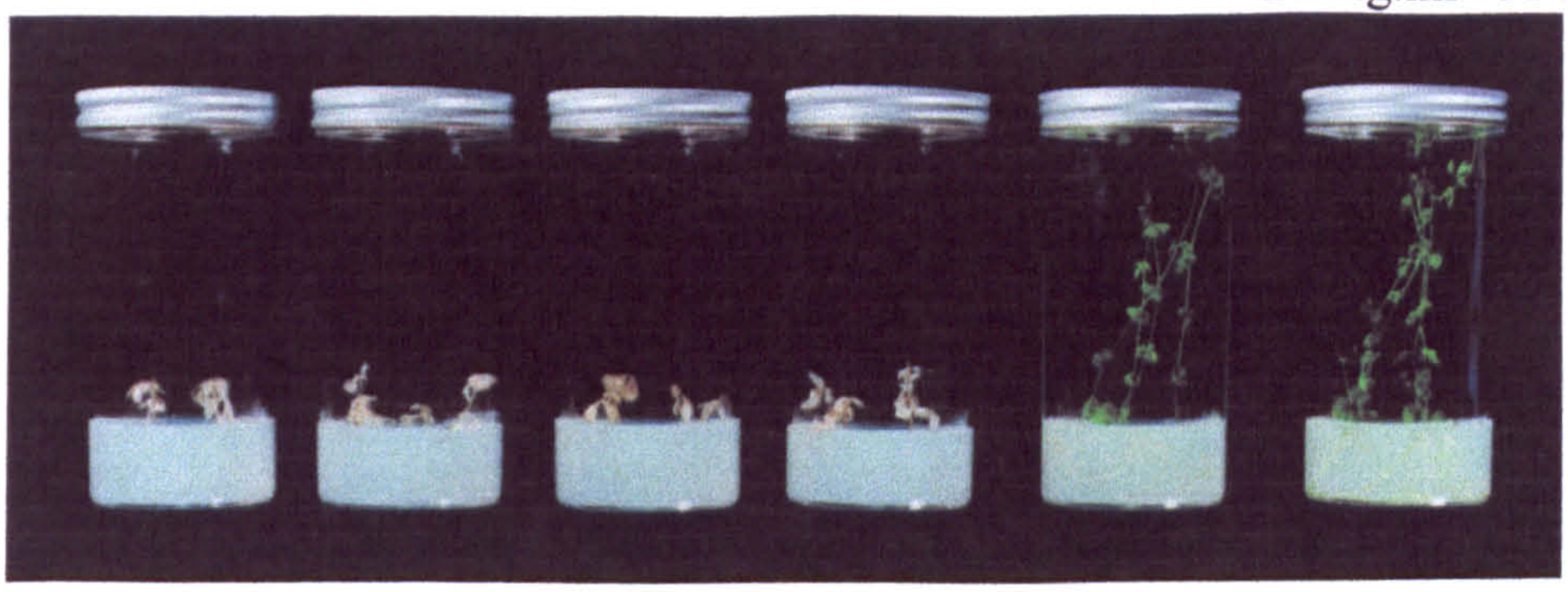

wild-type cA4 cD4 cD6 cC7 cD2

Figure 5.2 (continued): PPT resistance in *L. corniculatus* lines transformed with the 35S-PATGUS construct. Healthy stem segments were subcultured onto MS20 media supplemented with a range of concentrations of PPT and grown for 28 d under standard culture conditions as described in Section 2.9.1 before being photographed. Subculturing was as described in Section 2.9.1, but to ensure healthy growing tissue only the top 2-3 stem segments were used.

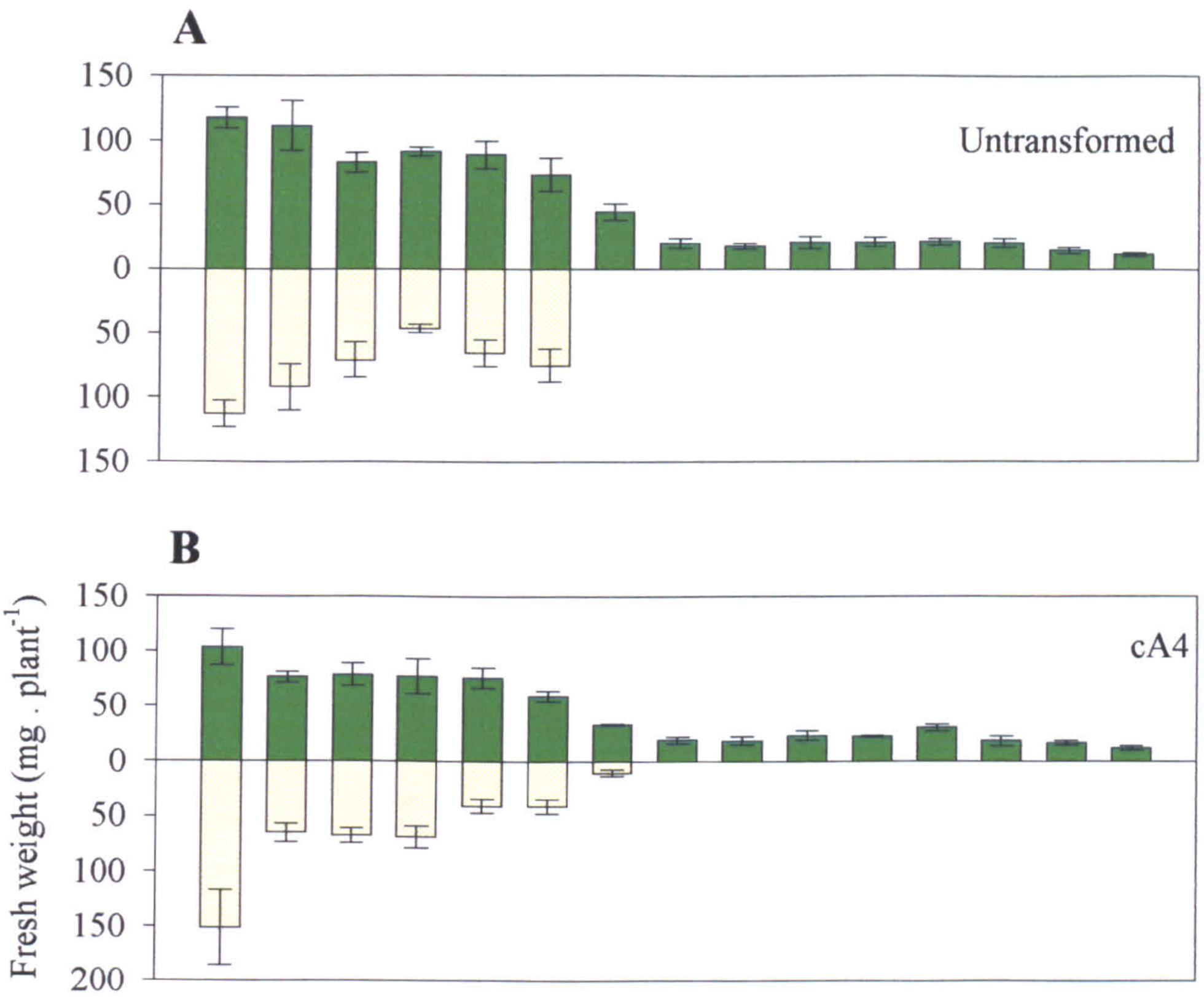

Figure 5.3: PPT resistance in *L. corniculatus* lines transformed with the 35S-PATGUS construct. Healthy stem segments were subcultured onto MS20 media supplemented with a variety of concentrations of PPT and grown for 28 d under standard culture conditions as described in Section 2.9.1. Shoots (■) and roots (■) were then harvested separately and fresh weights per plant determined. Subculturing was as described in Section 2.9.1, but to ensure healthy growing tissue only the top 2-3 stem segments were used. Values are shown are the mean of 4 replicates ± standard error. (*continued overleaf*)

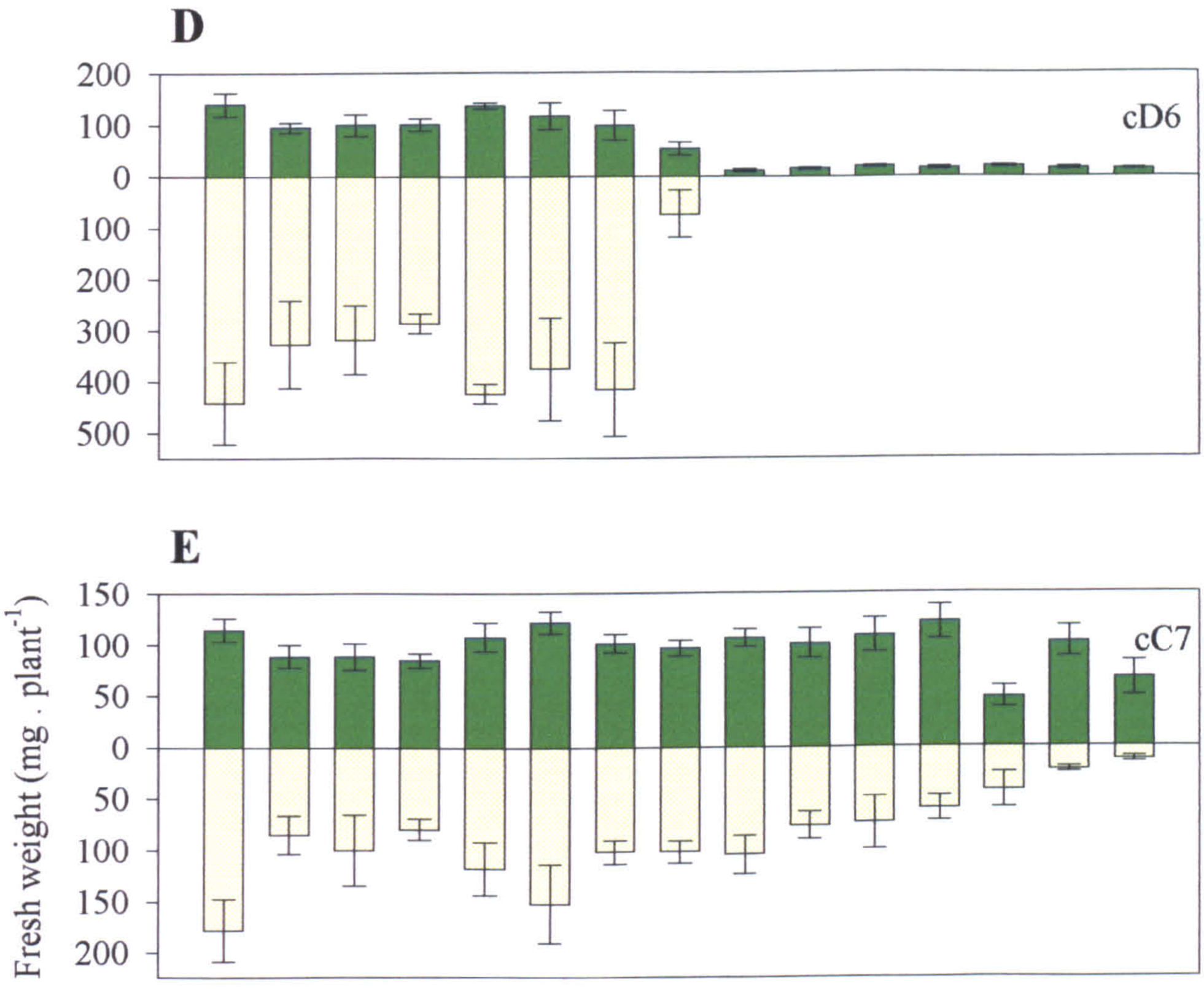

Figure 5.3 (continued): PPT resistance in *L. corniculatus* lines transformed with the 35S-PATGUS construct. Healthy stem segments were subcultured onto MS20 media supplemented with a variety of concentrations of PPT and grown for 28 d under standard culture conditions as described in Section 2.9.1. Shoots (■) and roots (■) were then harvested separately and fresh weights per plant determined. Subculturing was as described in Section 2.9.1, but to ensure healthy growing tissue only the top 2-3 stem segments were used. Values are shown are the mean of 4 replicates ± standard error.

A

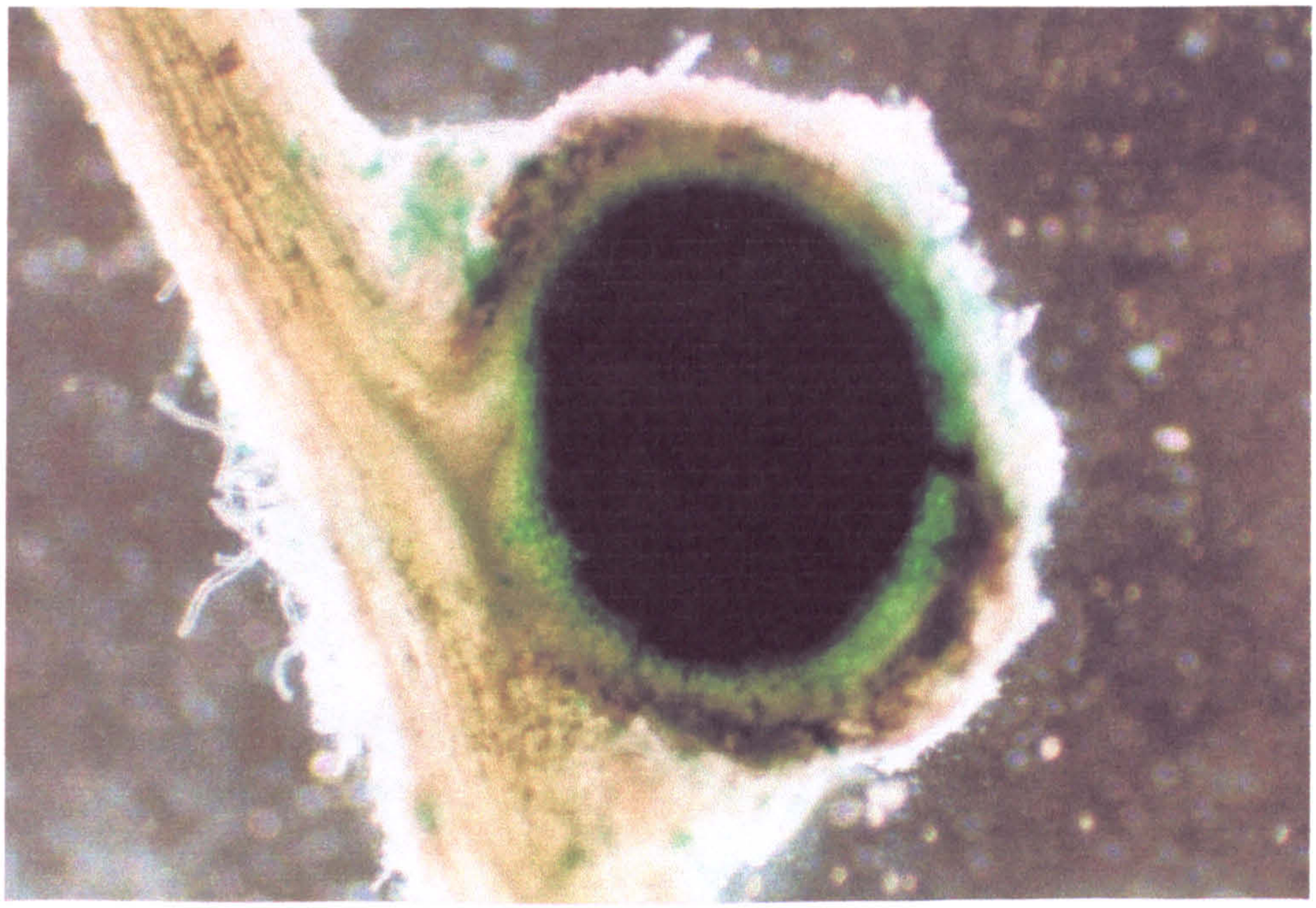

B

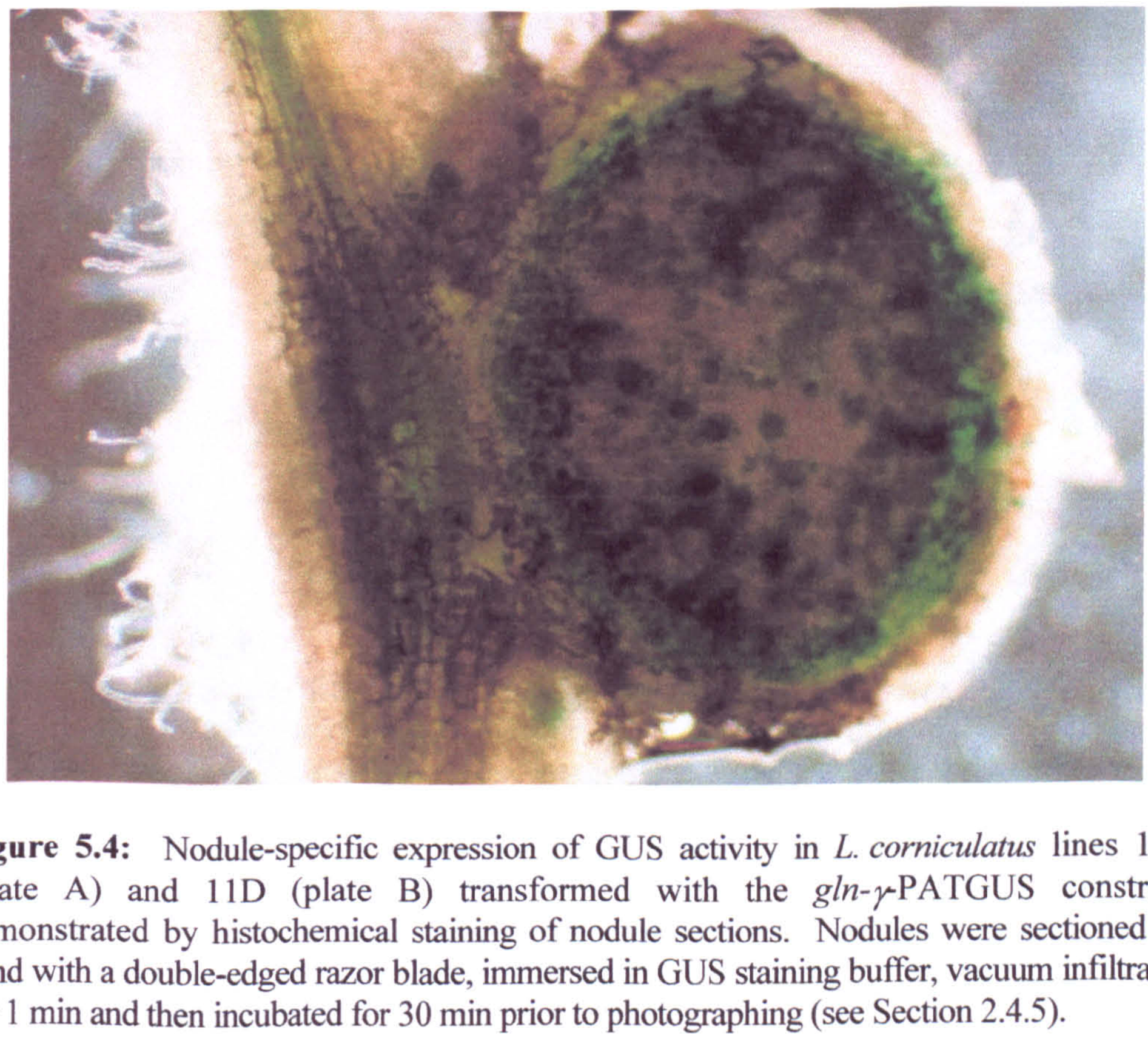

Figure 5.4: Nodule-specific expression of GUS activity in *L. corniculatus* lines 12E (plate A) and 11D (plate B) transformed with the *gln-γ*-PATGUS construct demonstrated by histochemical staining of nodule sections. Nodules were sectioned by hand with a double-edged razor blade, immersed in GUS staining buffer, vacuum infiltrated for 1 min and then incubated for 30 min prior to photographing (see Section 2.4.5).

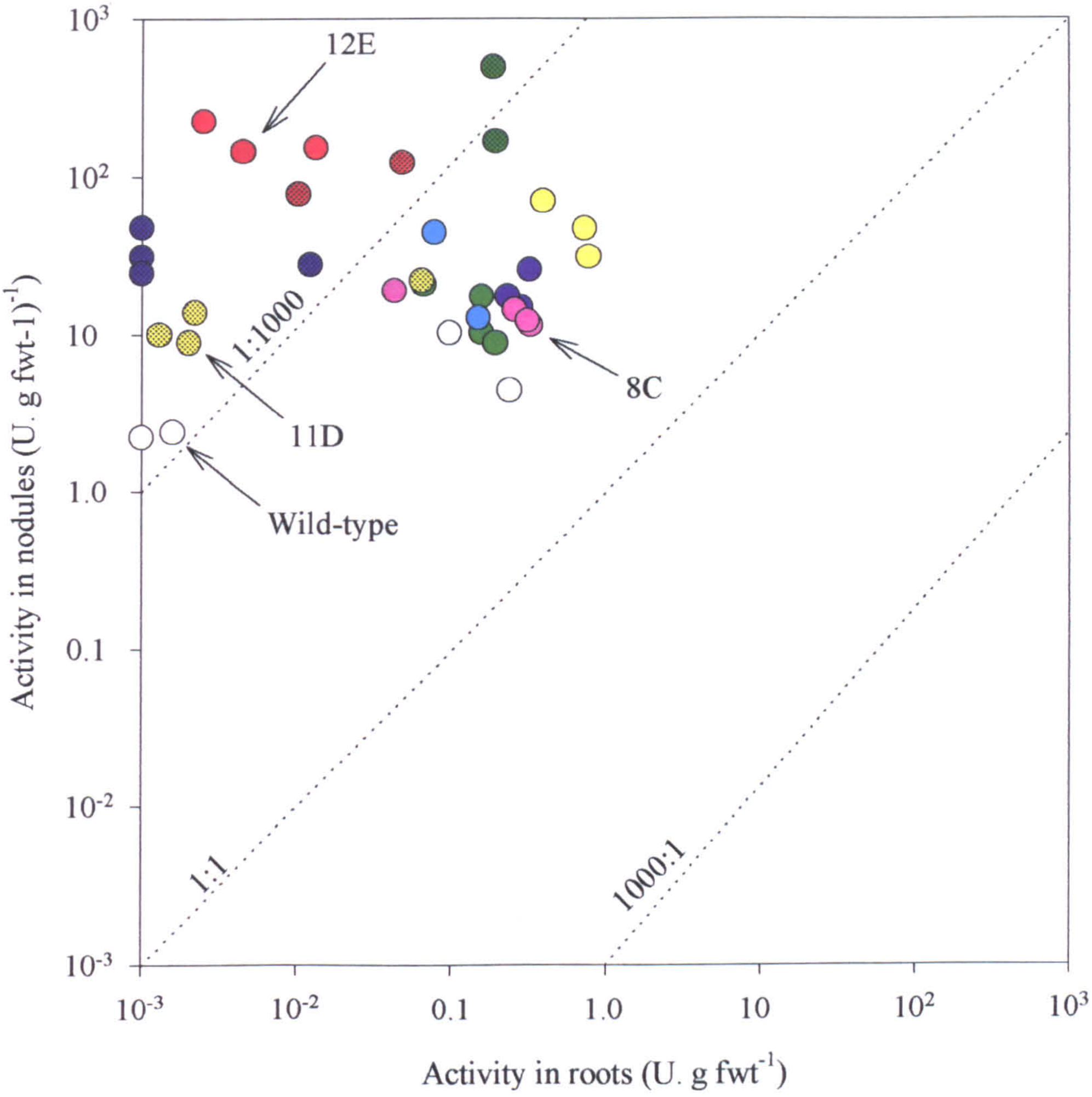

Figure 5.5: GUS activities in nodules of *L. corniculatus* plants transformed with the *gln*-γ-PATGUS construct, plotted against GUS activity in their roots. The dotted lines are plotted against the ratios of root activity to nodule activity as labelled. Plants were grown and nodulated as described in Section 2.9.1 and roots and nodules then harvested separately, extracted as described in Section 2.10.1, and GUS activity determined as described in Section 2.10.5. Symbols of the same colour represent individual plants of the same transgenic line. Untransformed plants and transformed lines 8C, 11D and 12E are marked. One unit of GUS activity catalyses the conversion of 1 µmol 4-MUG to 4-MU.

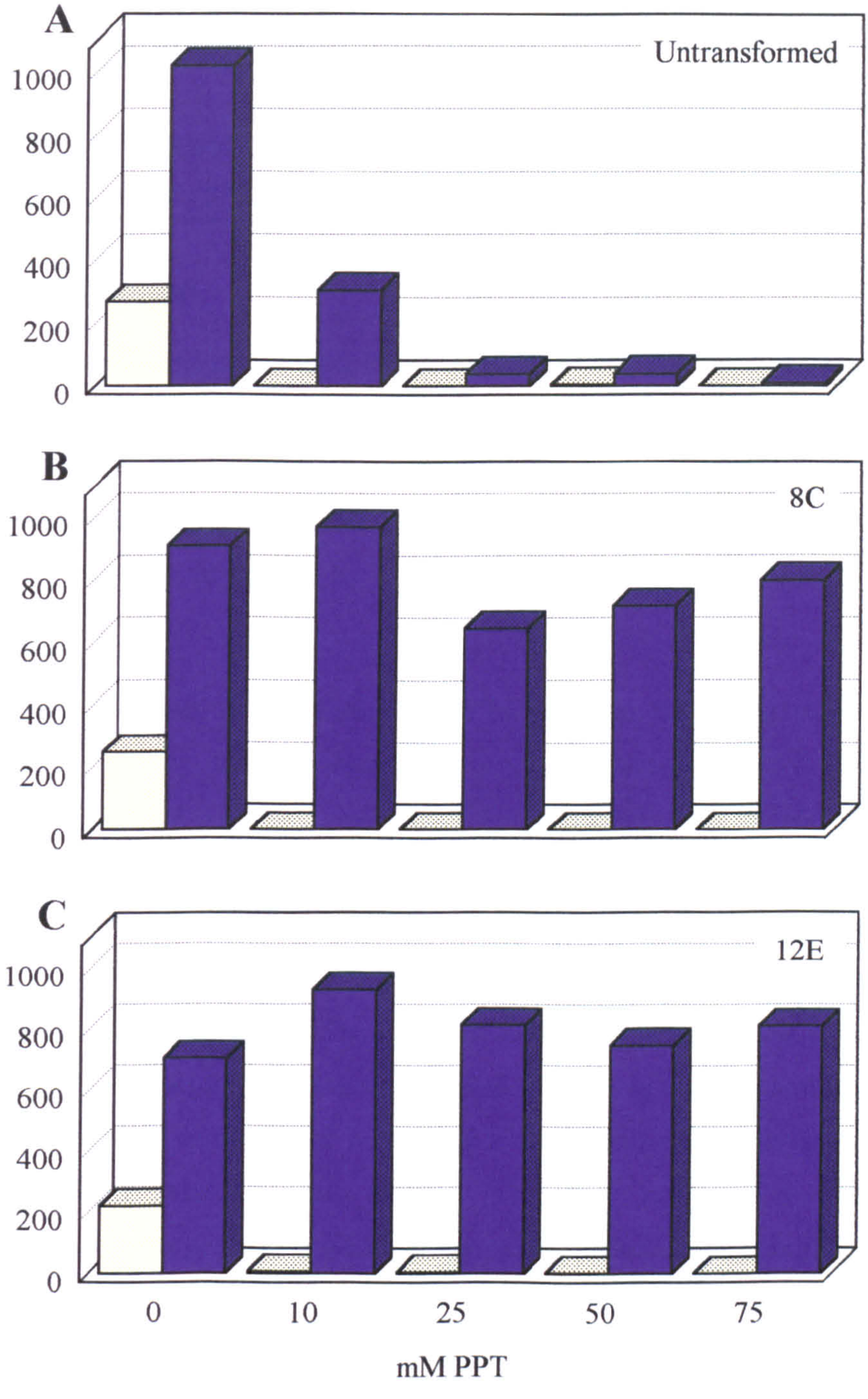

Figure 5.6: Measurements of GS activity in root (□) and nodule (■) extracts from *L. corniculatus* plants transformed with pBINGPG. Starting 38 d after rhizobial inoculation, Fåhreus solution supplemented with PPT was flushed through the soil as described in Section 5.6, and then nodules and roots harvested separately, extracted as described in Section 2.10.1, and assayed for GS transferase activity (GS_t) as described in Section 2.10.5.

CHAPTER 6:

THE EFFECT OF SPECIFIC INACTIVATION OF ROOT GLUTAMINE SYNTHETASE ON PLANT GROWTH AND NITROGEN METABOLISM IN NODULATED *LOTUS CORNICULATUS*

6.1 Introduction

The work presented in Chapter 5 demonstrated that the *pat::uidA* gene fusion produced a bifunctional PATGUS protein when expressed in transgenic *L. corniculatus*. Furthermore, GS activity in the nodules of transgenic plants, in which expression of the PATGUS protein was directed specifically to the nodules, was protected from inhibition by PPT, and thus the first major aim of the thesis was achieved.

The second aim was to use these plants to examine the effect of root-specific inhibition of GS by treating them with soil applications of PPT. The results presented in Chapter 5 showed that after 7 d of treatment with 10 mM PPT, the GS activity associated with the root was inhibited, but the nodule-specific activity was not significantly altered. In this Chapter, longer-term experiments are described that were designed to mimic the tabtoxin experiments of Knight and Langston-Unkefer as discussed in Section 1.2.3. Their results indicated that *M. sativa* plants infested with tabtoxin-producing *P. syringae* exhibited a doubling in fresh and dry weight, a doubling in nodule number and mass, and a 50% increase in nitrogenase activity (Knight and Langston-Unkefer, 1988). This they attributed to the shift in metabolism towards greater N_2 fixation that occurred due to the complete inhibition of root GS activity.

The experiments described in this Chapter were designed to determine the effect of PPT inhibition of the root form of GS on the same growth parameters mentioned above. The aim was to provide data that could be compared directly with those of Knight and Langston-Unkefer, but in a different plant species, and using a system that was more controllable.

6.2 Timing of the onset of nitrogenase activity in nodulated *L. corniculatus*

So that the start of the PPT treatment could be timed accordingly, the timing of the onset of nitrogenase activity was determined. Treatment with PPT prior to initiation of N_2 fixation would have been inappropriate for the study, and would probably have killed the plants. On the other hand, if the treatment began too late, then any potentially significant early changes due to changing the spatial distribution of GS would be missed. Therefore, to establish the timing of the onset of N_2 fixation, plants were transplanted individually into pots and assayed for nitrogenase at regular intervals over a 21-d period starting 27 d post-inoculation. The data from a number of such experiments, carried out on the wild-type (parental) line and a transgenic *gln-γ::PATGUS* line (12E), are collated in Fig. 6.1. Nitrogenase activity was first detected at 27 d after transplantation and rhizobial inoculation (d.a.i.), and extrapolation of the data suggests that N_2 fixation was initiated about 25-27 d after rhizobial inoculation in both the wild-type and transgenic lines.

There was a considerable quantitative difference between transformed and wild-type plants, with transformed plants exhibiting higher rates of nitrogenase activity, which may be related in some way to the hairy root phenotype of the transformed line.

6.3 Duration of the effect of a single PPT treatment on GS activity in nodules, roots, and shoots

The duration of the GS inhibition resulting from a single application of PPT to the soil was unknown, and the frequency of treatments that would be needed to maintain constant, long-term inhibition of GS in the root had to be determined. Therefore, wild-type plants were treated once with 10 mM PPT, and subsequently roots, nodules and stem parts harvested at daily intervals. Crude extracts were then prepared and assayed for GS activity. The concentration of PPT used was the lowest that had been identified as effectively inhibiting GS activity in roots and nodules of transformed plants by 100% after 7 d of daily application (as described in the previous Chapter). Within 24 h of the PPT treatment, the GS activity in roots (Fig. 6.2A) and nodules (Fig. 6.2B) was almost completely inhibited. While the GS

activity in the root remained low, the activity in the nodule recovered rapidly and by day 5 had increased to slightly higher levels than seen prior to treatment.

GS in the base (stem up to and including first set of leaflets) and tip (last internode and upper-most leaves) of the shoot was also inhibited by applying PPT to the soil solution. Here though, maximum inhibition was only 90% and, as might be expected, took longer to develop (2 d) than did the inhibition of GS in the root (Figs 5.7C and D). As with roots, the inhibitory effect was observable throughout the 7 d of the experiment, but there was evidence of some recovery in the shoot tip after 4-5 d.

Taking into account the above observations, watering with a 10 mM PPT solution every other day was considered necessary and sufficient for complete inhibition of root GS throughout the duration of the treatment.

6.4 Effect of long-term inhibition of root GS activity in transgenic *L. corniculatus* lines

The plants used in the long-term experiments described below were divided into two groups, and the timing of the start of the PPT treatment was different for each. The start of PPT treatments on one group of plants was timed to coincide with the onset of N_2 fixation as determined in earlier experiments, whereas the timing for the second group was delayed for a further 12 d. The second treatment was set up in case starting the treatment at the earlier stage would prove lethal.

6.4.1 Effect on plant growth and morphology

Sixteen plants of transformed line 12E (nodule-directed PATGUS) and sixteen wild-type plants were transplanted from tissue culture into individual pots and inoculated with *Rhizobium loti* as described in Section 2.9.1. After 7 d acclimatisation in the greenhouse, the plants were moved to a controlled environment room and grown under the conditions described in Section 2.9.1. Starting at either 26 d or 38 d after rhizobial inoculation (d.a.i.), the root systems of the plants were treated every other day with 10 mM PPT by flushing it through the soil. After 45 d of PPT treatment, the plants were removed carefully from their pots, their roots were washed, and they were photographed. These photographs are presented in Fig. 6.3. The plants shown in Plates A-D are representative of those for which the treatment

started 26 d.a.i. Whereas wild-type plants were clearly severely damaged by the PPT application compared to untreated plants (Fig. 6.3A and B), plants of line 12E were completely resistant (Fig. 6.3C and D).

The effect of delaying the start of the PPT treatment to 38 d.a.i. is shown in Plates E-H. Wild-type plants were severely affected by the treatment (Fig. 6.3E and F), but not so severely as those in the 26 d treatment. Again, there were no very obvious differences in the appearance of treated and untreated transformed plants (Fig. 6.3G and H).

The plants described above were subsequently divided into shoots, roots and nodules, and fresh weights, dry weights, root:shoot ratio and number of nodules per plant determined:

Fresh weight

Fresh weights obtained from each of the sets of eight plants are shown in Table 6.1, and the percentage change in fresh weight due to PPT treatment that this represents is shown in Figure 6.4. The fresh weights of all organs of wild-type plants (treated at either 26 or 38 d.a.i.) were dramatically reduced to between 12% and 36% of untreated controls. The shoot was most severely affected (12 to 15% of controls), whilst the fresh weights of roots and nodules were about one-third those of untreated plants. In contrast, the total fresh weight of the PATGUS plants treated from 26 d.a.i. was on average 25% greater than the untreated plants. This was mainly accounted for in the shoot, where there was a 38% increase in fresh weight due to treatment with PPT. When the start of the PPT treatment was delayed until 38 d.a.i., this stimulatory effect was lost, and the fresh weights of the PATGUS plants were actually reduced, although to a lesser extent than the wild-type (whole-plant fresh weight 54% of the untreated controls). Whereas shoot and root fresh weights were both reduced, there was no significant effect of PPT treatment on the total fresh weight of the nodules harvested from line 12E.

Dry weight

The dry weights of roots and shoots of the treated and untreated plants of the wild-type and line 12E are presented in Table 6.1 and Fig. 6.5. The trends observed in the fresh weights of the plants were mirrored in their dry weights, and the magnitude

of the differences in weights was the same. The most notable observation was that the PPT treatment beginning 26 d.a.i. produced a severe inhibition of dry weight accumulation in the wild-type, but a ~50% stimulation of dry weight accumulation in both roots and shoots of 12E. When the treatment was delayed to 38 d.a.i., this stimulatory effect on 12E was lost and dry weight accumulation was actually inhibited.

Root:shoot ratio

The effect that the PPT-treatments had on root:shoot ratios is shown in Table 6.1 and Fig. 6.6. Surprisingly, in wild-type plants, root applications of PPT had a greater effect on the fresh weight of the shoot than the root. Thus the root:shoot ratio of treated, wild-type plants was more than double that of untreated, wild-type plants, due to the severe stunting of the shoot (despite the PPT being applied to the soil). The opposite effect was observed with 12E, where the root:shoot ratio decreased as a result of treatment with PPT. This effect was strongest in the plants treated from 38 d.a.i. (a decrease of 37%, compared to 16% for the plants treated from 26 d.a.i.).

Number and fresh weight of nodules

In all cases, the number of nodules produced by plants subjected to the PPT treatment was significantly smaller than the number produced by untreated plants (Table 6.1; Fig. 6.7). However, the inhibitory effect on nodulation was greater for the wild-type than for 12E. PPT treatment of wild-type plants reduced the number of nodules by between 61% (26 d.a.i.) and 71% (38 d.a.i.) compared to the untreated controls. In comparison, nodulation by 12E was less affected by the PPT treatment (a 42% reduction for 26 d.a.i. and a 48% reduction for 38 d.a.i.).

An estimate of the average size of the nodules produced was derived from the number of nodules per plant and the total fresh weight of all the nodules on the plant, and is presented in Table 6.1 and Fig. 6.7. Treatment with PPT increased the fresh weight per nodule of wild-type plants by 40% if the treatment did not start until 38 d.a.i. This effect was not seen if the treatment started earlier (26 d.a.i.), in which case the treated plants were not significantly different to the controls (down by 15%). The effect of the PPT treatment on 12E was much greater, with the nodules of plants treated with PPT having on average double the fresh weight of those produced by untreated plants for both sets of treatments.

6.4.2 Effect on nodule metabolism

Nitrogenase activity

Just prior to harvesting, plants were assayed for nitrogenase activity by the acetylene reduction method as described in Section 2.10.8. The results are presented in Table 6.2, and Fig. 6.8 shows the average percentage change in the treated plants compared to untreated controls.

The fixation capacity of wild-type plants was strongly inhibited by PPT treatment irrespective of when the treatment started (by about 94% on average; Fig. 6.8A). This was mainly due to a reduction in the specific fixation capacity of the nodule which was reduced by about 85% (Fig. 6.8B and C). Nodules of line 12E that were treated with PPT from 38 d.a.i. did not show any significant alteration in N_2 fixation ability (Fig. 6.8B), but since the plants produced fewer nodules, the overall fixation capacity of the plants was on average about one third less than the untreated controls (Fig. 6.8A). Since these nodules were also larger than the controls, the fixation capacity per unit weight was also less (Fig. 6.8C). Plants treated earlier (26 d.a.i.) produced nodules with double the nitrogenase activity of the controls (Fig. 6.8B). This appeared to be mainly due to an increase in nodule size, as activity on a fresh weight basis was no different to the controls (Fig. 6.8C). However, as the treated lines produced fewer nodules than the controls (Fig. 6.7A), they had on average only 26% more N_2 fixation capacity on a whole plant basis.

GS activity

To determine the effect of the prolonged PPT treatment on GS activity, crude extracts were made from the harvested nodules as described in Section 2.10.1 and assayed for GS activity using the transferase method as described in Section 2.10.7. The results of this experiment are presented in Table 6.2.

Irrespective of the timing of the treatment, PPT application completely inhibited GS activity in the nodules of wild-type plants, but the long-term effect of PPT treatment on the plants expressing nodule-directed PATGUS activity was to stimulate nodule GS activity. GS activity per nodule at harvest was almost doubled (190% of control) by treatment with PPT starting 26 d.a.i., and nodules of transformants treated with

PPT starting 38 d.a.i. were found to have on average four times (408%) the specific activity of the untreated controls (Fig. 6.9B). Since the plants produced fewer nodules when subjected to the PPT treatment, the overall increase in plant GS activity associated with the nodule was more modest, with the plants treated at 26 d.a.i. exhibiting no significant increase relative to the controls (10%). Perhaps most surprisingly, the plants of line 12E in the 38 d.a.i. treatment had more than double (233%) the total nodule GS activity of the untreated controls. This effect was not apparent in the plants treated starting 26 d.a.i. when activity was expressed on a protein basis, there being a 63% reduction in specific activity. However, the plants treated starting 38 d.a.i. still showed a 121% increase in specific activity of nodule GS. Root GS was also measured and, in all cases, there was no detectable activity (data not shown).

6.5 Discussion

6.5.1 Soil applications of PPT inhibit GS activity in all plant tissues

Treating plants with PPT by flushing the herbicide through the soil at regular intervals is an unconventional method of application; the standard approach is to spray the leaves with dilute solutions of glufosinate-ammonium (Shelp *et al.*, 1992b; Padegimas *et al.*, 1994; McHughen and Holm, 1995) or Basta™, the commercial formulation of the product (Datta *et al.*, 1992; D'Halluin *et al.*, 1992a; Wan and Lemaux, 1994). Foliar application was unsuitable for this study as it was root GS that was to be targeted, and applications were to be repeated over a time period of a few weeks. A pilot study (data not shown) had also shown that repeated foliar applications of PPT killed both control and transgenic plants expressing PATGUS specifically in the nodule, confirming that this method was unsuitable for our purposes. Another concern was the presence of ammonium in the glufosinate-ammonium used (the only form commercially available), as the experiments were designed to be done under N_2-fixing conditions. Hence, PPT was first converted to the sodium salt using a cation exchange resin (see Section 2.12), and then applied to the soil, by adding it to the standard Fåhraeus medium used to water the plants (see Table 2.3). Since this use of PPT had not previously been reported in the literature, it was important to determine the time-course of inhibition resulting from soil applications of PPT, as

represented in Fig. 6.2. A number of conclusions can be drawn from the results of this experiment. Firstly, it is clear that applying 10 mM PPT to the soil in the manner described was sufficient to inhibit GS activity in all tissues of control plants. However, this effect varied greatly in both degree and duration, depending on the plant organ in question. In roots and shoots (Figs 6.2B-D), the effect was marked and long-lasting. However in nodules (Fig. 6.2A) the activity was at first strongly inhibited, but within another 48 h had fully recovered, and by 5 d after treatment was about 30% higher than at the start of the experiment.

The ability of the nodules not expressing PATGUS to recover from inhibition by PPT was surprising, as PPT is reported to be a potent irreversible inhibitor of GS (Lea and Ridley, 1989). To explain the recovery in GS activity, two processes would seem to be required: firstly the synthesis of new GS protein to replace that bound to PPT and secondly the depletion of PPT from the nodule tissues. There is surprisingly little literature addressing the subject of natural metabolism of PPT *in planta*, although there is evidence that some detoxification of PPT does occur. Komoßa and Sandermann (1992) reported that suspension cultures of *Z. mays* were capable of converting [3,4-^{14}C]PPT directly into 4-methylphosphinico-butyric acid (MPB), and into 3-methylphosphinico-propionic acid (MPP) and 4-methylphosphinico-2-hydroxybutyric acid (MHB) via the intermediate compound 4-methylphosphinico-2-oxo-butyric acid (PPO). They also found, to a much smaller extent, evidence of detoxification in *G. max* and *T. aestivum*, although only MPP was found in *G. max*, and MPP and MPB in *T. aestivum*. However, these results were obtained over a short (48 h) period, and they did not report any studies with whole plants.

Dröge-Laser and co-workers (1994) studied this phenomenon in intact plants of *Daucus carota*, *M. sativa* and *N. tabacum*, both wild-type and transformed with the PAT gene, and concluded that in both wild-type plants and transformants with low levels of PAT expression, a limited amount of endogenous detoxification of PPT was taking place via PPO to MHB and MPP. Thus, some of the depletion of PPT within the plant may be due to endogenous detoxification. It is possible that the enzymes responsible for this are more abundant in the nodule than in other organs, explaining the relatively rapid recovery of GS activity in this organ. Certainly, PPT is known to

be actively degraded by many soil microorganisms (Bartsch and Tebbe, 1989; Abell and Villafranca, 1991; Tebbe and Reber, 1991), and even used by them as a nitrogen source (Tebbe and Reber, 1988), so the concentration in the surrounding soil is likely to be declining during the course of the experiment.

Another possibility is that the bacteroids are capable of detoxifying PPT. Considering their bacterial origin, this may indeed be the case. However, Kriete and Broer (1996) found that free-living *R. meliloti* was sensitive to PPT, suggesting that at least some species of *Rhizobium* do not possess these detoxification mechanisms. It is also unclear to what extent this trait would be retained in the bacteroids.

In contrast to the apparently rapid replacement of PPT-inactivated GS in the nodules of the PPT-treated plants, there appears to be very little active synthesis in roots and shoots. This may indicate that the PPT treatment arrests plant development much earlier than the onset of symptoms suggests. The plants still appeared alive even at the end of the 7-d period, although signs of chlorosis and wilting were observable by this stage. Alternatively, this observation may merely be reflecting the fact that there is much less GS in these tissues, and the PPT concentration here is such that the inhibitor is not depleted as quickly by binding to the enzyme.

Finally, the strong inhibition of GS activity in the shoot system after 2 d indicates that PPT has systemic action in *L. corniculatus*, being translocated in the xylem from the roots to the above ground organs of the plant. This systemic action has been reported before in young shoots of *G. max* (Shelp *et al.*, 1992a), and Dröge-Laser and co-workers (1994) found radiolabelled PPT to be transported preferentially to the upper leaves of *N. tabacum* plants. The implications of this in the light of the long-term survival of PPT treated transgenic plants in subsequent experiments are discussed in Section 6.5.5.

6.5.2 Effect of the hairy root phenotype on nodulation

The observation, shown in Fig. 6.1, that plants of transformed line 12E had higher rates of N_2 fixation than the wild-type control corresponded with the number of nodules present on the roots of untreated plants at harvest (see Table 6.1): line 12E produced, on average, 25% more nodules. Since the inhibitor was not present, this is

likely to be due to expression in the transformed line of the hairy-root phenotype. This effect has been reported before by Pozárková *et al.* (1995), who transformed *L. corniculatus* with the *rolABC* genes from *A. rhizogenes*, using *A. tumefaciens*. They too observed a 25% increase in the number of nodules produced, although they made no comment on this aspect of their data.

A characteristic of the hairy root phenotype is known to be increased sensitivity of cells to the phytohormone, indoleacetic acid (IAA; see Gaudin *et al.*, 1994). Srinivasan *et al.* (1996) found that coinoculation of *P. vulgaris* with IAA-producing strains of *Bacillus* promoted nodulation and it seems likely that increased sensitivity to IAA would have a similar effect. A similar study by Sturz *et al.* (1997) found that coinoculation with *A. rhizogenes* promoted nodulation, although it is unclear whether the bacterium itself produces IAA.

6.5.3 Comparison of the effects of the two PPT treatments on line 12E, and their significance.

There were both similarities and differences in plant growth, morphology and metabolism that were attributable to the variation in timing of the PPT treatment. Tables 6.1 and 6.2 contain a comparison of the main effects that were observed. The main effect of delaying the treatment by 12 d was the loss of the majority of the promotive effect of PPT on nitrogenase activity in the nodule. The delay did not, however, have a similar effect on the number of nodules that developed (less than the untreated control for both treatments). Thus, whilst treatment with PPT clearly reduced the number of nodules formed, the 12-d delay was largely irrelevant. These observations may by explained in the following hypothesis:

Nodule initiation and development are rapid in the period between rhizobial inoculation and the onset of N_2 fixation. After N_2 fixation has begun (ca. 25-27 d.a.i.; see Fig. 6.1), production of new nodules slows down considerably, as demand for N is now increasingly being met by N_2 fixation. PPT treatment completely inhibits the formation of new nodules, accounting for the smaller number of nodules on the treated plants at harvest, compared to the untreated controls. Since the production of new nodules slows down after the onset of N_2 fixation, the number of nodules initiated in the 12-d period from 26 d.a.i. to 38 d.a.i. was relatively small, explaining

the apparent insensitivity of this parameter to the delay in treatment start. The N_2 fixation capacity of young nodules is plastic, and can be increased in response to an increase in N demand by production of more nitrogenase. However, this ability is gradually lost as the nodules mature. Thus, during the 12 days between 26 and 38 d.a.i., the nodules of plants under the earlier treatment regime produce more nitrogenase than the untreated ones of the later treatment. By 38 d.a.i., the majority of the nodules of plants in the second treatment are too old to respond in this way, and the promotive effect of the treatment is not seen.

The above hypothesis suggests that PPT initially inhibits nodule initiation and/or development. This results in N stress, which is compensated for in young, developing nodules by increased production of nitrogenase.

6.5.4 Comparison with the effects of *Pseudomonas syringae* on *Medicago sativa*

Table 6.4 also compares the results of this study with those of Knight and Langston-Unkefer (1988; see also Section 1.2.3). For many of the parameters measured, similar effects of inhibiting nodule GS were obtained. There were also some differences with their findings, for which some explanations are offered:

Nitrogenase activity

Arguably, the most important finding of Knight and Langston-Unkefer was the doubling of nitrogenase activity in the nodules due to infestation with the *Tox*$^+$ strain of *P. syringae*. This study has found that inhibition of root GS with PPT in line 12E mimics this effect, but only when the PPT treatment began around the onset of N_2 fixation (26 d.a.i.), and only if nitrogenase activity is expressed on a per nodule basis.

Number of nodules

Whereas Knight and Langston-Unkefer observed a doubling in the number of nodules as a result of the infestation, both PPT treatments had a strong inhibitory effect on the number of nodules produced by 12E. There are differences between the two studies that may explain this:

1. Nodulation capacity. The *M. sativa* plants used by Knight and Langston-Unkefer were very poorly nodulated (no more than 5 nodules per plant, on average).

Thus, a doubling in the number of nodules merely represented the production of a small number of additional nodules. To achieve a similar result in the well-nodulated *L. corniculatus* used here would have required the production of upwards of 100 extra nodules.

2. Inhibitor used. Knight and Langston-Unkefer (1988) reported the presence of a β-lactamase in the bacterial fraction of the nodule, which catalysed the cleavage of tabtoxin, and this protection mechanism may well be active in free-living *Rhizobium*. In contrast, some species of *Rhizobium* are known to be susceptible to PPT in their free-living state (see Section 6.5.1), and the treatment may well have killed any inoculum present in the soil, or at least rendered it incapable of infecting host plants. Kreite and Broer (1996) found that PPT inhibited nodulation of PPT-resistant *M. sativa* plants, when 100 mM PPT was applied to sterile soil fortnightly for 3 weeks. When this was repeated with unsterile soil, no decrease in nodulation rate was seen, which they attributed to the rapid degradation of PPT in the soil. In the experiments reported here, there is constant, if lower (10 mM) inhibitory pressure, which may have been sufficient to inhibit nodulation.

3. Delivery of the inhibitor. It seems likely that infestation of the root system with *P. syringae* would result in localised production of the toxin close to the root system of the host plant. This distribution would have been considerably different to the uniform coverage of PPT in the experiments described here. In a localised area, the effect of the toxin on soil microflora would be limited. However, the ubiquitous presence of PPT in the soil is likely to have a significant effect on the composition of microorganisms in the soil surrounding the *L. corniculatus* plants studied here. Of the seven species of bacteria studied in the experiments of Kreite and Broer (1996), four were found to be susceptible to PPT. One consequence of such an alteration in the make-up of bacterial populations in the soil may well be a reduction in nodulation efficiency. The beneficial effect of a range of species of soil bacteria on nodulation efficiency is well documented (see Srinivasan *et al.*, 1997), and significant reductions in their populations may have occurred over the course of the experiments described here. The delicate balance of species involved was demonstrated by Plazinski and Rolfe (1985) who found that certain *Azospirillium*

strains could either promote or inhibit nodulation of *Trifolium repens* depending on the ratio of the two bacterial species in the soil.

Nodule size

In line with the findings of Knight and Langston-Unkefer, the nodules of treated plants of line 12E were twice the size (based on fresh weight per nodule) of those produced by untreated plants, regardless of whether the treatment started 26 or 38 d.a.i. However, only nodules of plants treated at 26 d.a.i. had more nitrogenase activity, indicating that N_2 fixation capacity and nodule size were not tightly linked in these experiments.

Fresh- and dry- weights

Knight and Langston-Unkefer reported a remarkable doubling in fresh and dry weights of the alfalfa plants, which they attributed to the increased N_2 fixation capacity of the infested plants. In the experiment described here, the effects of the PPT treatment on the growth of line 12E were not obvious from a visual inspection (Fig. 6.3), but fresh and dry weight analysis did reveal that if the PPT treatment was started early enough (26 d.a.i.), then treated plants were larger (on both a fresh- and dry-weight basis) than the controls, due mainly to an increase in shoot weight. The whole-plant increase in dry weight (ca. 50%) was significant, although modest compared to the doubling reported by Knight and Langston-Unkefer. That the effect was not greater is probably due to the fact that, although nitrogenase activity per nodule was stimulated, there were fewer nodules per plant. As mentioned previously, nodules of plants treated starting 38 d.a.i. did not show increased nitrogenase activity, and thus the reduced number of nodules led to an overall reduction in N_2 fixation and an inhibition of plant growth.

Glutamine synthetase activity

The effects on nitrogenase activity were accompanied by even greater increases in GS activity per nodule (Fig. 6.9B), although the four-fold increase in GS activity per nodule seen in the 38 d.a.i. treatment was reduced to a two-fold increase on a whole plant basis, due to the decrease in the number of nodules produced. Knight and Langston-Unkefer presented their GS measurements on a protein basis, and found a

55% decrease in nodule GS activity due to infestation by the *Tox*$^+$ form of *P. syringae*. It is interesting that the data presented here, when expressed on a protein basis, show a comparable (63%) decrease in nodule GS activity in response to long-term treatment with PPT. It is unclear, either from the results presented here or from those of Knight and Langston-Unkefer, whether this is due to direct inhibition or to other changes in the nodule during long-term treatments. More work, such as western blotting to determine changes in GS protein, needs to be done to examine this phenomenon.

6.5.5 Other observations

Wild-type L. corniculatus *survived soil treatment with PPT*

Clearly, inhibition of GS in both roots and nodules of wild-type plants has a severe effect on their growth, with plants treated from 26 d.a.i. being almost killed by the PPT treatment (Fig. 6.3B). What is surprising is that the plants treated from 38 d.a.i. survived as well as they did under these conditions (Fig. 6.3F). Although these plants stopped growing (data not shown), they still managed to survive. This is especially surprising in the light of the results of the study presented in Fig. 6.2, which clearly show that these PPT-treated control plants would have had very little GS activity in the shoot. Thus it appears that wild-type *L. corniculatus* was capable of surviving with a fraction of the normal amount of GS activity present in any of the tissues examined. It is not known how much GS activity would be required by a plant that was not actively growing. In such a condition, only GS involved in metabolic pathways concerned with general cell maintenance would be required. One obvious concern is that of the potentially damaging effect of photorespiration. However, these plants may not have been prone to much photorespiratory activity as they would not have needed to photosynthesise as much as actively growing plants, and may consequently have had a much smaller quantity of active Rubisco.

Changes in root:shoot ratio

In wild-type plants. The dramatic increase in the root:shoot ratio of the wild-type plants in response to the PPT treatment was both unexpected and interesting, as it reflects an *increase* in partitioning to the root in response to the PPT treatment.

However, as Table 6.1 and Fig. 6.4 show, this increase in the ratio does not reflect an absolute increase in root fresh weight: it reflects the greater sensitivity of the shoots to the treatment. As discussed in Section 6.5.1, there is clear evidence for the systemic transport of PPT to the shoot (see Fig. 6.2). Any further interpretation of this result must be made with this in mind.

An increase in the root:shoot ratio is a frequently observed plant response to a deficiency in N relative to C (Rufty, 1997). The wild-type plants in this experiment would indeed be under considerable N stress, since the main enzymatic route for its assimilation was inhibited. This may explain the observed change in root:shoot partitioning in the wild-type plants.

In line 12E. In contrast to the dramatic increase in the root:shoot ratio of the wild-type plants, the ratio in PPT-treated plants of line 12E was slightly lower than untreated plants for both sets of treatment timings. Thus, these plants put relatively more resources into shoot growth when treated with PPT. As previously mentioned, the systemic action of PPT was demonstrated (see Fig. 6.2), and so it is unlikely that this can be explained by the presence of the inhibitor in the soil. On the basis that a decrease in root:shoot ratio is an indicator of high N status (Rufty, 1997), this result suggests that the PPT-treated transformant had a higher N status than the untreated controls.

6.5.6 Conclusion

The results presented in this Chapter have clearly shown that inhibition of GS activity specifically in the root has a profound effect on N metabolism within the nodule. This can be seen in the two-fold increase in nitrogenase activity, and the four-fold increase in GS activity in the nodule, over the levels seen in untreated control plants, with a corresponding increase in dry matter production. These results support the findings of Knight and Langston-Unkefer (1988), in that they also obtained unexpected increases in growth rate when root GS activity was inhibited in nodulated plants. A much greater stimulation of plant growth may have been seen if the PPT-treated transformants had not developed fewer nodules than the controls.

Table 6.1 (right): Effect of PPT treatment on the growth and morphology of wild-type *Lotus corniculatus* and of a line expressing PATGUS in the infected zone of the nodule (12E). Beginning either 26 or 38 d after rhizobial inoculation (d.a.i.), Fåhraeus solution supplemented with 10 mM PPT was flushed through the soil for 45 d as described in Section 6.4. Plants were then harvested and fresh weight, dry weight and number of nodules determined.

Table 6.1: Effect of PPT treatment on plant growth parameters

		PPT[††] treatment	Fresh weights					Dry weights		No. of nodules	Root:Shoot ratio (fwt)
			Shoot ($g.plant^{-1}$)	Root ($g.plant^{-1}$)	Nodule ($g.plant^{-1}$)	Nodule ($mg.nodule^{-1}$)	Plant ($g.plant^{-1}$)	Shoot ($g.plant^{-1}$)	Root ($g.plant^{-1}$)		
26 d.a.i.	wild-type	-	4.34 (0.27)	3.09 (0.21)	0.38 (0.03)	1.99 (0.15)	7.92 (0.49)	0.86 (0.05)	0.44 (0.03)	199 (27)	0.71 (0.03)
		+	0.53** (0.12)	1.01** (0.11)	0.13** (0.02)	1.70 (0.15)	1.67** (0.23)	0.13** (0.03)	0.20** (0.02)	77** (8)	2.56* (0.53)
	12E	-	1.89 (0.15)	1.07 (0.10)	0.31 (0.03)	1.28 (0.06)	3.36 (0.28)	0.39 (0.03)	0.17 (0.01)	242 (25)	0.57 (0.03)
		+	2.61** (0.16)	1.23 (0.07)	0.37 (0.03)	2.65** (0.15)	4.21* (0.23)	0.61** (0.04)	0.25** (0.01)	140** (8)	0.48* (0.03)
38 d.a.i.	wild-type	-	5.25 (0.42)	3.55 (0.27)	0.40 (0.03)	1.73 (0.11)	9.39 (0.71)	0.98 (0.09)	0.56 (0.05)	237 (23)	0.68 (0.03)
		+	0.76** (0.13)	1.27** (0.15)	0.16** (0.02)	2.42* (0.16)	2.18** (0.28)	0.19** (0.03)	0.26** (0.03)	69** (10)	1.84** (0.19)
	12E	-	4.58 (0.32)	3.62 (0.14)	0.37 (0.02)	1.27 (0.10)	8.81 (0.37)	1.07 (0.04)	0.54 (0.01)	303 (26)	0.83 (0.08)
		+	2.88** (0.24)	1.50** (0.11)	0.39 (0.04)	2.52** (0.17)	4.77** (0.37)	0.68** (0.05)	0.31** (0.03)	157** (12)	0.52* (0.01)

[†] Number of days between rhizobial inoculation and start of PPT treatment. [††] -: no PPT; +: 10 mM PPT. *Significantly different from untreated control of the same genotype at the 95% level. **Significantly different from untreated control of the same genotype at the 99% level. Values in brackets are standard errors of the mean.

Table 6.2 (right): Effect of PPT treatment on nodule GS and nitrogenase activities of wild-type *Lotus corniculatus* and of line 12E. Beginning either 26 or 38 d after rhizobial inoculation (d.a.i.), Fåhraeus solution supplemented with 10 mM PPT was flushed through the soil for 45 d as described in Section 6.4. Nodules were then harvested and enzyme activities determined. One unit (U) of GS activity catalyses the formation of one µmol of γ-glutamylhydroxamate from glutamine and hydroxylammonium per minute at 30°C. One U of nitrogenase activity catalyses the reduction of one nmol of acetylene to ethylene per min at room temperature.

Table 6.2: Effect of PPT treatment on nodule GS and nitrogenase activities

		PPT[††] treatment	Glutamine synthetase (U)				Nitrogenase (U)			
			/plant	*/nodule (x1000)*	*/g nodule fwt*	*/mg protein*	*/plant*	*/nodule*	*/g nodule fwt*	*/µg protein*
26 d.a.i.	wild-type	-	1.07 (0.15)	6.34 (1.07)	2.53 (0.50)	0.66 (0.11)	125.2 (12.1)	0.74 (0.09)	273.1 (13.7)	64.3 (6.71)
		+	0.000** (0.0002)	0.007** (0.003)	0.004** (0.002)	0.007** (0.003)	9.08** (3.55)	0.11** (0.03)	55.2** (12.0)	101.0** (8.69)
	12E	-	1.07 (0.12)	4.55 (0.69)	2.87 (0.58)	1.05 (0.15)	67.1 (5.54)	0.32 (0.03)	208.7 (13.5)	56.2 (6.07)
		+	1.18 (0.07)	8.66** (0.69)	3.31 (0.28)	0.39** (0.02)	84.7 (6.11)	0.65** (0.04)	205.5 (10.6)	30.0 (2.22)
38 d.a.i.	wild-type	-	0.47 (0.09)	2.25 (0.65)	0.85 (0.20)	0.29 (0.06)	157.5 (12.3)	0.78 (0.05)	313.5 (8.79)	81.1 (6.53)
		+	0.001** (0.0003)	0.01* (0.004)	0.006** (0.002)	0.004** (0.001)	8.71** (2.49)	0.13** (0.02)	50.3** (9.02)	45.2** (6.40)
	12E	-	0.45 (0.17)	1.72 (0.64)	0.76 (0.28)	0.29 (0.09)	154.8 (11.1)	0.59 (0.04)	318.5 (14.8)	92.0 (17.4)
		+	1.05** (0.13)	7.01** (0.96)	2.82** (0.38)	0.64* (0.07)	97.9* (9.87)	0.68 (0.06)	221.3** (11.6)	64.3 (6.62)

[†] Number of days between rhizobial inoculation and start of PPT treatment. [††] -: no PPT; +: 10 mM PPT. *Significantly different from untreated control of the same genotype at the 95% level. **Significantly different from untreated control of the same genotype at the 99% level. Values in brackets are standard errors of the mean.

Table 6.3: Comparison of the main effects of PPT treatment of line 12E with the findings of Knight and Langston-Unkefer (1988)

This work (*gln-γ:PATGUS* line 12E) PPT treatment beginning:		Knight and Langston-Unkefer (1988)
26 d.a.i.	*38 d.a.i.*	
Fresh weight:		
38% increase in shoot	*37% decrease* in shoot	*83% increase* in shoot
15% increase in root	*59% decrease* in root	*124% increase* in root
19% increase in nodule	*5% increase* in nodule	and nodule
Dry weight:		
56% increase in shoot	*46% decrease* in shoot	*95% increase* in plant
47% increase in root	*43% decrease* in root	
Root:shoot ratio:		
16% decrease	*37% decrease*	*113% increase*
Nodules:		
107% increase in size	*98% increase* in size	*No effect* on size
42% decrease in number	*48% decrease* in number	*141% increase* in number
Nitrogenase activity:		
No effect per g nodule fresh weight	*31% decrease* per g nodule fresh weight	*94% increase* per g nodule fresh weight
26% increase per plant	*37% decrease* per plant	Estimated *five-fold*
103% increase per nodule	*15% increase* per nodule	*increase* per plant
GS activity:		
63% decrease per mg soluble protein	*121% increase* per mg soluble protein	*45% decrease* per mg soluble protein
15% increase per g fresh weight of nodule	*271% increase* per g fresh weight of nodule	
No effect on activity per plant	*133% increase* per plant	

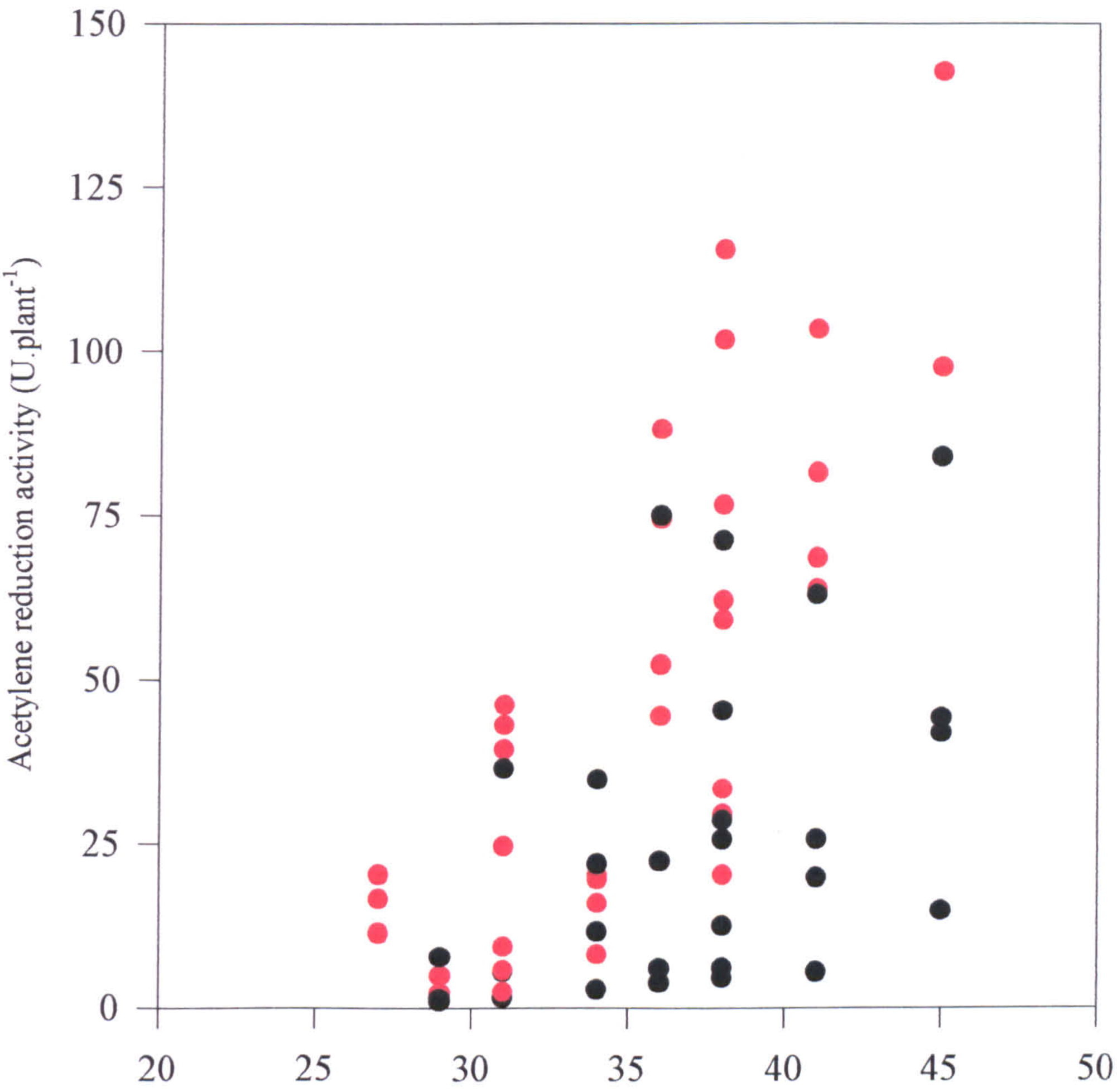

Figure 6.1: Time-course of increase in nitrogenase activity as measured by acetylene reduction in wild-type *L. corniculatus* plants (●) and in line 12E (●), which expresses PATGUS in the infected zone of the nodule. Plants were assayed for acetylene reduction as described in Section 2.4.8. Results are expressed as units of acetylene reduction activity per plant. One unit (U) of nitrogenase activity catalyses the reduction of one nmol of acetylene to ethylene per min at room temperature.

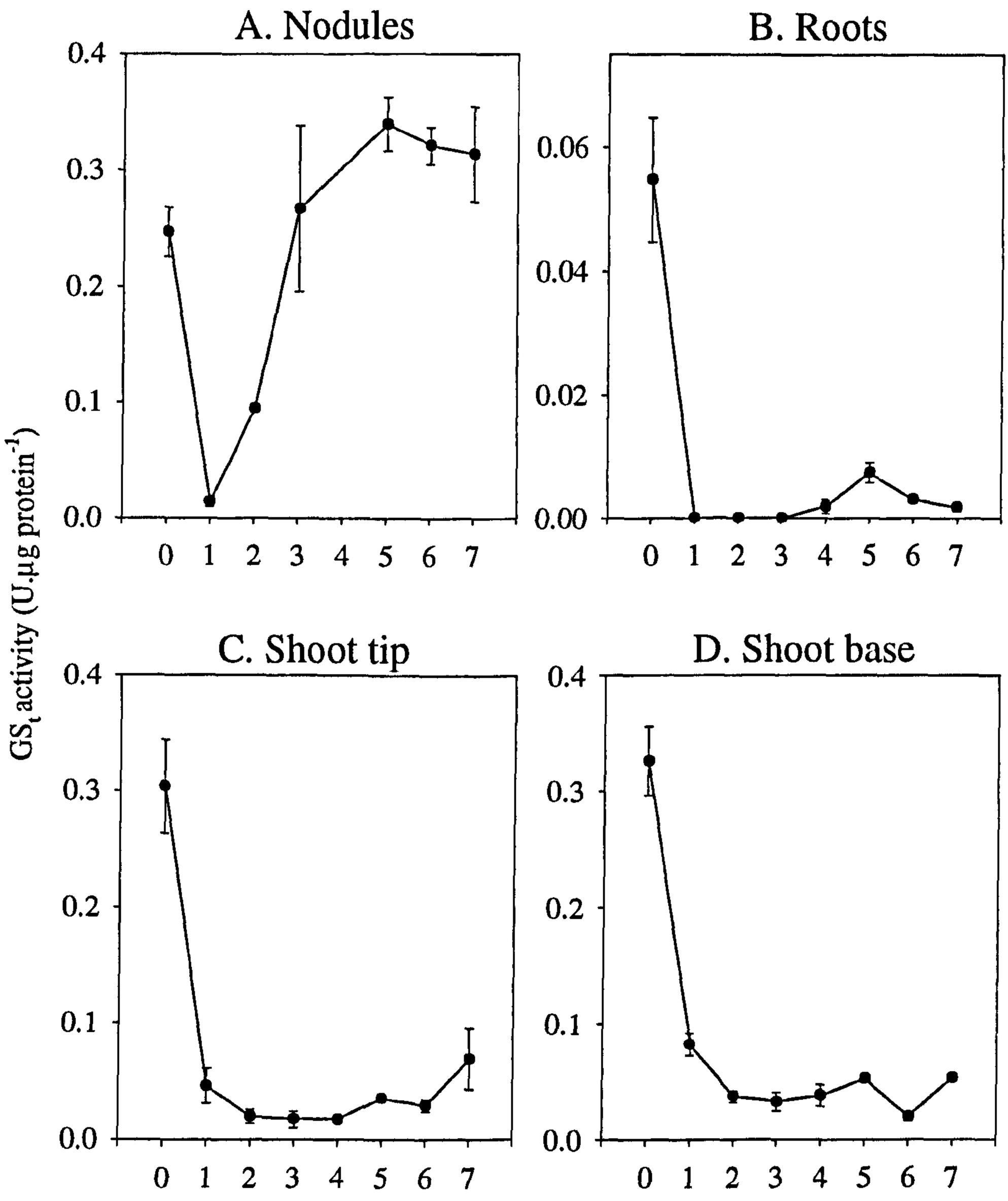

Figure 6.2: The effect of soil applications of PPT on GS activity in nodules, roots and shoots of wild-type *L. corniculatus*. Fåhraeus solution supplemented with 10 mM PPT was flushed through the soil as described in Section 6.3, and then nodules (A), roots (B) shoot tip (top-most internode and above; graph C) and shoot base (bottom-most leaflets and below; graph D) harvested separately and extracted as described in Section 2.4.1. GS transferase activity (GS_t) was determined as described in Section 2.4.7. One unit (U) of GS activity catalyses the formation of one µmol of γ-glutamylhydroxamate from glutamine and hydroxylammonium per min at 30 °C.

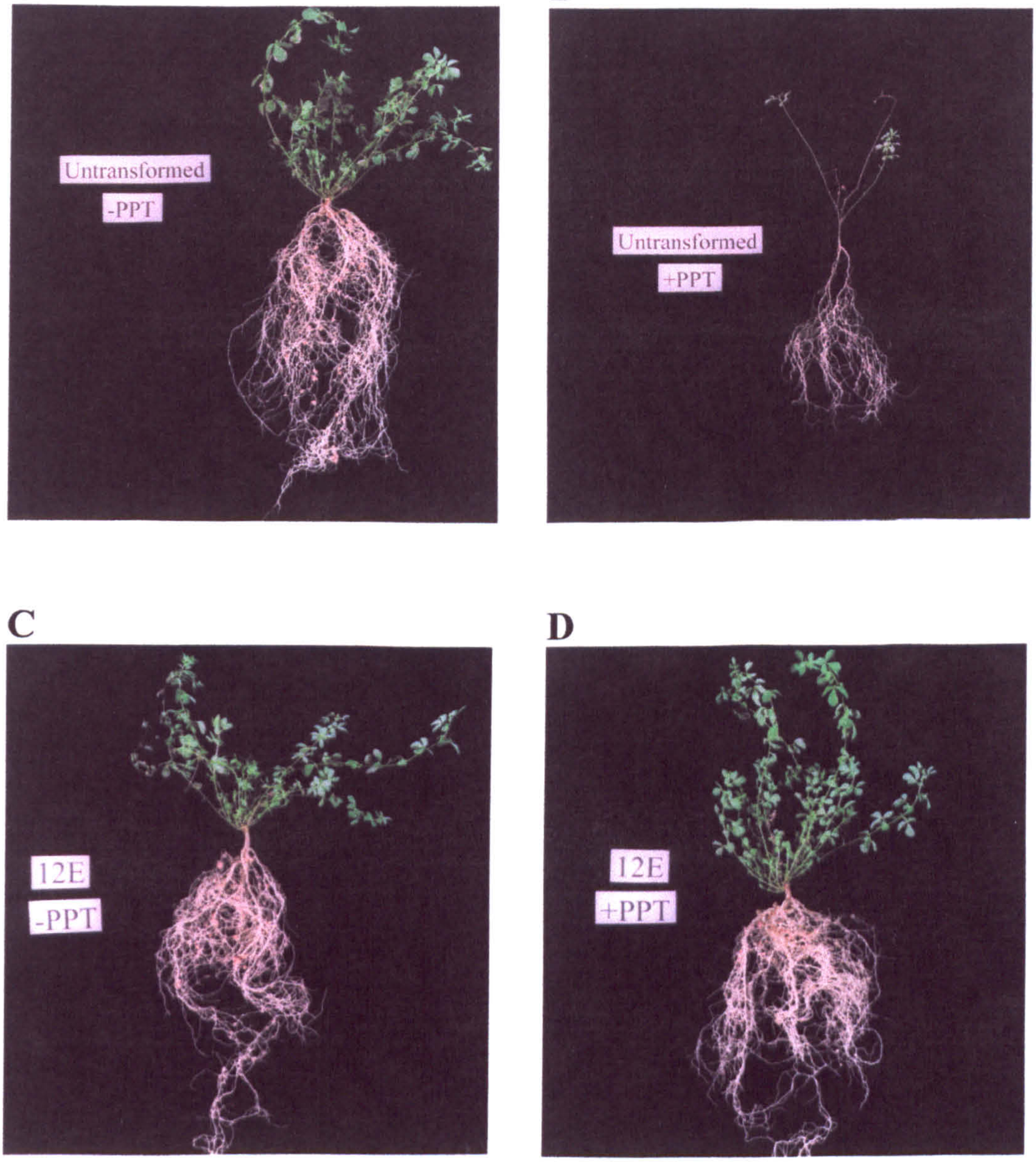

Figure 6.3: The effect of soil applications of PPT on the growth habit of *L. corniculatus*. Starting 26 d after inoculation with *R. leguminosarum*, Fåhraeus solution supplemented with 10 mM PPT was flushed through the soil every day for 45 d as described in Section 6.4 and then plants were removed from the growth medium, washed and photographed. (*continued overleaf*)

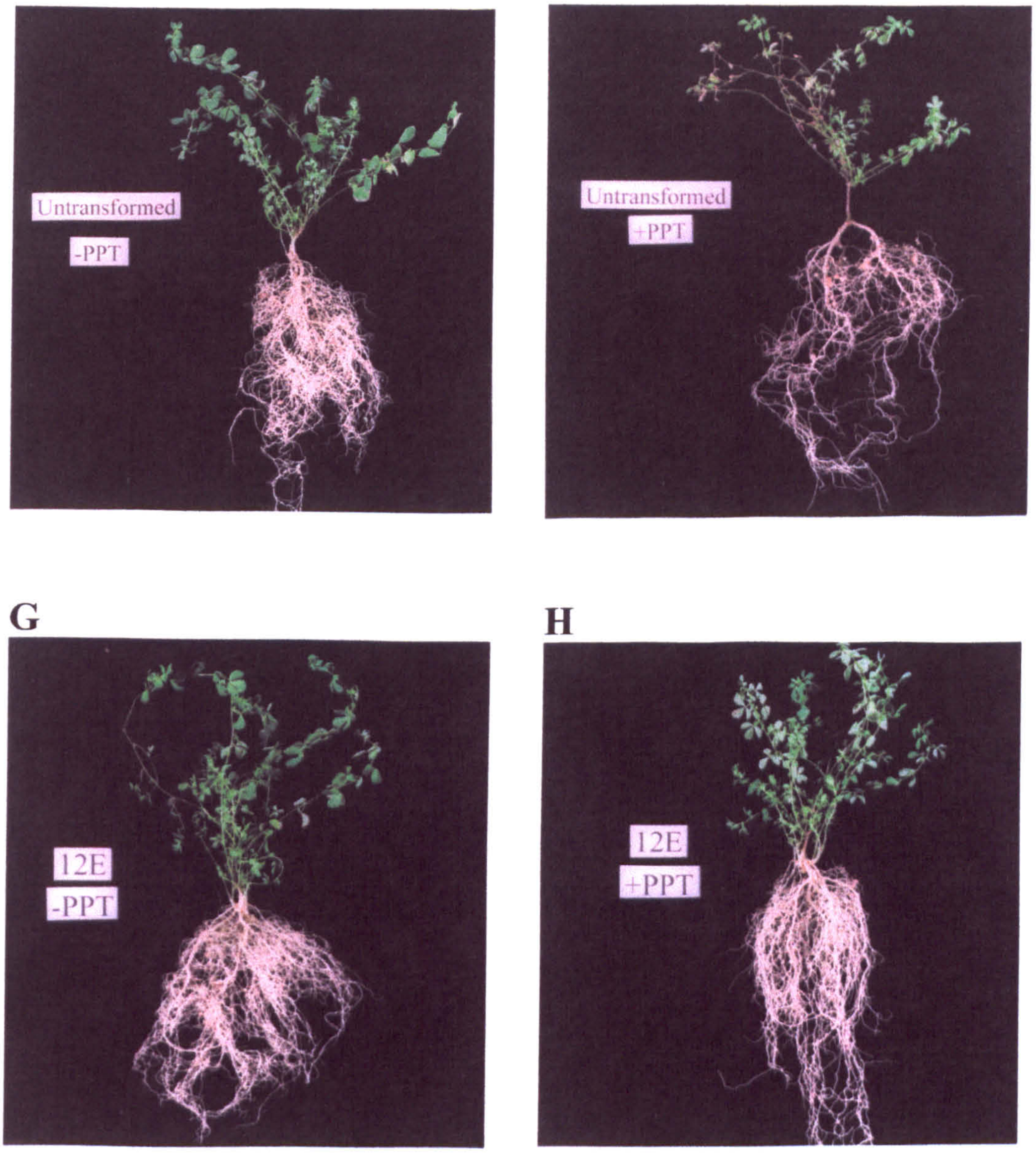

Figure 6.3 (continued): The effect of soil applications of PPT on the growth habit of *L. corniculatus*. Starting 38 d after inoculation with *R. leguminosarum*, Fåhraeus solution supplemented with 10 mM PPT was flushed through the soil every day for 45 d as described in Section 6.4 and then plants were removed from the growth medium, washed and photographed.

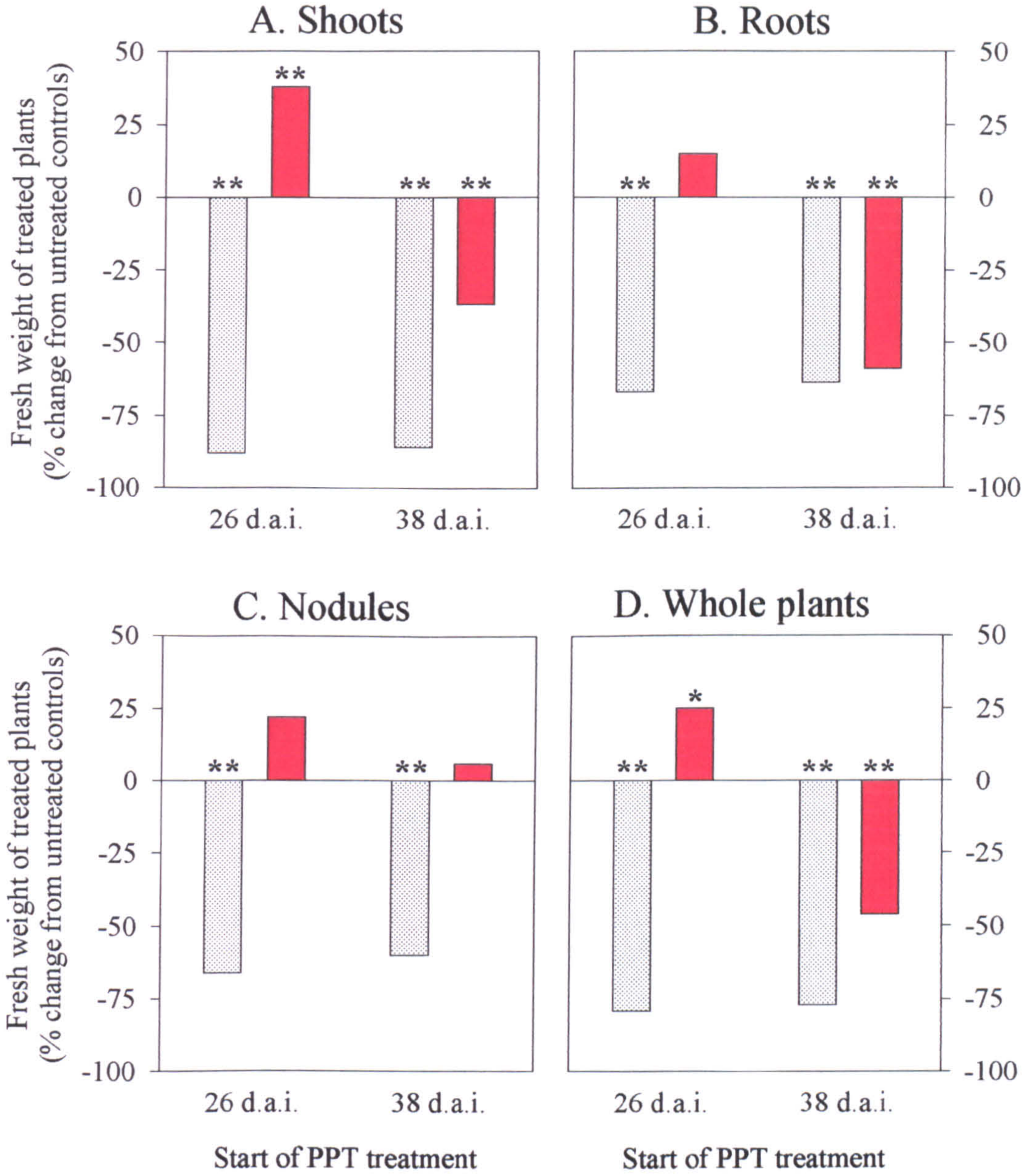

Figure 6.4: The effect of soil applications of PPT on the fresh weight of shoots (A), roots (B), nodules (C) and whole plants (D) of wild-type *L. corniculatus* and of line 12E. Beginning either 26 or 38 d after rhizobial inoculation (d.a.i.), Fåhraeus solution supplemented with 10 mM PPT was flushed through the soil for 45 d as described in Section 6.4, and then shoots, roots and nodules harvested and weighed. Bars indicate the percentage change in weight of treated plants compared to untreated controls. See also Table 6.1.

Key: ■ = wild-type; ■ = transformed line 12E; * = Significantly different from untreated control at the 95% confidence level; ** = Significantly different from untreated control at the 99% confidence level.

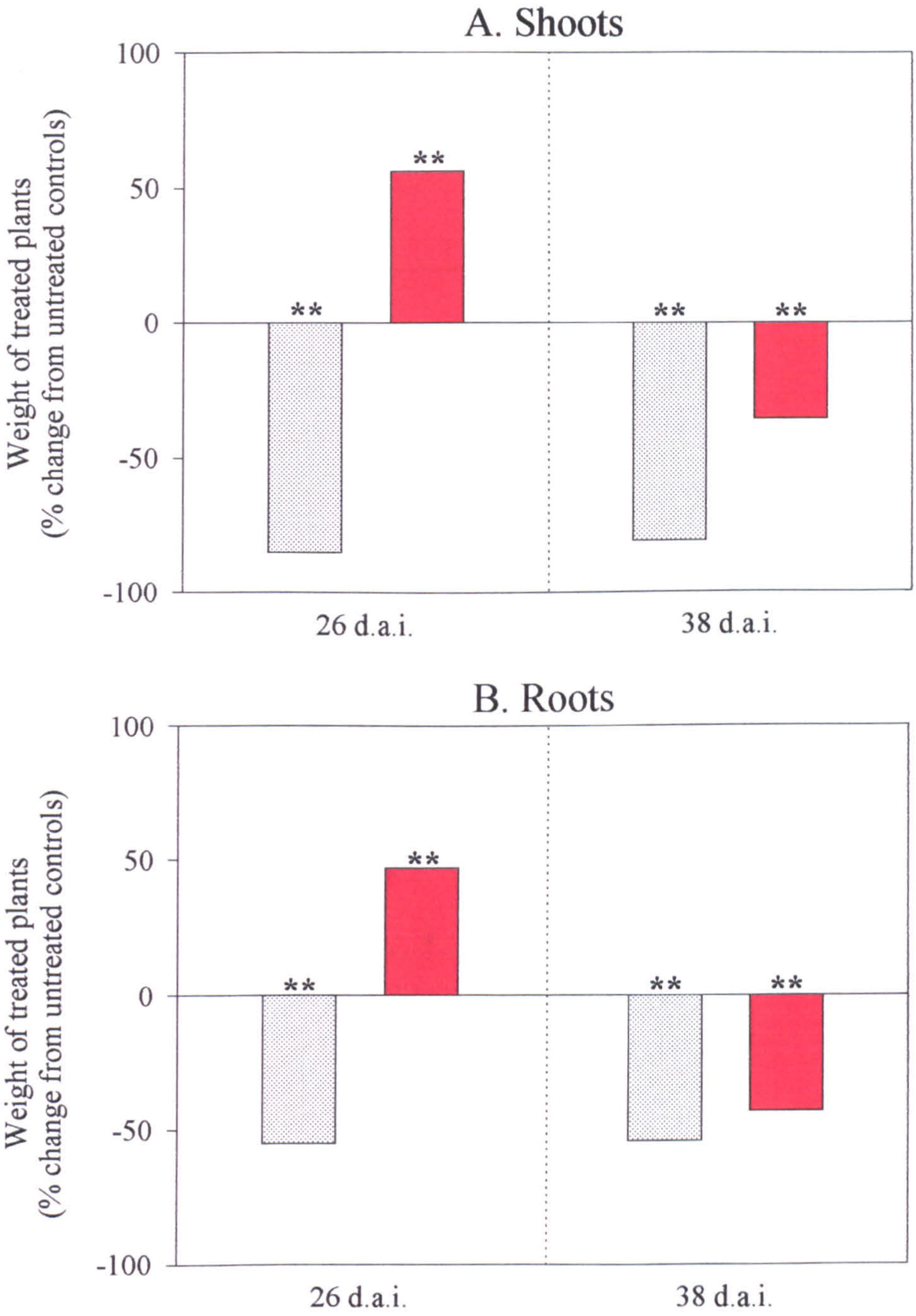

Figure 6.5: The effect of soil applications of PPT on the dry weight of wild-type *L. corniculatus* and of line 12E. See Fig. 6.4 for experimental details. After harvesting and fresh weight determination, shoots and roots were dried in an oven at 55°C for 48 h to remove the water content and reweighed. Bars indicate percentage change in weight of treated plants compared to untreated controls. See also Table 6.1. **Key:** ■ = wild-type; ■ = transformed line 12E; * = Significantly different from untreated control at the 95% confidence level; ** = Significantly different from untreated control at the 99% confidence level.

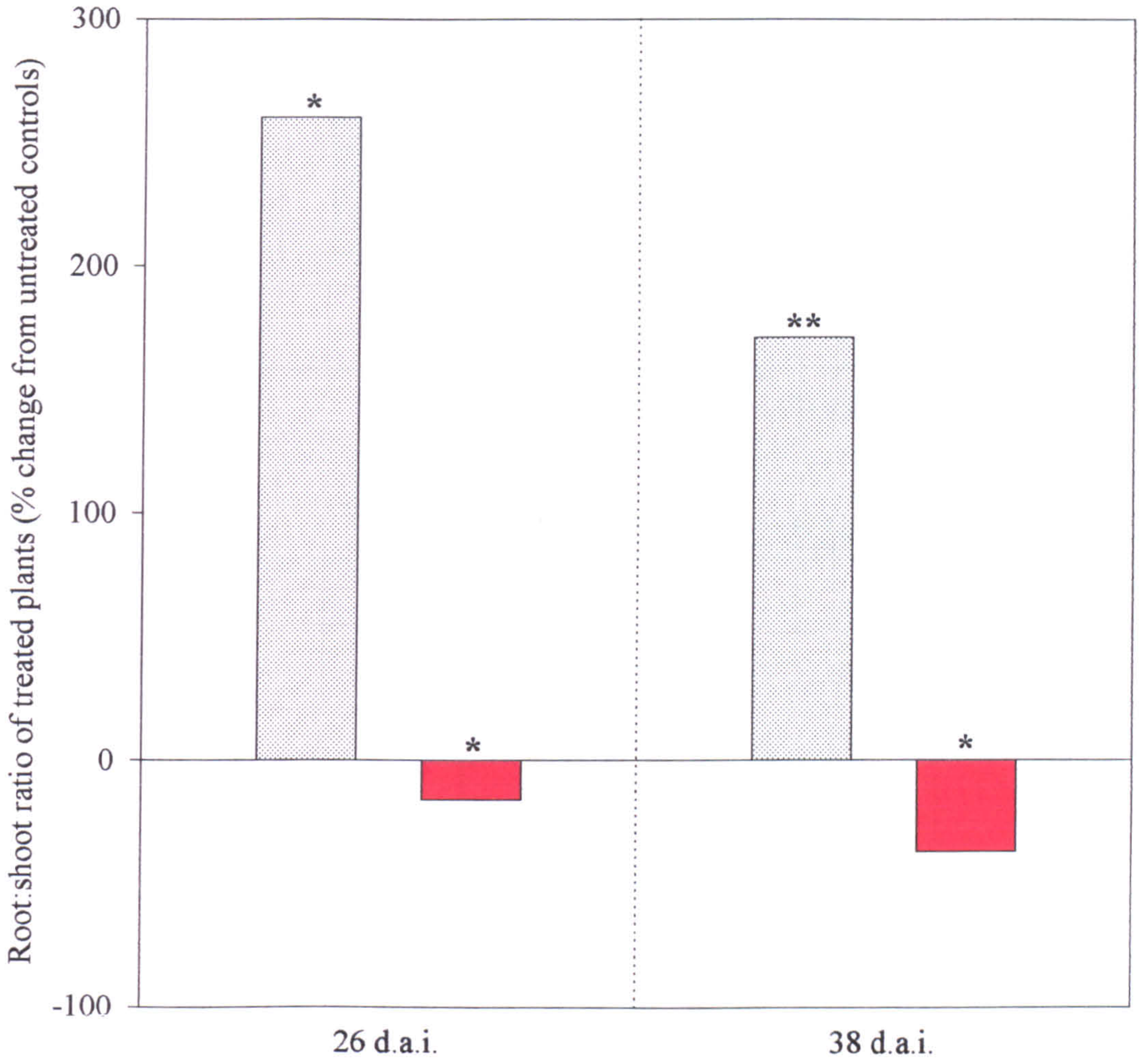

Figure 6.6: The effect of soil applications of PPT on the root:shoot ratio of wild-type *L. corniculatus* and of line 12E. See Fig 6.4 for experimental details. Bars indicate percentage change in root:shoot ratio of treated plants compared to untreated controls. See also Table 6.1.

Key: ■ = wild-type; ■ = transformed line 12E; * = Significantly different from untreated control at the 95% confidence level; ** = Significantly different from untreated control at the 99% confidence level.

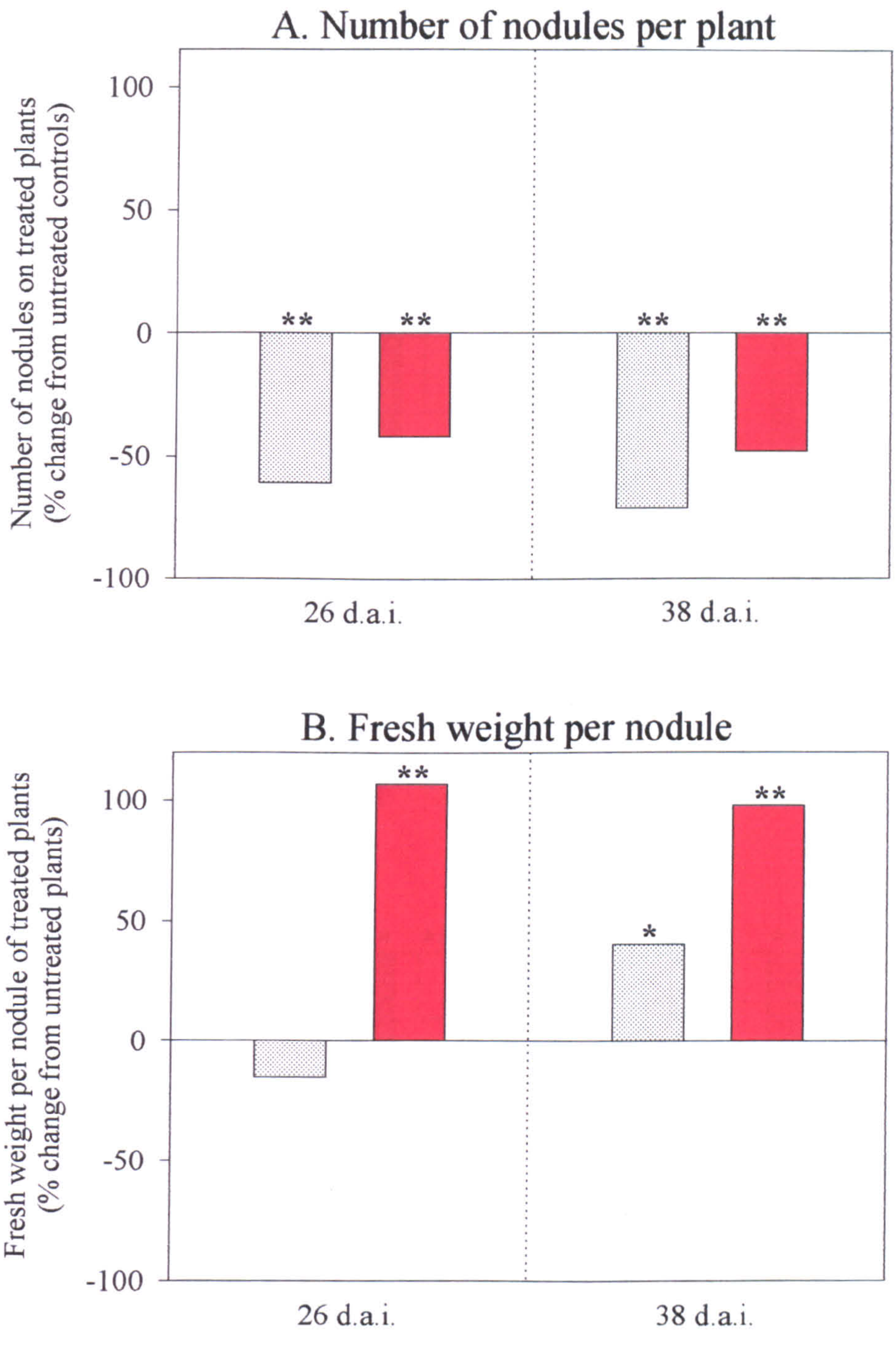

Figure 6.7: The effect of soil applications of PPT on the number and average fresh weight of nodules observed on the roots of wild-type *L. corniculatus* and of line 12E. See Fig. 6.4 for experimental details. Bars indicate percentage change in nodules of treated plants compared to untreated controls. See also Table 6.1.
Key: ■ = wild-type; ■ = transformed line 12E; * = Significantly different from untreated control at the 95% confidence level; ** = Significantly different from untreated control at the 99% confidence level.

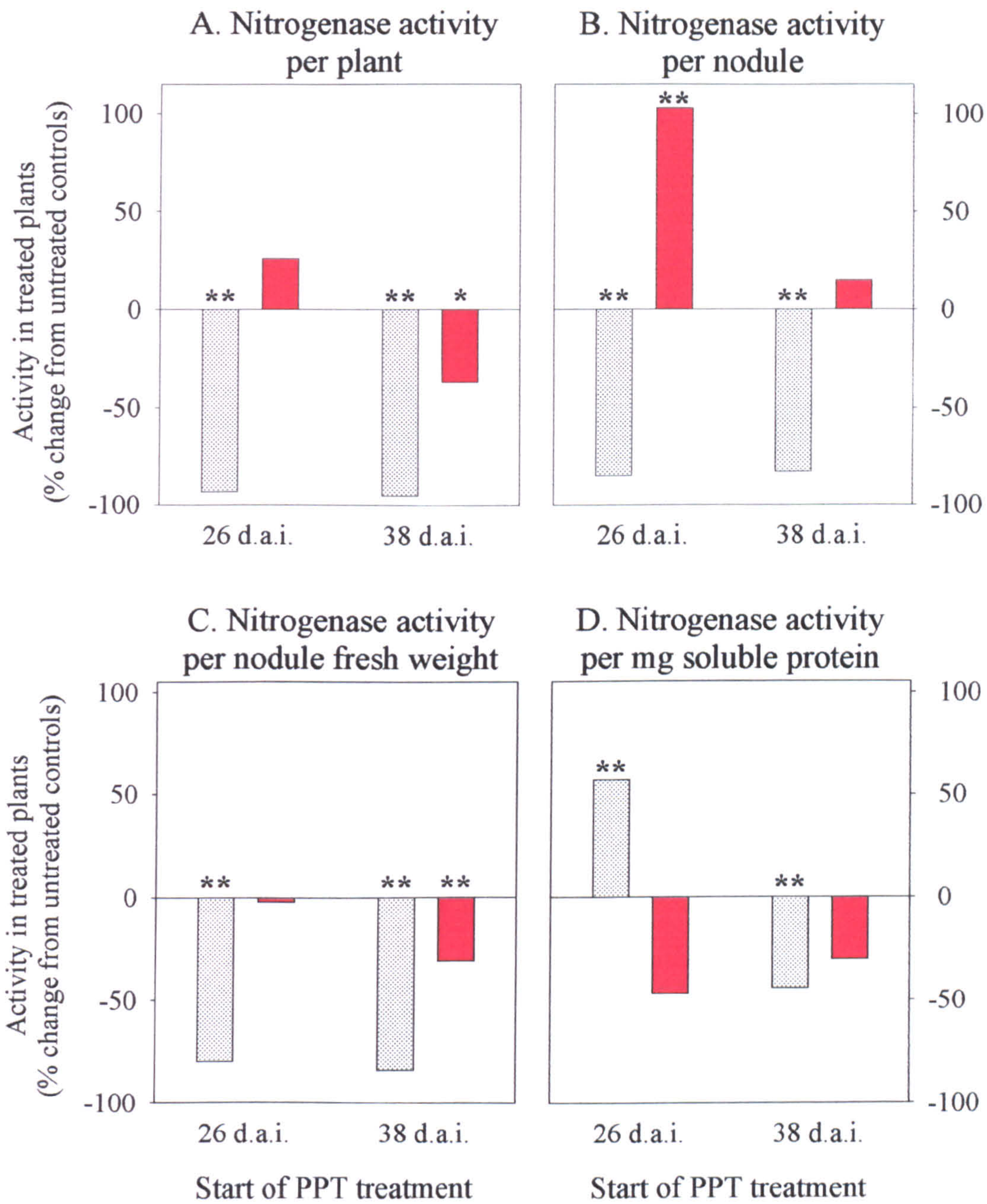

Figure 6.8: The effect of soil applications of PPT on nitrogenase activity, as measured by acetylene reduction, of wild-type *L. corniculatus* and in line 12E. See Fig. 6.4 for experimental details. Nitrogenase activity was determined as described in Section 2.4.8, and expressed per plant (A), per nodule (B), per g nodule fresh weight (C) and per mg soluble protein (D). Bars indicate percentage change in activity of treated plants compared to untreated controls. See also Table 6.2.
Key: ■ = wild-type; ■ = transformed line 12E; * = Significantly different from untreated control at the 95% confidence level; ** = Significantly different from untreated control at the 99% confidence level.

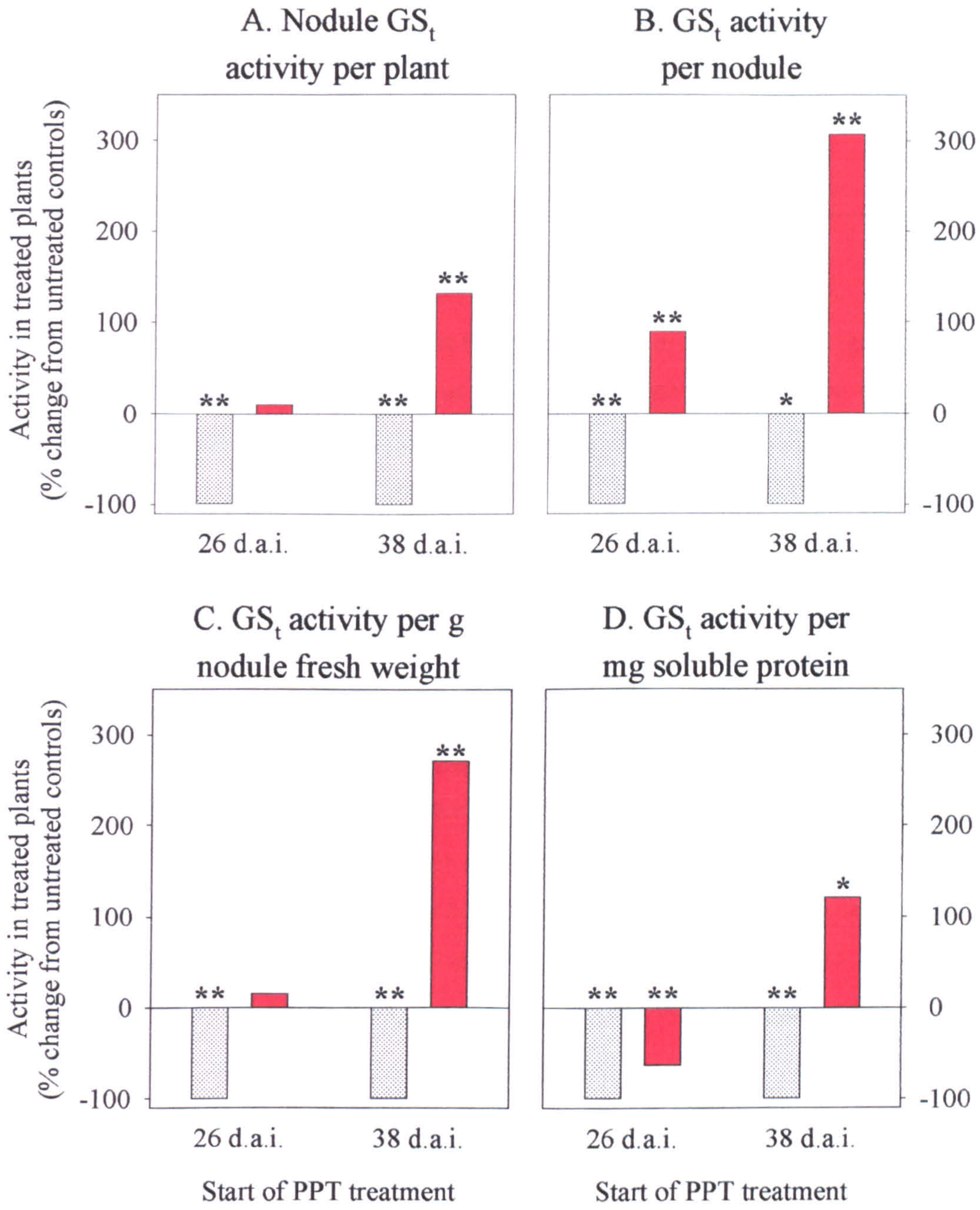

Figure 6.9: The effect of soil applications of PPT on GS activity in the nodules of wild-type *L. corniculatus* and of line 12E. See Fig. 6.4 for experimental details. GS transferase activity (GS_t) was determined as described in Section 2.4.7, and expressed per plant (A), per nodule (B), per g nodule fresh weight (C) and per mg soluble protein (D). Bars indicate percentage change in activity of treated plants compared to untreated controls. See also Table 6.2.

Key: ■ = wild-type; ■ = transformed line 12E; * = Significantly different from untreated control at the 95% confidence level; ** = Significantly different from untreated control at the 99% confidence level.

CHAPTER 7:

GENERAL DISCUSSION

7.1 The PATGUS gene fusion and its potential use

The first part of this thesis focussed on the construction of the *pat::uidA* gene fusion, and the demonstration of its activity in *E. coli* and *L. corniculatus* (see Chapters 3 and 5). The results presented clearly show that the product, PATGUS, retains both activities in *E. coli* and plant tissues, allowing the use of GUS activity as a histochemical marker for PAT activity (see Chapter 3). Furthermore, expression of PATGUS protects GS from inhibition by PPT, and this can be achieved in a tissue-specific way by the use of appropriate plant promoters (Chapter 5).

As mentioned in Section 3.4, there are other examples of the construction of selectable/scorable markers by gene fusion, by Datla *et al.* (*uidA::nptII*; 1991) and Sunito *et al.* (*lacZ::nptII*; 1994). However, this was the first reported use of the *pat* gene in such a construct. This study is also unique in that the expression of a gene fusion in specific tissues was shown to be able to effect selective protection of a target enzyme from inhibition; expression of the gene fusion was not an end in itself, but rather a tool for studying the selective protection of GS from inhibition by PPT (Chapter 6).

Through the use of appropriate promoters, the PATGUS gene could be used in the future to investigate the physiological effects of manipulating other GS isoenzymes. This ability to inhibit GS in certain tissue types at a specific, user-definable period of time, whilst leaving other tissues unaffected, should be a powerful tool in unraveling the respective roles of the sometimes numerous isoforms of this enzyme. For example, PATGUS could be expressed in the leaf using a mesophyll-specific promoter and used to study the role of GS at different stages in leaf development, examining the changing nature of the leaf from sink organ early on in development, through to source organ at maturity and into senescence.

This approach to the manipulation of GS has three considerable advantages over antisense technology (see Section 1.2.2): firstly, plants are physiologically normal up to the point of PPT treatment. Secondly, the timing of inhibition is under complete control, and does not rely on the availability of suitable developmentally regulated promoters. Finally, expression of PATGUS appears to have no deleterious effect on the fitness of transformants (see Chapter 5), and problems in regenerating transformants deficient in GS, such as those thought to have been encountered by Temple *et al.* (1994; see Section 1.2.2), are circumvented.

Outside of its use in the study of GS metabolism, PATGUS is a new tool for plant transformation. Both PAT and GUS have been used extensively: PAT as a selectable marker, and GUS as a histochemical and quantitative one. It is not uncommon for co-transformation with PAT and GUS genes to be used (see Wilmink and Donns, 1993; McElroy and Brittell, 1994). Using the PATGUS fusion would simplify the procedure, removing the need for co-transformations.

7.2 The nature and regulation of GS in *L. corniculatus*

The results presented in Chapter 4 clearly demonstrate the existence of a nodule-specific isoform of GS. Close examination of the isoenzyme profile, with the aid of the computer model described in Section 4.5, suggests that this isoenzyme in *L. corniculatus* is actually made up of an array of heterooctamers, similar to the situation found in *P. vulgaris*. Unlike *P. vulgaris*, however, it appears likely that the great majority (almost 80%) of the polypeptides in the infected cells are nodule-specific. Furthermore, the polypeptide species from which these are assembled do not appear to be resolvable by 1D gel electrophoresis.

Clearly, more work is needed to test this hypothesis. For example, more detailed western analysis of isoenzyme profiles would give a clearer picture of the changes in subunit composition of the nodule-specific peaks, along with 2D analysis to unravel any changes in the abundance of the four charge variants reported by Woodall (1994). It would also be extremely advantageous to follow up her work on cloning GS genes from *L. corniculatus*, as knowledge of the number of genes involved will help in knowing how many subunits to look for.

The effect of nitrate on the GS isoenzyme profile is another observation that deserves closer scrutiny. This thesis presents evidence that nitrate treatment apparently leads to a conversion of the nodule-specific isoenzyme into an isoform with the same elution characteristics as the root isoform. However, the precise nature of this transformation, and the factors determining its rate, are at present unknown. The experiment needs to be repeated; both in *L. corniculatus*, with much more attention paid to the subunit composition (using 2D western analysis), and in other species (e.g. *P. vulgaris*, *L. japonicus*, *M. sativa*), to determine the extent to which this phenomenon occurs in other legumes. Further information on the regulation of this effect will also be gained from experiments designed to measure the extent to which this effect is reversible, e.g. by removing the nitrate or switching from nitrate to ammonium after a set number of days.

There is also the question of other changes in metabolism that accompany the shift in the GS profile. The effects of nitrate on nodule metabolism are at present still highly controversial (Becana and Sprent, 1987; Vessey and Waterer, 1992; Arrese-Igor *et al.*, 1997). However, Arrese-Igor and co-workers (1997) have recently presented evidence that in nodules of *G. max*, nitrate does enter the infected zone, where it induces both NR and NiR. If this is the case in *L. corniculatus*, then the GS effect seen in this study may not be a primary effect of nitrate, but rather part of a physiological response within the nodule to a change in ammonium source from N_2 fixation to nitrate reduction.

This would imply that, at least in some species, the nodule is capable of changing from being a N_2-fixing organ to a nitrate-assimilating one in the short time before it ultimately succumbs to nitrate-induced senescence. This study found, like others before it (e.g. Schuller, 1986) that nitrate had little effect on the total amount of GS activity in the nodule, and the nodule therefore retained its ammonia assimilation capacity up to 7 d after the start of the nitrate treatment. By this time, N_2 fixation was almost completely inhibited.

The discrepancies between the amount of GS present and the GS activity of the corresponding fractions from the ion-exchange experiments indicate the presence of

inactive GS (see Chapter 4). This, along with the evidence for a qualitative shift in the GS composition and GS_t:GS_s ratios, the report by Peat and Tobin (1996) of inactive forms of GS in *H. vulgare* roots, the multiple isoforms found on the 2D western blots of Woodall, and a recent observation that *S. oleracea* GS binds to a 14-3-3 protein (C. MacKintosh, personal communication), certainly indicate that there is more to GS regulation than is currently known.

7.3 Comparison with the results of Knight and Langston-Unkefer (1988)

The results presented in Chapter 6 are generally complementary to the findings of Knight and Langston-Unkefer. Although significant differences exist between the two studies, it seems unlikely that these are due to anything more than differences in experimental design, rather than anything more fundamental. The results presented in Chapter 6 indicate that inhibition of the root form of GS results in a compensatory shift towards N_2 fixation, with the production of larger nodules with higher rates of nitrogenase activity. Nodulation may be directly inhibited by the presence of PPT (e.g. through effects on the *Rhizobia* or the populations of other soil microflora), which would explain the lack of a significant overall increase in plant weight due to the treatment. Repeating the experiments in Chapter 6 using a PPT-resistant strain of *Rhizobium* would help to clarify this.

Having demonstrated that the *L. corniculatus* plants of line 12E do benefit from PPT treatment, it is now necessary to determine in detail the metabolic status of these plants. Due to constraints of time, the amino acid composition, and total N content of the sap were not measured. These data would be valuable in determining the effects of the treatment on plant N metabolism, and elucidating the origin of the PPT-treatment-mediated increase in plant growth.

7.4 Conclusion

This study has achieved its two main aims: (a) to generate and test a chimaeric *pat::uidA* construct, which would provide a tool for the manipulation of GS and plant transformation. (b) To use this gene to study the role of GS in the infected

zone of the root nodule, by mimicking the earlier studies of Knight and Langston-Unkefer (1988). In addition, the GS isoenzyme profile in nodules and roots of *L. corniculatus* was elucidated, and an unexpected and novel effect of nitrate on this profile discovered. The results presented and discussed indicate new avenues for exploration of GS and its regulation.

APPENDIX I:

SUPPLIERS' NAMES AND ADDRESSES

AgrEvo Ltd.,
Chesterford Park,
Saffron Walden,
Essex CB10 1XL,
United Kingdom

Ai Cambridge Ltd.,
London Road,
Pampisford,
Cambridge CB2 4EF,
United Kingdom

Amersham International plc.,
Amersham Place,
Little Chalfont,
Buckinghamshire HP7 9NA,
United Kingdom

Berthold Instruments (UK) Ltd.,
35 High Street,
Sandridge, St. Albans,
Hertfordshire AL4 9DD,
United Kingdom

Bibby-Sterilin Ltd.,
Tilling Drive,
Stone,
Staffordshire ST15 0SA,
United Kingdom

Bio-Rad Laboratories Ltd.,
Bio-Rad House,
Maylands Avenue,
Hemel Hempstead,
Hertfordshire HP2 7TD,
United Kingdom

Boehringer Mannheim UK (Diagnostics & Biochemicals) Ltd.,
Bell Lane, Lewes,
East Sussex BN7 1LG
United Kingdom

Cambridge BioScience Ltd.,
24-25 Signet Court,
Newmarket Road,
Cambridge CB5 8LA,
United Kingdom

Clontech Laboratories UK Ltd.,
Unit 2, Intech 2,
Wade Road,
Basingstoke,
Hampshire RG24 8NE,
United Kingdom

Dynatech Laboratories Ltd.,
Daux Road, Billingshurst,
West Sussex RH1 49SJ,
United Kingdom

Fisher Scientific UK,
Bishop Meadow Road,
Loughborough,
Leicestershire, LE11 0RG,
United Kingdom

Fisons Scientific Equipment,
Bishop Meadow Road,
Loughborough,
Leicestershire, LE11 0RG,
United Kingdom

Greyhound Chromatography and Allied Chemicals,
88 Grange Road West,
Birkenhead,
Merseyside L43 4XF,
United Kingdom

ICN Flow Ltd.,
Eagle House,
Peregrine Business Park,
Gomm Road, High Wycombe,
Buckinghamshire, HP13 7DL,
United Kingdom

Jencons (Scientific) Ltd.,
Cherrycourt way Industrial Estate,
Stanbridge Road,
Leighton Buzzard,
Bedfordshire LU7 8UA,
United Kingdom

Jones Chromatography Ltd.,
New Road,
Hengoed,
Mid-Glamorgan CF8 8AU,
United Kingdom

Life Technologies International (UK) Ltd.,
Unit 5, The Ridgeway Centre,
Edison Road,
Basingstoke,
Hampshire RG21 6YH,
United Kingdom

Merck Ltd.,
Merck House,
Poole,
Dorset BH15 1TD,
United Kingdom

Millipore (UK) Ltd.,
The Boulevard,
Blackmoor Lane,
Watford,
Hertfordshire WD1 8YW,
United Kingdom

New Brunswick Scientific (UK) Ltd.,
Edison House,
163 Dixons Hill Road,
North Mymms,
Hatfield,
Hertfordshire AL9 7JE,
United Kingdom

New England Biolabs (UK) Ltd.,
67 Knowl Piece,
Wilbury Way,
Hitchin,
Hertfordshire SG4 0TY,
United Kingdom

Perkin Elmer Ltd.,
Kelvin Close,
Birchwood Science Park,
Warrington WA3 7PB,
United Kingdom

PerSeptive Biosystems UK Ltd.,
3 Harforde Court,
Foxholes Business Park,
John Tate Road,
Hertford SG13 7NW,
United Kingdom

Pharmacia Biotech,
23 Grosvenor Road,
St. Albans,
Hertfordshire AL1 3AW,
United Kingdom

Promega UK Ltd.,
Delta House,
Chilworth Research Centre,
Southampton SO16 7NS,
United Kingdom

Roussel Laboratories Ltd.,
Roussel House,
Broadwater Park,
Denham,
Uxbridge, UB9 5HP,
United Kingdom

Sigma-Aldrich Company Ltd.,
Fancy Road, Poole,
Dorset BH12 4QH,
United Kingdom

Stratagene Ltd.,
Cambridge Innovation Centre,
140 Cambridge Science Park,
Milton Road,
Cambridge CB4 4GF,
United Kingdom

Techmate Ltd.,
10 Bridgeturn Avenue,
Old Wolverton,
Milton Keynes MK12 5QL,
United Kingdom

Techne (Cambridge) Ltd.,
Duxford,
Cambridge CB2 4PZ,
United Kingdom

Turfpro Ltd.,
145 Church Street,
Staines,
Middlesex TW18 4XZ,
United Kingdom

Whatman International Ltd.,
St. Leonard's Road,
20/20 Maidstone,
Kent ME16 0LS,
United Kingdom

X-Ograph Ltd.,
Cotswold House,
Malmesbury,
Wiltshire SN16 9JS,
United Kingdom

APPENDIX II:

A VMS-BASIC PROGRAM FOR CALCULATION OF THE OPTIMUM ANNEALING TEMPERATURE FOR PCR PRIMERS

This program was written based on the equations of the thermodynamic calculations of Breslauer *et al.* (1986) and Rychlik *et al.* (1990). The source code for this program is presented is presented below. A World-Wide-Web based version of this program is also available for use by the research community at http://www.res.bbsrc.ac.uk/biochem/oligos/

```
10 %INCLUDE "SCREENCODES.H"
20 DIM H(4,4), G(4,4), S(4,4), BASE$(80), BASEPTR(80)

40 GOSUB Title
50 GOSUB Initialise
60 GOSUB Get_sequence
70 GOSUB Get_DNA_data
75 GOSUB Fill_possibles
80 GOSUB Find_best_nucleotides
90 GOSUB Do_work
100 GOTO 10

Get_sequence:
  400 INPUT "Name of input file";FILE$
  405 FLAG% = 0
Key_in:
  410 IF LEN(FILE$) = 0 THEN GOTO Manual_sequence
  415 IF LEFT$(FILE$,1) = "Q" THEN GOTO Finish
  420 WHEN ERROR USE Nofile
  425  OPEN FILE$ FOR INPUT AS #1%
  430 END WHEN
  435 IF FLAG% = 1 THEN GOTO Get_sequence
  445 WHEN ERROR USE Fileprobs
  450 INPUT #1%, Z$
  455 C$=Z$
  460 END WHEN
  461 GOSUB Remove_spaces
  465 IF FLG3% = 1 THEN GOTO Check_sequence
  470 GOTO 445

Check_sequence:
  475 GOSUB Convert_to_upper_case
  480 FOR Y=1 TO LEN(C$)
  490  X$=MID$(C$,Y,1)
  495  FOR Z=1 TO 16
  500       IF X$=MID$(ALLOWED$,Z,1) THEN GOTO 525
  510  NEXT Z
  520 GOTO No_match
  525 IF X$<>"A" AND X$<>"C" AND X$<>"G" AND X$<>"T"
      THEN NAME$="Highest: "
  530 NEXT Y
  535 RETURN
No_match:
  540 GOSUB Unknown
  545 IF LEN(FILE$)<>0 THEN GOTO Get_sequence
  547 GOTO Key_in

Manual_sequence:
  550 PRINT
  560 INPUT "Sequence";C$
  570 IF LEN(C$)=0 OR LEFT$(C$,1)="Q" THEN GOTO Finish
  580 IF LEN(C$)=1 THEN GOTO 600
  584 Z$=C$
```

```
  587 GOSUB Remove_spaces
  590 GOTO Check_sequence

  600 PRINT "ERROR:   Sequence can't be one base long!"
  610 PRINT "         Try again."
  620 PRINT
  630 GOTO 560

Get_DNA_data:
  680 PRINT "Please input target DNA data:";CHR$(9);
  690 INPUT "%CG (default=50)";PERCGC$
  691 WHEN ERROR USE Illegal_GC
  692  PERCGC=VAL(PERCGC$)
  693 END WHEN
  694 IF PERCGC>100 THEN GOTO Void_percgc
  695 IF PERCGC$="" THEN PERCGC=50
  700 PRINT CHR$(9);CHR$(9);CHR$(9);
  710 INPUT "Length (in bp, default=1000)";L$
  711 WHEN ERROR USE Illegal_length
  712  L=VAL(L$)
  713 END WHEN
  714 IF L$="" THEN L=1000
  720 IF L<=1 THEN GOTO Void_length
  730 GOTO 800
Void_length:
  740 PRINT "'Length' must be a positive integer!"
  750 GOTO 700
Void_percgc:
  760 PRINT "'%GC' must be a value between 0 and 100!"
  770 PRINT CHR$(9);CHR$(9);CHR$(9);
  780 GOTO 690
  800 RETURN

Remove_spaces:
  810 C$=""
  815 FOR LOOP=1 TO LEN(Z$)
  820 IF MID$(Z$,LOOP,1)=" " THEN GOTO 840
  830 C$=C$+MID$(Z$,LOOP,1)
  840 NEXT LOOP
  850 RETURN

Convert_to_upper_case:
  900 FOR Y=1 TO LEN(C$)
  910  CM$=MID$(C$,Y,1)
  920  IF ASC(CM$)>=97 THEN MID$(C$,Y,1)=CHR$(ASC(CM$)-32)
  930 NEXT Y

Initialise:
  1000 RESTORE
  1020 FOR X=0 TO 3
  1030 FOR Y=0 TO 3
  1040      READ H(X,Y), S(X,Y), G(X,Y)
  1050 NEXT Y
  1060 NEXT X
  1070 BEST$  = ""
  1075 WORST$ = ""
  1077 NAME$  = "Sequence  :"
  1080 FLG2%  = 0
  1090 FLG3%  = 0
  1092 DELTAG = 5.0
  1094 DELTAS = -10.8
  1096 DELTAH = 0.0
  1098 ALLOWED$ = "ACGTNHRYMWSKVDBX"
  1100 FOR X=1 TO 79
  1110 BASEPTR(X)=1
  1120 NEXT X
  1130 CTR=0
  1200 RETURN
```

```
2000 HANDLER Nofile
2010 PRINT
2020 PRINT "ERROR: Input file doesn't exist!"
2030 PRINT "   Try again (or press [RETURN] for direct entry.)"
2040 PRINT
2050 FLAG% = 1
2060 END HANDLER

2200 HANDLER Fileprobs
2210 FLG3% = 1
2230 END HANDLER

2400 HANDLER Illegal_GC
2410 PERCGC=50
2420 END HANDLER

2430 HANDLER Illegal_length
2440 END HANDLER

Unknown:
  2500 PRINT
  2510 PRINT "ERROR: Sequence contains unknown character:"
  2530 FOR Y=1 TO LEN(C$)
  2540      IF (Y-1)/3 = INT((Y-1)/3) AND Y<>1 THEN PRINT " ";
  2550 X$=MID$(C$,Y,1)
  2552 FOR Z=1 TO 16
  2554      IF X$=MID$(ALLOWED$,Z,1) THEN GOTO 2565
  2556 NEXT Z
  2560 PRINT INVRS$;BEEP$;
  2565      PRINT MID$(C$,Y,1);
  2570      PRINT NORM$;
  2580 NEXT Y
  2590 PRINT
  2600 RETURN

Fill_possibles:
  2700 FOR X=1 TO LEN(C$)
  2710 B$ = MID$(C$,X,1)
  2715 BASE$(X) = B$
  2720 IF B$="N" OR B$="X" THEN BASE$(X) = "ACGT"
  2722 IF B$="B" THEN BASE$(X) = "CGT"
  2724 IF B$="D" THEN BASE$(X) = "AGT"
  2726 IF B$="H" THEN BASE$(X) = "ACT"
  2728 IF B$="V" THEN BASE$(X) = "ACG"
  2730 IF B$="K" THEN BASE$(X) = "GT"
  2732 IF B$="Y" THEN BASE$(X) = "CT"
  2734 IF B$="S" THEN BASE$(X) = "CG"
  2736 IF B$="W" THEN BASE$(X) = "AT"
  2738 IF B$="R" THEN BASE$(X) = "AG"
  2740 IF B$="M" THEN BASE$(X) = "AC"
  2750 NEXT X
  2760 RETURN

Find_best_nucleotides:
  2800 PRINT "Calculating..."
  2805 GOSUB Construct_primer
  2810 BEST$=PRIMER$
  2820 WORST$=PRIMER$
  2830 GOSUB Try_possibility
  2840 TESTBEST=TOPTIMUM
  2850 TESTWORST=TOPTIMUM

Cont:
  3009 CTR=CTR+1
  3010 IF CTR>LEN(C$) THEN RETURN
  3020 IF BASEPTR(CTR)<LEN(BASE$(CTR)) THEN GOTO Change_base
  3030 BASEPTR(CTR)=1
  3040 GOTO Cont
```

```
Change_base:
  3050 BASEPTR(CTR)=BASEPTR(CTR)+1
  3060 CTR=0
  3070 GOSUB Construct_primer
  3080 GOSUB Try_possibility
  3090 GOTO Cont

Construct_primer:
  3200 PRIMER$=""
  3210 FOR X=1 TO LEN(C$)
  3220 PRIMER$=PRIMER$+MID$(BASE$(X),BASEPTR(X),1)
  3230 NEXT X
  3240 RETURN

Try_possibility:
  3300 GOSUB Calculate_result
  3310 IF TOPTIMUM <= TESTBEST  THEN GOTO 3340
  3320 TESTBEST = TOPTIMUM
  3330 BEST$ = PRIMER$
  3340 IF TOPTIMUM >= TESTWORST THEN GOTO 3370
  3350 TESTWORST = TOPTIMUM
  3360 WORST$ = PRIMER$
  3370 RETURN

Calculate_result:
  3600 DELTAH=0
  3605 DELTAS=-10.8
  3610 FOR X=1 TO LEN(PRIMER$)-1
  3620   C1$=MID$(PRIMER$,X,1)
  3630   C2$=MID$(PRIMER$,X+1,1)
  3700   IF C1$ = "T" THEN FIRST%  = 0
  3710   IF C1$ = "A" THEN FIRST%  = 1
  3720   IF C1$ = "G" THEN FIRST%  = 2
  3730   IF C1$ = "C" THEN FIRST%  = 3
  3800   IF C2$ = "T" THEN SECOND% = 0
  3810   IF C2$ = "A" THEN SECOND% = 1
  3820   IF C2$ = "G" THEN SECOND% = 2
  3830   IF C2$ = "C" THEN SECOND% = 3
  3900   DELTAH = DELTAH + H(FIRST%,SECOND%)
  3910   DELTAS = DELTAS + S(FIRST%,SECOND%)
  3920   DELTAG = DELTAG + G(FIRST%,SECOND%)
  3930 NEXT X
  3940 GOSUB Calculate_optimum
  3950 RETURN

Do_work:
  4000 GOSUB Title
  4010 PRIMER$ = BEST$
  4020 GOSUB Calculate_result
  4030 GOSUB Printout
  4040 IF LEFT$(NAME$,1) = "S" THEN 4080
  4045 NAME$ = "Lowest : "
  4050 PRIMER$ = WORST$
  4060 GOSUB Calculate_result
  4070 GOSUB Printout
  4080 PRINT
  4090 PRINT "PRESS ANY KEY TO RUN AGAIN OR [SPACE] TO QUIT";
  4110 A$=INKEY$(0%,WAIT)
  4120 IF A$="" THEN GOTO Finish
  4130 RETURN

Calculate_optimum:
  6000 GOSUB Calculate_primer
  6010 TPRODUCT = 81.5 + 0.41*PERCGC - 21.7 - 675/L
  6020 TOPTIMUM = 0.3*TPRIMER + 0.7*TPRODUCT - 14.9
  6030 RETURN
```

```
Calculate_primer:
  6100 TPRIMER  = (DELTAH*1000/(DELTAS-46.7)) - 294.8
  6110 RETURN

Printout:
  7000 PRINT NAME$;
  7010 FOR X=1 TO LEN(PRIMER$)
  7020 C2$=MID$(PRIMER$,X,1)
  7030 C1$=MID$(C$,X,1)
  7040 IF C1$<>C2$ THEN PRINT UNDRL$;
  7050 PRINT C2$;
  7060 IF C1$<>C2$ THEN PRINT NORM$;
  7070 IF INT(X/3) = X/3 THEN PRINT " ";
  7080 NEXT X
  7090 PRINT DOWN$;DOWN$;CHR$(13);"%CG      : ";PERCGC
  7100 PRINT "Length  : ";L
  7110 PRINT
  7120 PRINT "DELTA G = "; DELTAG;" ";TAB$;TAB$;TAB$;
             "TmPrimer  = ";TPRIMER
  7130 PRINT "DELTA H = "; DELTAH;" ";TAB$;TAB$;TAB$;
             "TmProduct = ";TPRODUCT
  7140 PRINT "DELTA S = "; DELTAS;" ";TAB$;TAB$;TAB$;
             "TaOptimum = ";TOPTIMUM
  7150 RETURN

Title:
  8900 PRINT CLEAR$;TAB$;TAB$;UNDRL$;
             "Optimum Annealing temperature calculator.";NORM$;DOWN$
  8910 RETURN

  9000 REM DELTA H, DELTA S, DELTA G
  9005 REM  _________TT_________ _________TA_________
  9010 DATA  -9.1,-24.0, -1.9,  -6.0,-16.9, -0.9
  9015 REM  _________TG_________ _________TC_________
  9020 DATA  -5.8,-12.9, -1.9,  -5.6,-13.5, -1.6
  9025 REM  _________AT_________ _________AA_________
  9030 DATA  -8.6,-23.9, -1.5,  -9.1,-24.0, -1.9
  9035 REM  _________AG_________ _________AC_________
  9040 DATA  -7.8,-20.8, -1.6,  -6.5,-17.3, -1.3
  9045 REM  _________GT_________ _________GA_________
  9050 DATA  -6.5,-17.3, -1.3,  -5.6,-13.5, -1.6
  9055 REM  _________GG_________ _________GC_________
  9060 DATA -11.0,-26.6, -3.1, -11.1,-26.7, -3.1
  9065 REM  _________CT_________ _________CA_________
  9070 DATA  -7.8,-20.8, -1.6,  -5.8,-12.9, -1.9
  9075 REM  _________CG_________ _________CC_________
  9080 DATA -11.9,-27.8, -3.6, -11.0,-26.6, -3.1

Finish:
 10000 PRINT
 10010 PRINT "Exiting."
 10020 END
```

APPENDIX III:

A VMS-BASIC PROGRAM FOR IMPLEMENTING A SIMPLE MODEL TO PREDICT THE ELUTION PROFILE OF GS FROM NODULE EXTRACTS

Calculations involved

The version of the program presented here calculates the relative peak heights for a range of subunit ratios from 100% A-type to 100% B-type. The steps involved are summarised below:

1. Set up a matrix, *gs()*, capable of holding 9 values, each corresponding to one arrangement of subunits from *gs(0)* = A-type$_8$ to *gs(8)* = B-type$_8$.
2. Generate a random number, *z*, between 0 and 100, 8 times.
3. Count the number of times that *z* is above the chosen % nodule form.
4. Increment the value in the matrix corresponding to this number.
5. Repeat steps 2 to 4 many times (in this case, 100,000) to simulate many randomly assembling polypeptides.

This procedure fills the matrix with values corresponding to the relative amounts of each octamer type.

Conversion to elution profile

To simulate the effect of running the profile down a column, the values for each peak were exported into SigmaPlot, and a normal distribution superimposed onto each peak using a purpose-built transform procedure. The transform subsequently computed the sum of peaks to produce the final, complex peak containing contributions from each individual holoenzyme combination (see Fig. 4.9).

Comparison with the observed elution profile

The model was run in a programmed loop which computed the expected amounts of each holoenzyme combination for all possible ratios of subunit types from 100% nodule-type to 100% root-type, in steps of 1%. The output of this exercise is collated in Appendix IV, and the effect on the predicted profile of a range of different subunit ratios can be seen in Fig. 4.9.

The program

```
100 REM ************************************************************
110 REM * This section creates the file which contains the relative *
120 REM * values for the peak heights.                              *
130 REM ************************************************************
140 open "gs.mod" for output as #1%
150 dim gs(101,9),percent_gamma(101)
155 for x=0 to 100
156   percent_gamma(x)=0
157 next x
160 array_count=-1
170 for this_percent=0 to 100
180   array_count=array_count+1
185   percent_gamma(array_count)=this_percent
190   random

200 REM *** Clear current line of array for input:
210   for x=0 to 8
220     gs(array_count,x)=0
230   next x

239 REM ************************************************************
240 REM **   Use random number generator to decided beta or gamma  **
250 REM **   polypeptide and use this to decide number of beta     **
260 REM **   polypeptides in a randomly assembled octamer.         **
265 REM **   Do this 100 000 (!) times...                          **
266 REM ************************************************************
270   for x=1 to 100000
280     beta_counter=0
290     for y=1 to 8
300       z=rnd*100
310       if z>this_percent then beta_counter=beta_counter+1
320     next y
330     gs(array_count,beta_counter)=gs(array_count,beta_counter)+1
340   next x

350 REM *** Let user know how we're getting on...
360 print "Done ";this_percent;"% gamma..."
370 next this_percent

375 REM *** Now output all of this data to file gs.mod, in ASCII
376 REM     white-space-delimited text suitable for SigmaPlot import:

380 for array_counter=0 to 100
385 print "Writing to file..."
400   print #1%, percent_gamma(array_counter);"% gamma"
410   for x=0 to 7
420     print #1%, gs(array_counter,x);" ";
430   next x
440   print #1%, gs(array_counter,8)

Empty_array:
460 next array_counter
470 close #1%
```

APPENDIX IV:

OUTPUT FROM THE PROGRAM IN APPENDIX III

% GS_{nod}	0:8	1:7	2:6	3:5	4:4	5:3	6:2	7:1	8:0
0	0	0	0	0	0	0	0	0	100000
1	0	0	0	0	0	2	280	7385	92333
2	0	0	0	0	0	41	937	13894	85128
3	0	0	0	0	2	123	2102	19146	78627
4	0	0	0	0	9	271	3476	23943	72301
5	0	0	0	1	34	540	5185	27862	66378
6	0	0	0	1	67	899	6973	31230	60830
7	0	0	0	6	129	1315	8865	33555	56130
8	0	0	1	14	212	1854	10722	35709	51488
9	0	0	2	30	304	2502	12918	37064	47180
10	0	0	4	48	439	3301	14764	38396	43048
11	0	0	5	71	696	4160	16788	38982	39298
12	0	0	5	117	881	5105	18805	38987	36100
13	0	0	10	154	1220	6125	20518	39001	32972
14	0	1	18	173	1493	7089	22067	39280	29879
15	0	1	26	270	1948	8299	23907	38128	27421
16	0	1	44	366	2353	9631	25178	37562	24865
17	0	2	50	469	2726	10769	26303	36940	22741
18	0	4	75	624	3402	12343	27455	35806	20291
19	0	8	97	778	3947	13110	28623	34740	18697
20	0	7	124	920	4540	14463	29634	33359	16953
21	1	6	163	1122	5251	16098	30118	32163	15078
22	1	16	199	1347	6164	17173	30542	30967	13591
23	0	21	243	1582	6870	18506	30749	29599	12430
24	1	27	306	1966	7753	19565	31006	28222	11154
25	1	40	373	2235	8689	20783	31308	26650	9921
26	2	49	458	2742	9639	21563	31323	25223	9001
27	3	54	562	3151	10645	22726	30957	23827	8075
28	2	99	723	3652	11527	23914	30642	22298	7143
29	8	98	804	4224	12693	24413	30248	21061	6451
30	4	122	960	4812	13330	25398	29638	19952	5784
31	10	166	1124	5310	14752	25921	29348	18230	5139
32	14	182	1350	5873	15647	26896	28098	17428	4512
33	17	230	1567	6630	16731	27099	27654	16007	4065
34	22	229	1905	7185	17732	27410	26867	15007	3643
35	20	313	2236	8063	18948	27970	25585	13743	3122
36	38	367	2465	8788	19647	28092	25115	12612	2876
37	24	489	2797	9714	20546	28205	23987	11855	2383
38	52	565	3229	10589	21658	28224	22867	10656	2160
39	53	660	3612	11497	22574	28020	21833	9808	1943
40	65	757	4104	12484	23228	27669	21027	9016	1650
41	77	918	4624	13405	23786	27558	19926	8281	1425
42	97	1033	5097	14139	24645	27451	18718	7570	1250
43	114	1288	5729	15181	25250	26789	17908	6654	1087
44	144	1449	6378	16107	25915	26380	16551	6096	980
45	149	1608	7136	16983	26201	25668	15858	5568	829
46	198	1867	7704	18171	26512	25258	14745	4824	721

% Gs_{nod}	0:8	1:7	2:6	3:5	4:4	5:3	6:2	7:1	8:0
47	251	2167	8523	19255	26857	24221	13645	4468	613
48	288	2469	9365	20074	27070	23560	12710	3887	577
49	313	2760	10030	20836	27399	22851	11838	3535	438
50	366	3137	11177	21947	27336	21756	10860	3055	366
51	480	3551	11740	22784	27492	20807	9967	2821	358
52	551	3951	12770	23361	27385	20025	9193	2464	300
53	603	4371	13708	24276	27080	19229	8342	2167	224
54	699	4861	14633	25072	26699	18234	7675	1883	244
55	877	5488	15609	25687	26177	17329	7031	1643	159
56	965	6056	16886	26318	25831	16194	6208	1395	147
57	1095	6829	17587	26833	25420	14950	5965	1193	128
58	1321	7449	18775	27269	24701	14176	5161	1040	108
59	1475	8231	19651	27538	24144	13356	4586	929	90
60	1691	8993	20758	27847	23216	12480	4215	738	62
61	1977	9812	21937	28267	22116	11540	3714	588	49
62	2132	10571	23168	28165	21702	10498	3164	553	47
63	2494	11630	23834	28166	20721	9821	2840	466	28
64	2721	12774	25038	28194	19534	8845	2456	406	32
65	3234	13643	25914	27761	18912	8074	2092	350	20
66	3519	14848	26405	27711	17850	7407	1928	314	18
67	4128	16250	27552	26879	16799	6582	1582	209	19
68	4530	17156	28397	26687	15639	5991	1369	218	13
69	5223	18202	29405	26030	14580	5203	1186	163	8
70	5711	19824	29786	25274	13664	4626	997	115	3
71	6408	21168	30241	24689	12473	4074	841	100	6
72	7366	22217	30653	23966	11380	3620	709	84	5
73	8096	23743	30778	23187	10522	3067	549	55	3
74	9056	24968	30984	21983	9741	2716	503	47	2
75	10009	26907	31211	20577	8555	2315	388	36	2
76	11109	27972	31328	19537	7742	1978	305	29	0
77	12252	29531	31083	18390	6837	1674	217	16	0
78	13827	30625	30525	17265	6132	1436	176	14	0
79	15207	32265	29913	16056	5282	1106	160	11	0
80	17006	33279	29254	14705	4673	945	133	5	0
81	18430	34786	28627	13310	3939	796	105	6	1
82	20421	35938	27725	12007	3230	606	67	6	0
83	22447	37083	26338	10789	2811	469	61	2	0
84	24766	37658	25210	9739	2261	333	31	2	0
85	27316	38366	23822	8387	1824	262	21	2	0
86	30071	38798	22183	7241	1496	194	16	1	0
87	32934	39325	20534	5868	1170	158	11	0	0
88	35910	39207	18841	5066	881	86	9	0	0
89	39327	38977	16856	4171	611	54	4	0	0
90	43107	38132	14944	3293	485	33	5	1	0
91	46983	37224	12895	2522	346	30	0	0	0
92	51502	35855	10570	1857	195	20	1	0	0
93	55976	33763	8786	1319	145	10	1	0	0
94	60966	31101	6960	903	70	0	0	0	0
95	66211	27995	5204	561	27	2	0	0	0
96	72043	24065	3573	303	16	0	0	0	0
97	78189	19493	2178	138	2	0	0	0	0
98	84907	14062	989	40	2	0	0	0	0
99	92256	7473	265	6	0	0	0	0	0
100	100000	0	0	0	0	0	0	0	0

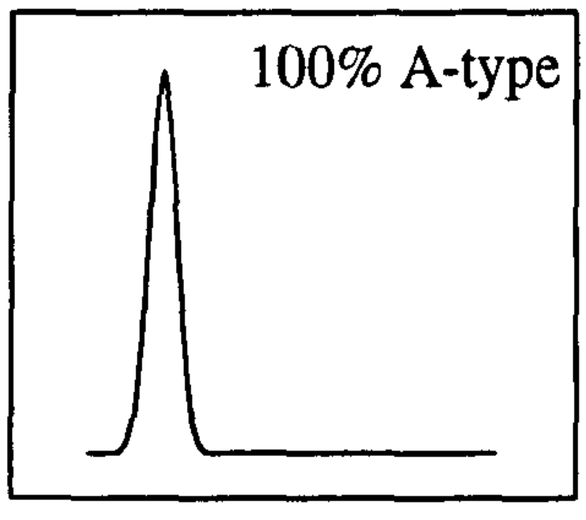

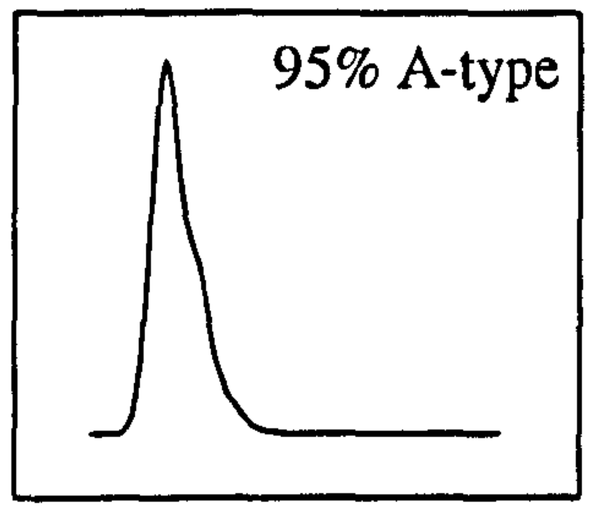

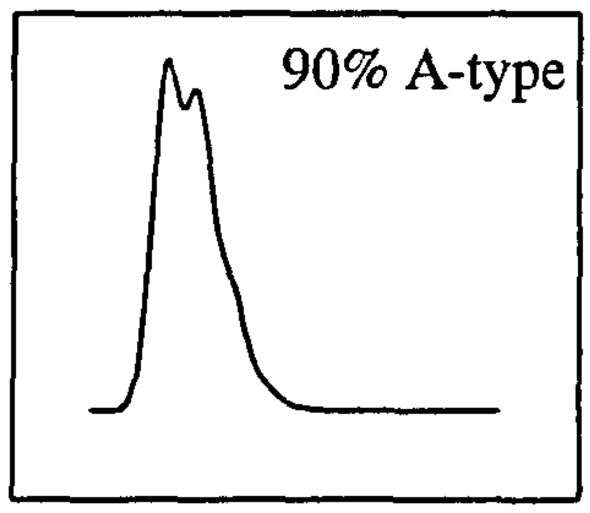

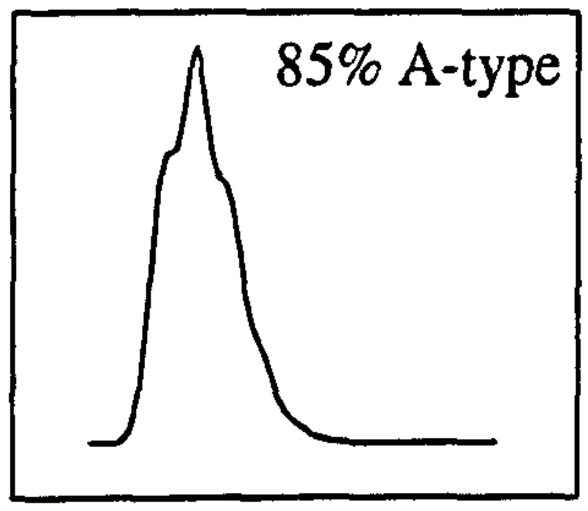

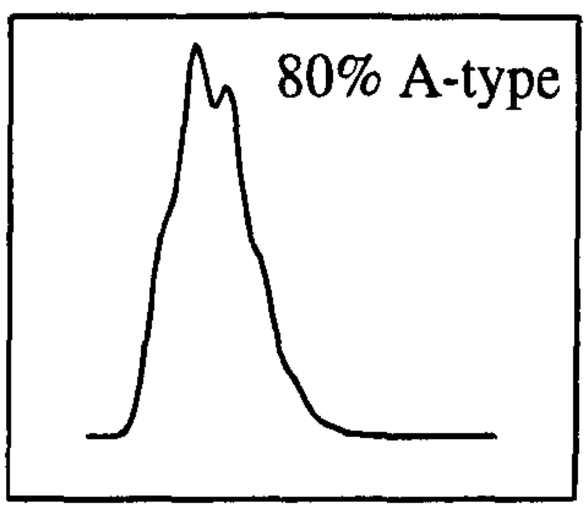

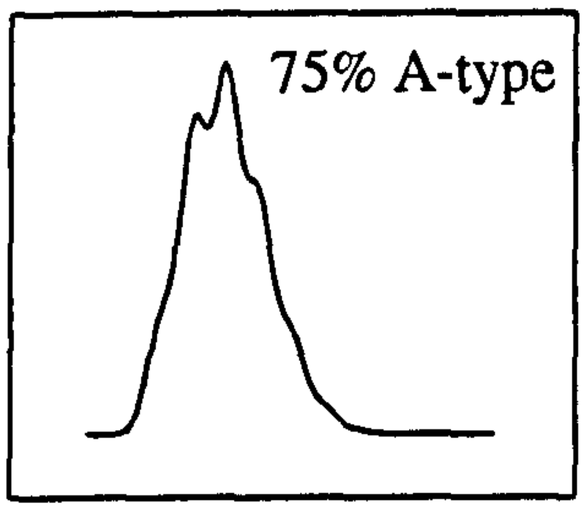

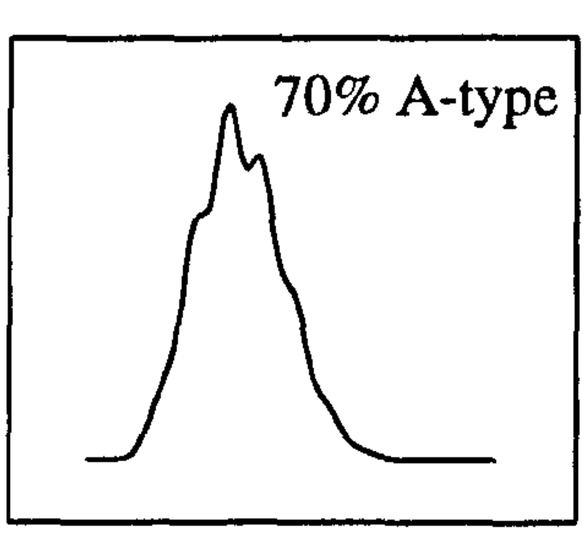

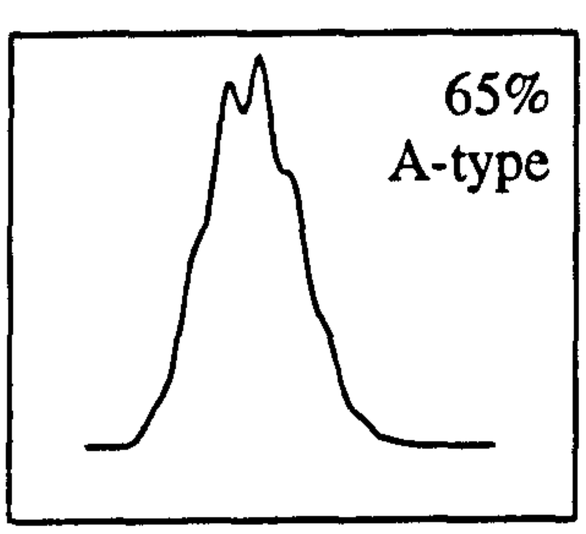

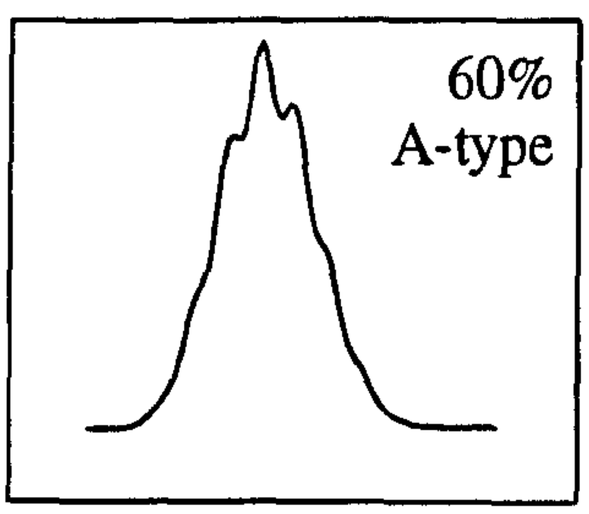

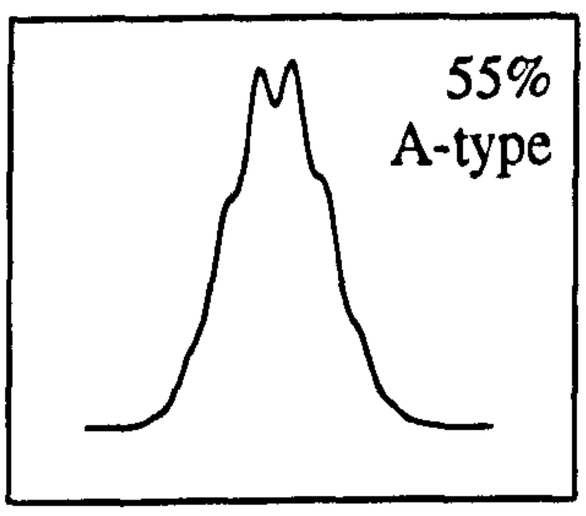

A range of profiles generated by the computer model described in Section 4.5, showing the variation in elution profile with polypeptide composition. The horizontal axis represents increasing elution time, and the vertical axis represents GS activity, both in arbitrary units. See Section 4.5 for more details.

REFERENCES:

Abell, L. M. and Villafranca, J. J. (1991). Investigation of the mechanism of phosphinothricin inactivation of *Escherichia coli* glutamine synthetase using rapid quench kinetic techniques. *Biochemistry* **30**, 6135-6141.

Alexander, D. C., McKnight, T. D. and Williams, B. G. (1984). A simplified and efficient vector-primer cDNA cloning system. *Gene* **31**, 79-89.

Alting-Mees, M. A. and Short, J. M. (1989). pBluescript II: gene mapping vectors. *Nucleic Acids Research* **17**, 9494.

Andersson, C. R., Llewellyn, D. J., Peacock, W. J. and Dennis, E. S. (1997). Cell-specific expression of the promoters of two nonlegume hemoglobin genes in a transgenic legume, *Lotus corniculatus*. *Plant Physiology* **113**, 45-57.

Andrews, M. (1986). The partitioning of nitrate assimilation between root and shoot of higher plants. *Plant, Cell and Environment* **9**, 511-519.

Arnheim, N. and Erlich, H. (1992). Polymerase chain reaction strategy. *Annual Review of Biochemistry* **61**, 131-156.

Arnone, J. A., Kohls, S. J. and Baker, D. D. (1994). Nitrate effects on nodulation and nitrogenase activity of actinorhizal *Casuarina* studied in split-root systems. *Soil Biology and Biochemistry* **26**, 599-606.

Arrese-Igor, C., Minchin, F. R., Gordon, A. J. and Nath, A. K. (1997). Possible causes of the physiological decline in soybean nitrogen fixation in the presence of nitrate. *Journal of Experimental Botany* **48**, 905-913.

Barratt, D. H. P. (1981). Identification of multiple forms of glutamine synthetase in field bean (*Vicia faba* L.). *Plant Science Letters* **20**, 273-279.

Bartsch, K. and Tebbe, C. C. (1989). Initial steps in the degradation of phosphinothricin (glufosinate) by soil bacteria. *Applied and Environmental Microbiology* **55**, 711-716.

Bayer, E., Gugel, K. H., Hägele, K., Hagenmaier, H., Jessipow, S., König, W. A. and Zähner, H. (1972). Stoffwechselprodukte von Mikroorganismen 98. Phosphinothricin und Phosphinothricyl-Alanyl-Alanin. *Helvetica Chimica Acta* **55**, 224-239.

Becana, M., Aparicio-Tejo, P. M. and Sanchez-Diaz, M. (1984). Root nodule enzymes of ammonia metabolism from *Medicago sativa* L. as influenced by nitrate levels. *Journal of Plant Physiology* **116**, 285-292.

Becker, T. W., Caboche, M., Carrayol, E. and Hirel, B. (1992). Nucleotide sequence of a tobacco cDNA encoding plastidic glutamine synthetase and light inducibility, organ specificity and diurnal rhythmicity in the expression of the corresponding genes of tobacco and tomato. *Plant Molecular Biology* **19**, 367-379.

Becker, T. W., Perrot-Rechenmann, C., Suzuki, A. and Hirel, B. (1993). Subcellular and immunocytochemical localization of the enzymes involved in ammonia assimilation in mesophyll and bundle-sheath cells of maize leaves. *Planta* **191**, 129-136.

Bedford, D. J., Lewis, C. G. and Buttner, M. J. (1991). Characterization of a gene conferring bialaphos resistance in *Streptomyces coelicolor* A3(2). *Gene* **104**, 39-45.

Bennett, M. J. and Cullimore, J. V. (1989). Glutamine synthetase isoenzymes of *Phaseolus vulgaris* L.: subunit composition in developing root nodules and plumules. *Planta* **179**, 433-440.

Bennett, M. J. and Cullimore, J. V. (1990). Expression of three plant glutamine synthetase cDNA in *Escherichia coli*. Formation of catalytically active isoenzymes, and complementation of a *glnA* mutant. *European Journal of Biochemistry* **193**, 319-324.

Bennett, M. J., Lightfoot, D. A. and Cullimore, J. V. (1989). cDNA sequence and differential expression of the gene encoding the glutamine synthetase γ-polypeptide of Phaseolus vulgaris L. *Plant Molecular Biology* **12**, 553-565.

Bentley, H. R., McDermott, E. E., Pace, J., Whitehead, J. K. and Moran, T. (1949). Action of nitrogen trichloride ('Agene') on proteins: Isolation of crystalline toxic factor. *Nature* **164**, 438-439.

Bernhard, W. R. and Matile, P. (1994). Differential expression of glutamine synthetase genes during the senescence of *Arabidopsis thaliana* rosette leaves. *Plant Science* **98**, 7-14.

Bevan, M. (1984). Binary *Agrobacterium* vectors for plant transformation. *Nucleic Acids Research* **12**, 8711-8721.

Birnboim, H. C. and Doly, J. (1979). A rapid alkaline extraction procedure for screening recombinant plasmid DNA. *Nucleic Acids Research* **7**, 1513.

Blackwell, R. D., Murray, A. J. S. and Lea, P. J. (1987). Inhibition of photosynthesis in barley with decreased levels of chloroplastic glutamine synthetase activity. *Journal of Experimental Botany* **38**, 1799-1809.

Blackwell, R. D., Murray, A. J. S., Lea, P. J., Kendall, A. C., Hall, N. P., Turner, J. C. and Wallsgrove, R. M. (1988). The value of mutants unable to carry out photorespiration. *Photosynthesis Research* **16**, 155-176.

Bloom, A. J., Sukrapanna, S. S. and Warner, R. L. (1992). Root respiration associated with ammonium and nitrate absorption and assimilation by barley. *Plant Physiology* **99**, 1294-1301.

Bolivar, F., Rodriguez, R. L., Greene, P. J., Betlach, M. C., Heyneker, H. L. and Boyer, H. L. (1977). Construction and characterization of new cloning vehicles. II. A multipurpose cloning system. *Gene* **2**, 95-113.

Boron, L., Szczyglowski, K., Konieczny, A. and Legocki, A. B. (1989). Glutamine synthetase in *Lupinus luteus*. Identification and preliminary characterization of a nodule specific cDNA clone. *Acta Biochimica Polonica* **36**, 295-301.

Botterman, J., Gossel, V., Thoen, C. and Lauwereys, M. (1991). Characterization of phosphinothricin acetyltransferase and C-terminal enzymatically active fusion proteins. *Gene* **102**, 33-37.

Bourque, J. E. (1995). Antisense strategies for genetic manipulations in plants. *Plant Science* **105**, 125-149.

Bradford, M. M. (1976). A rapid and sensitive method for the quantitation of microgram quantities of protein utilizing the principle of protein-dye binding. *Analytical Biochemistry* **72**, 248-254.

Bravo, A. and Mora, J. (1988). Ammonium assimilation in *Rhizobium phaseoli* by the glutamine synthetase-glutamate synthase pathway. *Journal of Bacteriology* **170**, 980-984.

Brears, T., Walker, E. L. and Coruzzi, G. M. (1991). A promoter sequence involved in cell-specific expression of the pea glutamine synthetase GS3A gene in organs of transgenic tobacco and alfalfa. *Plant Journal* **1**, 235-244.

Breslauer, K. J., Frank, R., Blocker, H. and Marky, L. A. (1986). Predicting DNA duplex stability from the base sequence. *Proceedings of the National Academy of Sciences of the USA* **83**, 3746-3750.

Brosius, J. and Holy, A. (1984). Regulation of ribosomal RNA promoters with a synthetic *lac* operator. *Proceedings of the National Academy of Sciences of the USA* **81**, 6929-6933.

Bullock, W. O., Fernandez, J. M. and Short, J. M. (1987). XL1-Blue: A high efficiency plasmid transforming *recA Escherichia coli* strain with ß-galactosidase selection. *BioTechniques* **5**, 376.

Caba, J. M., Lluch, C. and Ligero, F. (1994). Genotypic variability of nitrogen metabolism enzymes found in nodulated roots of *Vicia faba*. *Soil Biology and Biochemistry* **26**, 785-789.

Cabello, P., de la Haba, P. and Maldonado, J. M. (1991). Isoforms of glutamine synthetase in cotyledons, leaves and roots of sunflower plants. *Journal of Plant Physiology* **137**, 378-380.

Cabello, P., de la Haba, P. and Maldonado, J. M. (1994). Properties of the glutamine synthetase isoforms isolated from sunflower leaves. *Journal of Plant Physiology* **144**, 1-6.

Cai, X. and Wong, P. P. (1990). Mechanism for the variation in electrophoretic mobility of glutamine synthetase from *Phaseolus vulgaris* root nodules. *Plant Science* **72**, 199-206.

Cánovas, F., Valpuesta, V. and Núñez De Castro, I. (1984). Characterization of tomato leaf glutamine synthetase. *Plant Science Letters* **37**, 79-85.

Cánovas, F. M., Avila, C., Botella, J. R., Valpuesta, V. and Núñez de Castro, I. (1986). Effect of light-dark transition on glutamine synthetase activity in tomato leaves. *Physiologia Plantarum* **66**, 648-652.

Cao, J., Duan, X., McElroy, D. and Wu, R. (1992). Regeneration of herbicide resistant transgenic rice plants following microprojectile-mediated transformation of suspension culture cells. *Plant Cell Reports* **11**, 586-591.

Carroll, B. J. and Gresshoff, P. M. (1983). Nitrate inhibition of nodulation and nitrogen fixation in white clover. *Zeitschrift für Pflanzenphysiologie und Bodenkunde* **110**, 77-88.

Caruthers, M. H., Barone, A. D., Beaucage, S. L., Dodds, D. R., Fisher, E. F., McBride, L. J., Matteucci, M., Stabinsky, Z. and Tang, J. Y. (1987). Chemical synthesis of deoxyoligonucleotides. *Methods in Enzymology* **154**, 287-313.

Carvalho, H., Pereira, S., Sunkel, C. and Salema, R. (1992). Detection of a cytosolic glutamine synthetase in leaves of *Nicotiana tabacum* L. by immunocytochemical methods. *Plant Physiology* **100**, 1591-1594.

Castillo, A. M., Vasil, V. and Vasil, I. K. (1994). Rapid production of fertile transgenic plants of rye (*Secale cereale* L.). *BioTechnology* **12**, 1366-1371.

Chandok, M. R. and Sopory, S. K. (1996). Phosphorylation/dephosphorylation steps are key events in the phytochrome-mediated enhancement of nitrate reductase mRNA levels and enzyme activity in maize. *Molecular and General Genetics* **251**, 599-608.

Chen, F.-L., Bennett, M. J. and Cullimore, J. V. (1990). Effect of the nitrogen supply on the activities of isoenzymes of NADH-dependent glutamate synthase and glutamine synthetase in root nodules of *Phaseolus vulgaris* L. *Journal of Experimental Botany* **41**, 1215-1221.

Chen, F.-L. and Cullimore, J. V. (1989). Location of two isoenzymes of NADH-dependent glutamate synthase in root nodules of *Phaseolus vulgaris* L. *Planta* **179**, 441-447.

Chua, K.-Y., Pankhurst, C. E., MacDonald, P. E., Hopcroft, D. H., Jarvis, B. D. W. and Scott, D. B. (1985). Isolation and characterization of transposon Tn5-induced symbiotic mutants of *Rhizobium loti*. *Journal of Bacteriology* **162**, 335-343.

Clark, J. M. (1988). Novel non-templated nucleotide addition reactions catalyzed by prokaryotic and eukaryotic DNA polymerases. *Nucleic Acids Research* **16**, 9677-9686.

Cock, J. M., Brock, I. W., Watson, A. T., Swarup, R., Morby, A. P. and Cullimore, J. V. (1991). Regulation of glutamine synthetase genes in leaves of *Phaseolus vulgaris*. *Plant Molecular Biology* **17**, 761-771.

Cock, J. M., Mould, R. M., Bennett, M. J. and Cullimore, J. V. (1990). Expression of glutamine synthetase genes in roots and nodules of *Phaseolus vulgaris* following changes in the ammonium supply and infection with various *Rhizobium* mutants. *Plant Molecular Biology* **14**, 549-560.

Cullimore, J. V., Gebhardt, C., Saarelainen, R., Miflin, B. J., Idler, K. B. and Barker, R. F. (1984). Glutamine synthetase of *Phaseolus vulgaris* L.: organ-specific expression of a multigene family. *Journal of Molecular and Applied Genetics* **2**, 589-599.

Cullimore, J. V., Lara, M., Lea, P. J. and Miflin, B. J. (1983). Purification and properties of two forms of glutamine synthetase from the plant fraction of *Phaseolus* root nodules. *Planta* **157**, 245-253.

Cullimore, J. V. and Miflin, B. J. (1984). Immunological studies on glutamine synthetase using antisera raised to the two plant forms of the enzyme from *Phaseolus* root nodules. *Journal of Experimental Botany* **35**, 581-587.

Cullimore, J. V. and Sims, A. P. (1980). An association between photorespiration and protein catabolism: Studies in *Chlamydomonas*. *Planta* **150**, 392-396.

Cundliffe, E. (1989). How antibiotic-producing organisms avoid suicide. *Annual Review of Microbiology* **43**, 207-233.

Datla, R. S. S., Hammerlindl, J. K., Pelcher, L. E., Crosby, W. L. and Selvaraj, G. (1991). A bifunctional fusion between ß-glucuronidase and neomycin phosphotransferase: a broad-spectrum marker enzyme for plants. *Gene* **101**, 239-246.

Datta, S. K., Datta, K., Soltanifar, N., Donn, G. and Potrykus, I. (1992). Herbicide-resistant Indica rice plants from IRRI breeding line IR72 after PEG-mediated transformation of protoplasts. *Plant Molecular Biology* **20**, 619-629.

De Block, M., Botterman, J., Vandewiele, M., Dockx, J., Thoen, C., Gosselé, V., Movva, N. R., Thompson, C., Van Montagu, M. and Leemans, J. (1987). Engineering herbicide resistance in plants by expression of a detoxifying enzyme. *EMBO Journal* **6**, 2513-2518.

De Boer, H. A., Comstock, L. J. and Vasser, M. (1983). The *tac* promoter - a functional hybrid derived from the *trp* and *lac* promoters. *Proceedings of the National Academy of Sciences of the USA* **80**, 21-25.

De Greef, W., Delon, R., De Block, M., Leemans, J. and Botterman, J. (1989). Evaluation of herbicide resistance in transgenic crops under field conditions. *BioTechnology* **7**, 61-64.

Dean, C., Jones, J., Favreau, M., Dunsmuir, P. and Bedbrook, J. (1988). Influence of flanking sequences on variability in expression levels of an introduced gene in transgenic tobacco plants. *Nucleic Acids Research* **16**, 9267-9283.

Dellaporta, S. L., Wood, J. and Hicks, J. B. (1983). A plant DNA minipreparation: Version II. *Plant Molecular Biology Reporter* **1**, 19-21.

Denison, R. F. and Harter, B. L. (1995). Nitrate effects on nodule oxygen permeability and leghemoglobin: Nodule oximetry and computer modelling. *Plant Physiology* **107**, 1355-1364.

Denison, R. F., Hunt, S. and Layzell, D. B. (1992). Nitrogenase activity, nodule respiration, and O_2 permeability following detopping of alfalfa and birdsfoot trefoil. *Plant Physiology* **98**, 894-900.

Denison, R. F. and Kinraide, T. B. (1995). Oxygen-induced membrane depolarizations in legume root nodules - possible evidence for an osmoelectrical mechanism controlling nodule gas permeability. *Plant Physiology* **108**, 235-240.

D'Halluin, K., Bossut, M., Bonne, E., Mazur, B., Leemans, J. and Botterman, J. (1992a). Transformation of sugarbeet (*Beta vulgaris* L.) and evaluation of herbicide resistance in transgenic plants. *BioTechnology* **10**, 309-314.

D'Halluin, K., De Block, M., Denecke, J., Janssens, J., Leemans, J., Reynaerts, A. and Botterman, J. (1992b). The *bar* gene as a selectable and screenable marker in plant engineering. *Methods in Enzymology* **216**, 415-426.

Diaz, A., Maza, H., González-Moro, B. G., Lacuesta, M., González-Murua, C. and Muñoz-Rueda, A. (1995). Phosphinothricin reverts the ammonia-dependent enhancement of phosphoenolpyruvate carboxylase activity. *Journal of Plant Physiology* **145**, 11-16.

Douglas, P., Morrice, N. and Mackintosh, C. (1995). Identification of a regulatory phosphorylation site in the HINGE-1 region of nitrate reductase from spinach (*Spinacea oleracea*) leaves. *FEBS Letters* **377**, 113-117.

Downs, C. G., Borst, W. M., Hurst, P. L. and Stevenson, D. G. (1994a). Isoforms of glutamine synthetase in asparagus spears: the cytosolic enzyme increases after harvest. *Plant Cell and Environment* **17**, 1045-1052.

Downs, C. G., Christey, M. C., Davies, K. M., King, G. A., Seelye, J. F., Sinclair, B. K. and Stevenson, D. G. (1994b). Hairy roots of *Brassica napus*: II. Glutamine synthetase overexpression alters ammonia assimilation and the response to phosphinothricin. *Plant Cell Reports* **14**, 41-46.

Downs, C. G., Christey, M. C., Maddocks, D., Seelye, J. F. and Stevenson, D. G. (1994c). Hairy roots of *Brassica napus*: I. Applied glutamine overcomes the effect of phosphinothricin treatment. *Plant Cell Reports* **14**, 37-40.

Dröge-Laser, W., Siemeling, U., Pühler, A. and Broer, I. (1994). The Metabolites of the Herbicide L-Phosphinothricin (Glufosinate) - Identification, stability, and mobility in transgenic, herbicide-resistant, and untransformed plants. *Plant Physiology* **105**, 159-166.

Dunn, K., Dickstein, R., Feinbaum, R., Burnett, B. K., Peterman, T. K., Thoidis, G., Goodman, H. M. and Ausubel, F. M. (1988). Developmental regulation of nodule-specific genes in alfalfa root nodules. *Molecular Plant-Microbe Interactions* **1**, 66-74.

Dye, M. (1979). Functions and maintenance of a *Rhizobium* collection. In *Recent advances in biological nitrogen fixation*, N. S. Subba Rao, ed. (New Delhi: Oxford & IBH Publ. Co.), pp. 435-471.

Edwards, J. W. and Corruzzi, G. M. (1989). Photorespiration and light act in concert to regulate the expression of the nuclear gene for chloroplast glutamine synthetase. *Plant Cell* **1**, 241-248.

Edwards, J. W., Walker, E. L. and Coruzzi, G. M. (1990). Cell-specific expression in transgenic plants reveals non-overlapping roles for chloroplast and cytosolic glutamine synthetase. *Proceedings of the National Academy of Sciences of the USA* **87**, 3459-3463.

Egli, M. A., Griffith, S. M., Miller, S. S., Anderson, M. P. and Vance, C. P. (1989). Nitrogen assimilating enzyme activities and enzyme protein during development and senescence of effective and plant gene-controlled ineffective alfalfa nodules. *Plant Physiology* **91**, 898-904.

Elmlinger, M. W. and Mohr, H. (1992). Glutamine synthetase in Scots pine seedlings and its control by blue light and light absorbed by phytochrome. *Planta* **188**, 396-402.

Emes, M. J. and Fowler, M. W. (1974). The intracellular location of the enzymes of nitrate assimilation in the apices of seedling pea roots. *Planta* **144**, 249-253.

Emes, M. J. and Fowler, M. W. (1983). The supply of reducing power for nitrate reduction in plastids of seedling pea roots (*Pisum sativum* L.). *Planta* **158**, 97-102.

Ericson, M. C. (1985). Purification and properties of glutamine synthetase from spinach leaves. *Plant Physiology* **79**, 923-927.

Fåhraeus, G. (1957). The infection of clover root hairs by nodule bacteria studied by a simple glass slide technique. *Journal of General Microbiology* **16**, 374-381.

Faurie, O. and Soussana, J.-F. (1993). Oxygen-induced recovery from short-term nitrate inhibition of N_2 fixation in white clover plants from spaced and dense stands. *Physiologia Plantarum* **89**, 467-475.

Feller, U. and Fischer, A. (1994). Nitrogen metabolism in senescing leaves. *Critical Reviews in Plant Sciences* **13**, 241-273.

Forde, B. G. and Cullimore, J. V. (1989). The molecular biology of glutamine synthetase in higher plants. *Oxford Surveys of Plant Molecular and Cell Biology* **6**, 247-296.

Forde, B. G., Day, H. M., Turton, J. F., Shen, W. J., Cullimore, J. V. and Oliver, J. E. (1989). Two glutamine synthetase genes from *Phaseolus vulgaris* display contrasting developmental and spatial patterns of expression in transgenic *Lotus corniculatus* plants. *Plant Cell* **1**, 391-401.

Franck, A., Guilley, H., Jonard, G., Richards, K. and Hirth, L. (1980). Nucleotide sequence of cauliflower mosaic virus DNA. *Cell* **21**, 285-294.

Freeman, J., Marquez, A. J., Wallsgrove, R. M., Saarelainen, R. and Forde, B. G. (1990). Molecular analysis of barley mutants deficient in chloroplast glutamine synthetase. *Plant Molecular Biology* **14**, 297-311.

Frommer, W. B., Kwart, M., Hirner, B., Fischer, W. N., Hummel, S. and Ninnemann, O. (1994). Transporters for nitrogenous compounds in plants. *Plant Molecular Biology* **26**, 1651-1670.

Galangau, F., Daniel-Vedele, F., Moureaux, T., Dorbe, M.-F., Leydecker, M.-T. and Caboche, M. (1988). Expression of leaf nitrate reductase genes from tomato and tobacco in relation to light-dark regimes and nitrate supply. *Plant Physiology* **88**, 383-388.

Gallagher, S. R. (1992). GUS protocols: using the GUS gene as a reporter of gene expression. (London: Academic Press), pp. 221.

Gao, F. and Wong, P. (1994). Genotypes of the common bean (*Phaseolus vulgaris* L.) lacking the nodule-enhanced isoform of glutamine synthetase. *Plant Physiology* **106**, 1389-1394.

García-Fernández, J. M., López-Ruiz, A., Toribio, F., Roldán, J. M. and Diez, J. (1994). Occurrence of only one form of glutamine synthetase in the green alga *Monoraphidium braunii*. *Plant Physiology* **104**, 425-430.

Gaudin, V., Vrain, T. and Jouanin, L. (1994). Bacterial genes modifying hormonal balances in plants. *Plant Physiology and Biochemistry* **32**, 11-29.

Gebhardt, C., Oliver, J. E., Forde, B. G., Saarelainen, R. and Miflin, B. J. (1986). Primary structure and differential expression of glutamine synthetase genes in nodules, roots and leaves of *Phaseolus vulgaris*. *EMBO Journal* **5**, 1429-1435.

Givan, C. V., Joy, K. W. and Kleczowski, L. A. (1988). A decade of photorespiratory nitrogen cycling. *Trends in Biological Sciences* **13**, 433-437.

Goodwin, T. W. and Mercer, E. I. (1986). Introduction to plant biochemistry, 2nd Edition (Oxford: Pergamon Press).

Grant, M. and Bevan, M. W. (1994). Asparaginase gene expression is regulated in a complex spatial and temporal pattern in nitrogen-sink tissues. *Plant Journal* **5**, 695-704.

Grant, M. R., Carne, A., Hill, D. F. and Farnden, K. J. F. (1989). The isolation and characterization of a cDNA clone encoding *Lupinus angustifolius* root nodule glutamine synthetase. *Plant Molecular Biology* **13**, 484-490.

Green, P. D. and Wong, P. P. (1992). Subunit analysis of glutamine synthetase isozymes from root nodules of tepary bean (*Phaseolus acutifolius* Gray). *Plant Science* **82**, 179-186.

Griffith, O. W. and Meister, A. (1978). Differential inhibition of glutamine and γ-glutamylcysteine synthetases by α-alkyl analogs of methionine sulfoximine that induce convulsions. *Journal of Biological Chemistry* **253**, 2333-2338.

Griffith, O. W. and Meister, A. (1979). Potent and specific inhibition of glutathione synthesis by buthionine sulfoximine (S-*n*-butyl homocysteine sulfoximine). *Journal of Biological Chemistry* **254**, 7558-7560.

Groat, R. G., Vance, C. P. and Barnes, D. K. (1984). Host plant nodule enzymes associated with selection for increased N_2 fixation in alfalfa. *Crop Science* **24**, 895-898.

Grunstein, M. and Hogness, D. (1975). Colony hybridization: A method for the isolation of cloned DNAs that contain a specific gene. *Proceedings of the National Academy of Sciences of the USA* **72**, 3961.

Guivarch, A., Caissard, J. C., Azmi, A., Elmayan, T., Chriqui, D. and Tepfer, M. (1996). *In situ* detection of expression of the GUS reporter gene transgenic plants: 10 years of blue genes. *Transgenic Research* **5**, 281-288.

Guiz, C., Hirel, B., Shedlofsky, G. and Gadal, P. (1979). Occurrence and influence of light on the relative proportions of two glutamine synthetases in rice leaves. *Plant Science Letters* **15**, 271-277.

Gussin, G. N., Ronson, C. W. and Ausubel, F. M. (1986). Regulation of nitrogen fixation genes. *Annual Review of Genetics* **20**, 567-591.

Hatch, D. J. and Macduff, J. H. (1991). Concurrent rates of N_2 fixation, nitrate and ammonium uptake by white clover in response to growth at different root temperatures. *Annals of Botany* **67**, 265-274.

Haynes, R. J. (1986). Nitrification. In *Mineral nitrogen in the plant-soil system.*, R. J. Haynes, ed. (Orlando, Florida: Academic Press), pp. 483.

Hirel, B., Bouet, C., King, B., Layzell, D., Jacobs, F. and Verma, D. P. S. (1987). Glutamine synthetase genes are regulated by ammonia provided externally or by symbiotic nitrogen fixation. *EMBO Journal* **6**, 1167-1171.

Hirel, B. and Gadal, P. (1980). Glutamine synthetase in rice. A comparative study of the enzymes from roots and leaves. *Plant Physiology* **66**, 619-623.

Hirota, Y., Fujii, T., Sano, Y. and Iyama, S. (1978). Nitrogen fixation in the rhizosphere of rice. *Nature* **276**, 416-417.

Hirsch, A. M. (1992). Developmental biology of legume nodulation. *New Phytologist* **122**, 211-237.

Hobbs, S. L. A., Kpodar, P. and DeLong, C. M. O. (1990). The Effect of T-DNA copy number, position and methylation on reporter gene expression in tobacco transformants. *Plant Molecular Biology* **15**, 851-864.

Hoelzle, I., Finer, J. J., McMullen, M. D. and Streeter, J. G. (1992). Induction of glutamine synthetase activity in nonnodulated roots of *Glycine max*, *Phaseolus vulgaris*, and *Pisum sativum*. *Plant Physiology* **100**, 525-528.

Holmes, D. S. and Quigley, M. (1981). A rapid boiling method for the preparation of bacterial plasmids. *Analytical Biochemistry* **114**, 193-197.

Hooykaas, P. J. J. (1979). The role of plasmid determinated functions in the interactions of *Rhizobiaceae* with plant cells - A genetic approach. PhD Thesis, University of Wageningen

Höpfner, M., Ochs, G. and Wild, A. (1991). Detection of a single gene encoding glutamine synthetase in *Sinapis alba*. *Journal of Plant Physiology* **139**, 76-81.

Huber, S. C., Bachmann, M. and Huber, J. L. (1996). Post-translational regulation of nitrate reductase activity: a role for Ca^{2+} and 14-3-3 proteins. *Trends in Plant Science* **1**, 432-438.

Jacobsen, H., Klenow, H. and Ovargaard-Hansen, K. (1974). The N-terminal amino-acid sequences of DNA polymerase I from *Escherichia coli* and of the large and small fragments obtained by a limited proteolysis. *European Journal of Biochemistry* **45**, 623.

Jarvis, S. C., Macduff, J. H., Williams, J. R. and Hatch, D. J. (1989). Balances of forms of mineral N in grazed grassland soils: impact on N losses. *Proceedings of the XVI International Grassland Congress* (Nice, France), pp. 151-152.

Jefferson, R. A. (1985). DNA transformation of *C. elegans*: development and application of a new gene fusion system. PhD Thesis, University of Colerado, Boulder

Jefferson, R. A. (1987). Assaying chimaeric genes in plants: The GUS gene fusion system. *Plant Molecular Biology Reporter* **5**, 387-405.

Jefferson, R. A., Kavanagh, T. A. and Bevan, M. W. (1987). GUS fusions: β-glucuronidase as a sensitive and versatile gene fusion marker in higher plants. *EMBO Journal* **6**, 3901-3907.

Jones, J. D. G., Dunsmuir, P. and Bedbrook, J. (1985). High level expression of introduced chimaeric genes in regenerated transformed plants. *EMBO Journal* **4**, 2411-2418.

Joy, K. W. (1988). Ammonia, glutamine, and asparagine: a carbon-nitrogen interface. *Canadian Journal of Botany* **66**, 2103-2109.

Joyce, C. M. and Grindley, N. D. F. (1983). Construction of a plasmid that overproduces the large proteolytic fragment (Klenow fragment) of DNA polymerase I of *Escherichia coli*. *Proceedings of the National Academy of Sciences of the USA* **80**, 1830-1834.

Kado, C. I. and Heskett, M. G. (1970). Selective media for isolation of *Agrobacterium*, *Corynebacterium*, *Erwinia*, *Pseudomonas*, and *Xanthomonas*. *Phytopathology* **60**, 969-976.

Kamachi, K., Yamaya, T., Hayakawa, T., Mae, T. and Ojima, T. (1992). Vascular bundle-specific localization of cytosolic glutamine synthetase in rice leaves. *Plant Physiology* **99**, 1481-1486.

Keys, A. J., Bird, I. F., Cornelius, M. J., Lea, P. J., Wallsgrove, R. M. and Miflin, B. J. (1978). Photorespiratory nitrogen cycle. *Nature* **275**, 741-743.

Kim, K. H. and Rhee, S. G. (1987). Subunit interaction elicited by partial inactivation with L-methionine sulfoximine and ATP differently affects the biosynthetic and γ-glutamyltransferase reactions catalyzed by yeast glutamine synthetase. *Journal of Biological Chemistry* **262**, 13050-13054.

Knight, T. J., Bush, D. R. and Langston-Unkefer, P. J. (1988). Oats tolerant of *Pseudomonas syringae* pv. *tabaci* contain tabtoxinine-ß-lactam-insensitive leaf glutamine synthetases. *Plant Physiology* **88**, 333-339.

Knight, T. J. and Langston-Unkefer, P. J. (1988). Enhancement of symbiotic dinitrogen fixation by a toxin-releasing plant pathogen. *Science* **241**, 951-954.

Komoßa, D. and Sandermann Jr, H. (1992). Plant metabolism of herbicides with C-P bonds: phosphinothricin. *Pesticide Biochemistry and Physiology* **43**, 95-102.

Konieczny, A., Szczyglowski, K., Boron, L., Przybylska, M. and Legocki, A. B. (1988). Expression of lupin nodulin genes during root nodule development. *Plant Science* **55**, 145-149.

Kriete, G. and Broer, I. (1996). Influence of the herbicide phosphinothricin on growth and nodulation capacity of *Rhizobium meliloti*. *Applied Microbiology and Biotechnology* **46**, 580-586.

Kunjibettu, S., Temple, S. J., Roche, D. and Sengupta-Gopalan, C. (1996). The synthesis of nodule specific GS isoenzymes in developing soybean nodules is dependent on N_2 fixation. *Plant Physiology* **111**, 28.

Lacuesta, M., González-Moro, B., González-Murua, C. and Muñoz-Rueda, A. (1993). Time-course of the phosphinothricin effect on gas exchange and nitrate reduction in *Medicago sativa*. *Physiologia plantarum* **89**, 847-853.

Lacuesta, M., Muñoz-Rueda, A., González-Murua, C. and Sivak, M. N. (1992). Effect of phosphinothricin (glufosinate) on photosynthesis and chlorophyll fluorescence emission by barley leaves illuminated under photorespiratory and non-photorespiratory conditions. *Journal of Experimental Botany* **43**, 159-165.

Laemmli, U. K. (1970). Cleavage of structural proteins during the assembly of the head of bacteriophage T4. *Nature* **227**, 680-685.

Lam, H.-M., Coschigano, K. T., Oliveira, I. C., Melooliveira, R. and Coruzzi, G. M. (1996). The molecular genetics of nitrogen assimilation into amino acids in higher plants. *Annual Review of Plant Physiology and Plant Molecular Biology* **47**, 569-593.

Lang, P., Martín, R. and Golvano, M. P. (1993). Effect of nitrate on carbon metabolism and nitrogen fixation in root nodules of *Lupinus albus*. *Plant Physiology and Biochemistry* **31**, 639-648.

Langston-Unkefer, P. J., Robinson, A. C., Knight, T. J. and Durbin, R. D. (1987). Inactivation of pea seed glutamine synthetase by the toxin, tabtoxinine-β-lactam. *Journal of Biological Chemistry* **262**, 1608-1613.

Lara, M., Cullimore, J. V., Lea, P. J., Miflin, B. J., Johnston, A. W. B. and Lamb, J. W. (1983). Appearance of a novel form of plant glutamine synthetase during nodule development in *Phaseolus vulgaris* L. *Planta* **157**, 254-258.

Lara, M., Porta, H., Padilla, J., Folch, J. and Sánchez, F. (1984). Heterogeneity of glutamine synthetase polypeptides in *Phaseolus vulgaris* L. *Plant Physiology* **76**, 1019-1023.

Lauter, F. R., Ninnemann, O., Bucher, M., Riesmeier, J. W. and Frommer, W. B. (1996). Preferential expression of an ammonium transporter and of two putative nitrate transporters in root hairs of tomato. *Proceedings of the National Academy of Sciences of the USA* **93**, 8139-8144.

Layzell, D. B. and Hunt, S. (1990). Oxygen and the regulation of nitrogen fixation in legume nodules. *Physiologia Plantarum* **80**, 322-327.

Lea, P. J. (1991). The inhibition of ammonia assimilation: a mechanism of herbicide action. In *Herbicides*, N. R. Baker and B. V. Percival, eds. (Amsterdam: Elsevier), pp. 267-298.

Lea, P. J., Blackwell, R. D., Chen, F.-L. and Hecht, U. (1990). Enzymes of ammonia assimilation. In *Methods in Plant Biochemistry, Vol. 3*, P. J. Lea, ed. (London: Academic Press), pp. 257-276.

Lea, P. J. and Ridley, S. M. (1989). Glutamine synthetase and its inhibition. In *Herbicides and Plant Metabolism*, A. D. Dodge, ed. (Cambridge: Cambridge University Press), pp. 137-170.

Li, M. G., Villemur, R., Hussey, P. J., Silflow, C. D., Gantt, J. S. and Snustad, D. P. (1993). Differential expression of six glutamine synthetase genes in *Zea mays*. *Plant Molecular Biology* **23**, 401-407.

Lightfoot, D. A., Green, N. K. and Cullimore, J. V. (1988). The chloroplast-located glutamine synthetase of *Phaseolus vulgaris* L.: nucleotide sequence, expression in different organs and uptake into isolated chloroplasts. *Plant Molecular Biology* **11**, 191-202.

Lin, Z., Miao, G. H. and Verma, D. P. S. (1995). A cDNA sequence encoding glutamine synthetase is preferentially expressed in nodules of *Vigna aconitifolia*. *Plant Physiology* **107**, 279-280.

Logusch, E. W., Walker, D. M., McDonald, J. F. and Franz, J. E. (1989). Substrate variability as a factor in enzyme inhibitor design: Inhibition of ovine brain glutamine synthetase by α- and γ-substituted phosphinothricins. *Biochemistry* **28**, 3043-3051.

Lubben, T. H., Donaldson, G. K., Vitanen, P. V. and Gatenby, A. A. (1989). Several proteins imported into chloroplasts form stable complexes with the GroEL-related chloroplast molecular chaperone. *Plant Cell* **1**, 1223-1230.

Mäck, G. (1995). Organ-specific changes in the activity and subunit composition of glutamine-synthetase isoforms of barley (*Hordeum vulgare* L.) after growth on different levels of NH_4^+. *Planta* **196**, 231-238.

Mäck, G. and Tischner, R. (1990). Glutamine synthetase oligomers and isoforms in sugarbeet (*Beta vulgaris* L.). *Planta* **181**, 10-17.

Mäck, G. and Tischner, R. (1994). Activity of the tetramer and octamer of glutamine synthetase isoforms during primary leaf ontogeny of sugar beet (*Beta vulgaris* L.). *Planta* **194**, 353-359.

MacKintosh, C. (1997). Regulation of C/N metabolism by reversible protein phosphorylation. In *A molecular approach to primary metabolism in higher plants*, C. H. Foyer and W. P. Quick, eds. (London: Taylor and Francis).

Manco, G., Rossi, M., Defez, R., Lamberti, A., Percuoco, G. and Iaccarino, M. (1992). Dissociation by NH_4Cl treatment of the enzymatic activities of glutamine synthetase II from *Rhizobium leguminosarum* biovar *viceae*. *Journal of General Microbiology* **138**, 1453-1460.

Manhart, J. R. and Wong, P. P. (1980). Nitrate effect on nitrogen fixation (acetylene reduction). *Plant Physiology* **65**, 502-505.

Mann, A. F., Fentem, P. A. and Stewart, G. R. (1979). Identification of two forms of glutamine synthetase in barley (*Hordeum vulgare* L.). *Biochemical and Biophysical Research Communications* **88**, 515-521.

Marschner, H. (1995). Mineral nutrition of higher plants, 2nd Edition (London: Academic Press).

Marsolier, M. C., Carrayol, E. and Hirel, B. (1993). Multiple functions of promoter sequences involved in organ-specific expression and ammonia regulation of a cytosolic soybean glutamine synthetase gene in transgenic *Lotus corniculatus*. *Plant Journal* **3**, 405-414.

Marsolier, M. C. and Hirel, B. (1993). Metabolic and developmental control of cytosolic glutamine synthetase genes in soybean. *Physiologia plantarum* **89**, 613-617.

McCullough, H. (1967). The determination of ammonia in whole blood by a direct colorimetric method. *Clinica Chimica Acta* **17**, 297-304.

McElroy, D. and Brettell, R. I. S. (1994). Foreign gene expression in transgenic cereals. *Trends in Biotechnology* **12**, 62-68.

McHughen, A. and Holm, F. A. (1995). Development and preliminary testing of a glufosinate-ammonium tolerant transgenic flax. *Canadian Journal of Plant Science* **75**, 117-120.

McNally, S. and Hirel, B. (1983). Glutamine synthetase isoforms in higher plants. *Physiologie Végétale* **21**, 761-774.

McNally, S. F., Hirel, B., Gadal, P., Mann, A. F. and Stewart, G. R. (1983). Glutamine synthetases of higher plants - evidence for a specific isoform content related to their possible physiological role and their compartmentation within the leaf. *Plant Physiology* **72**, 22-25.

Mead, D. A., Pey, N. K., Herrnstadt, C., Marcil, R. A. and Smith, L. M. (1991). A universal method for the direct cloning of PCR-amplified nucleic acid. *BioTechnology* **9**, 657-663.

Meister, A. (1980). Catalytic mechanism of glutamine synthetase; overview of glutamine metabolism. In *Glutamine: Metabolism, enzymology and regulation*, J. Mora and R. Palacios, eds. (New York: Academic Press), pp. 1-40.

Mérida, A., Candau, P. and Florencio, F. J. (1991). Regulation of glutamine synthetase activity in the unicellular cyanobacterium *Synechocystis* sp. strain PCC 6803 by the nitrogen source: effect of ammonium. *Journal of Bacteriology* **173**, 4095-4100.

Mérida, A., Leurentop, L., Candau, P. and Florencio, F. J. (1990). Purification and properties of glutamine synthetases from the cyanobacteria *Synechocystis* sp. strain PCC 6803 and *Calothrix* sp. strain PCC 7601. *Journal of Bacteriology* **172**, 4732-4735.

Messing, J., Gronenborn, B., Muller-Hill, B. and Hopschneider, P. H. (1977). Filamentous coliphage M13 as a cloning vehicle: insertion of a *Hind*II fragment of the *lac* regulatory region in M13 replicative form *in vitro*. *Proceedings of the National Academy of Sciences of the USA* **74**, 3642-3646.

Miao, G. H., Hirel, B., Marsolier, M. C., Ridge, R. W. and Verma, D. P. S. (1991). Ammonia-regulated expression of a soybean gene encoding cytosolic glutamine synthetase in transgenic *Lotus corniculatus*. *Plant Cell* **3**, 11-22.

Miflin, B. J. (1974). The location of nitrate reductase and other enzymes related to amino acid biosynthesis in the plastids of roots and leaves. *Plant Physiology* **54**, 550-555.

Miflin, B. J. and Cullimore, J. V. (1984). Nitrogen assimilation in the legume-*Rhizobium* symbiosis: a joint endeavour. In *Genes involved in microbe-plant interactions*, D. P. S. Verma and T. Hohn, eds. (Wien: Springer-Verlag), pp. 129-178.

Miflin, B. J. and Lea, P. J. (1976). The pathway of nitrogen assimilation in plants. *Phytochemistry* **15**, 873-885.

Miflin, B. J., Lea, P. J. and Wallsgrove, R. M. (1980). The role of glutamine in ammonia assimilation and reassimilation in plants. In *Glutamine: Metabolism, enzymology and regulation*, J. Mora and R. Palacios, eds. (New York: Academic Press), 213-234.

Mitchell, A. P. and Magasanik, B. (1984). Biochemical and physiological aspects of glutamine synthetase inactivation in *Saccharomyces cerevisiae*. *Journal of Biological Chemistry* **259**, 2054-2062.

Mizukoshi, K., Nishiwaki, T., Ohtake, N., Minagawa, R., Ikarashi, T. and Ohyama, T. (1995). Nitrate transport pathway into soybean nodules traced by tungstate and $^{15}NO_3^-$. *Soil Science and Plant Nutrition* **41**, 75-88.

Mlynárová, L., Jansen, R. C., Conner, A. J., Stiekema, W. J. and Nap, J.-P. (1995). The MAR-mediated reduction in position effect can be uncoupled from copy number dependent expression in transgenic plants. *Plant Cell* **7**, 599-609.

Moffat, A. S. (1991). Making sense of antisense. *Science* **253**, 510-511.

Moorhead, G., Douglas, P., Morrice, N., Scarabel, M., Aitken, A. and MacKintosh, C. (1996). Phosphorylated nitrate reductase from spinach leaves is inhibited by 14-3-3 proteins and activated by fusicoccin. *Current Biology* **6**, 1104-1113.

Muhitch, M. J. (1989). Purification and characterization of two forms of glutamine synthetase from the pedicel region of maize (*Zea mays* L.) kernels. *Plant Physiology* **91**, 868-875.

Murashige, T. and Skoog, F. (1962). A revised medium for rapid growth and bioassays with tobacco tissue cultures. *Physiologia Plantarum* **15**, 473-497.

Naisbitt, T. and Sprent, J. I. (1993). The long-term effects of nitrate on the growth and nodule structure of the caesalpinioid herbaceous legume *Chamaecrista fasciculata* Michaux. *Journal of Experimental Botany* **44**, 829-836.

Nato, F., Hirel, B., Nato, A. and Gadal, P. (1984). Chloroplastic glutamine synthetase from tobacco leaves: a glycosylated protein. *FEBS Letters* **175**, 443-446.

Ninnemann, O., Jauniaux, J. C. and Frommer, W. B. (1994). Identification of a high-affinity NH_4^+ transporter from plants. *EMBO Journal* **13**, 3464-3471.

Oaks, A. (1992). A re-evaluation of nitrogen assimilation in roots. *Bioscience* **42**, 103-111.

Ochs, G., Schock, G. and Wild, A. (1995). Purification and characterization of glutamine synthetase isoenzymes from leaves and roots of *Brassica napus* (L.). *Journal of Plant Physiology* **147**, 1-8.

Odell, J. T., Nagy, F. and Chua, N. H. (1985). Identification of DNA sequences required for activity of the cauliflower mosaic virus 35S promoter. *Nature* **313**, 810-812.

Ogawa, Y., Yoshida, H., Inouye, S. and Niida, T. (1973). Studies on a new antibiotic SF-1293: III. Synthesis of a new phosphorus containing amino acid, a component of antibiotic SF-1293. *Meiji Seika Kenkyu Nempo* **13**, 49-53.

Õmura, S., Hinotozawa, K., Imamura, N. and Murata, M. (1984a). The structure of phosalacine, a new herbicide antibiotic containing phosphinothricin. *Journal of Antibiotics* **37**, 939-940.

Õmura, S., Murata, M., Hanaki, H., Hinotozawa, K., Õiwa, R. and Tanaka, H. (1984b). Phosalacine, a new herbicidal antibiotic containing phosphinothricin. Fermentation, isolation, biological activity and mechanism of action. *Journal of Antibiotics* **37**, 829-835.

Ortega, J. L., Sánchez, F., Soberón, M. and Flores, M. L. (1992). Regulation of nodule glutamine synthetase by CO_2 levels in bean (*Phaseolus vulgaris* L.). *Plant Physiology* **98**, 584-587.

Padegimas, L., Shul'ga, O. A. and Skryabin, K. G. (1994). Phosphinothricin-resistant transgenic *Nicotiana tabacum* and *Solanum tuberosum* plants. *Molecular Biology* **28**, 294-297.

Padilla, E. P., Campos, F., Conde, V., Lara, M. and Sánchez, F. (1987). Nodule-specific glutamine synthetase is expressed before the onset of nitrogen fixation in *Phaseolus vulgaris* L. *Plant Molecular Biology* **9**, 65-74.

Parsons, R., Stanforth, A., Raven, J. A. and Sprent, J. I. (1993). Nodule growth and activity may be regulated by a feedback mechanism involving phloem nitrogen. *Plant, Cell and Environment* **16**, 125-136.

Pate, J. S., Atkins, C. A., Hamel, K., McNeil, D. L. and Layzell, D. B. (1979). Transport of organic solutes in phloem and xylem of a nodulated legume. *Plant Physiology* **63**, 1082-1088.

Peach, C. and Velten, J. (1991). Transgene expression variability (position effect) of CAT and GUS reporter genes driven by linked divergent T-DNA promoters. *Plant Molecular Biology* **17**, 49-60.

Pearse, A. G. E. (1972). Histochemistry, theoretical and applied, 3rd Edition, Volume 2 (Edinburgh: Churchill Livingstone).

Pearson, J. and Ji, Y. M. (1994). Seasonal variation of leaf glutamine synthetase isoforms in temperate deciduous trees strongly suggests different functions for the enzymes. *Plant, Cell and Environment* **17**, 1331-1337.

Peat, L. J. and Tobin, A. K. (1996). The effect of nitrogen nutrition on the cellular localization of glutamine synthetase isoforms in barley roots. *Plant Physiology* **111**, 1109-1117.

Peeters, K. M. U. and Van Laere, A. J. (1994). Amino acid metabolism associated with N-mobilization from the flag leaf of wheat (*Triticum aestivum* L.) during grain development. *Plant, Cell and Environment* **17**, 131-141.

Pelsey, F. and Caboche, M. (1992). Molecular genetics of nitrate reductase in higher plants. *Advances in Genetics* **30**, 1-40.

Pereira, S., Carvalho, H., Sunkel, C. and Salema, R. (1992). Immunocytolocalization of glutamine synthetase in mesophyll and phloem of leaves of *Solanum tuberosum* L. *Protoplasma* **167**, 66-73.

Pérez-García, A., Cánovas, F. M., Gallardo, F., Hirel, B. and de Vicente, A. (1995). Differential expression of glutamine synthetase isoforms in tomato detached leaflets infected with *Pseudomonas syringae* pv. *tomato*. *Molecular Plant-Microbe Interactions* **8**, 96-103.

Peterman, T. K. and Goodman, H. M. (1991). The glutamine synthetase gene family of *Arabidopsis thaliana* - light-regulation and differential expression in leaves, roots and seeds. *Molecular and General Genetics* **230**, 145-154.

Pharmacia (1995). Gel filtration calibration kit instruction manual for protein molecular weight determinations by gel filtration. Pharmacia instruction manual no. 11-B-033-04, Pharmacia Laboratory Separation, Pharmacia Inc., Piscataway, NJ

Plazinski, J. and Rolfe, B. G. (1985). Influence of *Azospirillum* strains on the nodulation of clovers by *Rhizobium* strains. *Applied and Environmental Microbiology* **49**, 984-989.

Popp, M. (1993). Ecological aspects of nitrogen nutrition. *Progress in Botany* **54**, 448-460.

Pozárková, D., Siffelová, G., Nasinec, V. and Macháčková, I. (1995). Effects of the *rolABC*, *rolAB*, and 35S-*rolC* genes on growth and nitrogen fixation in *Lotus corniculatus* L. *Biologia Plantarum* **37**, 491-499.

Promega (1991). Magic minipreps™ DNA purification systems. Promega Technical Bulletin no. 117, Promega Corporation, Madison, WI

Rao, A. G. and Flynn, P. (1992). Microtitre plate-based assay for ß-D-glucuronidase: a quantitative approach. In *GUS protocols: using the GUS gene as a reporter of gene expression*, S. Gallagher, ed. (New York: Academic Press).

Redinbaugh, M. G. and Campbell, W. H. (1991). Higher plant responses to environmental nitrate. *Physiologia Plantarum* **82**, 640-650.

Redinbaugh, M. G. and Campbell, W. H. (1993). Glutamine synthetase and ferredoxin-dependent glutamate synthase expression in the maize (*Zea mays*) root primary response to nitrate. *Plant Physiology* **101**, 1249-1255.

Ridley, S. M. and McNally, S. F. (1985). Effects of phosphinothricin on the isoenzymes of glutamine synthetase isolated from plant species which exhibit varying degrees of susceptibility to the herbicide. *Plant Science* **39**, 31-36.

Robert, F. M. and Wong, P. P. (1986). Isozymes of glutamine synthetase in *Phaseolus vulgaris* L. and *Phaseolus lunatus* L. root nodules. *Plant Physiology* **81**, 142-148.

Robertson, J. G., Farnden, K. J. F., Warburton, M. P. and Banks, J.-A. M. (1975). Induction of glutamine synthetase during nodule development in lupin. *Australian Journal of Plant Physiology* **2**, 265-272.

Rufty, T. W. (1997). Probing the carbon and nitrogen interaction: a whole plant perspective. In *A molecular approach to primary metabolism in higher plants*, C. H. Foyer and W. P. Quick, eds. (London: Taylor and Francis).

Rychlik, W., Spencer, W. J. and Rhoads, R. E. (1990). Optimization of the annealing temperature for DNA amplification *in vitro*. *Nucleic Acids Research* **18**, 6409-6412.

Ryden, J. C., Ball, P. R. and Garwood, E. A. (1984). Nitrate leaching from grassland. *Nature* **311**, 50-53.

Sakakibara, H., Kawabata, S., Hase, T. and Sugiyama, T. (1992a). Differential effects of nitrate and light on the expression of glutamine synthetases and ferredoxin dependent glutamate synthase in maize. *Plant and Cell Physiology* **33**, 1193-1198.

Sakakibara, H., Kawabata, S., Takahashi, H., Hase, T. and Sugiyama, T. (1992b). Molecular cloning of the family of glutamine synthetase genes from maize: Expression of genes for glutamine synthetase and ferredoxin-dependent glutamate synthase in photosynthetic and non-photosynthetic tissues. *Plant and Cell Physiology* **33**, 49-58.

Sakakibara, H., Shimizu, H., Hase, T., Yamazaki, Y., Takao, T., Shimonishi, Y. and Sugiyama, T. (1996). Molecular identification and characterization of cytosolic isoforms of glutamine synthetase in maize roots. *Journal of Biological Chemistry* **271**, 29561-29568.

Sambrook, J., Fritsch, E. F. and Maniatis, T. (1989). Molecular Cloning - a laboratory manual, 2nd Edition, Volume 1-3, N. Ford, ed. (New York: Cold Spring Harbor Laboratory Press).

Sanger, F., Nicklen, S. and Coulsen, A. R. (1977). DNA sequencing with chain-terminating inhibitors. *Proceedings of the National Academy of Sciences of the USA* **74**, 5463-5467.

Schmidt, S. and Mohr, H. (1989). Regulation of the appearance of glutamine synthetase in mustard (*Sinapis alba* L.) cotyledons by light, nitrate and ammonium. *Planta* **177**, 526-534.

Schubert, S. (1995). Nitrogen assimilation by legumes - processes and ecological limitations. *Fertilizer Research* **42**, 99-107.

Schuller, K. A., Day, D. A., Gibson, A. H. and Gresshoff, P. M. (1986). Enzymes of ammonia assimilation and ureide biosynthesis in soybean nodules: Effect of nitrate. *Plant Physiology* **80**, 646-650.

Sengupta-Gopalan, C. and Pitas, J. W. (1986). Expression of nodule-specific glutamine synthetase genes during nodule development in soybeans. *Plant Molecular Biology* **7**, 189-199.

Shaw, W. V. (1975). Chloramphenicol acetyltransferase from chloramphenicol-resistant bacteria. *Methods in Enzymology* **43**, 737-755.

Shelp, B. J., Swanton, C. J. and Hall, J. C. (1992a). Glufosinate (phosphinothricin) mobility in young soybean shoots. *Journal of Plant Physiology* **139**, 626-628.

Shelp, B. J., Swanton, C. J., Mersey, B. G. and Hall, J. C. (1992b). Glufosinate (phosphinothricin) inhibition of nitrogen metabolism in barley and green foxtail plants. *Journal of Plant Physiology* **139**, 605-610.

Shen, W.-J. (1991). Expression of glutamine synthetase genes from *Phaseolus vulgaris* L. in transgenic plants. PhD Thesis, Imperial College, London

Shen, W.-J. and Forde, B. G. (1989). Efficient transformation of *Agrobacterium* spp. by high voltage electroporation. *Nucleic Acids Research* **17**, 8385.

Sinden, S. L. and Durbin, R. D. (1968). Glutamine synthetase inhibition: possible mode of action of wildfire toxin from *Pseudomonas tabaci*. *Nature* **219**, 379-380.

Somerville, C. R. and Ogren, W. L. (1979). A phosphoglycolate phosphatase-deficient mutant of *Arabidopsis*. *Nature* **280**, 833-835.

Spencer, T. M., O'Brien, J. V., Start, W. G., Adams, T. R., Gordon-Kamm, W. J. and Lemaux, P. G. (1992). Segregation of transgenes in maize. *Plant Molecular Biology* **18**, 201-210.

Sprent, J. I., Giannakis, C. and Wallace, W. (1987). Transport of nitrate and calcium into legume root nodules. *Journal of Experimental Botany* **38**, 1121-1128.

Srinivasan, M., Petersen, D. J. and Holl, F. B. (1996). Influence of indoleacetic-acid-producing *Bacillus* isolates on the nodulation of *Phaseolus vulgaris* by *Rhizobium etli* under gnotobiotic conditions. *Canadian Journal of Microbiology* **42**, 1006-1014.

Srinivasan, M., Petersen, D. J. and Holl, F. B. (1997). Nodulation of *Phaseolus vulgaris* by *Rhizobium etli* is enhanced by the presence of *Bacillus*. *Canadian Journal of Microbiology* **43**, 1-8.

Stanford, A. C., Larson, K., Barker, D. G. and Cullimore, J. V. (1993). Differential expression within the glutamine synthetase gene family of the model legume *Medicago truncatula*. *Plant Physiology* **103**, 73-81.

Stewart, G. R., Hegarty, E. E. and Specht, R. L. (1988). Inorganic nitrogen assimilation in plants of Australian rainforest communities. *Physiologia Plantarum* **74**, 26-33.

Stewart, G. R., Mann, A. F. and Fentem, P. A. (1980). . In *The Biochemistry of Plants*, B. J. Miflin, ed. (New York: Academic Press), pp. 271-327.

Stitt, M. and Sonnewald, U. (1995). Regulation of metabolism in transgenic plants. *Annual Review of Plant Physiology and Plant Molecular Biology* **46**, 341-368.

Strauch, E., Wohlleben, W. and Pühler, A. (1988). Cloning of a phosphinothricin N-acetyltransferase gene from *Streptomyces viridochromogenes* Tü 494 and its expression in *Streptomyces lividans* and *Escherichia coli*. *Gene* **63**, 65-74.

Streeter, J. (1988). Inhibition of legume nodule formation and N_2 fixation by nitrate. *Critical Reviews in Plant Sciences* **7**, 1-23.

Streit, W., Kosch, K. and Werner, D. (1992). Nodulation competitiveness of *Rhizobium leguminosarum* bv. *phaseoli* and *Rhizobium tropici* strains measured by glucuronidase (GUS) gene fusions. *Biology and Fertility of Soils* **14**, 140-144.

Studer, D., Gloudemans, T., Franssen, H. J., Fischer, H.-M., Bisseling, T. and Hennecke, H. (1987). Involvement of the bacterial nitrogen fixation regulatory gene (*nifA*) in control of nodule-specific host-plant gene expression. *European Journal of Cell Biology* **45**, 177-184.

Sturz, A. V., Christie, B. R., Matheson, B. G. and Nowak, J. (1997). Biodiversity of endophytic bacteria which colonize red clover nodules, roots, stems and foliage and their influence on host growth. *Biology and Fertility of Soils* **25**, 13-19.

Sunito, T. M. and Teeri, T. H. (1994). A new bifunctional reporter gene for in-vivo tagging of plant promoters. *Plant Molecular Biology Reporter* **12**, 43-57.

Sutton, W. D. (1983). Nodule development and senescence. In *Nitrogen fixation Vol. 3: Legumes*, W. J. Broughton, ed. (Oxford: Oxford University Press), pp. 144-212.

Suzuki, A., Gadal, P. and Oaks, A. (1981). Intracellular distribution of enzymes associated with nitrogen assimilation in roots. *Planta* **151**, 457-461.

Tachibana, K., Watanabe, T., Sekizawa, Y. and Takematsu, T. (1986). Inhibition of glutamine synthetase and quantitative changes of free amino acids in shoots of bialaphos-treated Japanese barnyard millet. *Journal of Pesticide Science* **11**, 27-31.

Tebbe, C. C. and Reber, H. H. (1988). Utilization of the herbicide phosphinothricin as a nitrogen source by soil bacteria. *Applied Microbiology and Biotechnology* **29**, 103-105.

Tebbe, C. C. and Reber, H. H. (1991). Degradation of [^{14}C]phosphinothricin (glufosinate) in soil under laboratory conditions: Effects of concentration and soil amendments on $^{14}CO_2$ production. *Biology and Fertility of Soils* **11**, 62-67.

Temple, S. J., Bagga, S. and Sengupta-Gopalan, C. (1994). Can glutamine synthetase activity levels be modulated in transgenic plants by the use of recombinant DNA technology. *Biochemical Society Transactions* **22**, 915-920.

Temple, S. J., Bagga, S. and Sengupta-Gopalan, C. (1995a). Regulation and functional analysis of glutamine synthetase genes in legumes. In *Nitrogen fixation: fundamentals and applications*, I. A. Tikhonovich, ed. (Dordrecht: Kluwer Academic Publishers), pp. 545-550.

Temple, S. J., Heard, J., Ganter, G., Dunn, K. and Sengupta-Gopalan, C. (1995b). Characterization of a nodule-enhanced glutamine synthetase from alfalfa: Nucleotide sequence, in situ localization, and transcript analysis. *Molecular Plant-Microbe Interactions* **8**, 218-227.

Temple, S. J., Knight, T. J., Unkefer, P. J. and Sengupta-Gopalan, C. (1993). Modulation of glutamine synthetase expression in tobacco by the introduction of an alfalfa glutamine synthetase gene in sense and antisense orientation: molecular and biochemical analysis. *Molecular and General Genetics* **236**, 315-325.

Temple, S. J., Kunjibettu, S., Roche, D. and Sengupta-Gopalan, C. (1996). Total glutamine-synthetase activity during soybean nodule development is controlled at the level of transcription and holoprotein turnover. *Plant Physiology* **112**, 1723-1733.

Temple, S. J. and Sengupta-Gopalan, C. (1997). Manipulating amino acid biosynthesis. In *A molecular approach to primary metabolism in higher plants*, C. H. Foyer and W. P. Quick, eds. (London: Taylor and Francis).

Thompson, C. J., Movva, N. R., Tizard, R., Crameri, R., Davies, J. E., Lauwereys, M. and Botterman, J. (1987). Characterization of the herbicide-resistance gene *bar* from *Streptomyces hygroscopicus*. *EMBO Journal* **6**, 2519-2523.

Thykjær, T., Danielsen, D., She, Q. and Stougaard, J. (1997). Organization and expression of genes in the genomic region surrounding the glutamine synthetase gene *Gln1* from *Lotus japonicus*. *Molecular and General Genetics* **255**, 628-636.

Tingey, S. V. and Coruzzi, G. M. (1987). Glutamine synthetase in *Nicotiana plumbaginifolia*. Cloning and in vivo expression. *Plant Physiology* **84**, 366-373.

Tingey, S. V., Walker, E. L. and Coruzzi, G. M. (1987). Glutamine synthetase genes of pea encode distinct polypeptides which are differentially expressed in leaves, roots and nodules. *EMBO Journal* **6**, 1-9.

Trueman, L. J., Onyeocha, I. and Forde, B. G. (1996). Recent advances in the molecular biology of a family of eukaryotic high affinity nitrate transporters. *Plant Physiology and Biochemistry* **34**, 621-627.

Tsuprun, V. L., Boekema, E. L., Pushkin, A. V. and Tagunova, I. V. (1992). Electron microscopy and image analysis of the GroEL-like protein and its complexes with glutamine synthetase from pea leaves. *Biochimica et Biophysica Acta* **1099**, 67-73.

Van der Hoeven, C., Dietz, A. and Landsmann, J. (1994). Expression of phosphinothricin acetyltransferase from the root specific *par* promoter in transgenic tobacco plants is sufficient for herbicide tolerance. *Plant Cell Reports* **14**, 165-170.

Vessey, J. K. and Waterer, J. (1992). In search of the mechanism of nitrate inhibition of nitrogenase activity in legume nodules: Recent developments. *Physiologia Plantarum* **84**, 171-176.

Vézina, L.-P., Hope, H. J. and Joy, K. W. (1987). Isoenzymes of glutamine synthetase in roots of pea (*Pisum sativum* L. cv Little Marvel) and alfalfa (*Medicago media* Pers. cv Saranac). *Plant Physiology* **83**, 58-62.

Vézina, L.-P. and Langlois, J. R. (1989). Tissue and cellular distribution of glutamine synthetase in roots of pea (*Pisum sativum*) seedlings. *Plant Physiology* **90**, 1129-1133.

Vézina, L.-P. and Margolis, H. A. (1990). Purification and properties of glutamine synthetase in leaves and roots of *Pinus banksiana* Lamb. *Plant Physiology* **94**, 657-664.

Vézina, L.-P., Margolis, H. A. and Ouimet, R. (1988). The activity, characterization and distribution of the nitrogen assimilation enzyme, glutamine synthetase, in Jack pine seedlings. *Tree Physiology* **4**, 109-118.

Vieira, J. and Messing, J. (1982). The pUC plasmids, an M13mp7-derived system for insertion mutagenesis and sequencing with synthetic universal primers. *Gene* **19**, 259-268.

Vinnemeier, J., Drogelaser, W., Pistorius, E. K. and Broer, I. (1995). Purification and partial characterization of the *Streptomyces viridochromogenes* Tü494 phosphinothricin-N-acetyltransferase mediating resistance to the herbicide phosphinothricin in transgenic plants. *Zeitschrift für Naturforschung C* **50**, 796-805.

Walker, E. L. and Coruzzi, G. M. (1989). Developmentally regulated expression of the gene family for cytosolic glutamine synthetase in *Pisum sativum*. *Plant Physiology* **91**, 702-708.

Wallsgrove, R. M., Keys, A. J., Bird, I. F., Cornelius, M. J., Lea, P. J. and Miflin, B. J. (1980). The location of glutamine synthetase in leaf cells and its role in the reassimilation of ammonia released in photorespiration. *Journal of Experimental Botany* **31**, 1005-1017.

Wallsgrove, R. M., Turner, J. C., Hall, N. P., Kendall, A. C. and Bright, S. W. J. (1987). Barley mutants lacking chloroplast glutamine synthetase - biochemical and genetic analysis. *Plant Physiology* **83**, 155-158.

Walsh, K. B. (1995). Physiology of the legume nodule and its response to stress. *Soil Biology and Biochemistry* **27**, 637-655.

Wan, Y. and Lemaux, P. G. (1994). Generation of large numbers of independently transformed fertile barley plants. *Plant Physiology* **104**, 37-48.

Watanabe, A., Hamada, K., Yokoi, H. and Akira, W. (1994). Biphasic and differential expression of cytosolic glutamine synthetase genes of radish during seed germination and senescence of cotyledons. *Plant Molecular Biology* **26**, 1807-1817.

Waterhouse, R. N., Smyth, A. J., Massonneau, A., Prosser, I. M. and Clarkson, D. T. (1996). Molecular cloning and characterization of asparagine synthetase from *Lotus japonicus*: Dynamics of asparagine synthesis in N-sufficient conditions. *Plant Molecular Biology* **30**, 883-897.

Wedler, F. C., Horn, B. R. and Roby, W. G. (1980). Interaction of a new γ-glutamyl-phosphate analog, 4-phosphonoacetyl)-L-α-aminobutyrate, with glutamine synthetase enzymes from *Escherichia coli*, plant, and mammalian sources. *Archives of Biochemistry and Biophysics* **202**, 482-490.

Wehrmann, A., Van Vliet, A., Opsomer, C., Botterman, J. and Schulz, A. (1996). The similarities of *bar* and *pat* gene products make them equally applicable for plant engineers. *Nature Biotechnology* **14**, 1274-1278.

Wendler, C., Barniske, M. and Wild, A. (1990). Effect of phosphinothricin (glufosinate) on photosynthesis and photorespiration of C_3 and C_4 plants. *Photosynthesis Research* **24**, 55-61.

Wendler, C., Putzer, A. and Wild, A. (1992). Effect of glufosinate (phosphinothricin) and inhibitors of photorespiration on photosynthesis and ribulose-1,5-bisphosphate carboxylase activity. *Journal of Plant Physiology* **139**, 666-671.

Wild, A., Sauer, H. and Ruhle, W. (1987). The effect of phosphinothricin (glufosinate) on photosynthesis: I. Inhibition of photosynthesis and accumulation of ammonia. *Zeitschrift für Naturforschung C* **42**, 263-269.

Wilkinson, J. E., Twell, D. and Lindsey, K. (1997). Activities of CaMV 35S and *nos* promoters in pollen: Implications for field release of transgenic plants. *Journal of Experimental Botany* **48**, 265-275.

Wilmink, A. and Donns, J. J. M. (1993). Selective agents and marker genes for use in transformation of monocotyledonous plants. *Plant Molecular Biology Reporter* **11**, 165-185.

Wilson, K. J. (1995). Molecular techniques for the study of rhizobial ecology in the field. *Soil Biology and Biochemistry* **27**, 501-514.

Wilson, K. J., Sessitsch, A., Corbo, J. C., Giller, K. E., Akkermans, A. D. L. and Jefferson, R. A. (1995). ß-glucuronidase (GUS) transposons for ecological and genetic studies of rhizobia and other Gram-negative bacteria. *Microbiology* **141**, 1691-1705.

Wohlleben, W., Arnold, W., Broer, I., Hillemann, D., Strauch, E. and Pühler, A. (1988). Nucleotide sequence of the phosphinothricin N-acetyltransferase gene from *Streptomyces viridochromogenes* Tü 494 and its expression in *Nicotiana tabacum*. *Gene* **70**, 25-37.

Woodall, J. (1994). Studies of glutamine synthetase in *Lotus* species and the occurrence of root GS2 in other legumes. PhD Thesis, University College, London

Woodall, J., Boxall, J. G., Forde, B. G. and Pearson, J. (1996a). Changing perspectives in plant nitrogen metabolism: the central role of glutamine synthetase. *Science Progress* **79**, 1-26.

Woodall, J. and Forde, B. G. (1996). Glutamine synthetase polypeptides in the roots of 55 legume species in relation to their climatic origin and the partitioning of nitrate assimilation. *Plant Cell and Environment* **19**, 848-858.

Woodall, J., Havill, D. C. and Pearson, J. (1996b). Developmental changes in glutamine synthetase isoforms in *Sambucus nigra* and *Trientalis europaea*. *Plant Physiology and Biochemistry* **34**, 697-706.

PUBLICATIONS:

Work presented in this thesis has been published in the following paper, which is attached at the back:

Woodall, J., Boxall, J. G., Forde, B. G. and Pearson, J. (1996). Changing perspectives in plant nitrogen metabolism: the central role of glutamine synthetase. *Science Progress* **79**, 1-26.

Published papers not copied on instruction from the university